UNIVERSITÉ LIBRE DE BRUXELLES

FACULTÉ DES SCIENCES

Département des Sciences de la Terre et de l'Environnement

Iron Biogeochemistry in the Antarctic Sea Ice Environment

PhD thesis presented by Delphine Lannuzel

to obtain the degree of "Docteur en Sciences"

Promotor: Prof. L. Chou
Laboratoire d'Océanographie Chimique et Géochimie des Eaux

Co-Promotor: Dr. V. Schoemann
Ecologie des Systèmes Aquatiques

Year 2006-2007

Table of contents

Chapter 1

General Introduction

1.1. Role of the Southern Ocean in climate change

1.1.1. Global Warming

Global warming is a term used to describe the trend of increases in the mean Earth's atmosphere and oceans temperature that has been recorded in the last few decades. Human-induced land-clearing, fossil-fuel burning and diverse industrial activities all contribute to the increase in the quantity of greenhouse gases (GHG) such as carbon dioxide (CO_2) and methane (CH_4) released to the atmosphere. Since the late 19th century, the anthropogenic gas emissions have led to a rise by 0.6 ± 0.2 °C in the averaged Earth temperature and it is likely that "most of the warming observed in the last 50 years is attributable to human-induced activities" (IPCC report, Climate Change 2001). Some ecological consequences are already conspicuous such as sea ice extent decrease and glacier retreats in the Arctic. The trend is less clear in the Antarctic as it is surrounded by massive volumes of cold waters keeping Antarctica insulated (Goosse and Renssen, 2001).

The Vostok (Antarctica) records of climate change provide a unique context for describing human-induced changes over the past 420,000 years (Petit et al., 1999; Sigman and Boyle, 2000). The main difference between climate records documented in the Vostok ice-cores and the present situation is the sharp increase in the concentrations of important GHG such as CO_2 that is being triggered by human activities at unprecedented rates (Falkowski et al., 2000) (Fig. 1.1).

This increase in the global Earth's temperature is expected to induce other climate changes such as sea level rises, slowdown or shutdown of the thermohaline circulation, and changes in the pattern of precipitation (IPCC report on Polar Regions: http://www.grida.no/climate/ipcc_tar/wg1/005.htm). Such changes may increase the intensity and frequency of extreme weather events like hurricanes, heat waves, floods, or even contribute to biological extinctions.

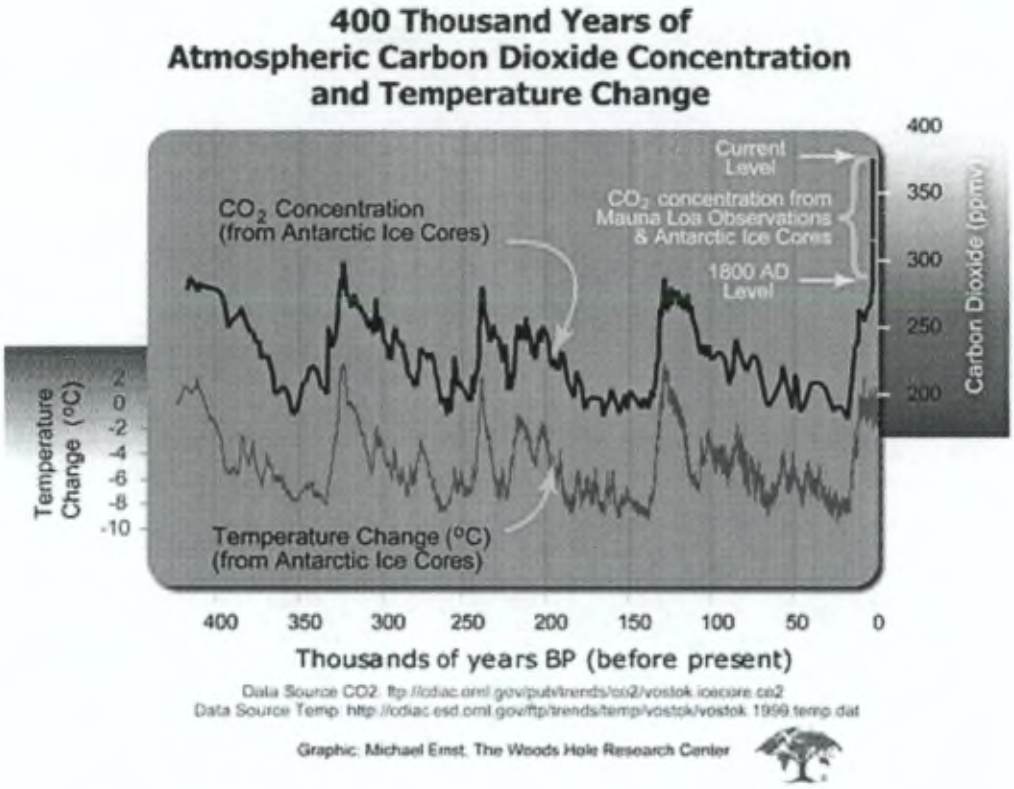

Figure 1.1. Plots of atmospheric CO_2 and averaged Earth temperature during the last 420, 000 years.

1.1.2. The Southern Ocean

The world ocean plays a key role in regulating the global climate system by buffering both heat and gases like atmospheric CO_2. Oceans behave either as a source or a sink of CO_2 and can therefore control the concentrations of this GHG in the atmosphere. Global model climates suggest that within the end of the current century, the Southern Ocean would be the ultimate oceanic sink for atmospheric CO_2 (Bopp et al., 2001). The Southern Ocean represents 20% of the world ocean surface and influences the global climate in many ways.

1.1.2.1. World Ocean circulation

The clockwise flow of the Antarctic Circumpolar Current (ACC) around Antarctica connects the Atlantic, Indian and Pacific basins and currents. The ACC redistributes heat and other properties around the Globe and thus influences the patterns of temperature and precipitation (Fig. 1.2).

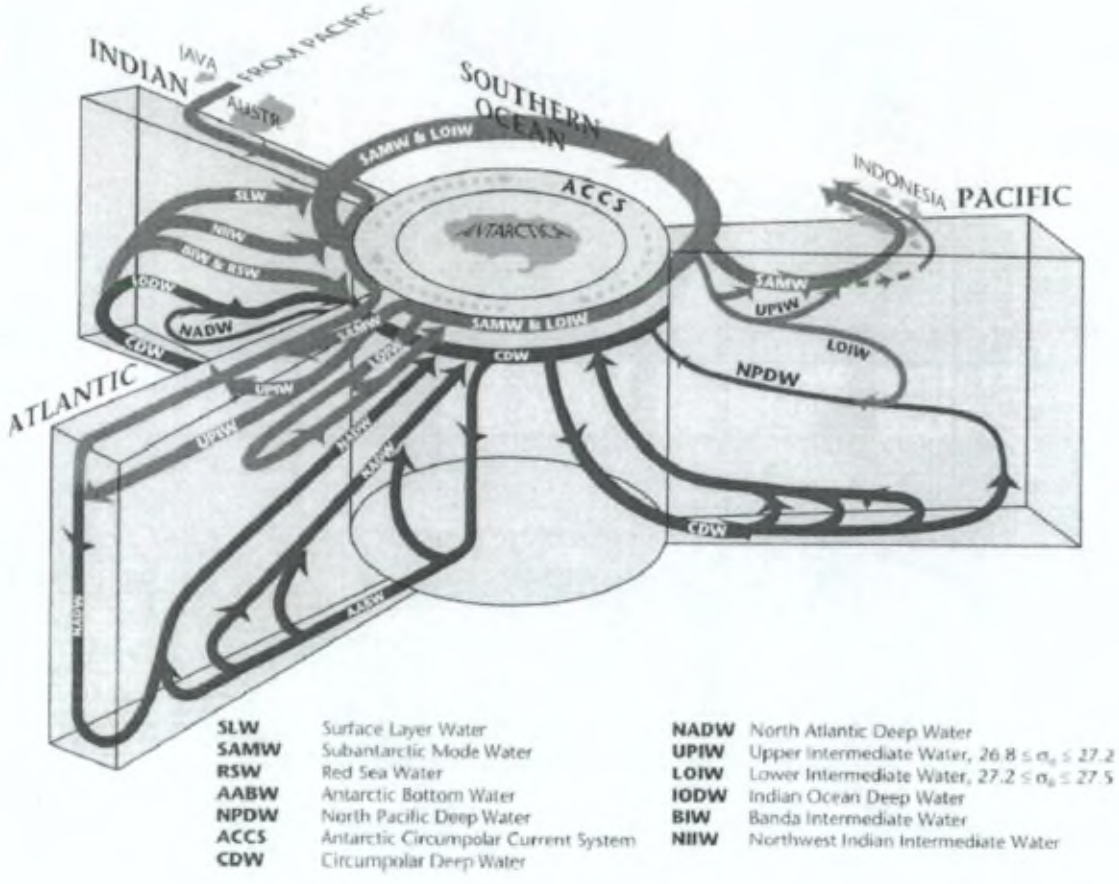

Figure 1.2. Schematic overview of the meridional overturning circulation (Rintoul et al., 2001)

1.1.2.2. Sea ice extent and thickness

Just at the interface between the surface ocean and the atmosphere, sea ice has a profound effect on climate processes. Its formation constitutes the largest single seasonal phenomenon on Earth (Brierley and Thomas, 2002). The size of Antarctica doubles each year with the ice freezing around the continent (Fig. 1.3). Because of its whiteness, the ice cover reflects the sun's heat back to space, thus intensifying the cold conditions (Dieckmann and Hellmer, 2003). Its patchy blanket also keeps the ocean insulated from the atmosphere and limits heat and gas loss (Bowman et al., 1997; Arrigo et al., 1998).

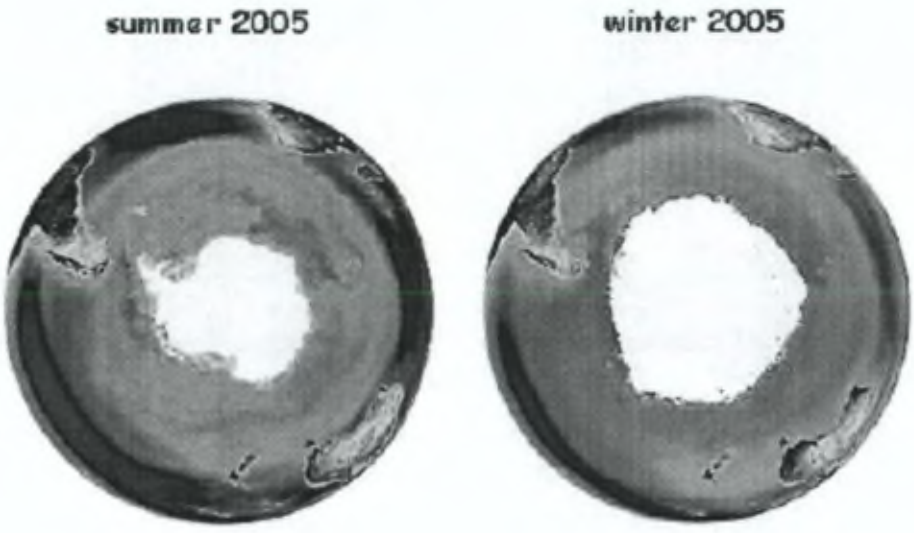

Figure 1.3. Summer (February 2005) and winter (September 2005) Antarctic sea ice extents (source: SeaWIFS http://oceancolor.gsfc.nasa.gov/).

1.1.2.3. Initiation of the thermohaline deep circulation

The cooling of the ocean, sea ice formation during winter and subsequent rejection of sea salts increase the density of the surface waters, which flow downwards to the deep sea (Fichefet et al., 2003; Marsland, 2004). These cold salty water masses include the Antarctic Bottom Waters (AABW) and the Antarctic Intermediate Waters (AAIW). The AABW forms on the continental shelf, travels northwards hugging the seafloor and carrying nutrients and carbon as far as the North Atlantic. The AAIW, less saline, forms further north as compared to the AABW (Figs. 1.2 and 1.4). These cold dense waters formed around the Antarctica, which sink and are transported laterally, constitute a major drive for the world's ocean circulation.

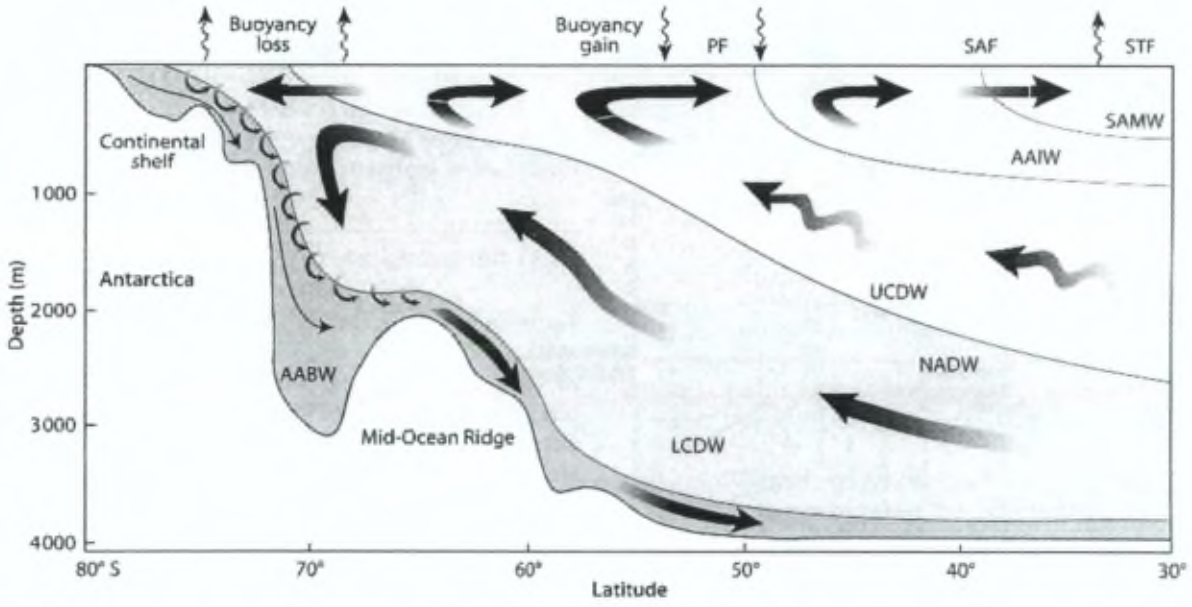

Figure 1.4. Scheme of the thermohaline circulation in the Southern Ocean AABW : Antarctic Bottom Water ; LCDW : Lower Circumpolar Deep Water; NADW: North Atlantic Deep Water; UCDW: Upper Circumpolar Antarctic Water; AAIW: Antarctic Intermediate Water; SAMW: Subantarctic Mode Water. PF: Polar Front; SAF: Subantarctic Front; STF: Subtropical Front (source: Trull et al., 2001).

1.1.2.4. Solubility and biological pumps

Oceans are able to take-up one third of the anthropogenic CO_2 emitted to the atmosphere from fossil-fuel burning and deforestation (Siegenthaler and Sarmiento, 1993) via the combination of abiotic and biotic processes that are referred as the solubility and biological pumps.

The surface ocean exchanges gases and heat with the low atmosphere. In the Southern Ocean, strong winds, waves and low temperatures favour CO_2 transfer into seawater. Carbon dioxide is exported 4 to 5 km beneath the ocean surface via the sinking of the cold dense water masses; this physical pump is called the "solubility pump". The efficiency of the solubility pump is driven by the thermohaline circulation, and by the spatial and temporal distribution in the ocean ventilation (Broeker and Peng, 1992; Stoker and Schmittner, 1998).

The "biological pump" is a key process in regulating atmospheric CO_2 via carbon fixation in the upper ocean and export towards the seafloor (Fig. 1.5). In surface waters, phytoplankton cells use light and inorganic nutrients to incorporate and transform dissolved inorganic carbon (CO_2) into organic carbon via photosynthesis. Part of this biologically formed organic matter is removed from the surface waters and exported to the deep ocean

under the form of dissolved and particulate organic carbon. This export occurs via sedimentation of aggregates, marine snow and faecal pellets. A large part of this organic carbon is however degraded during its transfer to the deep sea via remineralization processes, thus enabling only a small fraction of this organic carbon to be buried in the seafloor. The biological pump efficiency depends both on the biotic and abiotic processes controlling the algal growth in the photic zone (i.e. light and nutrients availability), but also on the fate of the organic matter during its export to the seafloor (remineralization or burial, Fig 1.5).

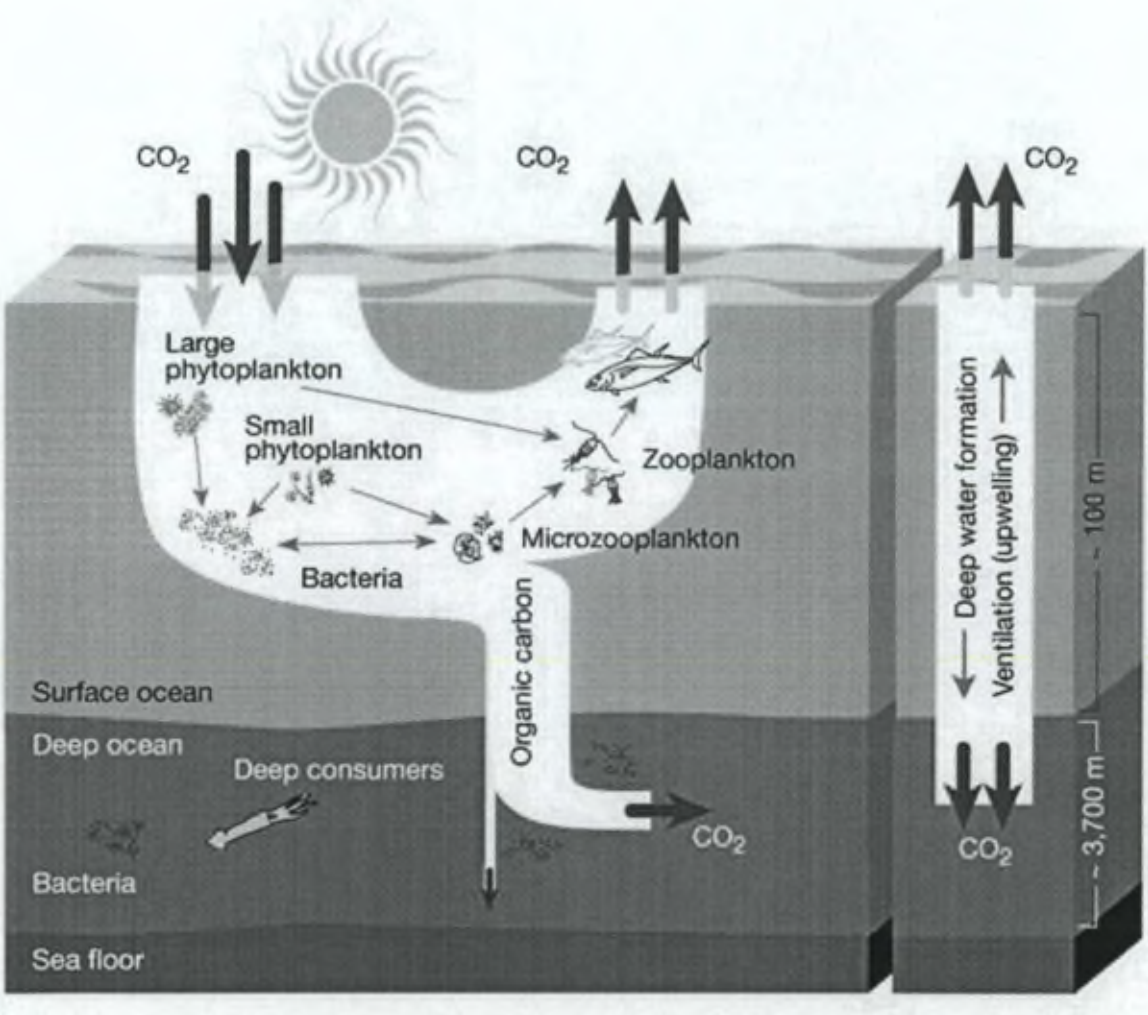

Figure 1.5. Planktonic foodweb and biological and solubility pumps (source: www.nature.com/nature/journal/v407/n6805/fig_tab/407685a0_F1.html)

1.1.3 *Limiting factors for algal growth in Antarctic surface waters*

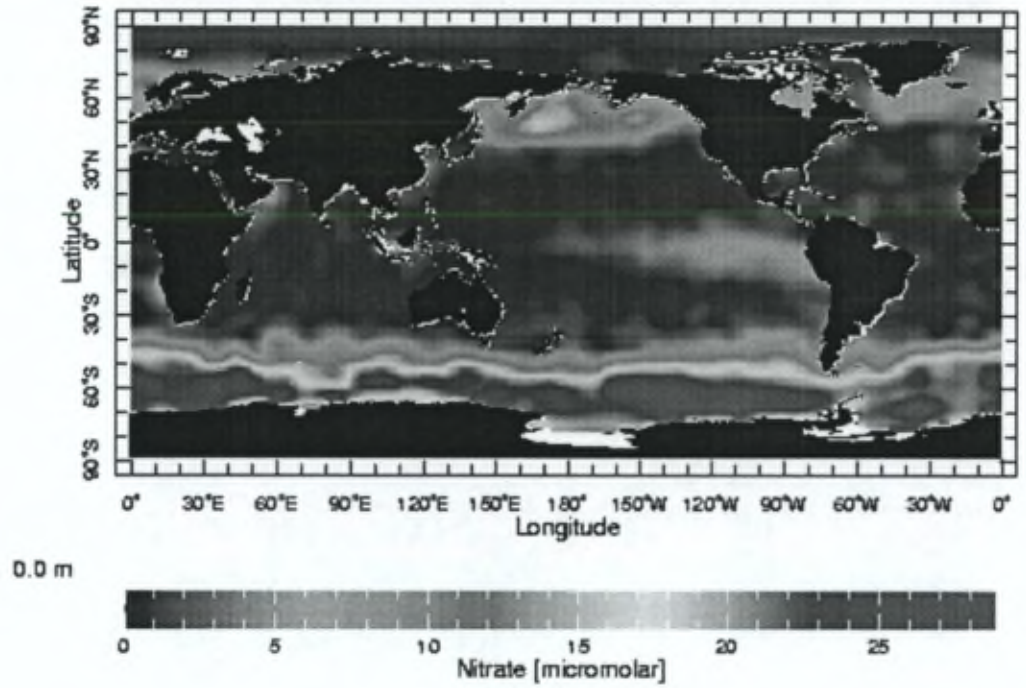

Figure 1.6. Map of annual average nitrate concentrations in the surface waters of the oceans. This image clearly shows the high levels of nitrate in the subarctic Pacific, the equatorial Pacific and the Southern Ocean. Data from the Levitus World Ocean Atlas 1994.

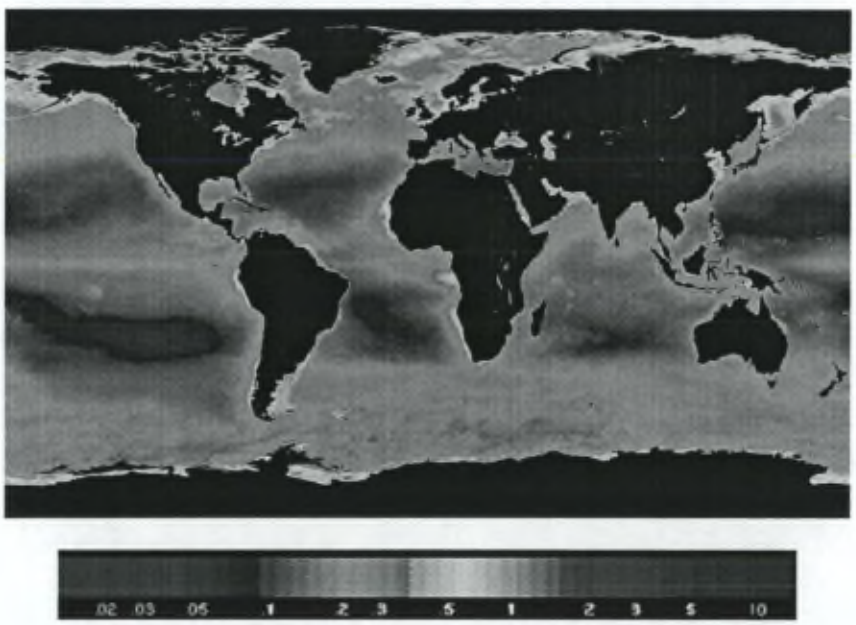

Figure 1.7. Chl *a* (mg/m^3) (source: SeaWIFS September 1997- August 2000 (http://oceancolor.gsfc.nasa.gov/cgi/image_archive.cgi?c=CHLOROPHYLL).

Nitrate and phosphate and, in a lesser extent, silicate, are the major nutrients for the algal growth in the oceans. In most surface oceans, phytoplankton grows until they have used up nitrates or phosphates, whichever becomes depleted first. The subarctic Pacific, the equatorial Pacific and the Southern Ocean, however, all have plenty of these macro-nutrients all year-round but contain low Chlorophyll *a* (Chl *a*) levels (Fig.1.6 and 1.7) (de Baar, 1994). These specific areas are known as the High Nutrient-Low Chorophyll (HNLC) regions and makes up about 40% of the total area of the ocean.

Factors such as irradiance (Nelson and Smith, 1991; Mitchell et al., 1991; Sunda and Huntsman, 1997), silicate availability (Dugdale et al., 1995; de Baar et al., 1999; Moore and Abbot, 2002), and extremely low iron concentrations (Martin and Fitzwater, 1988; de Baar, 1994) can co-limit and thus regulate primary production and planktonic composition in the Southern Ocean.

1.1.3.1. Light, silicates and grazing pressure

Light can be strongly limiting in the Southern Ocean as it is driven by the season, the depth of the mixed layer and the ice cover. Heavy black clouds absorbing solar radiation, strong winds and storms deepening the mixed layer, together with large ice covered areas which increase the albedo at the ocean surface all contribute to drastically limit algal productivity in the Antarctic ecosystem (Lancelot et al., 1991; Mitchell et al., 1991; Sakshaug et al., 1991).

Diatoms represent a significant part of the phytoplankton community and are key contributors to the primary production. These organisms use silicates ($Si(OH)_4$) to build their opaline frustules and are thus very sensitive to changes in silicates levels in the ocean. Concentrations in $Si(OH)_4$ are highly variable in the Antarctic surface waters and, depending on the areas, can become or not limiting for diatom growth (range from 2-3 µM in the North of the Polar Front to 70 µM in the Ross Sea; de Levitus et al., 1994; Baar et al., 1999).

While light and nutrient availabilities exert a "bottom up" control on phytoplankton growth, grazing by zooplankton affects algal mortality via "top down" control (Fig. 1.5). In the Southern Ocean grazing pressure can maintain low standing crops of pico- and nano-plankton and is thus a key factor in regulating primary production (Lancelot et al., 1993; Smetacek et al., 2004).

1.1.3.2. Iron limitation in the Southern Ocean

The hypothesis of algal growth limitation by low Fe supply in the Southern Ocean was first suggested by Gran (1931). Hart (1934) described the phytoplankton distribution in the Antarctic waters and presented a list of factors able to influence photosynthesis (i.e. light, nutrients, UV radiation, water column stability) upon which Fe availability was identified as one possible factor (Cullen, 1991). Martin (1990a) then based his iron hypothesis on the comparative observation of atmospheric CO_2 variations in the past and present climate: present-day high atmospheric CO_2 levels and Fe deficiency in surface waters are comparable to the conditions encountered during the last interglacial period. Contrastingly, enhanced Fe dust inputs to the Southern Ocean during the last glacial maximum would have stimulated primary production and drawn down atmospheric CO_2 levels.

Laboratory-based experiments (Martin et al., 1990b; de Baar et al., 1990; Buma et al., 1991), studies of naturally Fe enriched areas (de Baar et al., 1995; Blain et al., 2001) and large scale Fe fertilization experiments (SOIREE: Boyd et al., 2000 ; EisenEx: Smetacek et al., 2001; Gervais et al., 2002 ; SOFeX: Coale et al., 2004; EiFex: Hoffmann et al., 2005; de Baar et al., 2005) have been performed to investigate the algal response to Fe addition in the Southern Ocean: iron addition does stimulate major nutrients uptake by phytoplankton in the surface waters. It is not clear yet though to which extent the Fe fertilization would favour the export and burial of particulate material into the deep ocean (Boyd et al., 2004; Buesseler et al., 2004, de Baar et al., 2005) and thus regulate the climate.

1.2. Iron biogeochemistry

In order to address the many questions related to Fe metabolism in the Southern Ocean, it is of a paramount importance to describe and understand Fe chemistry and bio-availability in seawater. Iron (*Ferrum*, Fe) is the second most abundant metal on Earth after aluminium, and is believed to be the tenth most abundant element in the universe. Although highly abundant in the Earth's crust, Fe is found at concentrations rarely exceeding a few nM in modern surface oceanic seawater (de Baar and de Jong, 2001) and thus co-limit algal growth in the HNLC areas (de Baar et al., 2005). Iron is a bioactive metal which is necessary for photosynthesis and respiration processes (Chereskin and Castelfranco, 1982; Greene et al, 1992; Geider et al, 1993), nitrate metabolism (Timmermans et al., 1994; de Baar et al., 1997;

van Leeuwe et al., 1997), N_2 fixation (Mills et al., 2004), sulfate reduction and detoxification of reactive oxygen species (Sunda and Huntsman, 1995).

1.2.1. Iron speciation

1.2.1.1. Size-fractionation

The chemical forms of Fe are generally operationally defined via size-fractionation using filtration methods (Fig. 1.8) (Wells et al., 1995). In the marine environment, dissolved Fe (DFe) is commonly referred as the fraction collected after filtration of the sample through 0.2 µm or 0.45 µm pore filters, depending on the studies. If the dissolved (DFe, < 0.2 or 0.45 µm) and particulate (PFe, > 0.2 or 0.45 µm) forms originate from the 2 fractions separated during the filtration step, the total-dissolvable fraction (TDFe) refers to the unfiltered sample. Soluble Fe is filterable through 1 nm (Fig. 1.8) while colloids belong to the size-fraction between 1 nm and 0.2 or 0.45µm (Fig. 1.8).

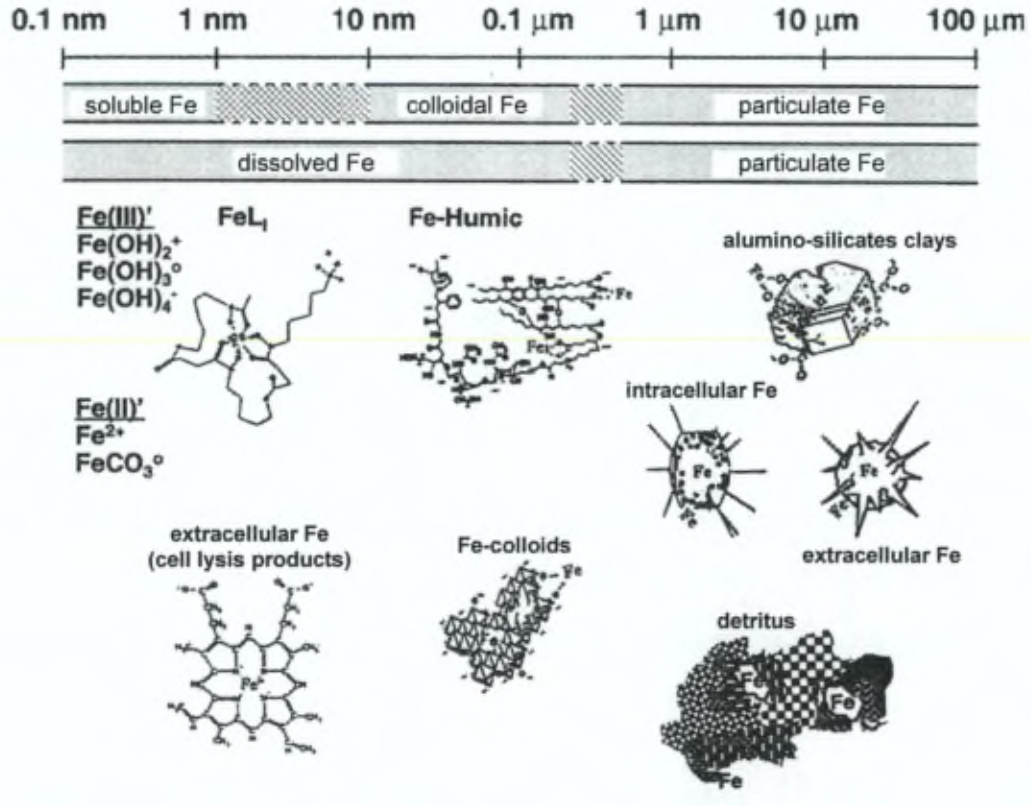

Figure 1.8. Various chemical forms and species of iron which can exist in dissolved and particulate phases (Bruland and Rue, 2001).

1.2.1.2. Redox state

Iron exists in two oxidation states: Fe (II) and Fe (III). Iron (III) is the main and thermodynamically most stable form of Fe in seawater at pH 8. Depending on pH, temperature, ionic strength and oxidising species present in the medium, oxidation rates can range from a few seconds (tropical waters) to a few hours (Antarctic waters) (Voelker et Sedlack, 1995; Sarthou et al., 1996; Croot and Laan, 2002). Iron (III) is highly reactive with respect to adsorption onto particle surfaces and complex formation. Hydrolysis of Fe (III) also tends to result in the formation of sparingly soluble oxyhydroxides particles (Millero and Sotolongo, 1989; Millero et al., 1995; Sunda and Huntsmann, 1995). Iron (III) thus tends to be rapidly removed from the upper ocean towards the deep sea via sedimentation of Fe particles (Sunda, 2001; de Baar and de Jong, 2001). While Fe (III) is sparely soluble in seawater, Fe (II) is the most kinetically labile redox specie. Fe (II) levels can be enhanced via dust deposition at the surface ocean of aerosols enriched in Fe (II) by photochemical reactions (Waite et al., 1995; Jickells and Spokes, 1999), photo-reduction in the upper waters or even reducing micro-environment such as marine snow (Wells et al., 1995).

1.2.1.3. Iron bio-availability for phytoplankton

Iron levels in oxygenated water are low and only part of it is available for phytoplankton uptake. Iron availability for marine micro-organisms can depend on i) its concentration, ii) its speciation (the chemical forms and species of Fe), iii) how the physico-chemical properties of the medium can alter Fe speciation and concentrations, (Buffle, 1988) and iv) biological uptake mechanisms. Iron exists in several species of which free Fe (II) and Fe (III) are preferred by the phytoplankton cells (Anderson and Morel, 1982). However, more than 99% of dissolved Fe is organically complexed to weak and/or strong ligands present in surface seawater (Gledhill and van den Berg, 1994, Rue and Bruland, 1995; Boyé et al., 2001). These ligands would maintain Fe into solution thus increase the residence time of Fe in the upper water column. Moreover, photochemical reactions with regards to Fe-ligand complexes could facilitate Fe biological uptake (Barbeau et al., 2001).

Marine organisms are able to transport Fe into their inner cell via various cellular mechanisms such as siderophore systems and surface reduction (Trick et al., 1983; Hudson and Morel, 1990, Völker and Wolf-Gladrow, 1999). Siderophores are Fe (III)-specific chelating compounds excreted by various micro-organisms such as marine bacteria (Gonye and Carpenter, 1974), cyanobacteria (Hutchins and Rueter, 1991) and a few species of

phytoplankton (Trick et al., 1983; Soria-Dengg and Horstmann, 1995). There is also a growing evidence suggesting that some phytoplankton species can directly access Fe bound to dissolved organic complex and colloids (Hutchins et al., 1999; Maldonado and Price, 1999; Maranger and Pullin, 2003).Some studies finally showed that mixotrophic algae could acquire Fe from grazing bacteria and Fe colloids (Maranger et al., 1998; Nodwell and Price, 2001).

1.2.2. Iron sources to the Southern Ocean

Low Fe concentrations in the Antarctic surface waters are the result of low Fe inputs. The conceivable sources of Fe to the Southern Ocean are suggested to be: a) atmospheric deposition of continental dusts from Transantarctic mountains, Australia, South America and South Africa (Duce and Tindale, 1991; Gao et al., 2001; Erickson et al., 2003) and extraterrestrial dusts (Johnson, 2001), b) continental shelf advection from e.g. the Argentine basin (de Baar et al., 1995) or Kerguelen Island platform (Blain et al., 2001), c) upwelling and vertical diffusion (de Baar and de Jong, 2001; Hoppema et al., 2003) and d) melting ice bergs and sea ice (Sedwick and DiTullio, 1997) (Fig. 1.9).

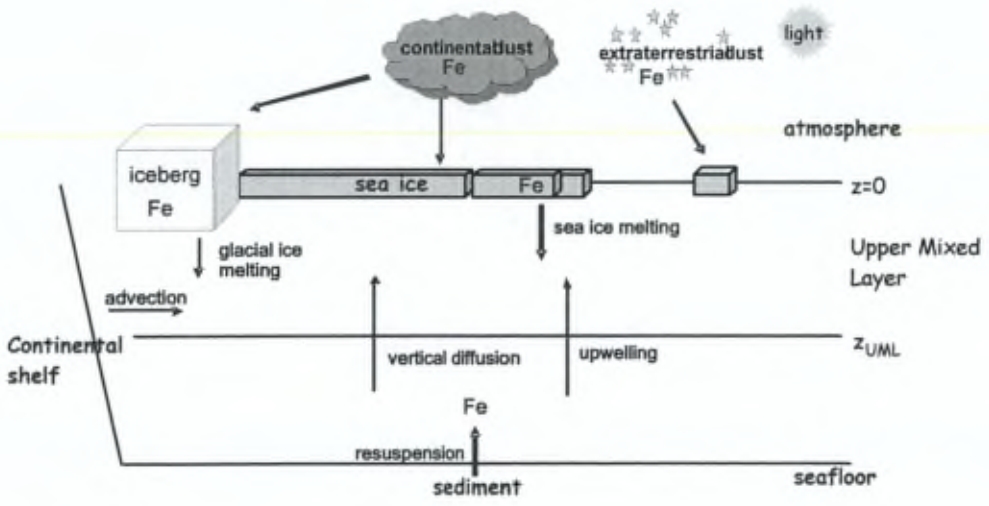

Figure 1.9. Schematic overview of the possible Fe sources to Antarctic surface waters.

1.2.2.1. Atmospheric input

Even though Fe is very abundant in dust and lots of dusts enter the ocean, its levels are extremely low in open ocean surface waters (de Baar and de Jong, 2001). Iron in dust mainly occurs as Fe (III) complexes that are not very soluble in seawater. As dust is transported through clouds, it encounters very acidic conditions which slightly increase Fe solubility (Jickells and Spokes, 2001; Jickells et al., 2005). However, depending on the areas, 1-54% of the Fe from the atmosphere entering seawater is soluble (Duce and Tindale, 1991; Sedwick et al., 2005; Baker et al., 2006). These eolian inputs are nevertheless low for the Antarctic waters because of their remoteness (Fig. 1.10). Continental dusts represent less than 0.1% of the total dissolved Fe supplied to the major oceans (Gao et al., 2001; 2003). Moreover, once deposited in the open ocean, Fe dusts are rapidly diluted and exported towards deep waters because of the strong mixing in the Antarctic sector. There are nevertheless other possible contributors to the atmospheric input such as extraterrestrial sources, for which Fe solubility when deposited on the surface ocean would be 100% (Johnson, 2001).

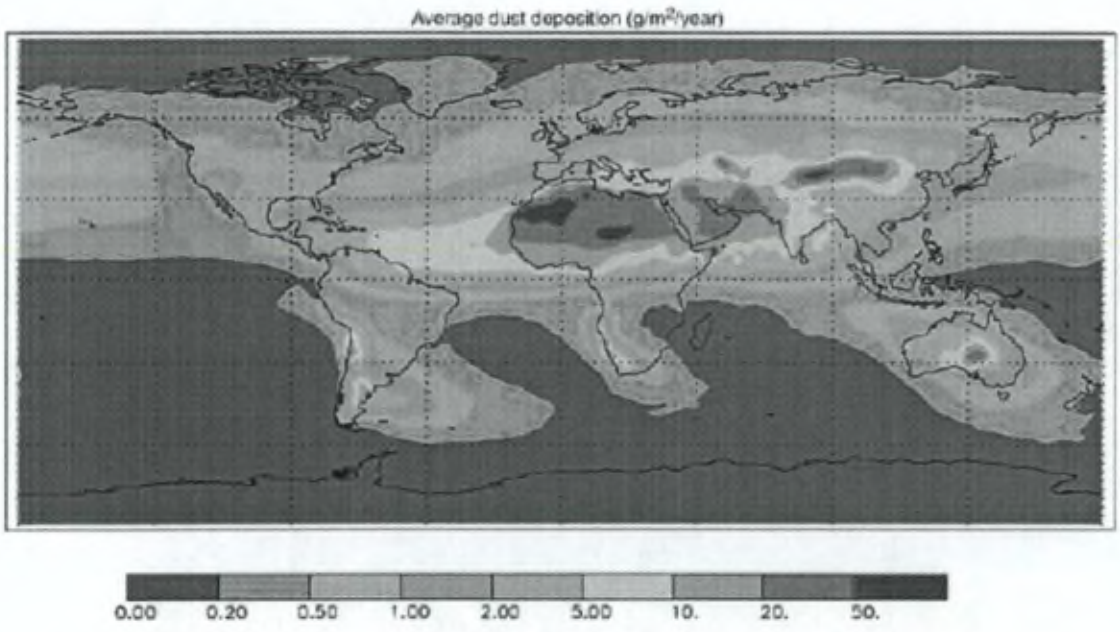

Figure 1.10. Dust fluxes to the world oceans based on a composite of three published modeling studies that match satellite optical depth, in situ concentration, and deposition observations (Ginoux et al., 2001; Mahowald and Luo, 2003; Tegen et al., 2004). Percentage inputs to ocean basins based on this figure are as follows: North Atlantic, 43%; South Atlantic, 4%; North Pacific, 15%; South Pacific, 6%; Indian, 25%; and Southern Ocean, 6% (source: Jickells et al., 2005).

1.2.2.2. Upwelling and vertical diffusion

In the AAC zone of the Southern Ocean, permanent strong winds and lack of land barrier would favour upwelling and eddy diffusion of Fe enriched deep waters (Löscher et al., 1997) as compared to the North Atlantic where the wind stress is twice as low (Trenberth et al., 1990). The opposite seasonality between enhanced upward supply of Fe over winter/early spring and better light availability over summer period would be favourable for algal growth in the AAC (Löscher et al., 1997).

1.2.2.3. Sediment resuspension and advection from the continental shelf

Some studies on seawater profiles in the Weddell Sea and the Gerlache Strait reported possible Fe inputs from shelf sediment of the Antarctic Peninsula and South Orkney (Martin et al., 1990a; Westerlund and Öhman, 1991; Nolting et al., 1991). Löscher et al. (1997) proposed that the high Fe levels encountered in the Polar Front could be explained by lateral advection from the South American continental shelf. Besides, particulate Fe from resuspended shelf material appeared to be a significant source which would eventually explain the elevated levels of Fe encountered in the western and southern areas of the Ross Sea (Fitzwater et al., 2000). Moreover, shallow shelves and slopes from Antarctic Islands may via sediment resuspension constitute an additional source of Fe to Antarctic nearshore waters (e.g. Kerguelen Islands: Bucciarelli et al., 2001).

1.2.2.4. Melting icebergs and sea ice

Glacial ice originates from snow accumulation and may contain Fe from atmospheric dust. These ice shelves or glaciers then eventually calve into the coastal ocean. The icebergs subsequently formed can travel towards open waters and slowly liberate Fe upon melting (de Baar et al., 1990). Iron contents of 26.0 nM, 20.4 nM and 20.0 nM were found in ice collected from a "clean" iceberg (i.e. not visibly covered with continental dirt) in the Polar Front (respectively from Martin et al., 1990a; de Baar et al., 1990; de Jong et al., 1999) and total-dissolvable Fe values up to 9 nM from surface water sampled in the wake of an iceberg (Löscher et al., 1997). .

While covering large areas around Antarctica, sea ice could yearly accumulate Fe not only from dust deposition but also from freezing of Fe-enriched coastal seawater (de Baar and de Jong, 2001). Total-dissolvable Fe values ranging from 4.5 to 50 nM in snow, 10 to 95

nM in sea ice (including bottom ice), and 20 to 65 nM in brine were measured in the Weddell Sea (Löscher et al., 1997; de Jong et al., 1999). Dissolved Fe concentrations ranging from 2.8 to 25 nM were reported for sea ice floes located at 70°S, 6°W (de Jong et al., 1999; Boyé et al., 2001). This Fe would then be released into stratified waters when the ice melts in spring (Sedwick and DiTullio, 1997; Löscher et al., 1997; Fitzwater et al., 2000).

1.3. Sea ice environment

1.3.1. Sea ice formation

Sea ice forms from seawater freezing at -1.9°C. (Land-)Fast ice is sea ice that has frozen along coasts and extends out from land to distances up to 35 km (Lange et al., 1989; Jeffries et al., 1993). Pack ice refers to floating consolidated sea ice that is either freely floating or has been blocked by land-attached ice while drifting. Pack ice is commonly associated to sea ice formed in the open ocean.

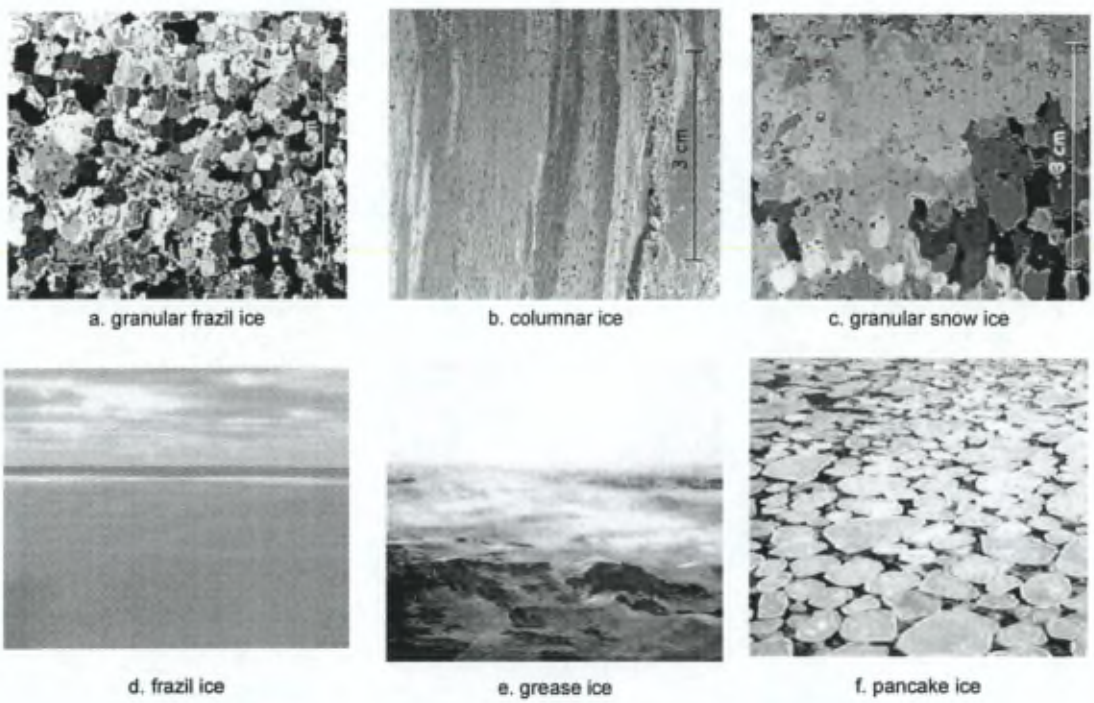

Figure 1.11. Pictures of textural types of ice taken under polarised light (a, b and c) and viewed from the ship (d, e and f). (Photos: J.-L. Tison/ V. Verbeke for a to c, T. Worby for d to f).

As surface seawater temperature drops down to -1.9°C, random shaped ice crystals of 2-4 mm in diameter begin to form (Figs 1.11a, and 1.12; Weeks and Ackley, 1982; 1986). These frazil ice crystals can either form on the sea surface or at depth (Penrose et al., 1994). Because these granular ice crystals formed up to several meters beneath the ocean surface are less dense than seawater, they rise towards the sea surface where they either float or are accumulated at the bottom of the existing ice sheet. The floating frazil ice crystals then form an amorphous suspension on the surface water (Fig. 1.11e). This ice stage is called grease ice (Horner et al., 1992).

Under quiet conditions the frazil ice crystal soon freeze together to form a continuous thin sheet 1-10 cm thick; in its early stage, when it is still transparent, this young granular ice is called nilas. In turbulent waters, waves and wind act to compress the frazil ice crystals together into larger units ranging from 30 cm to several meters in diameter floating on the ocean surface, called pancake ice (Fig. 1.11f, Maykut, 1985; Lange et al., 1989).

Once nilas or pancake ice have formed, a completely different growth process occurs. Water molecules, which are no longer in contact with the atmosphere, freeze onto the bottom of the existing ice sheet. This process, called congelation growth, slowly forms long oriented ice crystals called columnar ice (Figs. 1.11b and 1.12, Lange et al., 1989). This growth process yields first-year ice 0.5-1 m thick in Antarctic.

Snow falls are frequent in Antarctic so that a heavy snow layer generally accumulates on top of the ice cover a few days after it forms. Seawater may then infiltrate into the snow pack. "Snow ice" then may form by refreezing flooded snow and thus creates an ice solid layer bond to the top of the floe, and which is of granular type (Fig. 1.11c, Worby et al., 1998). The "superimposed ice" forms when the snow melts, percolates in the snow cover and refreezes at the sea ice-snow interface (Haas et al., 2001).

The Antarctic ice cover is highly seasonal, with very little ice in the summer (surface = 3.5×10^6 km^2, Comiso, 2003), expanding to an area roughly equal to that of the Antarctic continent in winter (surface=19×10^6 km^2, Gloersen et al., 1992). Consequently, most Antarctic sea ice is first-year ice, up to 1 m thick. The situation in the Arctic is very different as it is a polar sea surrounded by land, as opposed to the Antarctic that is a continent surrounded by the ocean. Seasonal variation is thus much less in the Arctic and most of the ice is multi-year up to 3-4 m thick with ridges building up to 20 m.

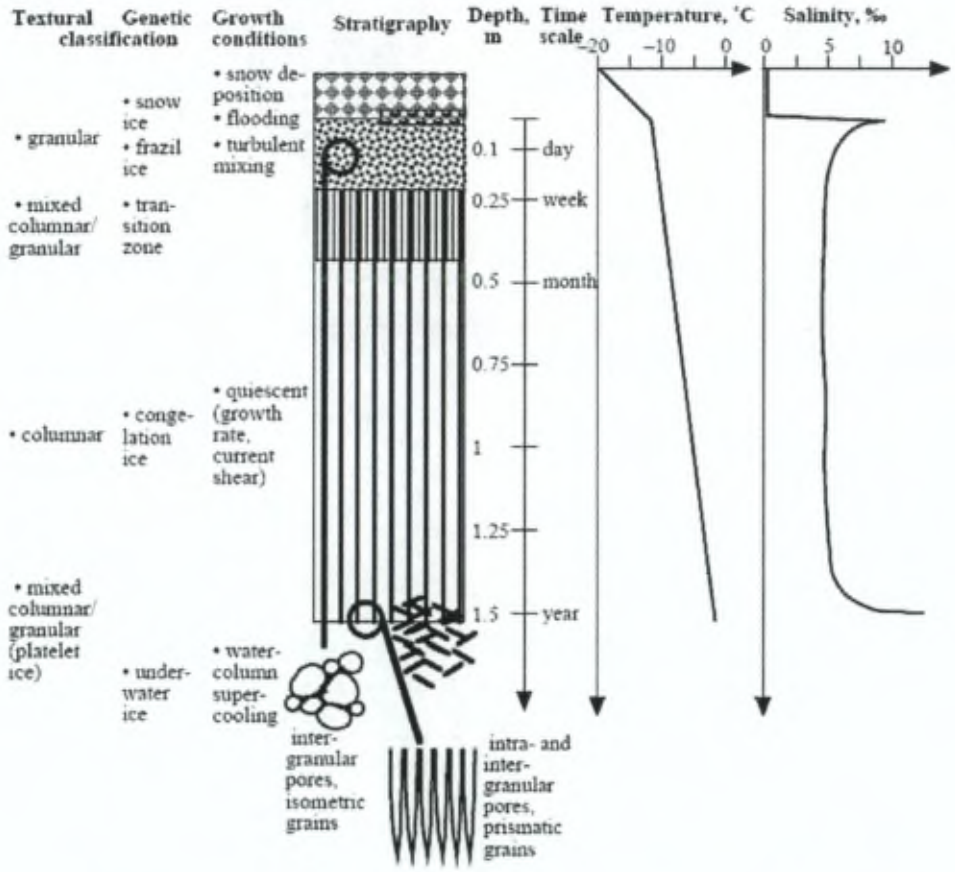

Figure 1.12. Scheme summarizing the main ice textures, growth conditions and time scale, as well as typical winter ice temperature and salinity profiles for first-year ice (source: Eicken, 2003).

1.3.2. Sea ice biogeochemistry

1.3.2.1. Sea ice algal communities

Sea ice is a vast area providing a habitat for marine organisms, which develop within the ice column. Although frozen coastal waters (land-fast ice) appear to be a favourable zone for primary production due to land vicinity, open pack ice can sustain high algal biomass as well. Chlorophyll *a* (Chl *a*) levels up to 6 mg/l in land-fast ice (McMurdo) and 0.2 mg/l in pack ice (Weddell Sea) have been reported (Arrigo, 2003). Algal communities can be observed at different levels within sea ice (e.g. Horner, 1985a, Fig. 1.13). Bottom assemblages are the most common. They often grow under low light conditions and consume major nutrients from the underlying seawater. Internal communities live in brine channels, where salinities and temperatures can be extreme as compared to bottom ice. Surface assemblages are thought to originate from seawater infiltration into the snow pack.

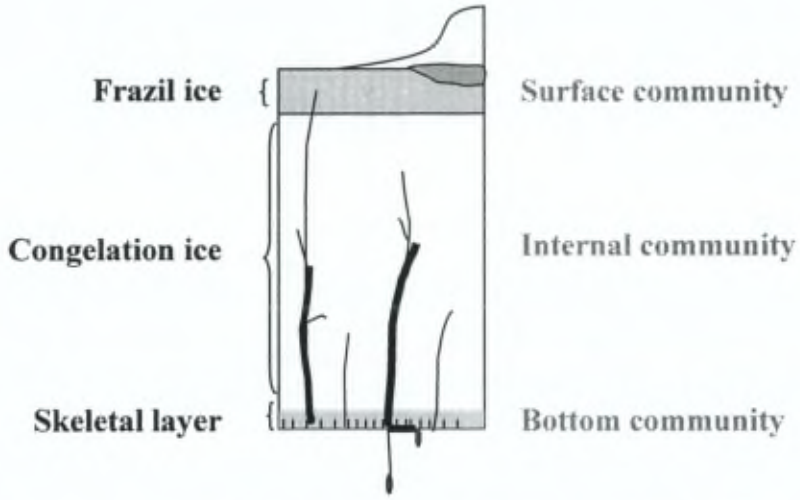

Figure 1.13. Schematic representation of biological communities encountered in pack ice (source: Arrigo and Thomas, 2004).

1.3.2.2. Possible limiting factors for sea ice algae

Within the sea ice, algal growth can be seasonally limited by a number of parameters such as light availability, high salinity, very low temperature (Eicken, 1992; Palmisano and Garrison, 1993; Kirst and Wiencke, 1995), brine pore space, grazing pressure (e.g. Garrison and Buck, 1991; Krembs et al., 2001; Schnack-Schiel et al., 1998) and deficiency in dissolved inorganic carbon, macro- and micro- nutrients such as Fe.

1.3.2.2.1. Irradiance, ice temperature and salinity

Sea ice habitats are often characterised by steep gradients in temperature, salinity and light conditions. Organisms inhabiting the pack ice can be subject to very low irradiance or even full darkness periods during winter time, which will considerably alter the development of autotrophic species in favour of heterotrophic processes (Garrison and Close, 1993; Kivi and Kuosa, 1994). Surface and near-surface assemblages may have optimal irradiance for growth, but are often restricted by nutrients supply. Micro-organisms residing in the internal layers of the ice cover are exposed to high brine salinities (e.g. up to 173; Arrigo and Sullivan, 1992) and extremely low temperatures (e.g. -16°C) during winter time, but can also experience low brine salinity when temperatures increase and flush nearly fresh melt water throughout the ice column when summer progresses (Brierley and Thomas, 2002). When enough light is available, most of sea ice algae are living in the bottom of the ice sheet where

temperature and salinity conditions are more stable and favourable for growth over spring and summer time (Arrigo, 2003).

1.3.2.2.2. Brine channel diameter and grazing pressure

Shapes and volumes of the brine channel system may control on one hand algal development of large phytoplankton species and favour smaller algal cells in the case brine pore sizes are restricted, and may on the other hand hamper infiltration of large grazers (e.g. amphipods, copepods) within the sea ice matrix. Depending on their size, swimming abilities and seasonal stage of the ice cover (i.e. permeability), grazers are able to colonize the inside of the ice habitat and/or feed on the underside of the ice (Brierley and Thomas, 2002). Sea ice algal crops do represent a major feeding ground for a wide variety of organisms, including krill, in autumn, winter and early spring when the phytoplankton biomass in the water column is scarce (Schnack-Schiel, 2003).

1.3.2.2.3. Macro- nutrients and Fe

Macro-nutrients can limit algal growth within the sea ice habitat. For the algal communities living at the snow-ice interface, infiltration and/or flooding events into the snow pack can provide resupply of nutrients from seawater which could induce important algal development (e.g. Arrigo et al, 1995; Thomas et al., 1998). Bottom ice phytoplankton communities commonly manage to stand high crops while taking advantage on the macro-nutrients from the underlying seawater. Theoretically, sea ice should contain little Fe since it is formed from Fe-deficient waters (Thomas, 2003). But this extreme environment can obviously meet chemical and physical conditions favourable for algal growth; in other words, Fe concentrations must be high enough to sustain biological activity in much of the sea ice.

1.4. Frame and scope of the study

1.4.1 Framework

The Belgian "SIBClim" project (Sea Ice Biogeochemistry in a Climate change perspective) aims at evaluating the contribution of polar oceans in the global climate regulation processes. This multidisciplinary program is a consortium of glaciologists, biologists, geochemists and modellers from the Université Libre de Bruxelles (ULB). The scopes are to quantify and understand the physical and biogeochemical processes associated

to the formation and melting of sea ice. The contribution of sea ice to the regulation of biogases involved in climate change is not well known and understood, and thus has been neglected in today's climate models. In this context, particular attention is paid to CO_2 and Dimethylsulfide (DMS), both actively involved in the metabolic processes of the sea ice microbial communities. On one hand, CO_2 is well known for its GHG properties, whereas on the other hand, DMS seems to be able to stabilize partially global warming by absorbing solar radiation via aerosols and cloud condensation nuclei formation. The SIBClim project thus focuses on the comparative study and modelisation of the biogeochemical cycles of Carbone, Sulfur, Azote, Phosphate, Siclate and Iron in the Antarctic sea ice environment and their impact on CO_2 exchanges and DMS emissions at the ocean-atmosphere interface.

1.4.2. Objectives of the study

The present work aims at studying the biogeochemical cycle of Fe in sea ice (sources, bio-availability and fate), as this element has been shown to play a crucial role in primary production and in the carbon pump efficiency in the Southern Ocean area. Iron biogeochemistry in sea ice is nearly unknown in the present-day because data are scarce (Löscher et al., 1997; de Jong et al., 1999) due, in large part, to the challenges encountered in this extreme environment with regard to sampling and analysis.

1.4.2.1. Trace metal sampling and analytical methods

The first objective of this thesis is to develop a trace metal clean sampling method suitable for such an extreme environment as sea ice. An analytical technique adapted to samples with high gradients of Fe concentrations and salinities is required; the Flow Injection Analysis (FIA) method is presented in Chapter 2.

1.4.2.2. Field data: Fe pools in Antarctic pack ice

The second scope is to evaluate the Fe distribution in the Antarctic sea ice and its associated snow, brine and seawater. Chapters 3 and 4 therefore focus on Fe data obtained along the course of two Antarctic cruises in the East Antarctic sector (September-October 2003, 64-65°S/112-119°E, "ARISE in the east" onboard the *RV Aurora Australis*) and in the Weddell Sea (ANT XXII-2, November 2004-January 2005, 67-68°S/54-55°W, ISPOL drifting station onboard the *RV Polarstern*).

1.4.2.3. Fe bio-availability, sources and fates to the Antarctic ecosystem

In the light of the results presented in Chapters 3 and 4, Chapter 5 compares both Antarctic areas and seasons investigated. Attempts are made to evaluate the overall bioavailability of Fe in pack ice and whether Fe distribution is preferentially driven by the spatial or temporal sampling collection. Based on data from the literature, estimates are then made of Fe inputs to the Southern Ocean surface waters -and possibly to sea ice- from various possible sources including atmospheric dust deposition, extraterrestrial input, continental advection, vertical diffusion, and upwelling. Finally, using data from the present study, Fe fluxes from melting sea ice to the Antarctic surface waters are evaluated to assess whether pack ice could be a significant Fe contributor to primary production in the Antarctic ecosystem.

Chapter 2

Material and Methods

Part of the Chapter 2 is available as an article published in Analytica Chimica Acta (Lannuzel et al., 2006a).

Abstract

A trace metal clean method for sampling and analysis of iron is set up and applied to sea ice and its associated snow, brine, and underlying seawater collected during the Antarctic expedition "ARISE in the East" (Antarctic Remote Ice Sensing Experiment, AA03-V1, September-October 2003, 64-65°S/112-119°E, RV *Aurora Australis*). For clean sampling, a non-contaminating electropolished stainless steel ice corer is designed in conjunction with a polyethylene lathe equipped with Ti chisels to remove outer layers of ice cores prone to contamination. A portable peristaltic pump with clean tubing is used on the ice to sample the underlying seawater (interface ice-water=0 m, 1 m and 30 m) and sea ice brine from access holes. Considering the extreme range of salinities (1-100) and Fe concentrations (0.1-100 nM) previously observed in similar environments, it is of paramount importance to set up a simple and sensitive Fe analyser adapted to such gradients. We use a Flow Injection Analysis (FIA) technique and demonstrate successfully its capability to measure directly Fe concentrations in the sample without an on-line preconcentration/matrix separation step. The sensitivity, accuracy, precision and long term stability of the analytical procedure are tested. Also interferences from a suite of other trace elements such as Ni, Cd, Cr, Mn, Cu, Zn and Co are explored and remediated. Analysis of reference materials NASS-5 and CASS-3 gives a good agreement with the certified values. Repeated measurements over a period of 5 months of an "in-house" Antarctic seawater standard yields a concentration of 1.02 ± 0.07 nM (n=17, 1σ). The detection limit (3σ of the blank) is on average 0.12 nM.

2.1. Trace metal clean sampling in a sea ice environment

Iron concentrations are typically very low in Antarctic surface ocean waters because of low Fe inputs, rapid removal by biological uptake and/or precipitation in the form of iron oxides. Until thirty years ago Fe concentrations in seawater may have been overestimated mainly because of contamination issues due to sampling (type of containers used, human manipulation, cables from the ship, material for CTDs...) and lack of analytical performances. Thanks to a huge international effort via for example intercalibration exercises (e.g. Bowie et al., 2003; 2006), sampling and analytical strategies for trace metal study in the ocean waters have been greatly improved over the past 3 decades.

Antarctic sea ice remained for a long period poorly investigated compared to other environments mainly because of the accessibility issues (Brierley and Thomas, 2002). But within the last 2 decades increasing amount of publications have been devoted to sea ice biota, physics and biogeochemistry (e.g. Horner, 1985b, Eicken, 1992, Thomas and Dieckmann, 2003). Amongst this growing interest for sea ice realm, very few investigations tackled trace metal study, most likely due to the challenges encountered both by sampling and analyses in such an extreme environment. This makes the biogeochemical cycle of Fe in sea ice virtually an unknown subject matter as to date.

2.1.1 Laboratory work

2.1.1.1. Trace metal clean room and container

To avoid possible metal contamination from the working environment, all manipulations dedicated to trace metal study are handled in a "clean room" at home-laboratory or in a "clean container" while at sea (Fig. 2.1). A class-100 laminar flow hood (i.e. supplying air with less than 100 particles per m^3) runs permanently and keeps the room under a little over-pressure so that eventual dusts are flushed out of the working area. Experimentalists wear Tyvek overall, overshoes, cap and Polyethylene and/or vinyl gloves (Cole-Parmer). The clean room is equipped with a Milli-Q system (18.2 MΩ, Millipore) supplying Ultra High Purity (UHP) water.

Figure 2.1. Laminar flow bench inside the trace metal clean container (property of MUMM, *RV Belgica*) onboard the *RV Polarstern* (Picture by J. de Jong).

2.1.1.2. Cleaning procedures

All plasticware (LDPE, HDPE, FEP, PFA) used for trace metal work is cleaned as follows: first soaking in a detergent bath (RBS 5% v:v) for 24h, followed by rinsing 3x with deionized water and then 3x with UHP water before being filled with 6M HCl (Merck, reagent grade) for 1 week. Inside the trace metal clean room, items are subsequently rinsed 5x with UHP water and dried inside the class-100 laminar flow hood. Bottles and containers, acid-cleaned, are then sealed in triple plastic bags until use.

Polycarbonate filters (0.2 µm porosity, 47 mm diameter, Nuclepore) and Sartorius polycarbonate filtration devices equipped with Teflon O-rings are treated in 1M HCl ultrapure (Ultrex, JT Baker) for 1 week before being rinsed 5x and stored in UHP before use. Pipette tips are manipulated inside a class-100 laminar flow hood and rinsed 5x with 6M HCl (J. T. Baker) and 5x with UHP before use.

Large polyethylene plastic bags dedicated to sea ice core storage are acid-cleaned in 1M HCl for 1 week and then rinsed 5x with UHP water, before being sealed in triple zip-lock bags.

2.1.2. Field sampling

Great attention has thus been paid to prevent contamination. The sampling site is located as far from the icebreaker as allowed and is off-limits to unauthorized personnel. Analysts are wearing clean room garments (Tyvek overall, overshoes and polyethylene

gloves) over their warm clothes, and items dedicated to sample collection and storage are acid-cleaned and sealed in plastic bags.

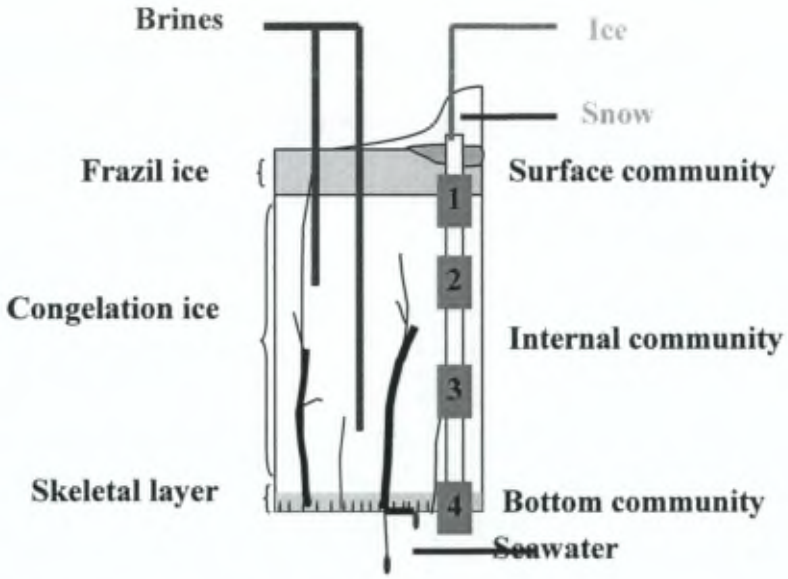

Figure 2.2. Samples to be collected in sea ice environment : brine at 2 depths (red), 4 to 6 sea ice sections (green), snow (grey) and underlying seawater (blue). (Source: adapted from S. Becquevort following Arrigo and Thomas, 2004)

Snow, brine (collected at 2 depths), seawater (0 m, 1 m and 30 m deep) and sea ice (4–6 sections chosen depending on the ice texture and visual observation of ice algae) were collected upwind from the ship under trace metal clean conditions (Fig 2.2). First, snow was collected with polyethylene shovels (Fig. 2.3a), upon which the ice-water interface was accessed using electropolished stainless steel ice corer (Fig. 2.3b) and seawater was pumped up with a portable peristaltic pump (Cole-Parmer, Masterflex E/P) and trace metal clean tubing (Fig. 2.3.c). Access holes ("sack holes") were drilled into the sea ice cover at various depths to allow gravity-driven brine collection and sampling with the electropolished stainless steel ice corer. Finally a set of sea ice cores was collected using the same non contaminating ice corer.

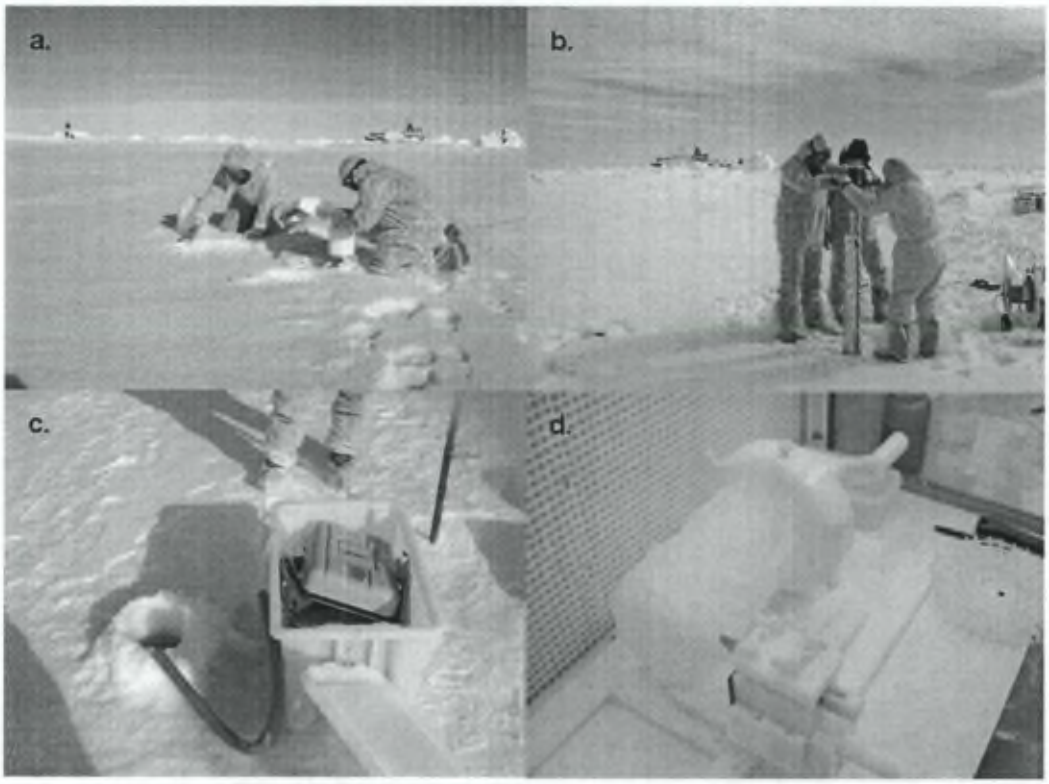

Figure 2.3. Field outfits and sampling steps for (a) snow, (b) sea ice cored with the electropolished stainless-steel corer, (c) underlying seawater collected using the peristaltic pump and plastic tubing, and (d) sea ice subsampling procedure under the laminar flow hood using the lathe and Ti chisels (pictures by J. de Jong/B. Delille/J.-L. Tison/D. Lannuzel).

2.1.3. Non-contamination tests

2.1.3.1. Test on the ice corer

For the ice corer the use of different materials was considered in order to comply with the following characteristics: (1) trace metal cleanliness, (2) mechanical strength, (3) resistance to below 0°C temperatures. Teflon, the material of choice for trace metal clean sampling, is unsuitable for sea ice coring because of its high plasticity. Teflon coated PVC and acrylate were also deemed unfit because these materials become brittle at low temperatures. Teflon coated stainless steel would be a good choice if the Teflon would not erode away during use. Titanium is a good option but the high cost makes it less attractive, although it could still be a useful alternative for smaller ice cutting accessories. The material finally chosen was electropolished stainless steel (Lichtert Industry, Belgium). Electropolished stainless steel is broadly used in bone surgery and in industries where hygiene is a major requirement (e.g. drinking water system, pharmaceutical production...): its

physical and mechanical properties, coupled with inert, easily cleaned surfaces capable of accepting a variety of finishes are perfectly suitable for trace metal ice coring purpose.

A leaching experiment was conducted on a piece of electropolished stainless steel, which was soaked in UHP water for several days. Subsamples taken at regular intervals from the leaching experiment were analysed by ICP-MS and the results indicated low Fe diffusion fluxes from the ice corer (Fig. 2.4 and Table 2.1). Contamination by the corer is thus negligible during the time period between the drilling of an ice core and its transfer into the protective plastic bags.

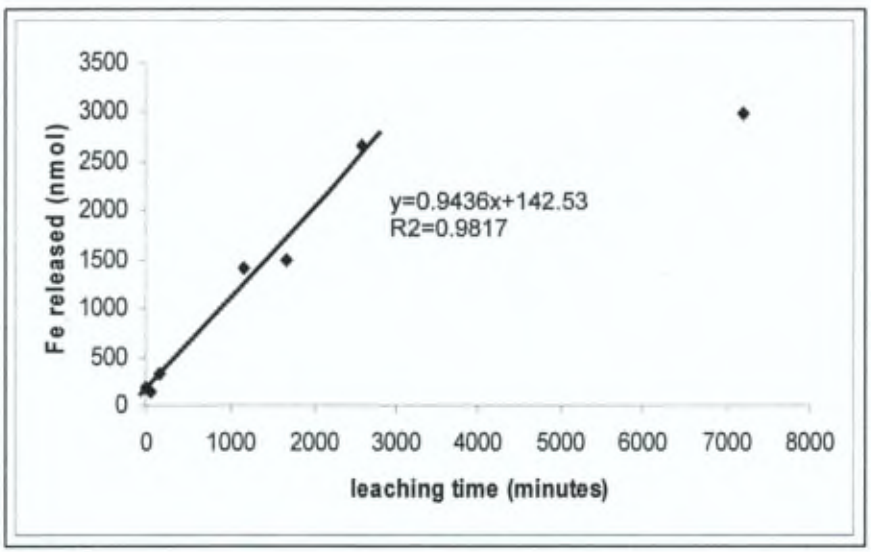

Figure 2.4. Fe released (nmol) as a function of time during a leaching experiment on an electroplished stainless steel testing piece in 100ml UHP water.

Table 2.1. Fe leaching of an electropolished stainless steel object [a] in 100 ml UHP water.

Slope ($nmol.min^{-1}$)	0.944
R	0.991
Dissolution flux ($fmol.\ cm^{-2}.min^{-1}$)	12.6
Typical sea ice Fe conc. ($nmol.l^{-1}$)	20
Total Fe amount sea ice core (nmol)	308
Fe added after 10min exposure (nmol)	0.6
% contamination	0.2%

[a] testing object surface area = 75.2 cm^2, inner surface ice corer = 4396 cm^2, volume ice corer = 15.4 dm^3

2.1.3.2. Sea ice sub-sampling procedure

To assess possible contamination during sampling, processing and/or storage, a duplicate sea ice core was decontaminated at the Glaciology Unit of the University of Brussels (AA03-V1 station XIII/ULB) and compared with the non-decontaminated core processed on board (AA03-V1 station XIII/Field). The decontamination procedure took place at -27° C, in a class-100 laminar flow bench (Figs. 2.5a and 2.5d). The core was mounted in a polyethylene lathe (Fig. 2.5b) and the 5 mm outer layer was removed mechanically using Ti chisels (Fig. 2.5c). The chisels are made of a glass/Epoxy handle with a Ti blade, which is the only part that comes into contact with the ice core. The inner core and ice chips falling off during the cleaning procedure were collected in clean polyethylene containers and melted, acidified to pH 1.8 and analysed for Fe by FIA. On the treated section depicted in Figure 2.6, outer layer and inner core TDFe values (24.3 ± 1.9 nM and 23.3 ± 2.7 nM respectively) suggest that there is no significant difference in concentration for the station XIII/Field core at approximately the same depth (22.6 ± 3.5 nM TDFe).

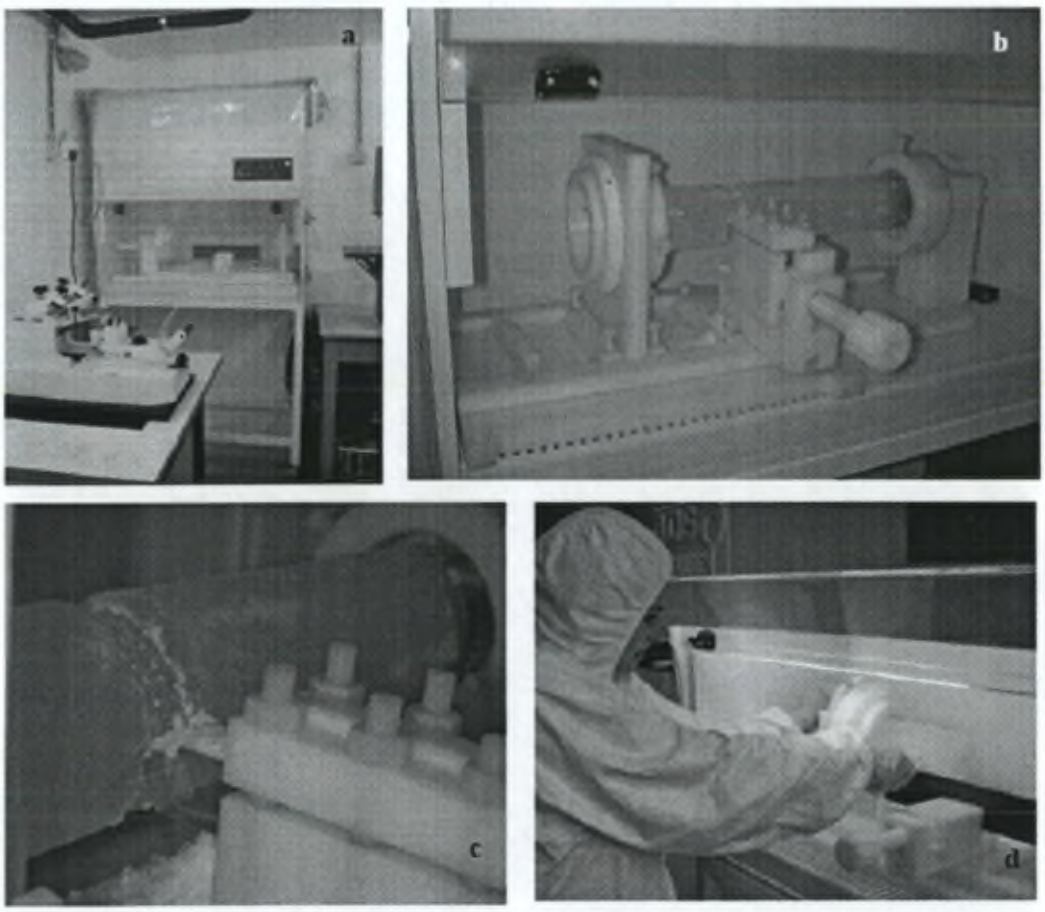

Figure 2.5. Ice core subsampling procedure in the cold room at -27°C under a class-100 laminar flow hood at Glaciology Unit ULB (pictures by A. Trevena/D. Lannuzel).

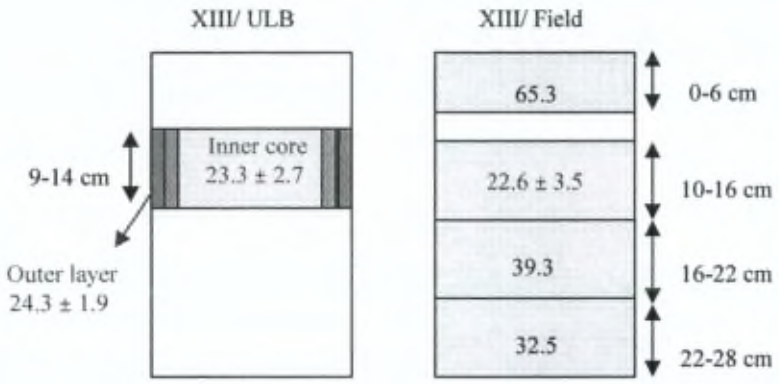

Figure 2.6. Schematic representation of the ice sections processed along the sub-sampling procedure. Total Dissolvable Fe in nM for cores XIII/ ULB (processed at ULB) and XIII/ Field (processed on board the ship).

2.1.4 Sample processing and storage

Inside a shipboard clean laboratory under a class-100 laminar flow hood, sea ice is cut in slices of 6 to 10 cm thick using a titanium coated stainless steel saw (Fig. 2.3d, Lichtert Industry, Belgium). Ice core slices are melted in PE containers and the meltwater was subsequently filtered using a Sartorius polycarbonate filtration device with Teflon O-rings. A gentle pressure of less than 0.3 atm is maintained with a hand pump to avoid the rupture of phytoplankton cells (Goldman and Dennett, 1985). Brine, snow and seawater are filtered on board as well. Membrane filtration (Nuclepore 0.2 µm, 47 mm diameter) operationally separates "dissolved" Fe species from suspended particulate matter. The filtrate (containing dissolved Fe, DFe hereafter) is acidified to pH 1.8 (14M HNO_3, J.T. Baker, Ultrex) at least 24h before being analysed. Total-dissolvable Fe (TDFe, unfiltered) is acidified and stored at pH 1.8 at least 6 months before measurement by Flow Injection Analysis (FIA) to release all but the most refractory Fe species into the dissolved form (Bowie et al., 2004). Filters are kept frozen until total digestion.

Filters are fully digested with 750 µl 12N HCl, 250 µl 14N HNO_3 and 250 µl 40% HF (Ultrex, J. T. Baker) in 15 ml Teflon PFA vials (Savillex) on a Teflon coated hot plate for 12h. The procedure is applied to estuarine and river sediment reference materials (respectively BCR-277 and BCR-320 available from Community Bureau of Reference, Fe indicative values are 45.5 ± 1.1 µg/g and 44.8 ± 1.1 µg/g of sediment) to verify the recovery of the treatment. After drying overnight at 50°C and shaking to homogenise the grains, the

sediment is left to equilibrate to room temperature in a desiccator. 10 to 40 mg is weighed in a 15 ml Teflon PFA vial (Savillex). Then the digestion step is realised by addition of the strong acid mixture and heating on the hot plate overnight. Some 7 to 10 ml of UHP water is subsequently added to the digested sediment sample before measurement of particulate Fe (PFe) by GF-AAS (Varian SpectrAA-300 Zeeman). The results of the recovery test are presented in the section 2.2.

2.2. Analytical techniques

2.2.1. Flow Injection Analysis (FIA)

Recent advances in shipboard flow injection techniques for the measurement of iron in seawater have greatly facilitated the collection of reliable data (Bowie et al., 2003; 2004). Not only can data now be acquired in near real-time mode, but also can contamination problems be quickly identified during sampling campaigns. Most of these methods use luminol chemiluminescence for detection (Obtata et al., 1993; O'Sullivan et al., 1995; Powell et al., 1995; Bowie et al., 1998; de Jong et al., 1998), while some rely on spectrophotometric detection (Sedwick et al., 2000; Weeks and Bruland, 2002). Another characteristic of the Fe-FIA methods used today, is that they nearly all apply on-line preconcentration/matrix separation using resins of 8-hydroxyquinoline (8-HQ) immobilized on a carrier of PVC based polymer (Landing et al., 1986) or alkoxyglass (Obata et al., 1993). Exceptions are the stopped-flow method by O'Sullivan et *al.* (1995) that measures total dissolved Fe directly in the sample, and the FIA applications for analysing reduced Fe (II) directly in ambient seawater in which it is required to measure the sample immediately to prevent loss of any Fe (II) by rapid re-oxidation (Rose and Waite, 2001; Croot and Laan, 2002).

The use of a column packed with 8-HQ resin aims at reaching low detection limits by on-line preconcentration followed by elution in a small volume of dilute acid. It also rejects sea-salts due to its high affinity for transition metals and low affinity for the major ions. Major ions not only would interfere with iron-luminol chemiluminescence, but also would clog the detector flow cell due to precipitation at the optimal high pH of the luminol reaction. The preconcentration technique requires tedious resin synthesis schemes, as well as column set up that can be problematic. Not every attempt to synthesize 8-HQ resin is successful and every new batch of the resin product needs careful characterization of its chromatographic properties and blank levels before it can be brought into use. Various factors control potential

occurrence of backpressure problems, which may lead to limited flow-through and even severe leaking problems. They concern the type of carrier resin (porosity, particle size), the length and diameter of the column, the connectors, the Teflon or polypropylene frits or nylon net to hold the resin in the column, and the flow speed. Another complication associated with 8-HQ resins is that their yield may be influenced by competition between natural organic ligands and the 8-HQ, resulting in underestimations of the concentration. This is especially crucial when standard additions are performed on one seawater sample only and all the others are related to this single calibration. When not using a pre-concentration step, dissolved organic matter can also interfere by absorbing the luminescent signal, competing for radical intermediates or complexing Fe (II) (O'Sullivan et al., 1995). But these matrix interferences can be cancelled out by applying standard addition calibration to every sample.

Luminol (3-aminophtalhydrazide) is well known to produce strong chemiluminescence with Fe or cobalt and, to a lesser extent, with other transition metals. FIA methods for Fe are based on the Fe-mediated chemiluminescent reaction between luminol and O_2 or H_2O_2. During the oxidation of luminol, blue light is emitted and detected by a photon counter. The peak area or peak height of the signal is proportional to the amount of dissolved Fe present in the analyte. The use of O_2 or H_2O_2 depends on whether Fe (II) or Fe (III) is the species of interest (Obata et al., 1993; King et al., 1995). The advantage of the Fe (II) driven chemiluminescence is that the reaction is instantaneous and can take place inside the detector flow cell so that analysis time can be kept short. Peak shapes are sharp and sensitivity is generally high, so that preconcentration volumes and times can be minimised. In the case of Fe (III) driven chemiluminescence, the Fe sample is delayed in a long reaction loop while being mixed with luminol, reaction buffer and H_2O_2 before being introduced in the detector flow cell. This leads to a longer analysis time, smearing of the signal due to wall friction in the flow circuit and lower sensitivity. The latter requires higher preconcentration factors hence higher sample volume. The Fe (II) based methods involve a lengthy reduction step, with for instance sodium sulphite to convert thermodynamically favoured Fe (III) into Fe (II), while the Fe (III) method can measure samples without this preliminary step. All FIA methods for dissolved Fe measurement require that filtered samples are acidified at least 24h before analysis to solubilize the iron, while unfiltered seawater samples for total dissolvable Fe should be kept for several weeks to months at low pH in order to release as much as possible the leachable particulate Fe species.

Our FIA instrument (Figs. 2.7 and 2.8) is an automated continuous flow system (FeLume, Waterville Analytical, USA) that detects chemiluminescence from the reaction of luminol and dissolved Fe (II) by directly injecting a natural water sample from a 1 ml sample loop into the detector flow cell. Sample preparation is adapted from Bowie *et al.* (1998) and O'Sullivan *et al.* (1995). To ensure that all the Fe is in the Fe (II) form, the reductant sodium sulphite (Na_2SO_3) in dilute ammonium acetate (NH_4Ac) solution is added to the acidified sample and allowed to react for 24h before analysis (O'Sullivan et al., 1995). A Valco 10-port selection valve (VICI, Switzerland, not shown in Fig. 2.7) switches between the samples to be analysed. A Valco 10-port injection valve with two 1 ml sample loops switches between load and inject mode. While one loop is being loaded with a sample (240s), the sample already in the other loop is being injected (240s) with a 0.1M HCl carrier into the detector where it mixes with a 0.5 mM luminol - 1M NH_3 ammonia buffer at an optimal reaction pH of 10.1. The detector consists of a 0.3 cm^3 Plexiglas spiral flow cell facing the photon counter (Hamamatsu HC-135). Pump tubing (Tygon), polypropylene reagents straws (Bran and Luebbe) and 1/8" and 1/16" ID teflon FEP tubing (Cole-Parmer) are used to transport reagents and sample to the detector via an 8-channel peristaltic pump (Minipuls 3, Gilson) at a rate of 8 rpm. The flow rates (Fig. 2.7) were optimised to minimize backpressure and to obtain a narrow peak.

Each sample is measured by the method of standard additions (sample plus increasing additions of fresh Fe (II) to three aliquots of the same sample). Each sample solution is measured in triplicate using peak area integrations. One analytical run takes 45 min and requires about 60 ml sample volume.

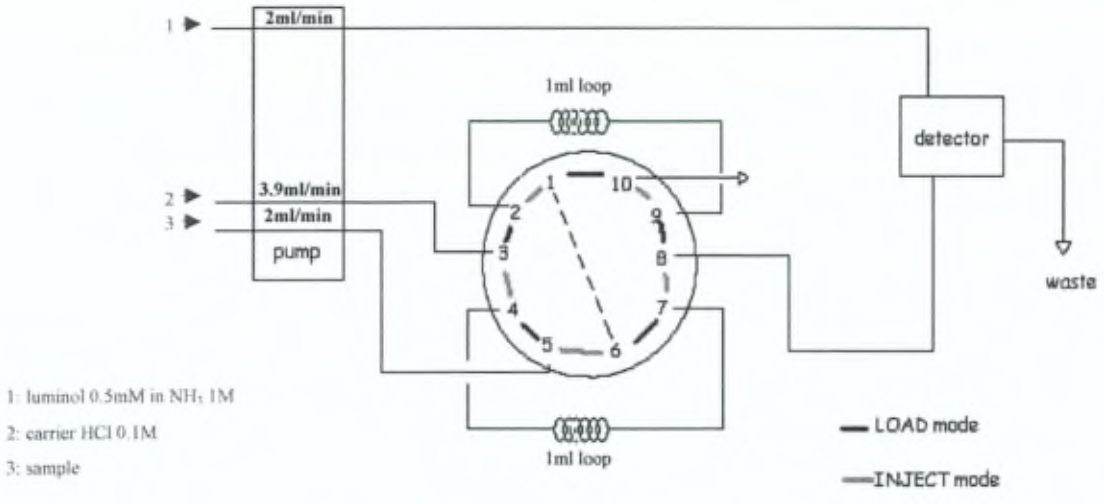

Figure 2.7. Schematic diagram of FeLume. Pump runs at 8rpm.

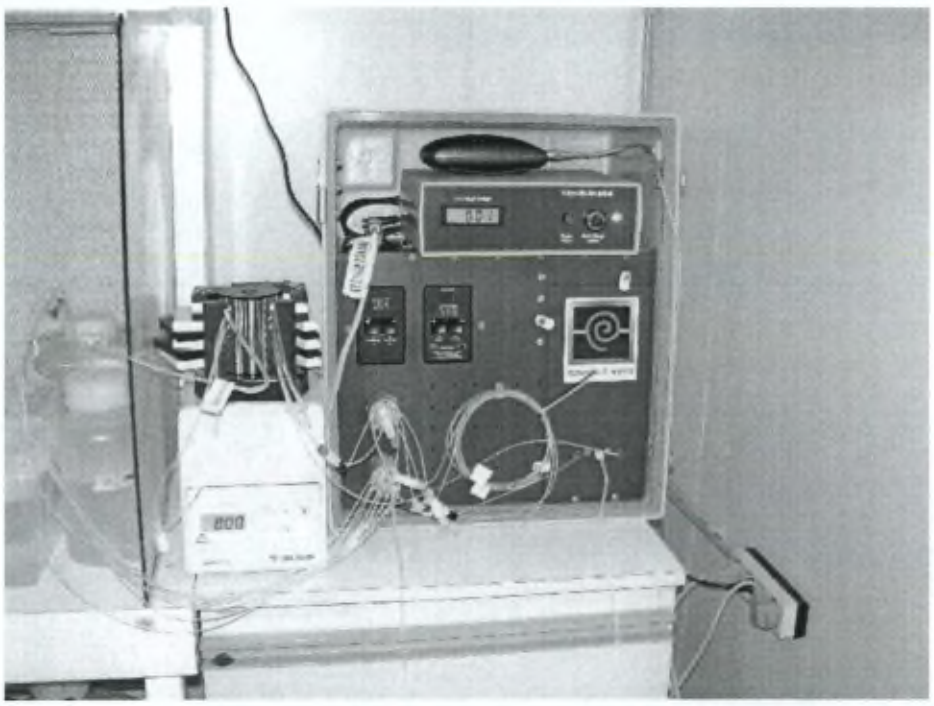

Figure 2.8. FIA instrument (Waterville Analytical) and peristaltic pump (Minipuls, Gilson).

2.2.1.1. Reagents

Acids:

Samples are acidified to pH 1.8 with 14M HNO_3 (J.T. Baker, Ultrex, 100µl per 100 ml sample). 0.1M HCl carrier and 0.2M HCl for Fe (II) working solutions are prepared by appropriate dilutions of 30% HCl (Merck, suprapure) in 1L UHP water. 1M HCl cleaning acid is prepared by diluting 32% HCl (Merck, reagent grade) in UHP water.

Fe(II) standards:

Fe (II) stock solution (4 mM) is prepared by dissolution in 0.2M HCl of 784.28 mg $FeSO_4.2H_2O$ in a 500 ml PE volumetric flask. This solution can be stored for 1 month. Two Fe (II) working solutions (40 µM and 400 nM) are prepared daily by serial dilutions of the stock solution in 0.2M HCl.

Luminol/ammonia buffer 1M NH_3:

One molar NH_3 is prepared by dilution of 73 ml of 25% NH_3 (Merck, reagent grade) in 1L UHP water. Luminol stock solution (10 mM) is prepared by the dissolution of 250 mg K_2CO_3 (Merck, suprapure) and 177 mg luminol (3-aminophtalhydrazide, Fluka) in 100 ml 1M NH_3, followed by ultrasonication for 30min (Bowie et al., 1998). Luminol working solution (0.5 mM) is prepared at least 24h in advance to ensure a stable pH by diluting 25 ml of luminol stock solution in 500 ml 1M NH_3. The luminol powder is used as received and solutions are not further purified.

Ammonium acetate buffer 2M NH_4Ac:

Two molar NH_4Ac buffer is prepared by adding 23.5 ml of 25% NH_3 (Merck, reagent grade) to 11.5 ml of 96% HAc (Merck, reagent grade) and made up to 100 ml with UHP water. The pH is then adjusted to 6.5 by dropwise addition of either NH_3 or HAc. Finally, the buffer is purified by pumping the solution at a rate of 1 $ml.min^{-1}$ through 2 sequential columns packed with Silica gel based-8HQ resin. 0.1M NH_4Ac buffer is prepared by diluting 20 times a 2M NH_4Ac buffer in UHP water.

Reducing agent:

Reducing agent is prepared daily by adding 108 mg Na_2SO_3 (Fluka) in 20 ml of 0.1M NH_4Ac buffer. Complete dissolution is achieved by a 10 min ultrasonicating step. The reducing agent solution is then cleaned by pumping through 2 sequential Si-8HQ columns

prior to its addition to the sample. 75 µl of reducing agent solution is added per 30 ml sample at pH 1.8 and allowed to react for 24h. The final reducing agent concentration in the sample is 100 µM (O'Sullivan et al., 1995).

Si-8HQ resin column set up:

Si-8HQ resin used to purify the reagents (see above) is prepared following the procedure of Hill (1973). Columns are constructed from 5 cm Tygon tube (3.17 mm ID) and filled with Si-8HQ resin by pipetting. Columns are closed at both ends with nylon nets (63 µm porosity) tightly folded to keep the resin in the tube. Polycarbonate connectors (Cole-Parmer) are used and attached to the Tygon tubing with some cyclohexanone solvant (Technilab). Columns are cleaned by passing 1M HCl and UHP water prior and after use.

Metal solutions:

For testing interferences, metal solutions are prepared by serial dilutions in 0.2 M HCl of 1000 ppm standards (Merck, CertiPUR) of $Co(NO_3)_2$, $Ni(NO_3)_2$, $Mn(NO_3)_2$, $Cu(NO_3)_2$, $Cd(NO_3)_2$, $Cr(NO_3)_3$ and $Zn(NO_3)_2$. The reducing agent and freshly prepared Fe (II) are first added to the unfiltered seawater matrix before spiking with other metals.

2.2.1.2. Metal ion interferences

Experiments to examine metal ion interferences were conducted with unfiltered Antarctic seawater from 30 m depth to which 2 nM fresh Fe (II) was added. Individual metal ions (Co (II), Mn (II), Cu (II), Zn (II), Cr (III), Cd (II) and Ni (II)) were then spiked to study possible changes in the Fe (II) signal as a function of the type and amount of metal added. Independent tests were performed on samples at pH 1.8 and at pH 5.3. The latter pH was chosen according to metal interference studies conducted by O'Sullivan et al (1995). The pH of the sample was brought from 1.8 to 5.3 by adding purified 2M NH_4Ac buffer to the sample (1 ml buffer pH 6.5 per 30 ml sample at pH 1.8) 4h prior to analysis by FIA. The 4h delay allows the sodium sulphite in the sample to reduce any Fe (III), which could have formed as a result of the increase of pH (Bowie et al., 1998). An overview of the spike experiment with added concentrations of each metal is given in Table 2.2.

Table 2.2. Response at pH 1.8 and 5.3 of interfering metals in Antarctic seawater from 30 m depth with 2 nM Fe(II) added, normalised to the response of 2 nM Fe(II) in 30 m Antarctic seawater.

% (signal metal added) / (signal Fe)	Metal						
	1.7 nM Co	17 nM Mn	8 nM Cu	20 nM Zn	20 nM Cr	20 nM Cd	20 nM Ni
pH 1.8	108 ± 2	103 ± 6	67 ± 5	113 ± 12	122 ± 4	140 ± 5	121 ± 8
pH 5.3	102 ± 2	96 ± 10	91 ± 13	98 ± 5	99 ± 5	102 ± 4	103 ± 8

Uncertainties represent the standard deviation for n=3 independent analyses.

The addition of 20 nM Zn, Cd, Cr or Ni seems to result in an increased chemiluminescent Fe (II) signal at a sample pH of 1.8, whereas no perturbation was encountered at a sample pH of 5.3 (Table 2.2). No Mn interferences were observed at both pH 1.8 and 5.3. Co (II) did not interfere at sample pH 1.8 and 5.3 when added at similar or lower concentrations as Fe (II). At higher Co (II) concentrations there is an overestimation of Fe (II) signal (e.g.: 146 ± 10% when 3.4 nM added). However, Co (II) is unlikely to interfere since it would be present at picomolar levels in most natural samples (Boyle et al., 1987; Martin et al., 1990; Sanudo-Wilhelmy et al., 2002).

In the case of Cu, an underestimation of Fe was observed with only 67% (± 5%) of the signal recovered at pH 1.8 with an 8 nM Cu addition to 2 nM Fe, whereas at pH 5.3 the yield is 91% (± 13%) of the signal (Table 2.2). This result was confirmed with CASS-3 seawater, measured at both pHs (1.8 and 5.3). This certified reference seawater contains 8.5 nM Cu and 22.56 nM Fe. At sample pH 1.8, the instrument measured 59% (± 3.5%, n=5) of the true value, whereas the results were satisfactory at pH 5.3 (Table 2.2). The reduced Fe signal can be explained by the fact that at pH 1.8, Cu is in its free ionic form and oxidizes Fe (II) present in the sample, which results in a suppression of the signal:

$$Cu\ (II) + Fe\ (II) = Fe\ (III) + Cu\ (I)$$

The Cu (I) formed is oxidized by O_2 at the reaction pH causing a catalytic oxidation of Fe (II) without involving luminol (O'Sullivan et al., 1995). Tests were conducted by adding Cu (II) at different timing prior to and during analysis, however observations were the same independently of the timing of the Cu addition, suggesting that the reaction is probably instantaneous.

An explanation for the absence of positive or negative interference at pH 5.3, could be that the interfering metal ions recombine with the natural organic ligands present in the

sample, which impedes their reaction with Fe (II) or with luminol. The metals we tested for interference are predominantly complexed by organic ligands in natural waters. Another explanation could be that these metals no longer contribute (or at least much less) to luminol chemiluminescence as a result of the pH shift to somewhat higher values inside the flow cell. This would lead to a stronger formation of $Mg(OH)_2$ precipitates, effectively masking these metals.

2.2.1.3. Analytical figures of merit

Sensitivity

The sensitivity of a method can be deduced from the slope of the linear regression line from the calibration curve. Rose and Waite (2001) used a model to study the chemiluminescence of luminol in the presence of Fe (II) and O_2: they obtained a non-linear response, which has been observed by Croot and Laan (2002) as well. In our case, the calibrations show a slight upward curvature which can be fitted with a second order polynomial of the form $y = ax^2+bx+c$. The first derivative of the latter equation, when x approaches x_0, gives the slope of the tangent at the point of abscissa x_0 on the curve. We chose a concentration of x_0 at halfway the standard addition range (e. g.: $x_0 = 2$ when range is 0-4 nM Fe added) where we compared sensitivities.

As can be seen in Table 2.3, one of the consequences of measuring the in-house standard at pH 5.3 is a lower sensitivity by nearly a factor 3. At reaction pH>10, Mg^{2+} precipitates as $Mg(OH)_2$. At sample pH 1.8 and reaction pH of 10.1 there is only a weak formation of precipitates in the flow cell, but at sample pH 5.3 this happens more intensely because the pH shift upon mixing of sample and luminol/buffer is smaller. These magnesium hydroxides can interfere by either scavenging Fe (II) and/or scattering the luminescent emission, which results in reduced signal intensity (O'Sullivan et al., 1995). However, the accuracy of the method is not affected (see in-house value Table 2.3).

Table 2.3. Fe values and sensitivities (slope of the tangent at x_0=2 nM) for n independent calibrations of the in-house standard at pH 1.8 and 5.3.

	In-house value (nM Fe)	Sensitivity (counts/ nM Fe)
pH 1.8 (n=13, 1σ)	1.02 ± 0.09	8661 ± 4227
pH 5.3 (n=4, 1σ)	1.03 ± 0.05	3405 ± 1607

Table 2.4. Fe values and sensitivities (slope of the tangent at x_0=4 nM) for a brine sample salinity 80.1 (TDFe=36.7 nM) diluted 2.5x, 5x and 10x in UHP water.

Salinity	32.0	16.0	8.0
TDFe value (nM) pH 5.3	34.1	35.1	34.7
Sensitivity (counts/nM Fe)	22020	17050	11395

Salinity in samples from the sea ice environment may range from 0 up to 100. Experiments conducted at different salinities exhibited higher sensitivity at higher salinity (Table 2.4). This may be due to an enhancing effect of chloride ions on the chemiluminescence reaction (Bowie et al., 1998).

The age of the luminol and carrier solutions seems to affect also the sensitivity of the instrument. Practically, the sensitivity was improved when using luminol working solution prepared at least 24h before analysis.

Blanks and detection limit

The reagent blank of the FeLume results from the addition to a sample of the following chemicals: (1) HNO_3 (JT Baker, Ultrex) used to acidify the samples, (2) sodium sulphite reducing agent in dilute NH_4Ac buffer and (3) 2M NH_4Ac buffer to change the pH of the sample from 1.8 to 5.3 in order to minimize possible metal interferences. These three reagents were all added in single and double volumes to assess their possible contamination. The Fe content of the added reagents was not detectable. The detection limit (DL) was estimated by repeated analysis of UHP water and calculated as 3σ of the UHP concentration. This was carried out at sample pH 1.8 and pH 5.3. At pH 1.8 the DL is 0.12 ± 0.07 nM (n=12) and at pH 5.3 DL is 0.20 ± 0.08 nM (n=8).

Accuracy and Reproducibility

Certified reference materials CASS-3 (coastal seawater) and NASS-5 (open ocean) available from the National Research Council of Canada, were both measured and results were in good agreement with certified values (Table 2.5). For quality control purpose (monitoring long term stability and accuracy of the FeLume) a low Fe in-house standard that was cross-calibrated with the above reference materials, was measured together with the

samples. Our "in-house" standard is a batch of filtered under-ice seawater from 30 m depth acidified to pH 1.8 with 14M HNO_3 (J.T. Baker, Ultrex). The long-term stability over a period of 5 months was excellent and averaged 1.02 ± 0.07 nM, n=17, 1σ (Table 2.3).

Table 2.5. Results for dissolved Fe (II+III) in certified seawater solutions.

	NASS-5	CASS-3
Certified value (nM Fe)	3.70 ± 0.63	22.56 ± 3.04
FIA value (nM Fe) pH 5.3	3.95 ± 0.61 (n=4, 2σ)	21.99 ± 4.61 (n=5, 2σ) 19.6 (n=1)[a]
FIA value (nM Fe) pH 1.8	3.81 (n=1)	13.22 ± 1.08 (n=5, 2σ)

[a] 3x diluted CASS-3 in MQ (salinity 11.3 after dilution).

2.2.2. *Graphite Furnace Atomic Absorption Spectrometry (GF-AAS)*

2.2.2.1. Principle

The Graphite Furnace Atomic Absorption Spectrometry (GF-AAS, Varian SpectrAA-300 Zeeman) requires smaller sample volumes (typically 5-25 µl per replicate), reduced analytical time (2-3 min per replicate) and is hardly affected by highly saline matrix. The GF-AAS technique is nevertheless less sensitive (typically detection limit yields 1 ppb for Fe) but is convenient for particulate metal determination.

Briefly, the technique is based on:

1) Vaporization followed by an atomization at high temperature of a droplet of the sample deposited in a pyrolytically coated graphite furnace (wall or platform);
2) The free atom of the metal will absorb the light emitted by a lamp (i.e. Fe) at a wavelength characteristic of the element of interest;
3) The amount of light absorbed by the atomized sample is proportional to the concentration of the metal present in the deposited sample;

2.2.2.2. Methods for digested samples (Fe)

Each analytical session starts with several "blank" atomizations of the graphite furnace until an absorbance below 0.015 is reached. The chemical modifier permits the use of a higher ashing temperature. Triplicates of the sample of interest are then atomised and the

contents of the metal of interest are automatically determined via the absorbance and the calibration curve. After 10 analyses, a blank and a reslope (intermediate standard) are processed to assess the stability of the instrument. Furthermore, BCR-320 and BCR-277 reference sediments materials are regularly measured together with blanks to check the recovery of the digestion treatment (Table 2.6).

Table 2.6. Fe indicative (i.e. "theo') and obtained (i.e. "gf-aas") values in µg/g for digested reference sediments diluted 4000x in HNO_3 5%.

	Fe (µg/g) theo	Fe (µg/g) gf-aas
BCR-277 n°2 09/06/06	45.5 ± 1.1	45.3 ± 1.6 (n=2,1σ)
BCR-277 n°12 09/06/06	45.5 ± 1.1	44.6 ± 3.4 (n=2,1σ)
BCR-277 n°2 26/06/06	45.5 ± 1.1	47.5 ± 2.8 (n=8,1σ)
BCR-320 n°12 26/06/06	44.8 ± 1.1	42.8 ± 2.5 (n=6,1σ)

For Fe analysis, a 25 ppb standard (CertiPure®, 1000 ppm stock) in 5% HNO_3 is used and self-diluted with decreasing volumes of 5% HNO_3 to achieve a calibration (e.g. 150-300-450 pg for 5µl sample). The modifier used is a Palladium Chloride (500-2000 ppm, Specpure Alfa), together with a wall graphite furnace (SP012 Spectrotech®, Germany) and the ashing and atomising temperatures are 1100°C and 2500°C respectively.

Chapter 3

Spatial and temporal distribution of Fe in the East Antarctic pack ice

The present Chapter focuses on the distribution of Fe in sea ice and associated snow, brine and underlying seawater collected during the "ARISE in the East" Antarctic expedition (Antarctic Remote Ice Sensing Experiment, voyage AA03-01, September-October 2003, 64-65°S/112-119°E, RV *Aurora Australis*). This work is in press in Marine Chemistry Wollast Memorial Special issue.

Abstract

We have attempted to evaluate the relative importance, compared to other possible sources, of sea ice in supplying Fe to East Antarctic surface ocean waters. Samples of snow, brine, seawater and sea ice were collected and processed for Fe analysis during the "ARISE in the East" Antarctic cruise that took place in September-October 2003 (64-65°S/112-119°E, *RV Aurora Australis*). Total-dissolvable and dissolved Fe (TDFe and DFe respectively) concentrations were measured together with relevant physical, chemical and biological parameters. The most striking feature observed is that TDFe concentrations in sea ice are up to an order of magnitude higher than those measured in the underlying seawater. Moreover, TDFe in sea ice is more concentrated at cold "winter" type stations than at the warm "spring" ones. This probably results from the enhanced ice permeability as spring arrives, which allows brine drainage within the ice cover and renders exchanges with the water column possible. During the melting period, Fe inputs to surface waters from sea ice may represent as much as 70% of the estimated daily total flux into surface seawater when taking into account available data on dust deposition, extraterrestrial Fe, vertical diffusion and upwelling. Our results highlight the potentially important contribution of pack ice to the biogeochemical cycle of Fe in the East Antarctic oceanic Ecosystem.

3.1. Material and Methods

3.1.1. Studied area and sample collection

Samples of sea ice and associated snow, brine and underlying seawater were collected during the "ARISE in the East" Antarctic expedition (Antarctic Remote Ice Sensing Experiment, voyage AA03-01, September-October 2003, 64-65°S/112-119°E, RV *Aurora Australis*). The 6 stations sampled were located in the seasonal sea ice zone in the deep ocean (Fig. 3.1 a and b).

A full description of the sample collection technique for Fe measurement in sea ice is detailed in chapter 2. Briefly, snow was first collected in Polyethylene (PE) containers using polypropylene (PP) shovels. A set of closely spaced ice cores (10-20 cm apart from each other) was then sampled on a uniform, levelled sea ice cover, using an electropolished stainless-steel corer previously tested for trace-metal cleanness in order to assess relevant physical, chemical and biological parameters (temperature, salinity, nutrients and chlorophyll *a*). Cores were stored in acid-cleaned plastic bags at -28°C in the dark until further processing. Access holes ("sack holes") were drilled into the sea ice cover at one or two different depths to allow gravity-driven brine collection (ice levels above or below -5°C threshold when applicable as described by Golden et al., 1998; see 3.2 below). Brines and under ice seawater (0 m, 1 m and 30 m deep) were then pumped up using a portable peristaltic pump (Cole-Parmer, Masterflex E/P) and silicon tubing. Snow and ice sections of 5-10 cm thickness were melted in trace-metal clean PE containers in the dark at shipboard ambient temperature.

3.1.2. Physical and biological parameters

In-situ ice temperatures were measured on site using a calibrated probe (TESTO 720) inserted every 5 or 10 cm along the freshly sampled core. Bulk salinity was determined from conductivity measurement using a WP-84-TPS meter. Vertical ice thin-section photographs taken under polarized light (Langway, 1958) indicated ice crystalline shapes and were used as an indicator for ice texture (e.g. columnar vs. granular).

Sea ice sections for chlorophyll *a* (Chl *a*) determination were melted in seawater filtered through 0.2 µm filters (1:4 volume ratio) to avoid cell lysis by osmotic shock. Chl *a* was quantified fluorimetrically following Yentsch and Menzel (1963) after 90% v:v acetone

extraction of the particulate material retained on glass-fibre filters (Whatman GF/F) for 12 h at 4°C in the dark.

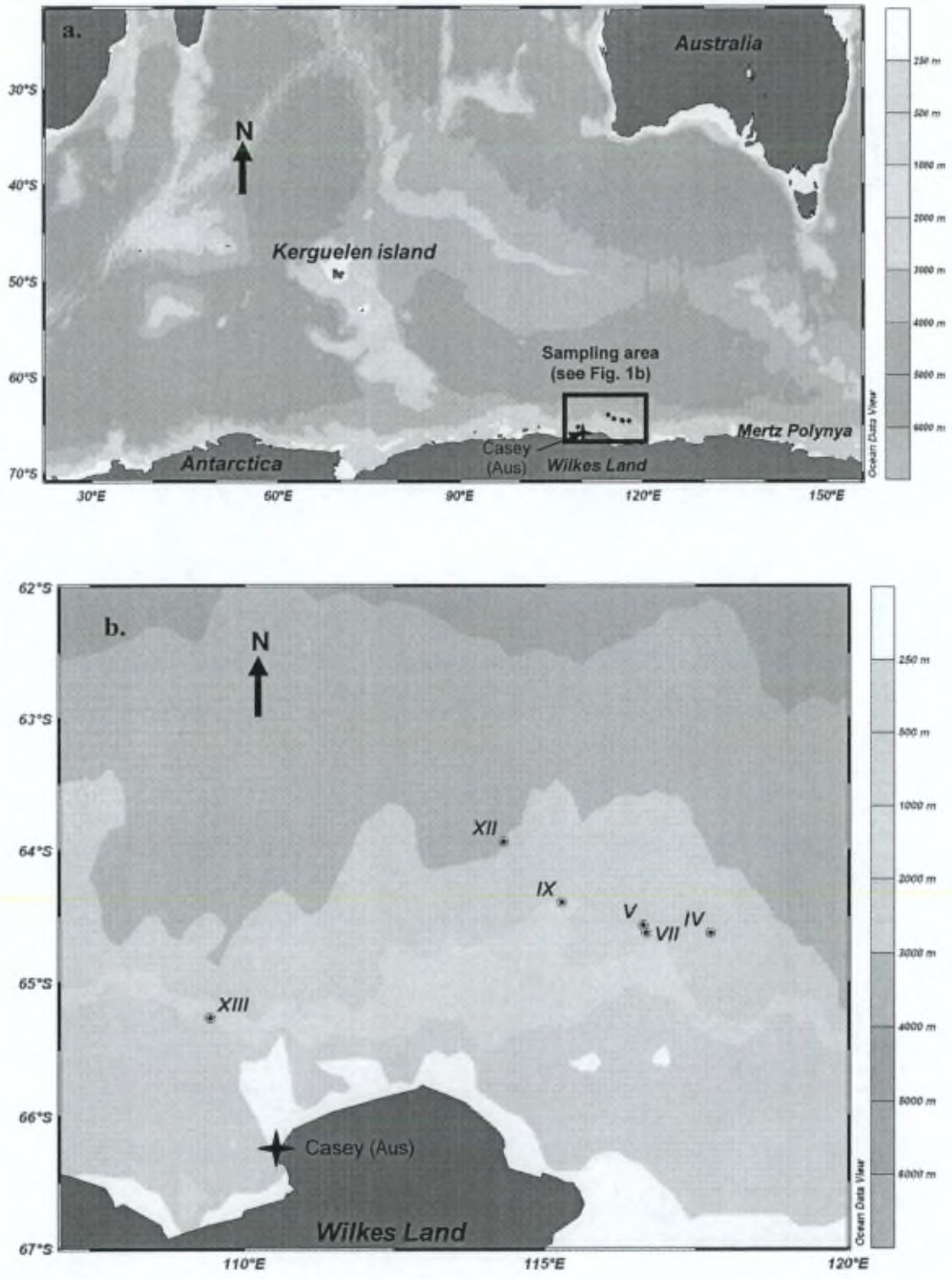

Figure 3.1. Maps of the sampling area in the East Antarctic sector (Schlitzer, R., Ocean Data View, http://www.awi-bremerhaven.de/GEO/ODV, 2005).

3.1.3. Iron

Seawater, brine, and melted snow and sea ice samples dedicated for analysis of various Fe fractions were processed onboard the ship. All labware was acid-cleaned according to the procedure described in Chapter 2. Total-dissolvable Fe (TDFe, unfiltered) was stored at pH 1.8 (addition of 100 µl 14M HNO_3, J.T. Baker, Ultrex for 100 ml of sample) for a period of at least 6 months before Fe measurement by flow injection analysis (FIA), which should dissolve all but the most refractory Fe species. The dissolved Fe fraction (DFe) was collected after filtration through 0.2 µm pore Nuclepore Polycarbonate (PC) membrane filters, mounted on Sartorius PC filtration devices equipped with Teflon O-rings. The filtrate was acidified to pH 1.8 with 14M HNO_3 (J.T. Baker, Ultrex) at least 24 h prior to analysis. We adapted a FIA technique (FeLume, Waterville Analytical) to measure TDFe and DFe concentrations in our samples without a pre-concentration step. Details of the analytical procedures are described in Chapter 2. Analysis of reference material NASS-5 and CASS-3 gives a good agreement with the certified values and detection limit (3σ of the blank) is on average 0.12 nM (cf. Chapter 2; Lannuzel et al., 2006). Particulate-dissolvable Fe (PDFe) refers to the difference in concentration between TDFe and DFe.

3.2. Results

3.2.1. Ice texture

Sea ice thickness at our selected sampling sites ranged from 0.3 m (station XIII) to 0.8 m (station V) thickness. Thin section observations reveal a typical pack ice structure, with snow ice and/or frazil ice, underlain by congelation ice (Fig. 3.2). Station IV apparently underwent a similar genesis as station IX, with about 15 cm of frazil ice growing then into columnar ice (~30 cm). Both stations V and VII show a thick snow ice layer (~20 cm deep) with contrasted snow metamorphism, then a frazil ice layer followed by a columnar structure. Stations XII and XIII display a somewhat more complex sequence of genesis, probably involving rafting. This is suggested by the repeated occurrence of bent columnar crystals at station XII and the "flattened" frazil ice crystals in the lower part of the core XIII (Fig. 3.2). Stations IV, V, VII and IX are located at the same latitude (64.3°S), whereas stations XII and XIII are located at 63.6°S and 65.2°S, respectively (Fig. 3.1).

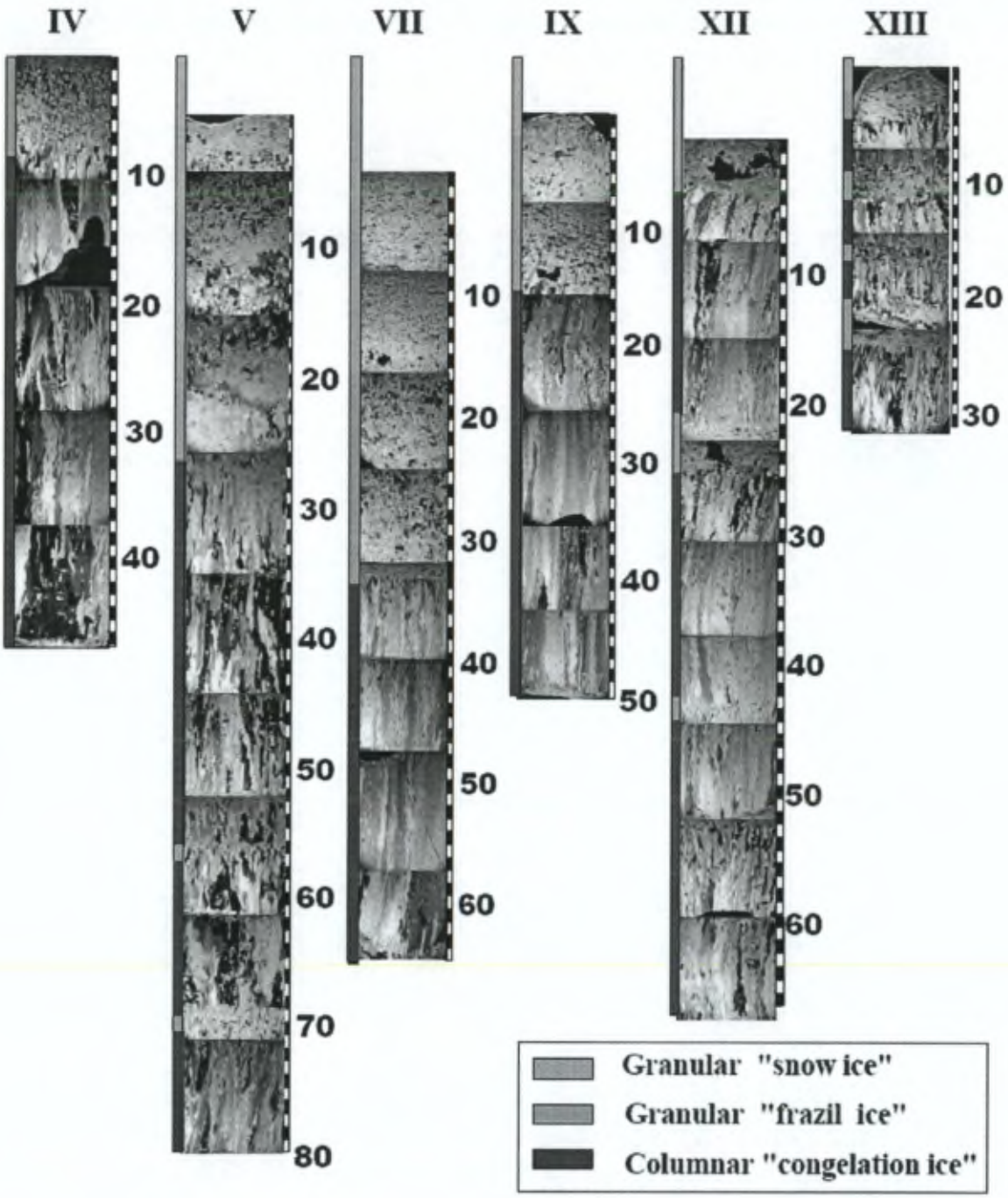

Figure 3.2. Ice textures from vertical thin sections, viewed under crossed polarizers, of ice cores for each stations. Depths have been adjusted so that snow thickness is taken into account.

3.2.2 Temperature, bulk ice salinity, brine volume and Chl a profiles

In sea ice, the upper layer is colder than the bottom layer because of the relatively low air temperature compared to underlying seawater. Sea ice indeed exhibits a marked transition in its fluid transport properties at a brine volume fraction of about 5%, which roughly corresponds to a -5°C ice temperature at a bulk ice salinity of 5 (Golden et al., 1998). For brine volume fractions higher than 5%, brine inclusions become interconnected and can carry heat and nutrients through the ice, whereas for lower porosities the ice is impermeable. Golden et al. (1998) referred this threshold behaviour as the "law of fives".

Temperature profiles allow a possible classification of our stations in terms of the thermal stages (Fig. 3.3a). Station IV had the coldest ice, with its upper half exhibiting the lowest ice temperatures. Then ice at stations VII, XII and XIII appeared to be in a later seasonal stage compared to station IV, as ice temperatures were slightly higher in the upper half of the ice cover. Finally, both stations V and IX showed a warmer regime as most of the ice cover was above -5°C.

Most stations exhibited the typical C-shaped bulk salinity profile described in many other field studies devoted to sea ice (e.g. Nakawo and Sinha, 1981; Weeks and Ackley, 1986; Eicken, 1992; 1998) (Fig. 3.3b). Higher salinities at the top result from enhanced initial entrapment under faster growth rates, brine expulsion upwards on cooling, and eventually seawater infiltration in snow ice, later in the season. Lower salinities in the middle levels reflect enhanced salt rejection after initial entrapment under slower growth rates and brine drainage, whilst higher salinities in the warmer bottom layers result from higher porosities and lack of brine drainage in the fragile skeletal layer. Sea salts tend to be more easily trapped in surface frazil ice because of its rapid formation (a few hours to a few days, depending on air temperature), whereas congelation ice forms slowly (weeks to months) and expels salts more efficiently. This contrast supports the previous assumption of ice rafting at station XII, which shows the repetition of such a sequence with depth.

The evolutionary stages described from the various temperature profiles are also shown in the calculated brine volume fraction (Vb/V = Brine volume/Bulk ice volume; Eicken, 2003) profiles (Fig. 3.3c). This variable is of critical importance since brine drainage within the ice towards the underlying water can be regarded as a key physical process for Fe transfer. Station IV clearly shows Vb/V < 5% in the upper ice column because cold ice temperature favours smaller brine volumes and higher brine salinity. On the contrary, the

lower section of this core indicates increased porosity and permeability (Vb/V being > 5%), and possible exchanges with underlying seawater. In contrast, ice porosity at stations V, VII and IX was considerably higher, with brine volumes typically being ≥ 5% along all cores. Stations XII and XIII displayed a somewhat intermediate profile in the upper half of the ice cover. One should bear in mind that air temperature, ice thickness and texture, snow cover and solar irradiance all contribute to the control of ice temperature, salinity and permeability. Within a few hours, meteorological conditions may act together and affect the brine volumes at different locations along the core. It is thus not surprising that the complex interplay between different physical properties renders a clear seasonal characterization for all stations difficult, especially in the spring.

Chl *a* profiles indicate that maximum values (i.e. from 9.1 to 34.2 μg/l) are systematically located in the lower portions of the ice at all stations (Fig. 3.4). Algal biomass is however also observed at other levels in the cores of stations V, VII and IX. This probably reflects increased ice permeability at these stations, supplying major nutrients from seawater and possibly Fe from the sea ice, in addition to improved light conditions.

In light of the physical parameters and Chl *a* profiles, stations V and IX can be regarded as typical "spring" stations, as revealed by ice temperatures > -5°C and brine volume fractions > 5% throughout the ice cover. The latter physical characteristic allows vertical ice-water exchanges, and thus algal development along the entire core (Fig. 3.4). Note that in the case of station V, one cannot preclude snow ice formation (i.e. seawater infiltration into the snow pack) as an efficient process for initial algal "seeding" and major nutrients enrichment of the top ice layer. In contrast, station IV is more likely a "winter" type station. Figure 3.3 (a-c) demonstrates that the ice is impermeable to brine exchange in the upper part of the ice cover, therefore preventing algal development in the upper ice (Fig. 3.4). Stations VII, XII and XIII exhibit a transitional regime, with the upper 30 cm of stations XII and XIII still reflecting low permeability.

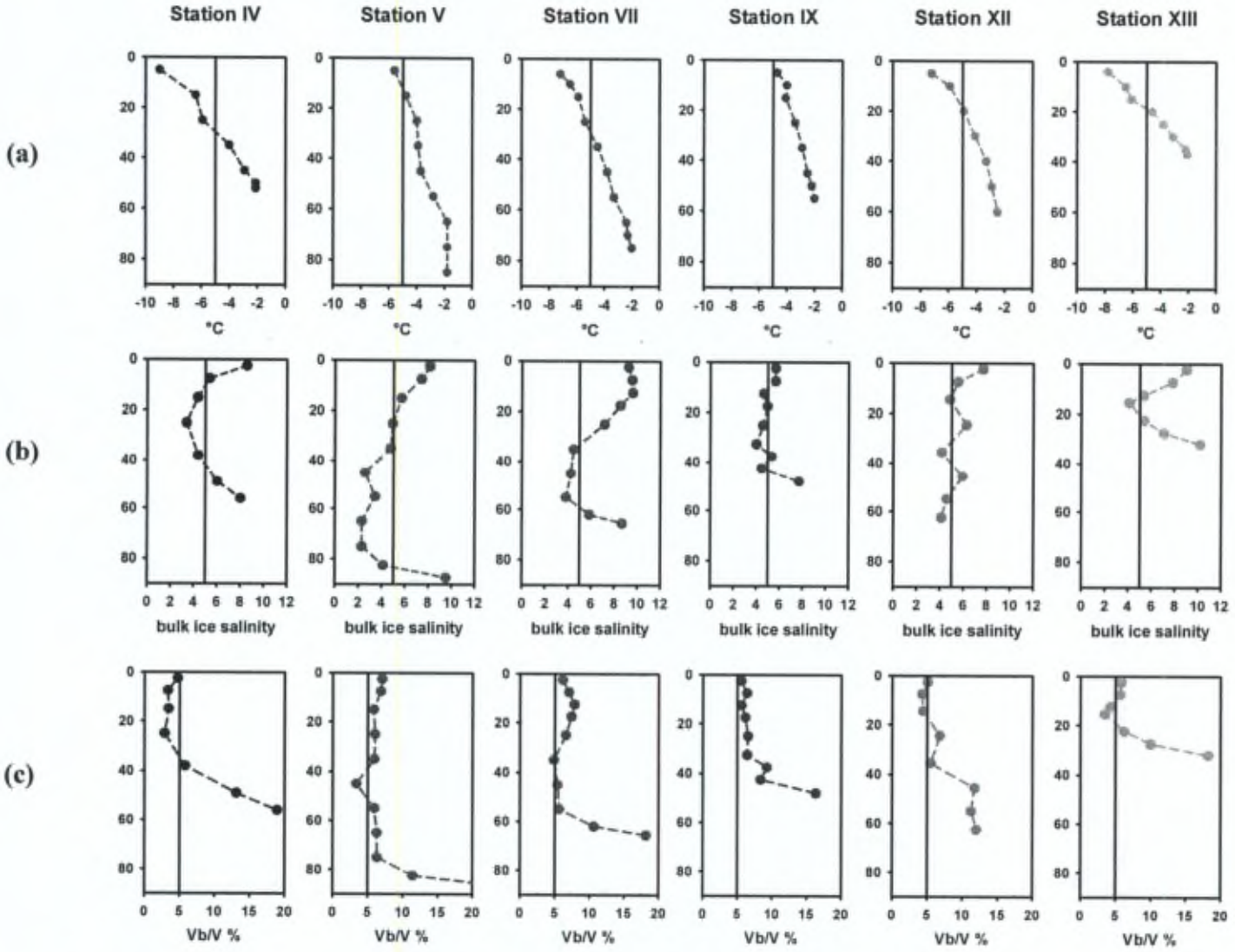

Figure 3.3. Sea ice profiles of (a) temperature (°C) , (b) bulk ice salinity, and (c) brine volume fraction percentage (Vb/V) as a function of depth (cm). Solid vertical lines represent respectively in (a) the -5°C isotherm, (b) the salinity 5 threshold and (c) the 5% brine volume threshold.

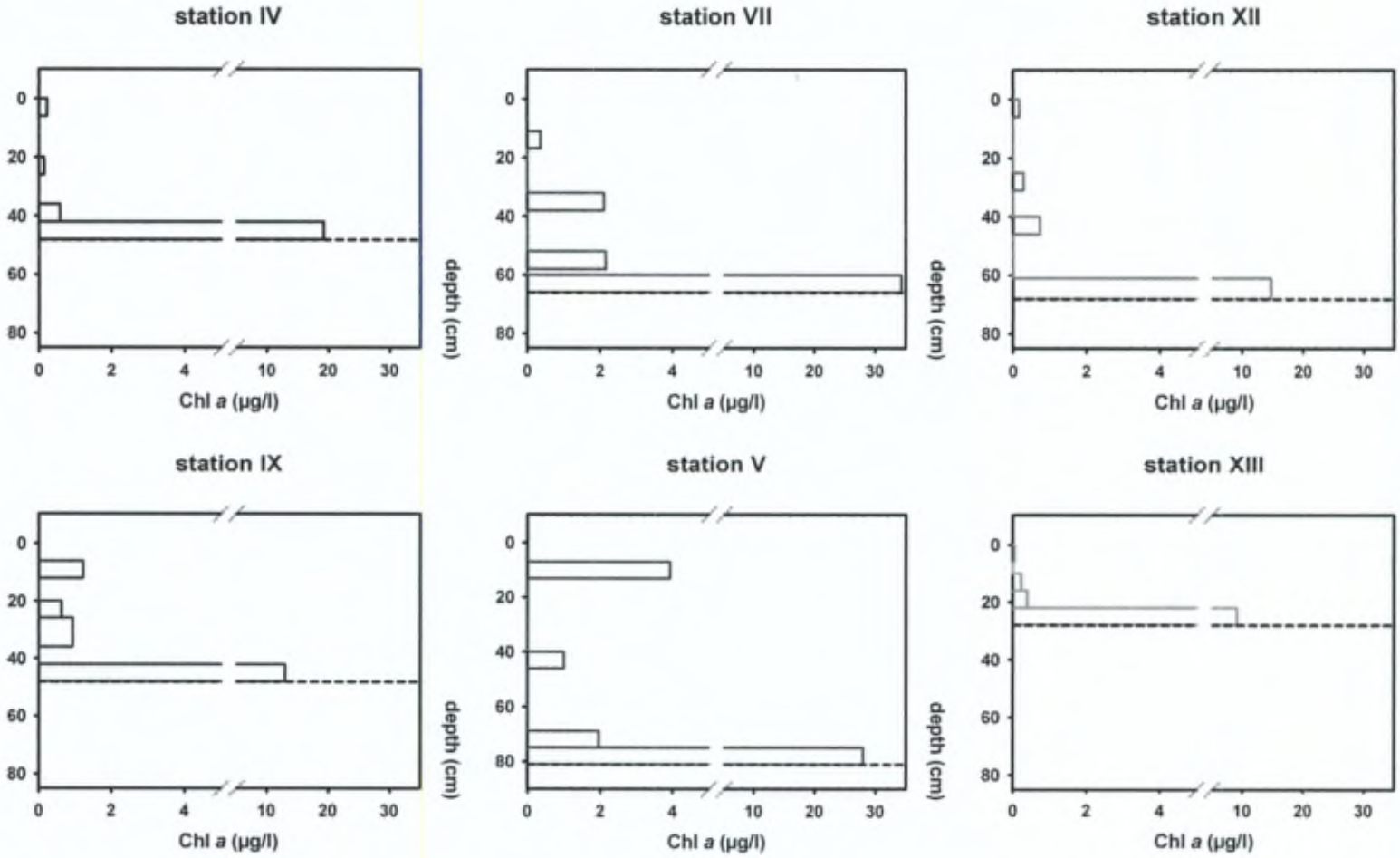

Figure 3.4. Cholophyll *a* (Chl *a* in ug/l) distributions in 4 sea ice sections 6-10cm thick along the ice cores.

3.2.3. Spatial and temporal distribution of Fe

Figures 3.5, 3.6 and 3.7 show the profiles of TDFe, DFe and PDFe in our East Antarctic pack ice cores (bars), including surface snow (dashed bars). "Sack hole" brine (> -5°C and < -5°C when present) concentrations are indicated by solid vertical lines.

Our results tend to show relatively high Fe contents in the sea ice compared to under-ice seawater (Table 3.1). Generally, sea ice and brines exhibit the highest Fe levels, followed by snow. These three media are more concentrated in Fe than the underlying seawater. The ranges are: 3.3-65.8 nM TDFe and 2.6-26.0 nM DFe in sea ice, 6.0-28.9 nM TDFe and 4.7-25.5 nM DFe in brines, 1.8-23.7 nM TDFe and 1.0-6.5 nM DFe in snow, and 1.2-3.8 nM TDFe and 1.1-4.5 nM DFe in under-ice seawater. Seawater contains a major DFe fraction that is higher compared to the sea ice, as reflected by DFe percentages of 78 ± 23% (1σ, n=15) in seawater and 60 ± 32% (1σ, n=24) in sea ice.

On the whole, station IV exhibits higher levels of TDFe, DFe and PDFe in sea ice, brines and snow compared to other sampled stations (Figs. 3.5, 3.6 and 3.7). Based on the data collected at 4 levels along the core, we vertically integrated the concentrations of TDFe, DFe and PDFe per core at each station. This provides an estimate of a mean bulk concentration of Fe in ice at each station (Table 3.2). The mean TDFe bulk concentration estimated for station IV is the highest at 48.9 nM, followed by stations XIII and IX, where average integrated TDFe concentrations are 40.7 and 24.0 nM respectively. The averaged integrated bulk concentrations of Fe (1σ standard deviation) estimated in sea ice for all stations investigated are respectively 25.7 ± 15.8 nM TDFe, 10.7 ± 4.6 nM DFe and 15.0 ± 12.8 nM PDFe.

In the same ice core, the Fe concentration measured in cold shallow brine is typically higher than in warm deep brine; for example, TDFe at station VII is 28.9 nM at 20 cm and 10.4 nM at 45 cm sampled depths (Table 3.1). Another notable feature is that most of the Fe in the brines is in the dissolved phase, as can be observed at station XIII, where DFe and TDFe are 14.1 nM and 14.6 nM at 15 cm depth. As a result, DFe represents on average 78 ± 14% (1σ, n=9) of TDFe in brines. Both brines and seawater therefore exhibit a high DFe percentage of TDFe, as compared to sea ice.

Finally, Fe levels in snow are relatively low, with a somewhat higher value at "winter" station IV (Table 3.1); concentrations of TDFe range from 1.8 nM (station XIII) to 23.7 nM (station IV). Dissolved Fe is on the average 56 ± 26% (1σ, n=6) of TDFe in the snow.

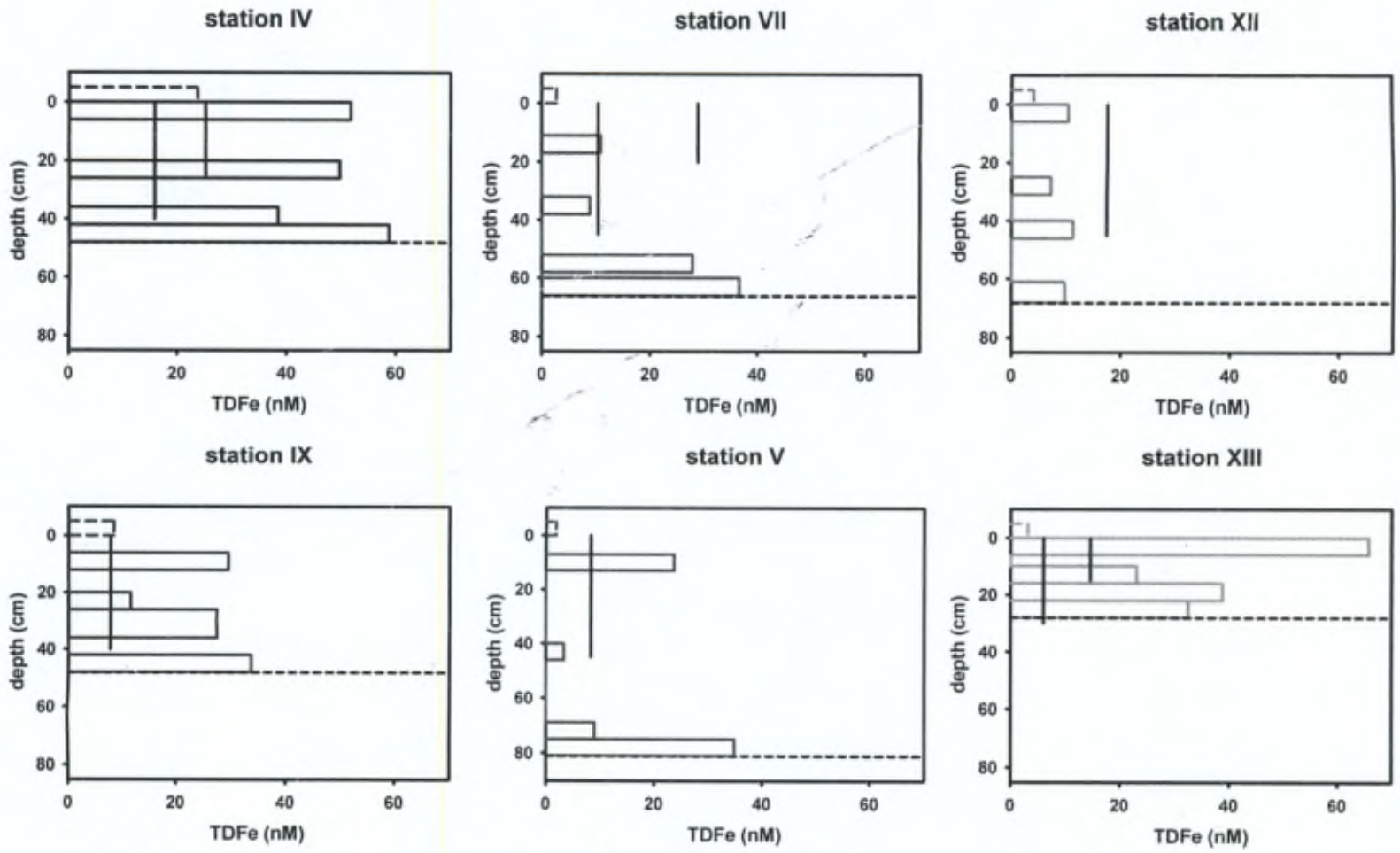

Figure 3.5. Distribution of total-dissolvable Fe (TDFe in nmol/l, unfiltered, pH 1.8) in East Antarctic pack ice cores. Surface snow concentration is indicated by dashed bars. "Sack hole" brine (> -5°C and < -5°C when present) concentrations are shown by solid vertical lines. The dashed horizontal line represents the ice-water interface.

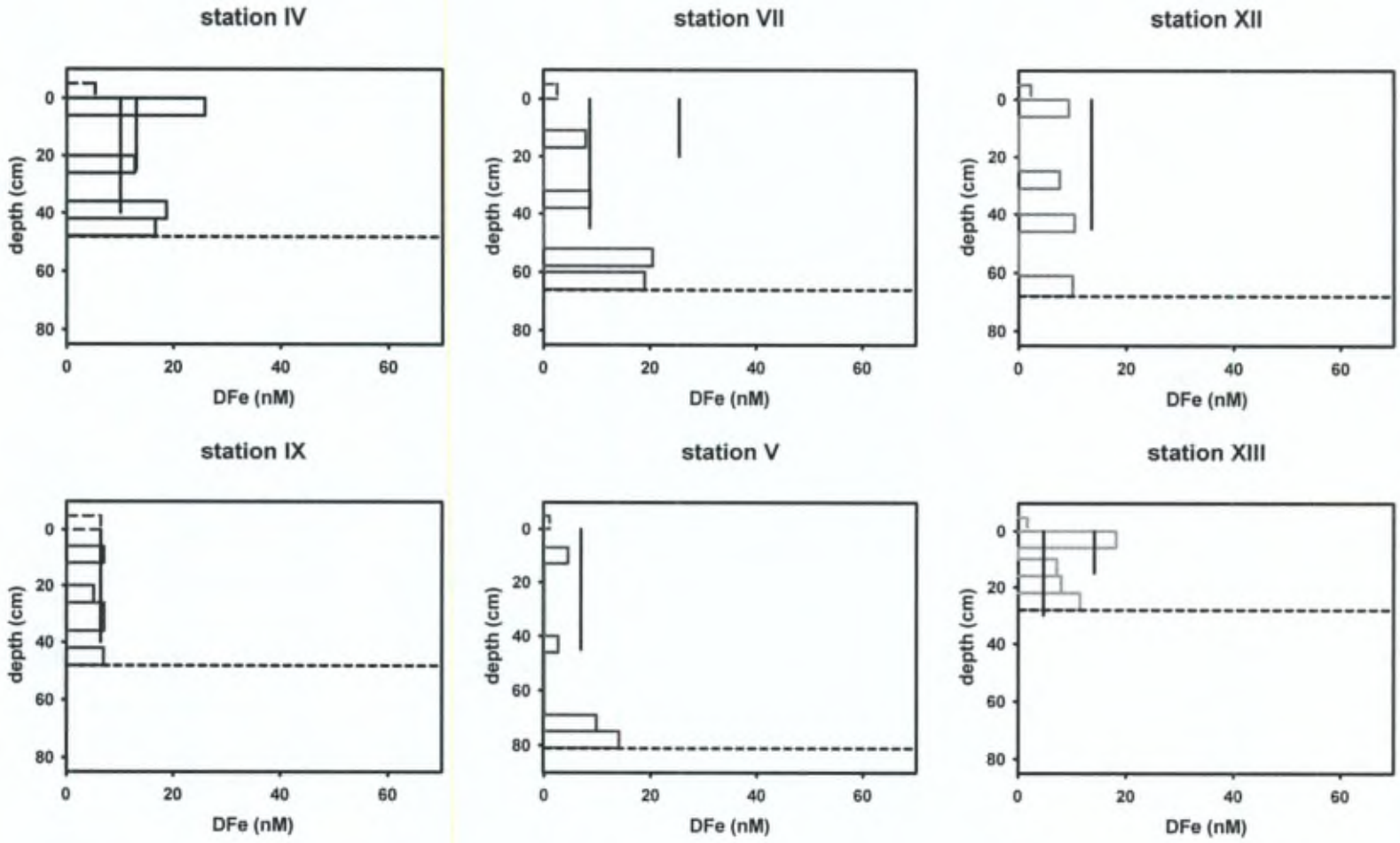

Figure 3.6. Distribution of dissolved Fe (DFe in nmol/l, filtered on 0.2µm, pH 1.8) in East Antarctic pack ice cores. Surface snow concentration is indicated by dashed bars. "Sack hole" brine (> -5°C and < -5°C when present) concentrations are shown by solid vertical lines. The dashed horizontal line represents the ice-water interface.

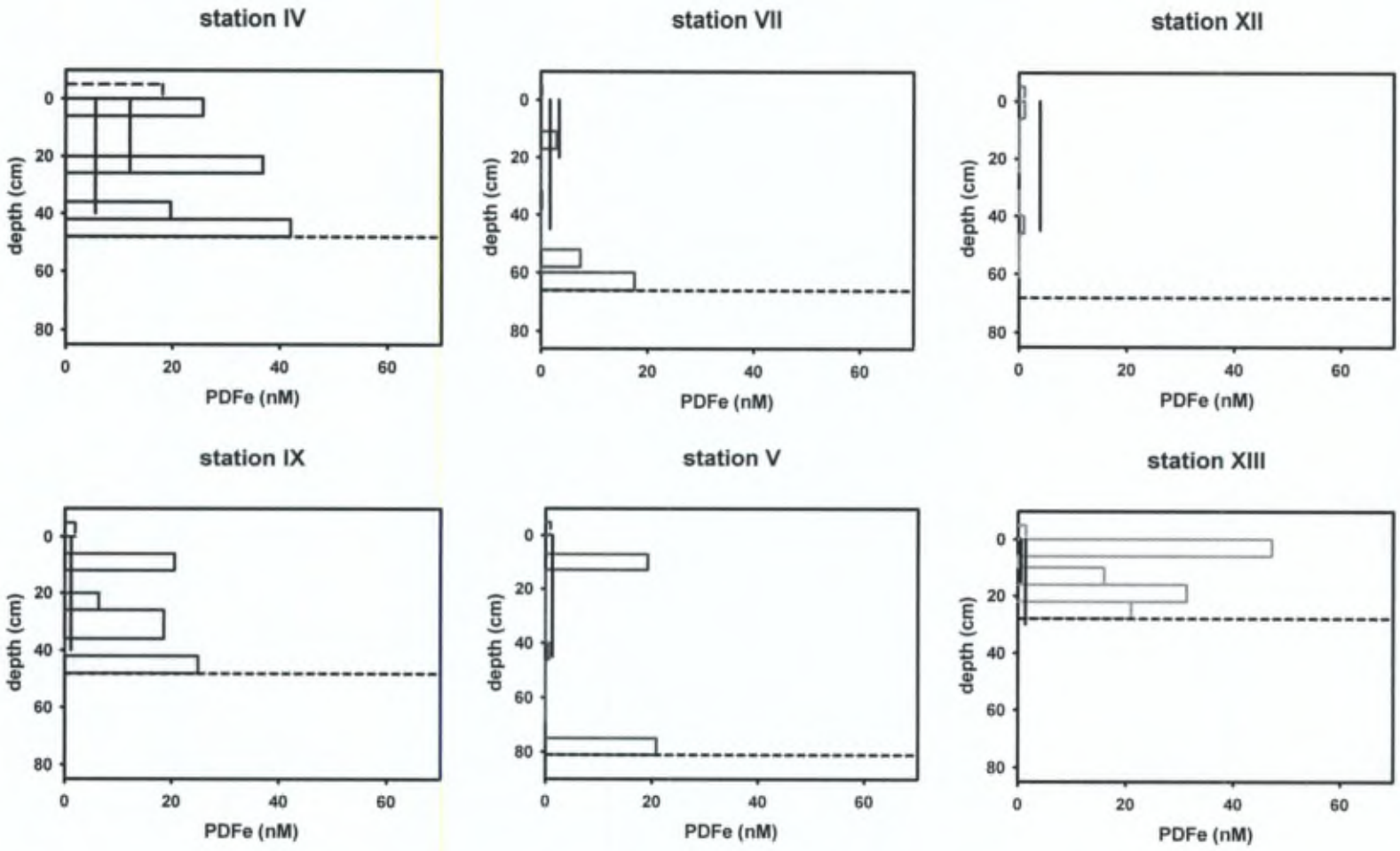

Figure 3.7. Distribution of particulate-dissolvable Fe (PDFe in nmol/l) in East Antarctic pack ice cores. Surface snow concentration is indicated by dashed bars. "Sack hole" brine (> -5°C and < -5°C when present) concentrations are shown by solid vertical lines. The dashed horizontal line represents the ice-water interface.

Table 3.1. TDFe, DFe and PDFe (all in nM), temperature (in °C) and salinity at the visited stations. The sampling date and location are also indicated for each site, in addition to media, sampling depths and sea ice textures.

		Depth	ice texture	T°	salinity	TDFe	DFe	PDFe
station IV	snow					23.7	5.4	18.3
01-oct-03	Sea ice	0 - 6 cm	frazil	-8.9	8.6	51.8	26.0	25.8
64°37.7 S		20 - 26 cm	columnar	-5.9	3.6	49.8	12.9	37.0
117°44.5 E		36 - 42 cm	columnar	-3.7	4.4	38.5	18.8	19.7
		42 - 48 cm	bottom	-3.0	6.0	58.8	16.7	42.1
	brine	0 - 25 cm		-8.2	103.5	25.2	13.1	12.1
		0 - 40 cm		-6.0	89.9	15.8	10.1	5.6
	seawater	0 m			34.3	3.0	2.4	0.5
		1 m			34.3	2.7	2.4	0.3
		30 m			34.3	1.4	1.1	0.2
station V	snow					1.8	1.0	0.9
07-oct-03	Sea ice	7 - 13 cm	snow ice	-5.2	6.6	23.7	4.5	19.2
64°34.0 S		40 - 46 cm	columnar	-3.5	3.1	3.3	2.6	0.6
116°37.8 E		69 - 75 cm	columnar	-1.9	2.3	8.9	9.8	[a]
		75 - 81 cm	bottom	-1.8	3.3	34.9	14.1	20.8
	brine	0 - 45 cm			78.6	8.2	6.9	1.3
	seawater	0 m			34.3	3.0	1.3	1.7
		1 m			34.2	2.3	1.3	1.0
Station VII	snow					2.7	2.6	0.1
09-oct-03	Sea ice	11 - 17 cm	snow ice	-6.2	9.1	10.9	8.0	2.9
64°38.0 S		32 - 38 cm	columnar	-4.7	4.5	8.9	8.8	0.1
116°40.7 E		52 - 58 cm	columnar	-3.2	3.8	27.9	20.5	7.4
		60 - 66 cm	bottom	-2.7	7.3	36.6	19.0	17.6
	brine	0 - 20 cm			89.1	28.9	25.5	3.4
		0 - 45 cm		-6.7	80.1	10.4	8.7	1.7
	seawater	0 m			34.2	2.0	1.1	0.9
		1 m			34.2	2.9	1.9	1.0
station IX	snow					8.4	6.5	1.9
11-oct-03	Sea ice	6 - 12 cm	frazil	-4.3	5.2	29.5	8.0	21.5
64°24.1 S		20 - 26 cm	columnar	-3.6	4.7	11.5	4.8	6.7
115°17.5 E		36 - 42 cm	columnar	-2.8	4.9	27.6	7.1	20.5
		42 - 48 cm	bottom	-2.4	6.1	33.8	7.0	26.8
	brine	0 - 40 cm		-2.8	61.5	7.6	6.4	1.1
	seawater	0 m			34.3	1.9	1.7	0.2
		1 m			34.3	3.3	1.9	1.4
		30 m				2.1	1.7	0.4
Station XII	snow					4.1	2.3	1.8
14-oct-03	Sea ice	0 - 6 cm	snow ice	-6.7	7.7	10.3	9.3	1.0
63°56.2 S		25 - 31 cm	columnar	-4.7	5.2	7.2	7.6	[a]
114°19.4 E		40 - 46 cm	frazil/column	-3.4	5.9	11.3	10.4	0.9
		61 - 68 cm	bottom	-1.9	4.1	9.8	10.0	[a]
	brine	0 - 40 cm		-3.8	63.0	17.4	13.5	3.9
	seawater	0 m			34.2	2.2	2.1	0.1
		1 m			34.2	3.8	4.5	[a]
Station XIII	snow					3.1	1.7	1.4
20-oct-03	Sea ice	0 - 6 cm	frazil/column	-7.9	9.0	65.8	18.1	47.6
65°16.1 S		10 - 16 cm	frazil/column	-6.1	5.3	23.1	7.2	15.9
109°27.8 E		16 - 22 cm	frazil/column	-5.1	4.7	38.8	8.0	30.8
		22 - 28 cm	bottom	-4.0	6.2	32.5	11.5	21.0
	brine	0 - 15 cm		-6.0	93.7	14.6	14.1	0.5
		0 - 25 cm		-4.2	88.0	6.0	4.7	1.4
	seawater	0 m			34.3	2.1	1.5	0.6
		1 m			34.3	1.7	1.4	0.3
		30 m			34.3	1.2	1.3	[a]

[a] not detectable within measurement error

Table 3.2. Estimated averaged bulk concentrations (in nM) of total-dissolvable Fe (TDFe), dissolved Fe (DFe) and particulate-dissolvable Fe (PDFe).

stations	TDFe (nM)	DFe (nM)	PDFe (nM)
station IV	48.9	18.3	30.6
station V	13.5	5.6	7.9
station VII	17.7	13.1	4.6
station IX	24.0	6.7	17.3
station XII	9.5	9.3	0.3
station XIII	40.7	11.4	29.2

3.3. Discussion

3.3.1. Distribution and biogeochemical behaviour of Fe

3.3.1.1. Sea ice, seawater and snow

Patchiness can be a recurrent factor within the same ice floe (Eicken et al., 1991). Sea ice is indeed a highly dynamic and heterogeneous medium in terms of thickness, texture, nutrients distribution, gas content, light penetration, biological activity and probably Fe distribution. As we present here a spatial study of cores collected on different ice floes, it is important to compare stations exhibiting similar ice structure. Hypothetically, stations IV, V, VII and IX, which are located at the same latitude and similar water depth, should have received similar Fe inputs from atmospheric deposition and advection from the continent shelf. Ice at station XII (farther from the coast) and station XIII (closer to the coast) probably reflect rafting processes; it is therefore difficult to assess whether stations XII and XIII received the same external Fe inputs as stations IV, V, VII and IX. Based on similarities in ice textures, we thus compare here below station IV to station IX, station V to station VII, and finally stations XII to XIII.

Station IV clearly shows high DFe and TDFe contents in the sea ice compared to station IX. This is probably due to the difference in the stage of seasonal ice evolution. Station IV can be associated with "winter" type ice in terms of ice temperature, brine volume and Chl *a* profiles (Fig. 3.3 a-c). In contrast, station IX ice demonstrates "spring" type features, which could favour brine drainage and Fe transfer from the ice pack to the water

column below. Besides thermodynamic controls, biological activity is likely to have a strong impact on Fe distribution in the sea ice environment. In nutrient-replete Antarctic waters, light conditions are improving in spring and Fe may become available from the sea ice as it starts to melt. All environmental conditions are then met to favour an algal bloom. Although internal melting has probably occurred, lower DFe and relatively high PDFe concentrations in sea ice at station IX together with increases in Chl *a* levels suggest biological uptake of Fe within the ice (see Table 3.1 and Fig. 3.5). Decreases in major nutrient concentrations throughout the ice core between the winter and spring type stations were also observed (ranges for stations IV and IX are respectively: 0.4-14.4 μM and 0.4-5.65 μM NO_3^-, 1.3-12.8 μM and 2.2-10.2 μM $Si(OH)_4$, and 0.04-10.4 μM and 0.03-4.0 μM PO_4^{3-}; data not shown). This comparison is valid only if the two stations had similar initial inventory; a situation that is likely since similar ice structures suggest similar sea ice history, and thus similar Fe accumulation processes.

In the same way, station VII can be regarded as a colder station with regard to station V (see temperature profile in Fig. 3.3a). Chl *a* profiles (Fig. 3.4) and apparent DFe "drawdown" (Table 3.2) support the idea that station V is in a later stage of the seasonal ice evolution compared to station VII.

Stations XII and XIII both underwent a perturbed genesis as revealed by the succession of frazil and congelation ice sections which lead to strong differences in thickness and probably age. Comparisons of Fe distributions between these two stations are therefore difficult, as we cannot assume that initial Fe stocks were similar. Note, however, that station XII shows a larger proportion of ice with increased permeability, suggesting that it is in a later seasonal stage as compared to station XIII. Levels of PDFe in brine at station XII are amongst the highest measured for our sites, suggesting that Fe release via brine channels had occurred.

To summarize, comparisons of station IV with station IX, station VII with station V, and station XIII with station XII suggest that, as the spring progresses, both ice melting and biological activity are important processes in controlling the distribution and speciation of Fe in the sea ice.

The inferred release of Fe from the ice pack as spring progresses is not obvious from the seawater Fe profiles. This may reflect rapid scavenging, vertical mixing and/or diffusion below the ice, both leading to Fe removal from the upper water column and transfer to deeper

water. Seawater Fe concentrations are nevertheless relatively high compared to levels usually encountered in ice-free surface waters (e.g. 0.05-0.3 nM DFe, de Jong et al., 1998; 0.1 nM DFe, Bowie et al., 2001).

Reported Fe concentration levels in snow from previous studies suggest that this medium could potentially contribute to the high Fe values observed in sea ice and underlying seawater (Westerlund and Öhman, 1991; Löscher et al., 1997; Edwards, 2000). However, the snow sampled at our locations did not, in general, exhibit Fe concentrations as high as those observed in sea ice, reflecting possibly the remoteness of our study area with respect to dust sources, compared to other investigated sites. Our snow TDFe values are consistent with other published data for the East Antarctic sector, ranging from 1.2 to 31.7 nM (Edwards and Sedwick, 2001). Long-term deposition of aerosol Fe could be responsible for the high Fe values in the sea ice topmost layers, with the low ice temperature in the upper half of the sea ice cover preventing transfer of this surface enrichment to the lower levels via the brine system (e.g. station IV).

3.3.1.2. Brines

Concentrations of TDFe and DFe in sea ice were up to two orders of magnitude higher than in typical Antarctic seawater. When seawater freezes, sea-salts are expelled together with other impurities (e.g. gases, particles) into the brine system and the water below (Eicken, 1998). In this context, and given the mean calculated brine volumes at our stations (Vb/V = 3-27%, Fig. 3.3c) the TDFe and DFe concentrations should be about 4 to 33 times higher in brine than in bulk sea ice. However, we observed similar levels in both media. A potential explanation for this apparent discrepancy is that the brine collection technique ("sack-hole") might lead to an underestimation of the particulate Fe content in brines. Due to its high particle affinity, the Fe associated with micro-organisms and derived organic matter could remain attached to the walls of the brine channels during sample collection, and thus could not be recovered (Krembs et al., 2001). For the same reason, it might well be that Fe does not behave in the same way as other nutrients during sea ice formation. Iron would not be expelled into the liquid brine, but could use the solid phase, such as wall channels, pure ice crystals or even particulate matter (organic or inorganic), as sorptive surfaces. Comparing TDFe and DFe concentrations in sea ice and brine at station XIII provides evidence to support this hypothesis. Indeed, TDFe and DFe concentrations are nearly identical in the brine, while TDFe is considerably higher than DFe in the ice. This suggests that particulate

Fe might not be easily drained into the brine sack hole, and is perhaps retained in the ice medium.

The difference in Fe content between shallow (< -5°C) and deep (> -5°C) brines might be a consequence of brine exchanges between the bottom ice cover and the surface seawater. Density difference between brine and underlying seawater can initiate brine convection, as rising temperatures in the bottom ice re-establish connection between brine in the lower sea ice and the seawater below. Comparison of winter and spring brine profiles also tends to show a decline in salinity and Fe as spring progresses. This can be attributed to brine dilution by freshwater from melting pure ice and/or by seawater due to brine convection.

3.3.2. Fe and ice texture relationships

Ice texture provides information on the ice growth history, and may help in deciphering Fe sources and pathways in the ice column. Iron accumulates within pack ice at concentrations clearly exceeding that of the underlying seawater. In the case of planktonic organisms, enrichment has been attributed to physical concentration mechanisms, via scavenging by frazil ice crystals rising through the water column (Garrison et al., 1983; 1989; Reimnitz et al., 1990). In this process, suspended organisms are thought to adhere to individual ice crystals (frazil ice) that develop and rise in surface waters. Alternatively, particulates of micro-organisms may be concentrated by wave fields pumping water through the freshly formed frazil ice layer, causing particles to become attached to, or trapped between, the ice crystals (Weissenberger et al., 1998). Thus, sea ice genesis could eventually lead to physical enrichment of particulate or colloidal Fe within the pack ice, together with planktonic organisms. However, such enrichment would mainly be confined to frazil ice layers as it is probably the case at stations IV and XIII.

Within our cores, however, no clear overall relationship was observed between ice texture and Fe content (Table 3.1). For example at station IV, TDFe is 51.8 nM in frazil ice, 49.8 nM and 38.5 nM in columnar sections, and 58.8 nM in bottom ice (also of columnar nature). Bottom ice TDFe enrichment could be caused by phytoplankton DFe uptake in the bottom ice assemblages. On one hand, we might expect higher Fe levels in snow ice, because of accumulation of atmospheric deposition, and in frazil ice via planktonic enrichment. But on the other hand, columnar ice should expel more efficiently sea salts and particles during formation, especially at depth, and therefore might not accumulate Fe. Our observations

support neither scenarios and point toward the need for further research on the processes of Fe enrichment and transfer in sea ice.

3.3.3. Requirements and potential sources for Fe inputs to the sea ice cover

In our investigation, station IV can be regarded as a "winter" type station and its Fe content might thus be taken as representative of the initial Fe distribution before significant melting taking place (Table 3.2). Considering a 9 month residence time of 0.5 m thick ice, the required Fe flux in to sea ice in order to accumulate 49 nM TDFe and 18 nM DFe would be 0.09 µmol TDFe /m^2/d and 0.03 µmol DFe /m^2/d (Table 3.3).

Table 3.3. Upper ocean iron input estimates during sea ice melting.

		Remarks
Sea ice formation Fe uptake		
Winter TDFe (nM)	49	station IV
winter DFe (nM)	18	station IV
thickness (m)	0.5	station IV
residence time sea ice (9 months) in days	274	
Required flux to sea ice (TDFe µmol/m^2/d)	0.09	external supply 0.13, Table 3.4
Required flux to sea ice (DFe µmol/m^2/d)	0.03	external supply 0.28, Table 3.4
Sea ice melting Fe release		
TDFe inventory (µmol/m^2)	24.5	0.49 nM TDFe addition to upper 50m if melted at once
DFe inventory (µmol/m^2)	9	
melting time (d)	30	
release TDFe (µmol/m^2/d)	0.82	
Release DFe (µmol/m^2/d)	0.30	
DFe total flux to the upper ocean during sea ice melting	µmol/m^2/d	
Atmospheric/extraterrestrial	0.0016	
vertical diffusion	0.01	
upwelling	0.12	
sea ice melting	0.30	
total	0.43	

Table 3.4. Upper ocean iron input estimates for the Antarctic Ocean.

		Remarks	References
Aerosol flux J_{atm}			
dust input (mg/m^2/yr)	5	range 1-10	Duce and Tindale,
TFe flux (μmol/m^2/d)	0.011	assuming 4.3% Fe content	Wedepohl, 1995
DFe flux (μmol/m^2/d)	0.0005	solubility mineral dust 5%	Baker et al., 2006
TDFe flux (μmol/m^2/d)	0.003	SSIZ, 32% mean solubility	Edwards and
DFe flux (μmol/m^2/d)	0.0010		Edwards and
Average DFe flux (μmol/m^2/d)	0.0008		
Extraterrestrial flux J_{space}			
DFe (μmol/m^2/d)	0.0008	assumed 100% soluble	Johnson, 2001
Vertical diffusion J_{diapyc}			
K_z (m^2/s)	3.0E-05	ACC (56°S, 15°W)	de Baar et al., 1995
d[DFe]/dz (μmol/m^4)	0.006		
DFe flux (μmol/m^2/d)	0.016		
TDFe flux (μmol/m^2/d)	0.031 [a,b]		
K_z (m^2/s)	2.4E-05	SOIREE (61°S, 140°E)	Law et al., 2003
d[DFe]/dz (μmol/m^4)	0.003		Bowie et al., 2001
DFe flux (μmol/m^2/d)	0.006		
TDFe flux (μmol/m^2/d)	0.012 [a,b]		
K_z (m^2/s)	6.6E-05	FeCycle (46°S, 179° E)	Boyd et al., 2005
d[DFe]/dz (μmol/m^4)	0.00066		
DFe flux (μmol/m^2/d)	0.004		
TDFe flux (μmol/m^2/d)	0.008 [a,b]		
Average DFe flux (μmol/m^2/d)	0.009		
Average TDFe flux	0.017		
Upwelling $J_{upwelling}$			
upwelling velocity (m/s)	1.5E-06	ACC (56°S, 15°W)	de Baar et al., 1995
deep water concentration (nM)	1		
DFe flux (μmol/m^2/d)	0.13		
TDFe flux (μmol/m^2/d)	0.26 [a]		
Surface (m^2)	1.08E+13 [c]		Watson, 2001
upwelling flux (Sv)	25		
deep water concentration (nM)	0.6		
DFe flux (μmol/m^2/d)	0.12		
TDFe flux (μmol/m^2/d)	0.24 [a]		
Average DFe flux(μmol/m^2/d)	0.12		
Average TDFe flux	0.25		
TOTAL FLUX J_{tot}			
Average DFe flux (μmol/m^2/d)	0.13		
Average TDFe flux	0.28		

$J_{diff}=Kz \times d[DFe]/dz$ $J_{upwelling}=v_{upwelling} \times [DFe]_{deep}$ $J_{tot}=J_{atm}+J_{space}+J_{diff}+J_{upwelling}$

[a] assuming TDFe = 2x DFe

[b] assuming the same vertical diffusivity for TDFe and DFe

[c] surface based on biogeochemical provinces from Longhurst et al.

Based on data from the literature, we attempted to estimate Fe inputs to the Southern Ocean surface waters from various possible sources including atmospheric dust deposition (J_{atm}), extraterrestrial input (J_{space}), vertical diffusion (J_{diapyc}) and upwelling ($J_{upwelling}$). The calculations suggest a possible total flux of 0.28 μmol/m^2/d for TDFe and 0.13 μmol/m^2/d for DFe to the surface Antarctic waters (Table 3.4). Amongst the considered sources, upwelling should dominate the Fe inputs, accounting for about 90% of the total. This means that potential sources of Fe to the upper waters of the Southern Ocean are sufficient to account for the total DFe and TDFe trapped in pack ice based on our data (Table 3.4).

3.3.4 Importance of sea ice as a source of Fe to Antarctic surface waters

Table 3.3 shows estimated TDFe and DFe fluxes from melting East Antarctic pack ice to the upper water column. For an ice floe of 0.5 m thickness containing an average of 49 nM TDFe and 18 nM DFe (station IV), and assuming a melting period of one month, the estimated releases to the upper ocean would be 0.82 μmol/m^2/d for TDFe and 0.30 μmol/m^2/d for DFe - this equates to a 0.49 nM TDFe addition over a 50 m mixed layer. During spring melting, compared to other sources, sea ice could thus represent a significant Fe source to the Antarctic surface waters (Table 3.4 and Fig. 3.8). When integrating the DFe fluxes from atmospheric dust and extraterrestrial deposition (0.0016 μmol/m^2/d), vertical diffusion (0.01 μmol/m^2/d), upwelling (0.12 μmol/m^2/d) and sea ice melting (0.30 μmol/m^2/d), the total flux of DFe to the ocean surface would be 0.43 μmol/m^2/d (Table 3.3), of which sea ice could represent 70% of the total input. Hence, sea ice melting during austral spring may be important, as a source of Fe, in favouring ice edge spring blooms.

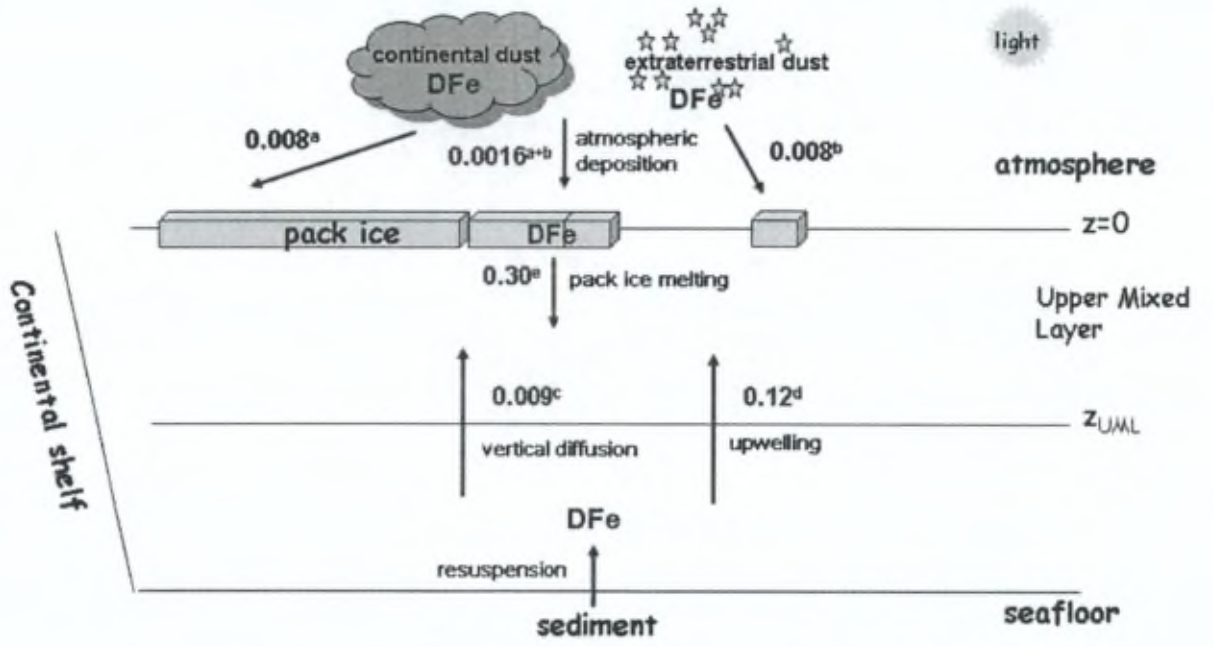

Figure 3.8. Summary of the conceivable DFe sources and estimated fluxes to East Antarctic surface waters upon 1 month melting period. (a) Duce and Tindale, 1991; Wedepohl, 1995; Bakker et al., 2005, Edwards and Sedwick, 2001. (b) Johnson, 2001. (c) de Baar et al., 1995; Law et al., 2003; Bowie et al., 2000; Boyd et al., 2005. (d) de Baar et al., 1995; Watson, 2001. (e) This study for a 0.5 m ice thick, DFe winter station=18 nM.

3.4. Conclusions

The East Antarctic pack ice investigated in the present study reveals high Fe contents in sea ice as compared to under-ice seawater. Both thermodynamic and biological processes are likely key factors controlling the Fe distribution, as spring progresses and the ice warms. Comparison of Fe content and ice texture sheds some light on possible pathways involving Fe biogeochemical cycling in pack ice. Complementary field data and laboratory experiments simulating ice growth could provide further mechanistic insights into the enrichment processes for Fe in the sea ice environment. Mass balance calculations show that melting sea ice may provide a significant input of Fe to Antarctic surface waters during spring, in comparison to other sources, which may thus play an important role in fuelling algal blooms in the seasonal ice zone.

Chapter 4

Iron study along a time series in the western Weddell pack ice

Delphine Lannuzel, Véronique Schoemann, Jeroen de Jong, Jean- Louis Tison,

Bruno Delille, Sylvie Becquevort and Lei Chou

To be submitted to Geophysical Research Letters

Abstract

Samples of sea ice, snow, brine and underlying seawater were collected in the western Weddell pack ice at the ISPOL drifting station (Ice Station POLarstern, 68°S/55°W) in early spring - summer period (November 2004 - January 2005). Total-dissolvable, dissolved and particulate Fe concentrations in the sea ice environment were determined every 5 days during the time series, together with relevant physical, chemical and biological parameters. From November 29th to December 30th, a drastic drawdown in Fe contents was observed (e.g. averaged total estimated bulk level of Fe drops from 66.0 nM to 10.6 nM). This overall decrease is likely the result of enhanced ice permeability as summer sets in. In addition, brine-water convection process takes place. This would enable the fuelling of Fe from the ice matrix towards the stable upper water column below. Another information brought to light is that a major fraction of the Fe accumulated in the pack ice investigated would be associated with particles. During this one-month sea ice decay, additional Fe inputs from the melting ice would represent 0.23 nM DFe and 1.0 nM TFe over a 50 m deep upper mixed layer. Flux estimates from the sampled area highlight furthermore the presumably important role of the western Weddell pack ice in the biogeochemical cycle of Fe in the Weddell Sea ecosystem.

4.1. Introduction

Being a scarce dissolved element in the present day oxygenated oceanic waters and micro-nutrient essential for algal growth, iron (Fe) has been clearly shown to play a crucial role in primary production and in the carbon pump efficiency in the Southern Ocean area (Martin and Fitzwater, 1988, de Baar et al., 1990; 2005). The low Fe concentrations in the Antarctic surface waters are the result of low Fe inputs. Potential sources of Fe are: a) atmospheric deposition of continental dusts (Duce and Tindale, 1991; Gao et al., 2001; Erickson et al., 2003) and extraterrestrial dusts (Johnson, 2001), b) continental shelf advection from e.g. the Argentine basin (de Baar et al., 1995) or Kerguelen Island platform (Blain et al., 2001), c) upwelling and vertical diffusion (de Baar and de Jong, 2001; Hoppema et al., 2003) and d) melting ice bergs and sea ice (de Baar et al., 1990; Sedwick and Ditullio, 1997). In an earlier study, high Fe contents were revealed in the East Antarctic pack ice as compared to under-ice seawater (Chapter 3, Lannuzel et al., 2006b). The Fe ranges encountered were in accordance with previously investigated areas widespread around Antarctica (de Baar et al., 1990, Löscher et al., 1997, de Jong et al., 1999, Grotti et al., 2005). In the light of the results obtained along our East Antarctic pack ice investigation, melting sea ice would provide a significant input of Fe to Antarctic surface waters during spring (Chapter 3, Lannuzel et al., 2006b).

Sea ice is known to be far from homogeneous. Most of the ship-based expeditions rely on a few hours stays per spatially visited stations (e.g. "Arise in the East" cruise in late winter-early spring, chapter 3) and therefore barely allow the long-term temporal study of a given Fe pool. An alternative for this is the long-term observation of pack ice from a drifting ice station which enables the study of Fe distribution ice sea ice environment as the season progresses. The present study will therefore focus on Fe biogeochemistry along a time series performed in the western Weddell ice in late spring-early summer (i.e. one month later in the season as compared to our previous study) and attempts will be made to evaluate Fe biogeochemical cycle and potential inputs from the visited melting ice floe to the upper ocean as a function of time.

4.2. Material and Methods

4.2.1 Sampling site

Samples of sea ice, snow, brine and underlying seawater were collected during the ISPOL Antarctic expedition in early spring - summer (Ice Station POLarstern, 68°S/55°W, November 2004 - January 2005, onboard the *RV Polarstern)*. From November 29th to December 30th, one ice station was sampled every 5 days in order to follow the evolution of Fe biogeochemistry in pack ice as a function of time. Depending on the floe location while drifting, the visited western Weddell ice floe was between 1500 m and 1900 m above the seafloor (Fig. 4.1). Our 20 m x 20 m trace metal sampling site was distanced at 1 km away from the anchored vessel until the ice floe broke on December 25th; the 2 ice stations collected afterwards were then 500 m away from the *RV Polarstern* (Fig. 4.2).

Collection methods and parameters to be studied together with processing steps and analytical techniques are detailed elsewhere (in Lannuzel et al., 2006a; Chapter 2). Briefly, snow was first sampled in polyethylene (PE) containers using polypropylene (PP) shovels and then ice cores were collected using an electropolished stainless-steel corer previously tested for trace-metal clean sampling, in order to assess metal contents and other relevant parameters (temperature, salinity, nutrients and Chl *a*). Holes were drilled into the ice cover until 20 cm and 60 cm deep to allow gravity-driven brine collection ("sack hole" brine sampling technique). Brines and under ice seawater (0 m, 1 m and 30 m deep) were then pumped up using a portable peristaltic pump (Cole-Parmer, Masterflex E/P) and tubing. Ice cores dedicated to trace metal determination were set in the polyethylene lathe under the onboard class-100 laminar flow bench and sections of 5-10 cm thickness were cut using Ti chisels. Snow and sea ice sections dedicated to metal study were then melted in trace-metal clean containers in the dark at shipboard ambient temperature until further processing. Sea ice sections for Chlorophyll *a* (Chl *a*) determination were melted in seawater filtered through 0.2 µm filters (1:4 volume ratio) to avoid cell lysis by osmotic shock.

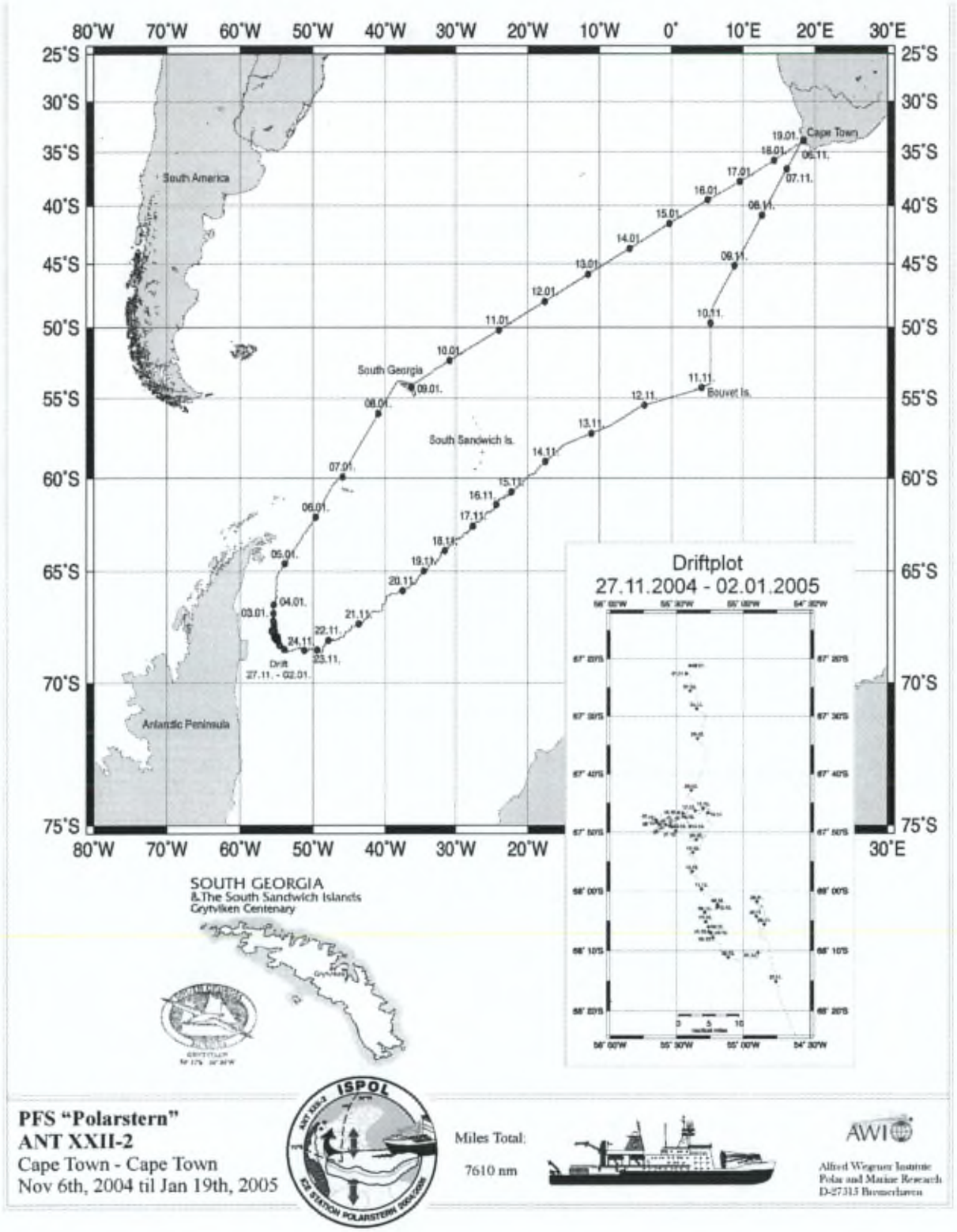

Figure 4.1. Cruise track and ISPOL ice floe drift in the Western Weddell Sea.

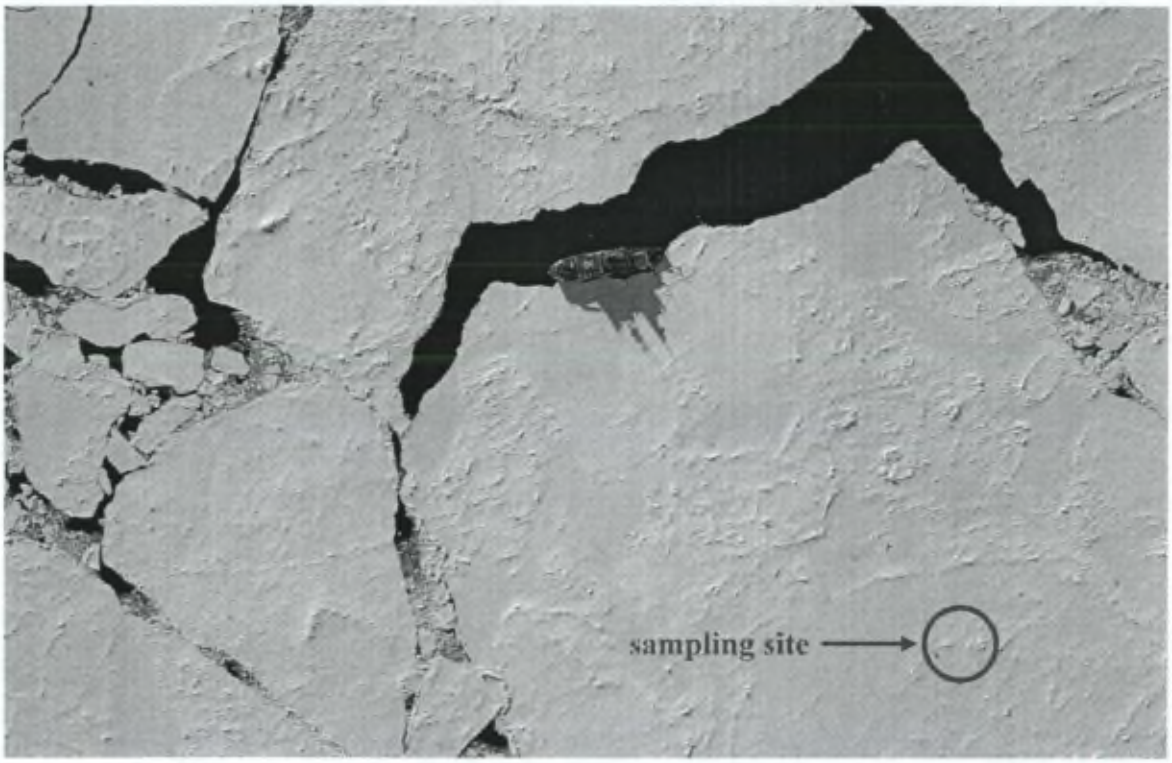

Figure 4.2. Helicopter view of the ISPOL floe (picture taken the 26th December by T. Worby, after the break up event). Our sampling site is indicated by the pink circle.

Two deep seawater profiles were collected for Fe determination at 12 depths throughout the water column using the onboard Niskin bottles thoroughly rinsed with Antarctic seawater from previous casts. One profile was sampled just below the visited ice floe (station n° PS 67/06-142, water depth at 1386 m, 67°22 S/ 55°24 W, 1st January 2005, Fig. 4.1) while another one was collected up north throughout a 4270 m deep water column (station n° PS 67/011-3, 59°55 S/ 45°55 W, 7th January 2005, Fig. 4.1). Results are presented in section 2.4.

4.2.2 Studied parameters

4.2.2.1. Physico-chemical and biological parameters

Granular (frazil and/or snow ice) and columnar (congelation growth) ice textures were determined from thin ice section photographs taken under polarised light.. *In-situ* ice temperatures were measured on site using a calibrated probe (TESTO 720) inserted every 5

or 10 cm along the freshly sampled core. Bulk ice salinity (5 cm definition) was measured onboard using a portable salinometer and brine volume fraction was calculated based on the ice temperature and brine and bulk ice salinities (Cox and Weeks, 1988; Eicken, 2003). Chlorophyll *a* was quantified fluorimetrically following Yentsch and Menzel (1963) after 90% v:v acetone extraction of the particulate material retained on glass-fibre filters (Whatman GF/F) for 12h at 4°C in the dark.

4.2.2.2. Iron

Total-dissolvable Fe (TDFe hereafter, unfiltered fraction, pH 1.8) samples were stored for at least 6 months before measurement by FIA in the home laboratory, while dissolved Fe (DFe, fraction filterable through 0.2 µm) was analysed onboard the ship 24h after acidification at pH 1.8. Filters (Polycarbonate Nuclepore 0.2µm) retaining particulate Fe (PFe) were stored frozen until total digestion in a mixture of strong acids (750 µl 12N HCl, 250 µl 40% HF, 250 µl 14N HNO_3, all ultrapure, Ultrex JT Baker) on a Teflon coated hot plate for 12h and were analysed by GF-AAS (Varian SpectrAA-300 Zeeman, see section 2.1.4 and 2.2.2 in Chapter 2). Total Fe (TFe) refers to the sum of DFe and PFe concentrations, while particulate-dissolvable Fe (PDFe) is estimated by substracting the DFe content from the TDFe fraction.

4.3. Results

4.3.1. Physico-chemical and biological features

4.3.1.1. Ice types

Figure 4.3 gives vertical thin ice section photographs taken under polarized light (Langway, 1958), which indicate crystalline ice shapes (e.g. columnar vs. granular). Both of granular type, snow ice and frazil ice were distinguished by δO^{18} measurement (snow ice has a $\delta O^{18}<0$, while frazil ice has a $\delta O^{18}>0$; Lange and Eicken, 1991). Based on field observations, thin sections and $\delta^{18}O$ measurements, natural breaks, permeability stage and seawater infiltration events occurring within the ice cover are reported as well (scheme on the right of the thin section photograph). The freeboard (i.e. the surface of the ice floe is above sea level) and snow layers are respectively indicated by the numbers in red and blue.

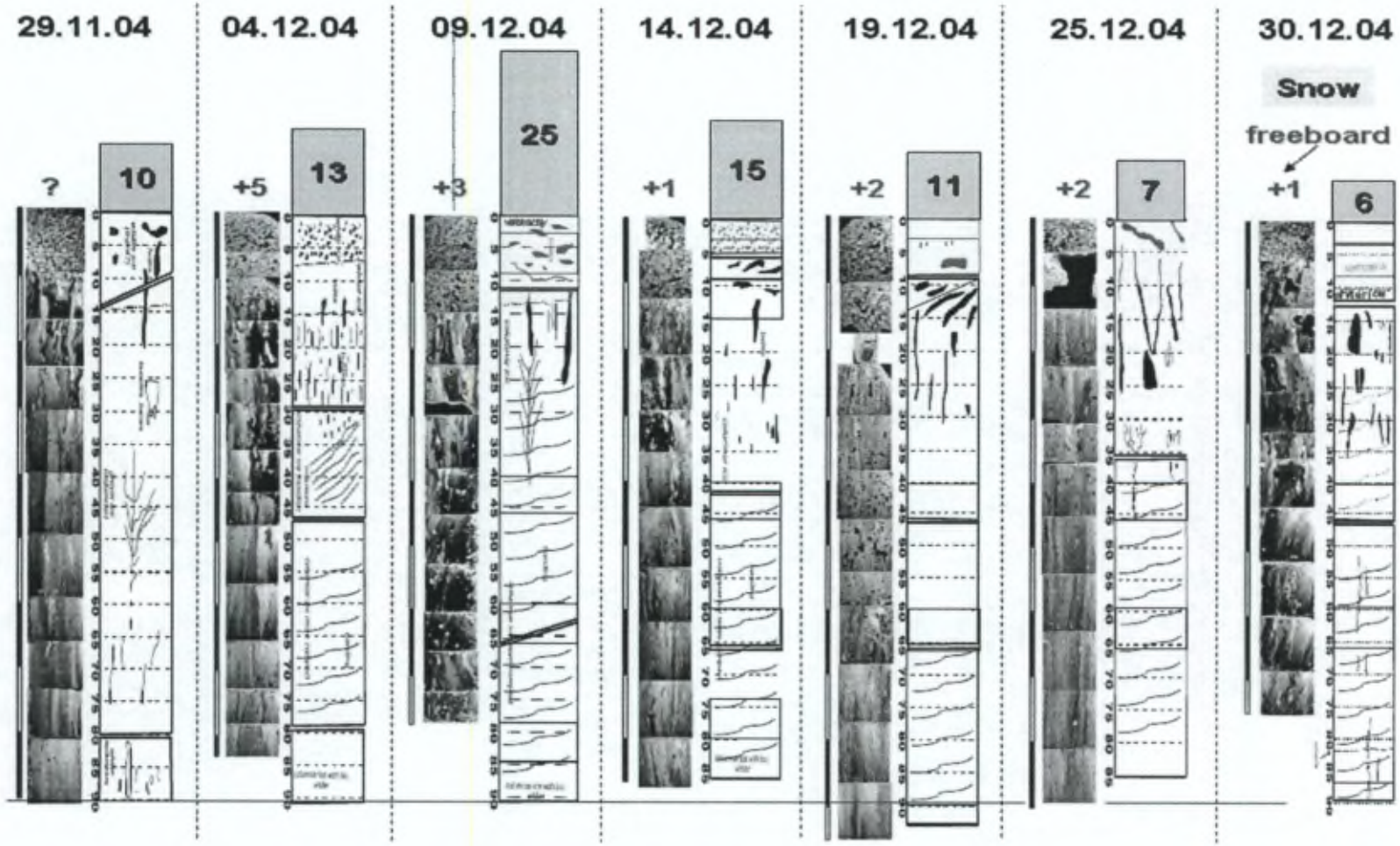

Figure 4.3. Ice textures from vertical thin sections, viewed under crossed polarizers of ice cores for each stations. The freeboard layer is indicated in red while snow depths are indicated in blue on top of the cores (e.g. freeboard=+5 cm and snow pack=13 cm the 04th of December).

Apart from the ice station sampled on the 9th of December located close to a ridge, sea ice cores collected along the ISPOL cruise were sampled on a 5x5 m uniform, levelled ice sheet. Cores were about 90 cm thick and exhibited a typical pack ice structure: frazil ice about 10 cm thick underlain by columnar ice (November 29th and December 4th in Fig. 4.3). The freeboard always remained positive: this means the ice level was above the seawater level during the whole duration of our sampling period. Snowfalls accumulated into a thick snow layer on top of our ice floe and formed snow ice via infiltration of seawater into the snow pack from the 9th December until the 30th December. The maximum snow layer is 25 cm thick on 9th December, quite probably because of the ridge vicinity. The seawater infiltration into the melted snow layer resulted in the formation of "slushes" (i.e. viscuous mix of snow and seawater) on the top of this 5x5 m area. Finally, the relatively warm air temperature induced the melting of snow pack and superimposed ice subsequently formed on the top of the ice floe at the 3 last stations.

4.3.1.2. Ice temperature

The visited area was already in a warm "spring-summer" regime when arriving on site, as all the ice temperature profiles were above -5°C (Fig 4.4.a). Our 1st sampled station shows ice temperature greater than -5°C with temperature profiles in the upper ice clearly shifting as a function of time towards ice warmer than the ice section below (e.g. 19th December to 30th December).

4.3.1.3. Bulk ice and brine salinity

Figure 4.4.b supports the spring-summer regime of the ISPOL sampling site as ice salinities were below 5 along almost the entire ice cover. Increased ice salinities in the bottom are probably due to seawater vicinity and brine transfer from the ice cover towards the water column via the skeletal layer (i.e. dendritic layer a few mm thick at the ice-water interface). Increased salinities in the top most layers of the two 1st sampled stations could be explained by the relatively lower ice temperatures which lead to increased brine salinities and smaller brine volume fractions. Brine salinities were higher than seawater salinities until the 9th of December, where brine salinities became lower than seawater salinity (Fig. 4.4.c).

4.3.1.4. Brine volume fraction

Brine volume fractions are depicted in Figure 4.4.d and show that the ice cover is already highly permeable upon arrival on site (November 29th), with Vb/V being greater than 5% along the whole profile. From November 29th to December 30th, the ice permeability increases, mostly in the top most sections, supporting the hypothesis of a melting starting from the top due to relatively warm air temperature and solar radiations. Huge cavities were actually conspicuous in the top part of the freshly sampled ice cores. This hypothesis is further supported by the fact that the length of the collected cores remained globally even during the whole duration of the study; if a melting from the bottom part would have occurred, the length of the cores would have probably been shorten as a function of time.

4.2.1.5. Chl a profiles

Chlorophyll *a* profiles show enhanced concentrations in the top and bottom 10 cm of the ice cover, where maxima values ranging from 16.3 to 28.4 $\mu g.l^{-1}$ Chl *a*. As the summer settles in and the upper water column stabilizes due to the ice melting, underlying seawater profiles exhibit also an algal increase: Chl *a* at the ice-water interface evolve from 0.03 µg/l on November 29th to 0.14 µg/l on December 30th (Fig. 4.5 a-h).

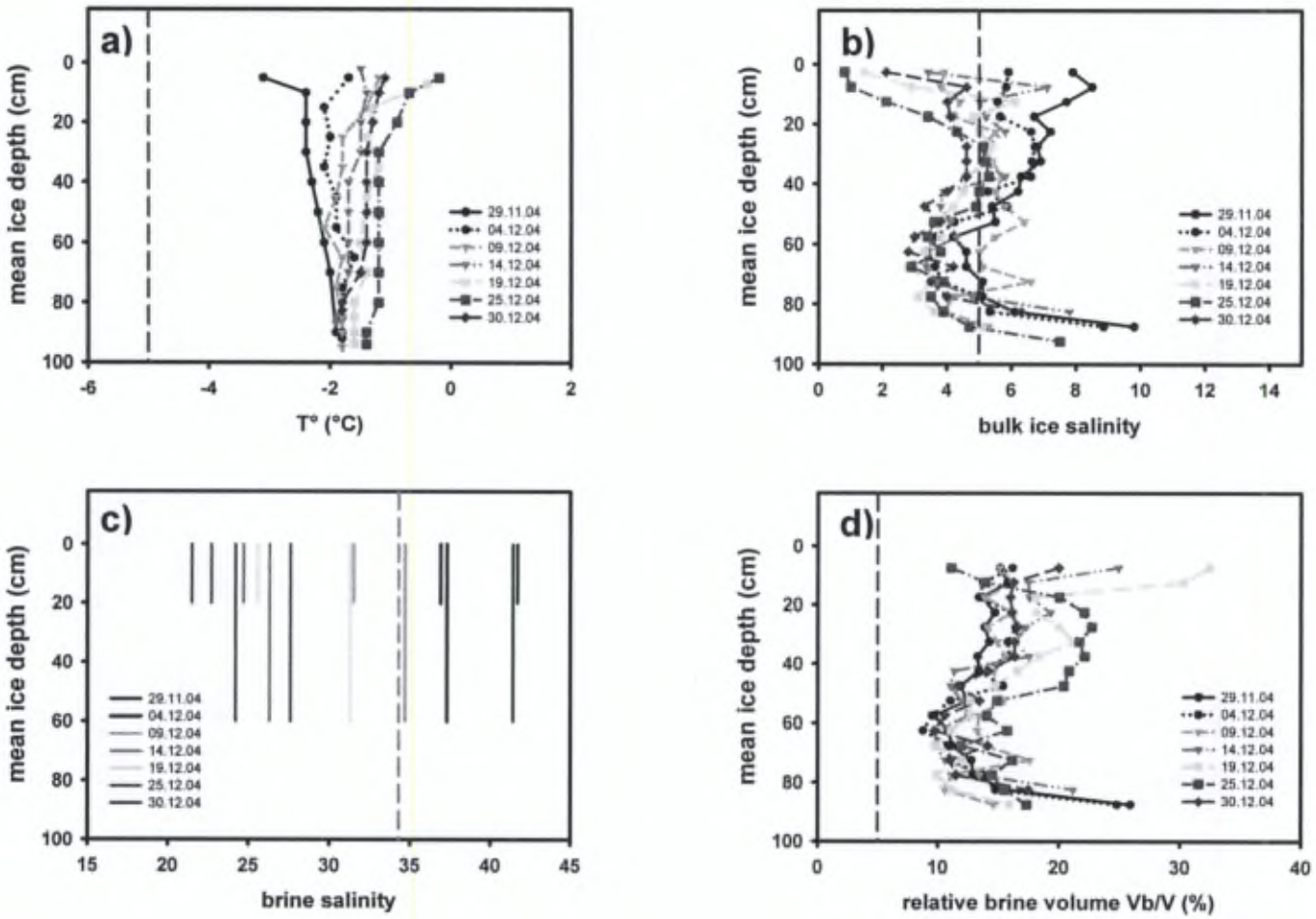

Figure 4.4. Temporal evolution of the ice cover along the ISPOL time series from November 29th to December 30th for: a) sea ice temperatures (°C). The vertical dashed red line indicates the -5°C threshold. b) Bulk ice salinity. Critical salinity 5 threshold is indicated by the vertical red long dashed line. c) brine salinities at 20 cm and 60 cm deep. The seawater salinity is indicated at 34.3 by a vertical grey dashed line. d) calculated relative brine to bulk ice volume fraction (Vb/V) in %. The 5% threshold is indicated by the red dashed vertical line.

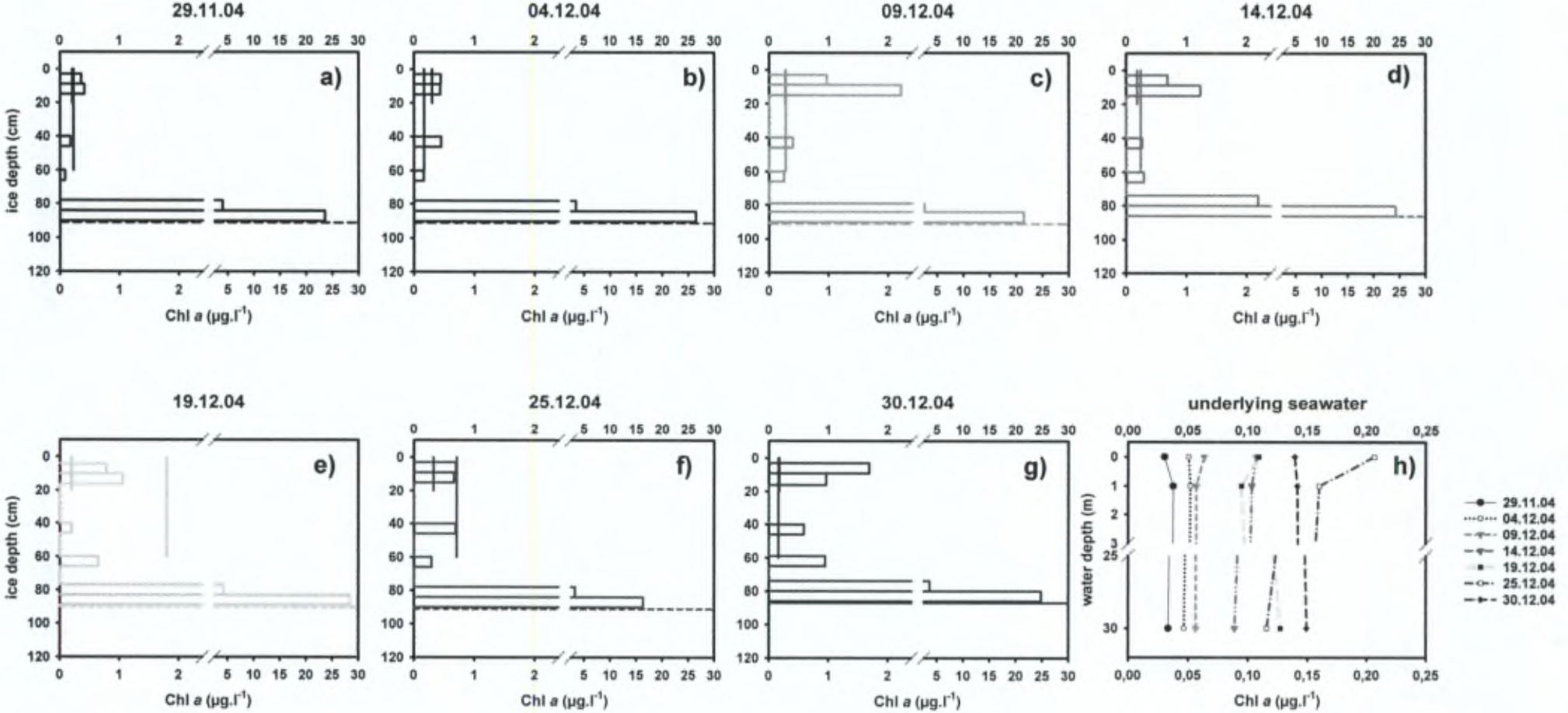

Figure 4.5. a-g. Chlorophyll *a* profiles in ISPOL pack ice (solid bars) and collected brines at 20 cm and 60 cm integrated depths (vertical lines) in µg/l. The break on the x axis is at 2.5 µg/l; h. temporal evolution of Chl *a* in underlying seawater at 0m, 1m and 30m deep.

4.3.2. Iron distribution

At a first glance, the five studied forms of Fe adopt a slightly C-shaped Fe profile, the trend being clearer early in the study where Fe levels encountered are greater. The potential discrepancies observed between the TFe and TDFe results presented in Table 4.1 are meant to result from an artefact upon sample filtration. Strains of algae were visible in the melted sea ice section and Fe-aggregates may not have been fairly distributed between the unfiltered sample and fraction retained on the filter for PFe determination. Total Fe concentrations in sea ice at the beginning of the time series are up to 2 orders of magnitude higher than in the underlying seawater, with brine levels being in between (see Table 4.1). The most striking feature is indeed this drastic drawdown of the Fe contents in the total, dissolved and particulate fractions as a function of time. The overall decrease in the bulk ice is very efficient at the two first stations, as for example observed by the <10 nM DFe levels reached the 9th December and for which middle-ice values remain as low as in the underlying seawater for the rest of the time series. Likewise, TDFe and TFe levels in sea ice after the 9th December are globally about the same as or even lower than the sampled brines concentrations (Fig. 4.6). On average 22 ± 12% (n=25, 1σ) of the TFe in sea ice belongs to the dissolved phase. This means a major part of the Fe in the ice medium would be associated to particulate matter.

Table 4.1. TDFe (in nM), DFe (in nM), PDFe (in nM), PFe (in nM), TFe (in nM) and DFe/TFe (%) at sampled date, media and depths.

			TDFe	DFe	PDFe	PFe	TFe	DFe/TFe
29.11.04	snow		7.8	2.5	5.3	7.8	10.2	24%
	sea ice	0 - 15 cm	57.0	12.4	44.6	44.2	56.6	22%
		40 - 46 cm	21.7	9.1	12.6	10.4	19.5	47%
		60 - 67 cm	42.6	7.2	35.4	39.0	46.2	16%
		80 - 90 cm	97.8	36.8	61.1	141.5	178.2	21%
	brine	0 - 20 cm	27.9	17.2	10.6	3.2	20.4	84%
		0 - 60 cm	15.3	9.8	5.5	10.0	9.9	50%
	seawater	0 m	1.4	0.9	0.4	0.4	1.3	70%
		1 m	1.5	1.7	<dl	1.3	3.0	57%
		30 m	1.6	0.9	0.7	*	nd	
04.12.04	snow		12.1	0.8	11.3	*	*	
	sea ice	0 - 7 cm	55.1	29.9	25.2	24.4	54.3	55%
		40 - 46 cm	10.1	2.4	7.7	13.2	15.6	16%
		60 - 67 cm	8.2	4.8	3.4	*	nd	
		80 - 90 cm	21.2	19.6	1.6	*	nd	
	brine	0 - 20 cm	17.3	17.9	<dl	5.6	23.4	76%
		0 - 60 cm	17.0	9.6	7.4	5.8	15.4	62%
	seawater	0 m	1.6	0.9	0.7	1.1	2.0	45%
		1 m	1.7	0.9	0.8	<1.1	nd	
		30 m	*	*	*	*	nd	
09.12.04	snow		12.2	0.7	11.4	13.8	14.4	5%
	sea ice	0 - 10 cm	22.7	8.1	14.6	50.5	58.6	14%

			TDFe	DFe	PDFe	PFe	TFe	DFe/TFe
		43 - 48 cm	2.7	1.2	1.5	6.6	7.8	15%
		60 - 67 cm	5.1	1.2	3.9	6.4	7.7	16%
		83 - 90 cm	12.5	10.8	1.7	19.1	29.9	36%
	brine	0 - 20 cm	20.6	19.0	1.6	5.0	24.0	92%
		0 - 60 cm	29.7	16.9	12.8	7.2	24.1	57%
	seawater	0 m	2.6	0.8	1.8	<1.9	nd	
		1 m	1.6	1.1	0.5	<1.3	nd	
		30 m	*	1.2	*	<1.8	nd	
14.12.04	snow		20.4	2.7	17.6	*	nd	
	sea ice	0 - 7 cm	19.3	3.2	16.1	*	nd	
		7 - 17 cm	7.1	2.5	4.6	*	nd	
		53 - 60 cm	5.3	0.9	4.4	5.4	6.3	14%
		60 - 67 cm	3.5	1.0	2.5	2.6	3.6	28%
		80 - 87 cm	22.0	8.3	13.7	15.1	23.4	36%
	brine	0 - 20 cm	22.0	13.0	8.9	7.1	20.1	65%
		0 - 60 cm	15.8	12.0	3.8	8.4	20.4	59%
	seawater	0 m	1.8	0.7	1.1	<1.3	nd	
		1 m	0.5	0.7	<dl	<1.3	nd	
		30 m	1.8	1.2	0.6	<1.8	nd	
19.12.04	snow		8.1	1.3	6.8	*	nd	
	sea ice	0 - 7 cm	10.9	4.4	6.5	12.7	17.1	26%
		40 - 46 cm	5.1	1.1	4.1	11.9	12.9	8%
		60 - 67 cm	3.0	0.9	2.1	5.9	6.8	13%
		80 - 87 cm	14.7	3.0	11.7	24.4	27.4	11%
	brine	0 - 20 cm	25.1	18.4	6.7	8.4	26.9	69%
		0 - 60 cm	21.7	24.8	<dl	12.8	37.6	66%
	seawater	0 m	3.2	1.5	1.7	1.6	3.1	49%
		1 m	2.2	1.0	1.1	1.1	2.1	49%
		30 m	*	1.1	*	2.1	3.2	35%
25.12.04	snow		*	1.7	*	*	*	
	sea ice	0 - 7 cm	10.7	1.6	9.1	17.2	18.8	9%
		40 - 46 cm	4.0	0.8	3.1	7.5	8.3	10%
		60 - 67 cm	2.3	0.8	1.5	8.1	8.9	9%
		80 - 87 cm	8.4	2.3	6.1	6.1	8.4	28%
	brine	0 - 20 cm	21.2	17.9	3.2	26.4	44.3	40%
		0 - 60 cm	21.0	8.5	12.5	26.7	35.2	24%
	seawater	0 m	2.4	1.2	1.2	1.4	2.6	47%
		1 m	1.6	1.1	0.5	3.2	4.3	25%
		30 m	2.3	1.4	0.9	*	nd	
30.12.04	snow		22.3	3.2	19.1	*	nd	
	sea ice	0 - 7 cm	14.1	2.8	11.3	17.8	20.6	14%
		40 - 46 cm	4.8	1.9	2.9	7.6	9.6	20%
		60 - 67 cm	2.7	0.7	1.9	2.3	3.1	24%
		84 - 89 cm	15.8	2.9	12.8	5.4	8.3	35%
	brine	0 - 20 cm	14.0	7.4	6.6	7.6	15.0	49%
		0 - 60 cm	13.0	6.6	6.4	5.9	12.5	53%
	seawater	0 m	2.3	1.0	1.3	3.4	4.4	23%
		1 m	1.5	0.9	0.6	2.5	3.4	27%
		30 m	4.1	1.2	2.9	4.0	5.2	23%
overall range	snow		7.8-20.3	0.7-3.2	5.3-19.1	7.8-13.8	10.2-14.4	
	sea ice		2.3-97.8	0.7-36.8	1.5-61.1	2.3-141.5	3.1-178.2	
	brine		13.0-29.7	6.6-24.8	<dl-12.8	3.2-26.7	9.9-44.3	
	seawater		0.5-4.1	0.7-1.7	<dl-2.9	0.4-4.0	1.3-5.2	

* no samples
nd: not determined
< dl: below analytical detection limit

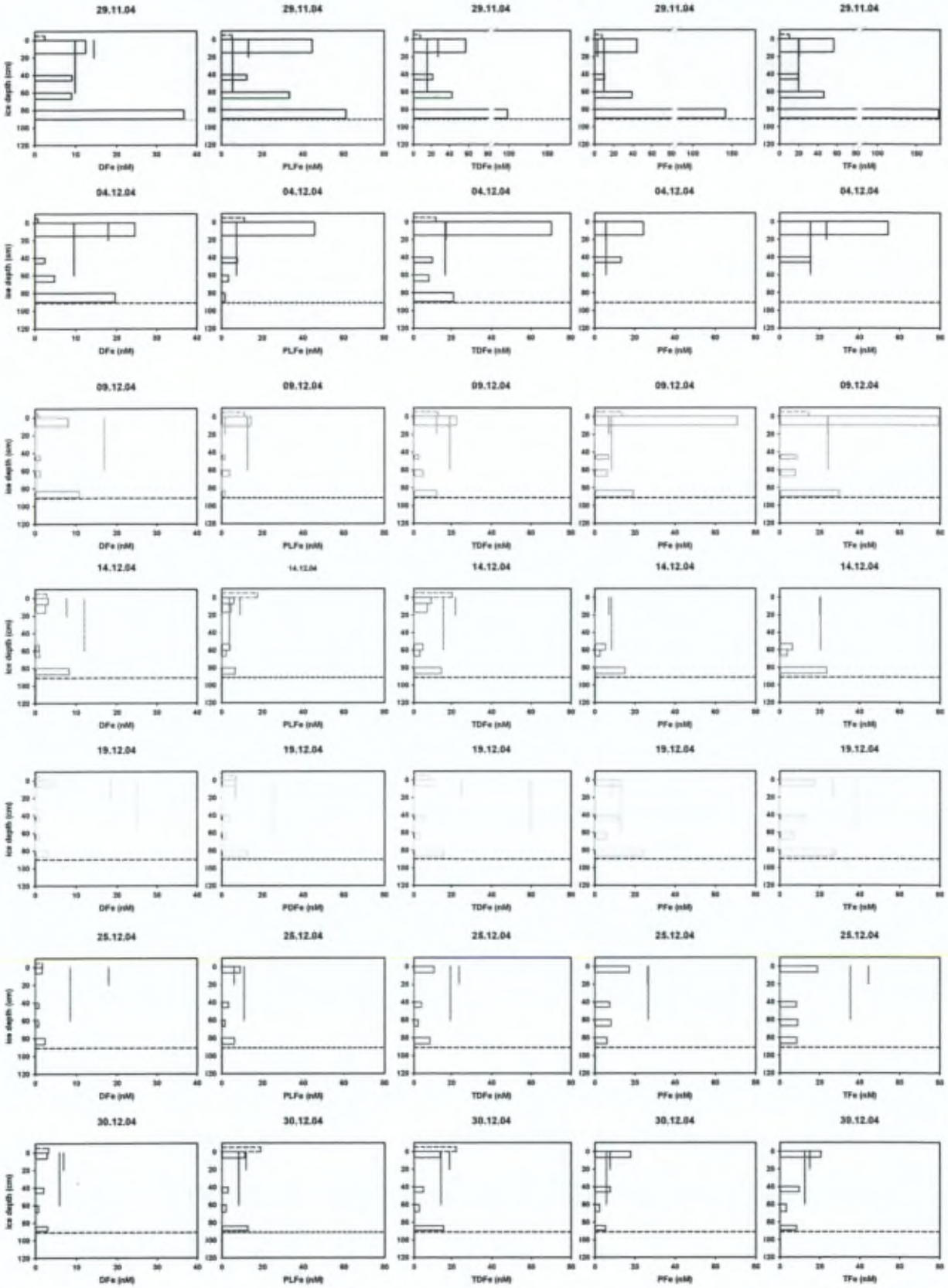

Figure 4.6. Total-dissolvable Fe (TDFe, unfiltered), dissolved Fe (DFe, filtered <0.2µm), particulate Fe (PFe, >0.2µm), particulate-dissolvable Fe (PDFe=TDFe-DFe) and total Fe (TFe=DFe+PFe) distribution in nM in sea ice (solid bars), snow (dashed bars) and collected brine at 20 cm and 60 cm deep (vertical solid lines). The dashed horizontal line represents the ice-water interface. * : no ice samples.

Total-dissolvable Fe levels in snow seem to be increasing from November 29th (7.8 nM TDFe) to December 14th (20.4 nM TDFe) and seem to be related to snow events. The highest value of the time study is reported for the 30th December (i.e. 22.4 nM TDFe). Dissolved Fe reported values in snow are together with DFe in seawater samples amongst the lowest, all media included. Averaged DFe concentration in snow is 1.9 ± 1.0 nM (n=7, 1σ) and would represent 15 ± 9% (n=6, 1σ) of the total-dissolvable Fe. Based on the TFe results from the two digested filters, iron solubility (i.e. DFe/TFe) in snow would range from 5% (December 9th) to 24% (November 29th).

Seawater sampled at 0 m, 1 m and 30 m globally range from 0.7 to 1.8 nM DFe, 0.5 to 4.1 nM TDFe and 1.3 to 5.2 nM TFe. Particulate Fe values are close to or below the GF-AAS detection limit (i.e. 3 x blank) at the first sampled stations, but then become detectable and increase as the season progresses (see Table 4.1 and Fig. 4.7c). Total Fe and TDFe contents in the upper water column globally increase at all sampled depths as a function of time as can be observed on Figure 4.7a and b, while DFe concentrations exhibit a fairly uniform distribution spatially and temporally (Fig. 4.7e). Dissolved Fe represents on average 41 ± 16% (n=12, 1σ) of the total Fe.

The Fe enclosed in the brine system seems to slightly differ in its behaviour as compared to Fe associated with the bulk ice. On the whole, brine also exhibits a decrease in their Fe contents as summer progresses: for example, DFe is 17.2 nM on November 29th and 7.4 nM on December 30th at 20 cm integrated depth (Table 4.1). For most of the stations, DFe values in the cold shallow brine are greater than in the deep warm brine (e.g. DFe is 17.2 nM at 20 cm and 9.9 nM at 60 cm on November 29th, Fig. 4.6 and Table 4.1). The DFe/TFe fraction is higher in the shallow brine than in the deep brine as reported by the respectively 84% and 50% on November 29th, and 76% and 62% on December 4th. Along the rest of the temporal study and mostly at the 2 last sampling days, we observe a rough equilibration together with a drawdown in DFe fractions and concentrations at both brine sampling depths (Fig. 4.6). Brine indeed exhibits the highest dissolved fraction, as compared to sea ice, seawater and snow, with 60 ± 16% (n=14, 1σ) of the DFe.

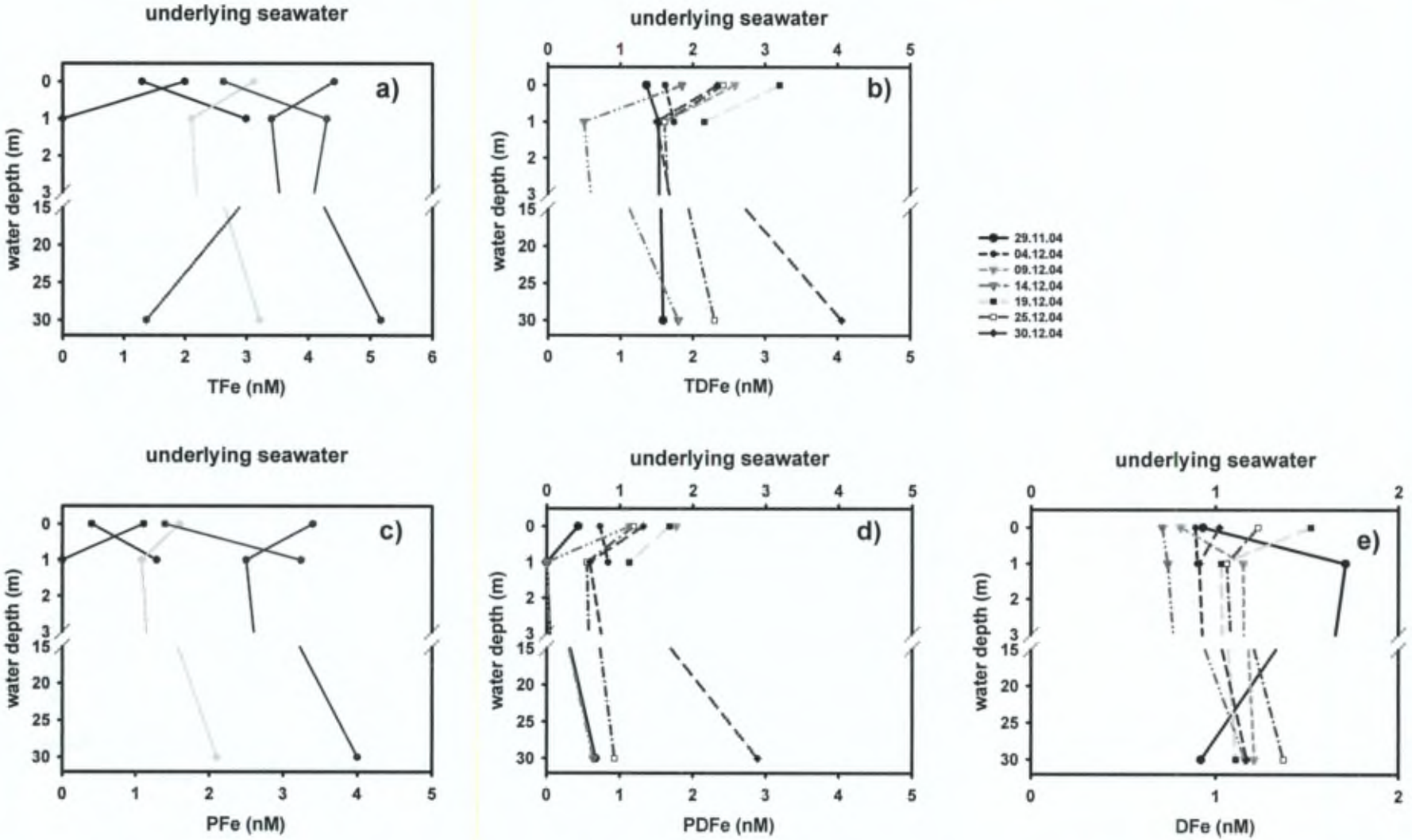

Figure 4.7. Profiles of a) total, b) total-dissolvable, c) particulate, d) particulate-dissolvable and e) dissolved Fe in under-ice seawater along the ISPOL time series. Note that the horizontal scale for DFe has been expanded and that a few data are <dl for profiles a) and c) (see Table 4.1).

4.3.3. Vertical distribution of DFe and TDFe in the water column at the ISPOL site and on the ice edge

Both profiles exhibit a subsurface maximum at about 500 m deep for the 07th Jan (DFe levels up to 4 nM for the deep water profile, Figure 4.8). Another feature is that the DFe levels increase to 5-6 nM close to the seafloor whereas concentrations are close to nanomolar levels at the seawater surface. Both TDFe profiles exhibit similar shape with the recurrent peak at 500 m deep in the water column. The near-bottom TDFe concentrations yield 66 nM at 1376 m for the shallow profile and 42 nM at 4270 m for the deep profile.

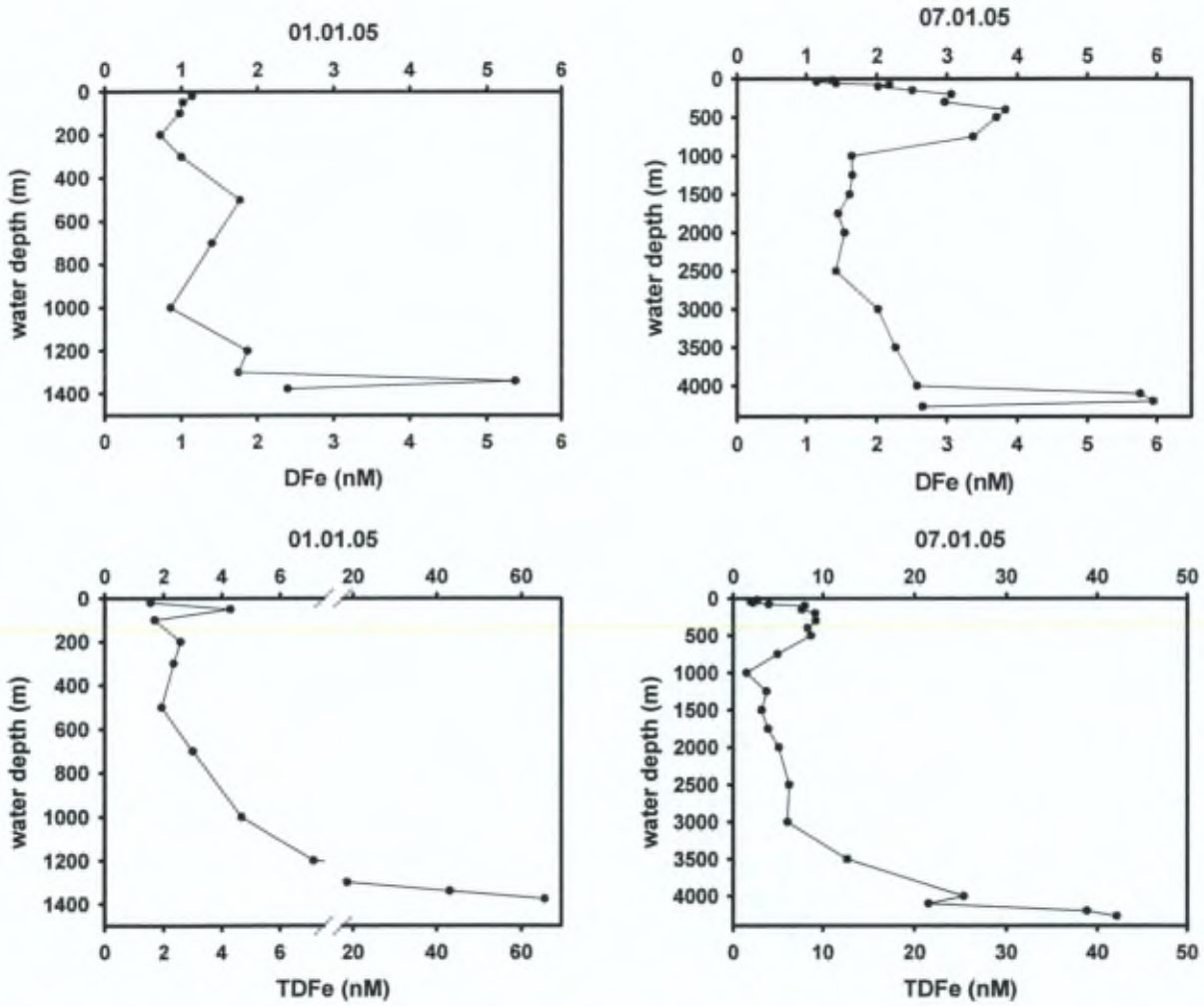

Figure 4.8. Vertical DFe and TDFe seawater profiles in the ISPOL pack ice zone (01.01.05) and on the ice edge (07.01.05).

4.4. Discussion

Our previous pack ice study revealed the very close links between the distribution of Fe in the sea ice environment and the physical and biological features of the ice (structure, temperature, salinity and presence of micro-organisms, Chapter 3: Lannuzel et al., 2006b). The 7 sampled stations are located a few meters away from each other with, apart from the station sampled on December 09th, similar lengths, textural type of ice and genesis. This quite reasonably allow us to assume that they all had the same Fe stock and ancillary parameters initially.

4.4.1. Temporal evolution of the thermodynamic properties of the sampled ice cover

Figure 4.4 supports the spring-summer regime of the ISPOL sampled area as a consequence of relatively warm air temperature. Ice temperatures were >-5°C and Vb/V > 10% along the whole ice cover as the summer progresses. This late seasonal stage is in contrast with our previous study which took place in September-October and where ice temperatures were <-5°C in some of the visited stations, thus displaying winter, transitional and spring type regimes (see Chapter 3). In the current spring-summer study, the brine enclosed in the ice cover can move freely within the highly permeable bulk ice system, as a consequence of the re-establishment of the connections between the brine pockets and channels. From November 29th to December 9th, heavy saline brine renders the densities unstable thus allowing exchanges between the ice matrix and the underlying seawater (see brine salinities greater than seawater in Fig. 4.4.c; Weeks and Ackley, 1982; 1986). The 9th of December and the days after, brine volumes increase as weather conditions are improving: pure ice melting becomes very active and dilutes the brines in the channels. Therefore, brine salinities become lower than seawater salinity and densities are rendered stable (see brine salinities < 34.3 from December 9th to December 30th in Figure 4.4.c). The aforementioned convection process is thus stopped and exchanges between the ice and the water column are severely slowed down or even shut down. A much slower process that is the molecular diffusion would remain as the pathways for nutrients transfer at the ice-water interface (i.e. skeletal layer).

4.4.2. Temporal evolution of the Fe distribution

4.4.2.1. In sea ice and the underlying seawater

Conspicuous drawdown in sea ice (Fig. 4.6) and global TFe increase in the under-ice water (Fig. 4.7) would support a loss of Fe from the ice pack towards the water column as a function of time. As spring progresses and light condition improves, the increased ice porosity allows brine carrying Fe to move through the ice system. The enhanced permeability in the top most sections would favour gravity-driven brine drainage and thus potentially explain the drawdown in bulk ice PFe levels in the upper ice observed in Figure 4.6 between 29th Nov and 04th Dec. The overall drastic decrease occurring at the two first stations would also be related to the brine-seawater convection occurring at the ice-water interface, which would therefore lead to an efficient flushing of Fe. This convection process nevertheless becomes severely limited after the 9th December and molecular diffusion, which is a much slower process, would therefore remain as the only pathway for Fe loss.

Based on the data collected at 4 levels along the core, we vertically integrated the concentrations of TDFe, DFe, PFe, PDFe and TFe per core sampled every 5 days at our ISPOL site. This integration led to an estimate of a mean bulk concentration of Fe in nM per station (Table 4.2). Results indicated in Table 4.2 further support the Fe profiles discussed here above. The mean Fe bulk ice concentrations estimated for November 29th are the highest amongst the time series and then decrease drastically within the following days. Dissolved Fe estimated bulk content averaged from 14.8 nM for November 29th down to seawater levels the 14th December and remained low until the end of the study (Table 4.2). Total Fe contents constantly decrease throughout the time series: the 66.0 nM TFe present on November 29th draws down to 10.6 nM on December 30th (Table 4.2).

Table 4.2. Estimated averaged bulk concentrations (in nM) of total-dissolvable Fe (TDFe), dissolved Fe (DFe), particulate-dissolvable Fe (PDFe), particulate Fe (PFe) and total Fe (TFe).

	TDFe	DFe	PDFe	PFe	TFe
29.11.04	51.2	14.8	36.5	51.3	66.0
04.12.04	25.5	14.5	11.0	21.9	36.4
09.12.04	10.8	4.8	6.0	21.6	25.3
14.12.04	9.3	2.8	6.6	10.9	13.7
19.12.04	7.7	2.2	5.4	12.6	14.8
25.12.04	6.1	1.3	4.8	10.0	11.3
30.12.04	8.3	2.0	6.3	8.6	10.6

4.4.2.2. In brine

As mentioned in Chapter 3, DFe levels and Fe solubility in shallow brine are enhanced as compared to deep brine. When sea ice forms, the 20 cm deep brine is colder and saltier as compared to the 60 cm deep which is influenced by the vicinity of warm seawater. The relatively warmer temperature in the deep brine system causes a melting of pure ice and a decrease in brine salinity via this dilution, as compared to the shallow brine. Not only the freshwater addition dilutes the Fe initially entrapped in the brine pockets thus explaining lower Fe levels as compared to shallow brine, but also gravity brine drainage acts for Fe loss towards the underlying seawater. In our study, this trend is still observed at the two first sampled stations for which DFe and TDFe values were enhanced in the shallow brine as compared to the deep brine (Table 4.1 and Fig. 4.6).

Furthermore, DFe fraction in brine has been reported to be greater (on average 60 ± 16%) than in sea ice, snow and seawater (Table 4.1). On one hand, DFe would be favoured at higher brine salinity as a consequence of ice formation and exclusion of salts together with dissolved Fe into the brine inclusions; thus the saltier the brine, the more dissolved Fe into the liquid phase of the bulk ice (see DFe and DFe/TFe values in brine sampled at the first station and for which brine salinity remain higher than seawater salinity). On the other hand, the brine collection technique ("sack hole": incomplete core holes are drilled into the ice cover and the brine that drains into the hole is collected; see chapter 2, section 2.1.2) suggested particulate Fe is likely to be associated to colloidal and particulate organic matter adsorbed to brine walls, thus not being recovered upon brine sampling (Schoemann et al., in prep and see explanation in Chapter 3, section 3.1.2). This sorption of the PFe to the walls of the ice inclusions would be less efficient in the deep brine system presumably because of the dilution via pure ice melting and seawater infiltration upon brine-water convection process. This is supported by the 3.2 nM PFe at 20 cm as compared to 10.0 nM PFe at 60 cm at the first station. Particulate Fe values in the brine system then equilibrate at values roughly between 5 to 8 nM at both depths, probably as a consequence of the shut down of the convection process.

4.4.2.3. Biological control and possible limiting factors for algal growth

At the same time, biological uptake could potentially play a role in the Fe distribution as the summer progresses. Enhanced Chl *a* values were observed in the top and lower most sections of the ice cover. This is probably as a consequence of better light penetration

together with a resupply of macro-nutrients upon seawater infiltration into the snow pack for the surface community, while the bottom community indeed benefits from seawater vicinity for major nutrients uptake. Chlorphyll *a* levels in under-ice seawater increased along the time series study, quite evidently as a consequence of a seeding from the ice medium of Fe together with sea ice algae and enhanced light availability as the pack ice becomes highly permeable (see Fig. 4.5h).

Station sampled on Decembre 9th close to the ridge demonstrates exotic features as compared to the rest of the sampling dates. High PFe and Chl *a* values in the top section of the core could be linked to slush occurence (see PFe in Figure 4.6 and Table 4.1, Chl *a* in Figure 4.5c and snow ice texture in Figure 4.2). While 25 cm thick snow was building on 09.12.04, seawater infiltrated into this snow pack to form a slush layer. The seawater infiltration favoured major nutrients and algal seeding into the top ice medium; this supply of nutrients in a section of the ice cover particularly advantaged with regards to irradiance and Fe concentrations could easily enhanced Fe algal uptake and therefore possibly explains the observed PFe peak.

The present late spring-early summer time series study reveals subnanomolar DFe levels in some part of the bulk ice as the season evolves (Table 4.1). However DFe brine contents remained high (i.e. the lowest reported value is 6.6 nM DFe) and presumably still sufficient to sustain micro-organism growth within the sea ice habitat. Macro-nutrients were nevertheless severely exhausted in much of the ice cover a few days after our arrival on site (e.g. the minimum measured contents in the collected brine are <dl for NO_3^- and < 2 μM $Si(OH)_4$; data not shown) and would have therefore been potentially limiting for primary production in sea ice. For the algal communities living at the snow-ice interface, infiltration and/or flooding events into the snow pack can provide sporadic resupply of major nutrients from seawater which could enhance algal development (e.g. December 9th and the following days). Bottom ice algal communities would thrive via the uptake of macro-nutrients supplied from the underlying seawater and Fe fuelled from the ice medium. Finally, grazing pressure may presumably co-limit primary production within the sampled pack ice as evidenced by the conspicuous presence of grazers below and within the sampled ice matrix.

4.4.3 *Iron sources and pathways*

4.4.3.1. Ice textures

Genetic types of ice (i.e. congelation, frazil, superimposed and/or snow ice) are key indicators of the ice growth history and hence could give insights on Fe accumulation pathways before and during our time series. Apart from our slightly C-shaped profile of Fe distribution in pack ice, our results do not demonstrate striking differences between snow ice, frazil and columnar ice (Fig. 4.6 and Table 4.1). This confirms the observations already arising in Chapter 3 (Lannuzel et al., 2006b). Snow ice would receive atmospheric Fe, eventually diluted by seawater infiltration. Within the few days of its formation, frazil ice would accumulate Fe associated with organic matter via adsorption onto/in between the granular ice crystals rising through the water column, via wave field pumping and/or Langmuir circulation (Garrison et al., 1993; Weissenberger and Grossmann, 1998; Schoemann et al., 2005; in prep). Our results do point out that up to 80% of Fe in the bulk ice would be associated to the particulate phase. While frazil ice forms quickly under agitated conditions into randomly-shaped ice crystals (i.e. granular), congelation ice grows under a much slower process into elongated ice crystals (i.e. columnar). Though columnar ice expels salts very efficiently, both Fe and particulate organic carbon (POC) attain levels way greater than in seawater (e.g. range from 140 to 740 $\mu g.l^{-1}$ POC in columnar ice on day 0 while underlying seawater is found around 50 $\mu g.l^{-1}$ POC, data not shown). Iron in columnar ice is also mostly associated to particulate Fe and would thus support the close links between Fe and particulate organic matter. Finally, enhanced Fe values in the warmer bottom ice may be associated with the presence of freshly formed ice algae as evidenced by high Chl *a* concentrations (Figs. 4.5 and 4.6).

There might therefore be a very intimate link between Fe and organic matter accumulation pathways in sea ice (Schoemann et al., in prep). Ice texture can give insights on the growth history and how/when the Fe was scavenged together with organic matter in the Antarctic pack ice.

4.4.3.2. Iron inputs to the western Weddell pack ice

Both seawater profiles presented in Figure 4.7 exhibit a first maximum in their DFe and TDFe profiles at 500 m deep (except for the DFe the 01st of January) and a sharp increase when approaching the seafloor. The anomaly in Fe signal at 500 m might be correlated to the Weddell Warm Deep Water (circumpolar water) which forms below the permanent

pycnocline at 200-650 m South-East from our floe location and then travels northwards at 500-650 m deep. The high TDFe and DFe values in the bottom nepheloid layer reflect Fe supplied from sediment resuspension (maxima at 42 nM TDFe the 07th Jan and 66 nM TDFe the 1st Jan; Symes and Kester, 1985). The DFe values encountered in the very deep sampled waters enable estimation of Fe fluxes from the seafloor to Weddell surface waters by vertical diffusion. For a measured 5.4 nM DFe at 1340 m deep, d[DFe]/dz would yield 0.004 $\mu mol/m^4$. This value is in good agreement with the mean of previous estimates (de Baar et al., 1995; Bowie et al., 2001and Boyd et al., 2005) reported in Table 3.4 (Chapter 3). When using a $Kz=3.0x10^{-5}$ m^2/s (ACC area after de Baar et al., 1995), the diapycnal DFe flux would equate 0.01 $\mu mol/m^2/d$. This value coincides well with the aforementioned estimated annual flux in the East Antarctic pack ice study (Table 3.4). The other possible sources previously reported for DFe (Table 3.4 in Chapter 3) would represent a total annual flux of 0.13 $\mu mol/m^2/d$. This includes atmospheric dust deposition (J_{atm} = 0.0008 $\mu mol/m^2/d$), extraterrestrial input (J_{space} = 0.0008 $\mu mol/m^2/d$), vertical diffusion (J_{diapyc} = 0.01 $\mu mol/m^2/d$) and upwelling ($J_{upwelling}$ = 0.12 $\mu mol/m^2/d$).

Though ice melting already started and some Fe may have been lost before our arrival on site, the station sampled the 29th of November will be regarded as the initial pool of Fe for our study. Considering a 9 month residence time of 0.9 m thick ice, the required Fe fluxes to sea ice in order to accumulate 66 nM TFe and 14.8 nM DFe would yield 0.18 $\mu mol/m^2/d$ for TFe and 0.04 $\mu mol/m^2/d$ for DFe. The aforementioned possible Fe sources and associated annual fluxes to Antarctic surface waters would therefore be sufficient to accumulate in sea ice the DFe and TFe levels observed in the present study.

4.4.4. Importance of pack ice as a source of Fe to western Weddell Sea surface waters

Underlying seawater profiles do show a global increase in Fe contents as the summer settles in (Fig. 4.7). The observed additional Fe supplied to the upper ocean waters is presumably originating from sea ice decay. Ice melting not only stabilizes the upper water column via low salinity water addition but also seeds the stratified water column with Fe and micro-organisms. During one month melting period, for an ice floe of 0.9 m thickness with on average of 53.7 nM TFe and 12.8 nM DFe (i.e. Fe losses upon 1 month time series) the estimated releases to the upper ocean would be 1.61 $\mu mol/m^2/d$ TFe and 0.38 $\mu mol/m^2/d$ DFe. This would give rise to an increase of 0.23 nM DFe and 1.0 nM TFe over a 50 m deep mixed layer upon ice melting. Sea ice retreat might therefore be a non negligible source of Fe

to the upper ocean and may explain the observed phytoplankton blooms in the marginal ice zone.

4.5. Conclusion

The current time series performed along spring-summer in the western Weddell pack ice first demonstrated a drastic drawdown of the initial Fe stock in sea ice, together with a discernible increase of Fe in the under-ice water column. This conspicuous loss of Fe from the ice cover would be a consequence of brine-seawater convection process, then probably relayed by the much slower molecular diffusion process as the summer acts in rendering brine density stable. Another information arising from this study is that up to 80% of the Fe accumulated in pack ice would be associated with particles phase. Finally, fluxes and Fe addition estimates of melting ice to the upper water column during late spring-early summer would point out the key role of the pack ice as an additional source of Fe to the western Weddell surface waters.

Chapter 5
General discussion and conclusion

5.1. General discussion

The first objective of this thesis was to develop a trace metal clean sampling technique and an analytical method suitable for Fe determination in the sea ice environment. The second scope was then to evaluate the Fe distribution in the Antarctic sea ice and its associated snow, brine and seawater. Based on the field data collected in the East Antarctic and Weddell pack ice, attempts can then be made to evaluate whether Fe biogeochemical behaviour in sea ice is preferentially driven by the spatial or temporal features of the Antarctic sea ice cover. Data from the literature enable the estimation of Fe fluxes to the Southern Ocean surface waters - and possibly to sea ice- from various possible sources including atmospheric dust deposition, extraterrestrial input, lateral advection from the continent, vertical diffusion, and upwelling. Finally, using data from both investigated areas, Fe fluxes from melting sea ice to the Antarctic surface waters are evaluated to assess whether pack ice could be a significant contributor to primary production in the Antarctic ecosystem.

5.1.1. Trace metal clean sampling and analytical method used for Fe determination in sea ice

For sea ice sampling, a non-contaminating electropolished stainless steel ice corer was designed in conjunction with a polyethylene lathe equipped with Ti chisels used to remove possibly contaminated outer layers of the collected ice cores. A portable peristaltic pump with plastic tubing was used on the ice to collect the underlying seawater (0 m, 1 m and 30 m) and sea ice brine from access holes (incomplete holes drilled at 2 different depths in the ice cover). We used a Flow Injection Analysis (FIA) technique and successfully demonstrated its capability to measure Fe concentrations without an on-line preconcentration step. The sensitivity, accuracy, precision and long term stability of the analytical procedure were satisfactory. Analysis of reference materials NASS-5 and CASS-3 gave a good agreement with the certified values. Repeated measurements over a period of 5 months of an "in-house" Antarctic seawater standard yields a concentration of 1.02 ± 0.07 nM (n=17, 1σ). Our methodology has been successfully applied to Antarctic sea ice samples and Fe data were consistent with previously reported values.

5.1.2. *Overall distribution of Fe in a sea ice environment*

Table 5.1. Overview of Fe data from the literature and the present study for the Antarctic ice environment.

Medium	TDFe	DFe	PFe	Latitude, longitude	reference
Glacial ice	26.0				Martin et al., 1990a
	20.4			48°S, 6°W	de Baar et al., 1990
	20.0	4.0		70°S, 6°W	de Jong et al., 1999
Global range	20.0-26.0				
Snow	5.7-16.0			Weddell Sea	Westerlund and Öhman, 1991
	31.3-52.6			58-60°S, 6-7°W	Löscher et al., 1997
	25.0	4.0		70°S, 6°W	de Jong et al., 1999
	1.2-31.7			64-66°S, 75-76°E	Edwards and Sedwick, 2001
	1.8-23.7	1.0-6.5		64-65°S, 112-119°E	This study
	7.8-22.3	0.7-3.2		67-68°S, 54-55°W	This study
Global range	1.2-52.6	0.7-6.5			
sea ice (bottom not included)	10.8-26.3			58-60°S, 6-7°W	Löscher et al., 1997
	95.0	25.0		70°S, 6°W	de Jong et al., 1999
		1.1-3.7	26-627	74°S, 164°E	Grotti et al., 2005
	3.3-65.8	2.6-20.5	3.0-90.3	64-65°S, 112-119°E	This study
	2.3-57.0	0.7-29.9	2.3-44.2	67-68°S, 54-55°W	This study
Global range	2.3-95.0	0.7-29.9	2.3-627		
Bottom sea ice	99.3			58-60°S, 6-7°W	Löscher et al., 1997
		5.6-6.0	869-1162	74°S, 164°E	Grotti et al., 2005
	9.8-58.8	7.0-19.0	5.9-100.8	64-65°S, 112-119°E	This study
	8.4-97.8	2.3-36.8	5.4-41.5	67-68°S, 54-55°W	This study
Global range	8.4-99.3	2.3-36.8	5.4-1162		
Brine	19.8-64.6			58-60°S, 6-7°W	Löscher et al., 1997
	6.0-28.6	4.7-25.5		64-65°S, 112-119°E	This study
	13.0-34.3	6.6-24.8		67-68°S, 54-55°W	This study
Global range	6.0-64.6	4.7-25.5			
Seawater	0.4-12.9[a]	0.2-8.6[a]		Weddell Sea	Westerlund and Öhman, 1991
	1.0 -9.0[b]			48°S, 6°W	Löscher et al., 1997
	0.3-9.2[c]	0.1-3.8[c]		66-77°S, 164-179°E	Sedwick et al., 2000
		0.4-4.2[d]		74°S, 164°E	Grotti et al., 2001
		0.5-31.0[e]		63-65°S, 41-56°W	Sanudo et al., 2002
	1.2-3.8[f]	1.1-4.5[f]		64-65°S, 112-119°E	This study
	0.5-4.0[f]	0.7-1.7[f]		67-68°S, 54-55°W	This study
Global range	0.3-9.2	0.1-8.6			

(a) surface seawater 50m deep, Weddell Sea
(b) surface seawater sampled in the wake of an iceberg, Weddell Sea
(c) seawater down to 300m deep, Ross Sea
(d) water column from 2m to 380m deep, 2km away from the coast,Terra Nova Bay
(e) surface seawater <1m deep, Weddell Sea
(f) under ice seawater 0m to 30m deep, East Antarctic and Weddell Sea

Table 5.1 gives an overview as to date of Fe data in Antarctic sea ice and glacial ice environments. The first values reported for glacial ice sample (Table 5.1, Martin et al., 1990a; de Baar et al.; 1990) hinted on the potential of such an extreme and poorly investigated environment in supplying Fe to the highly Fe-depleted Antarctic surface waters (e.g. 0.05-0.3 nM DFe, de Jong et al., 1998; 0.1 nM DFe, Bowie et al., 2001). A few years later, Löscher et al. (1997) measured surface waters Fe concentrations in the wake of an iceberg yielding 9 nM TDFe.

5.1.2.1. Iron ranges in the sea ice environment

For both pack ice studies presented in chapters 3 and 4, under-ice seawater Fe concentrations are relatively high (i.e. 0.5 - 4.0 nM TDFe in Table 5.1) compared to levels usually encountered in ice-free surface waters. Our reported values are however in the same range as values reported for other polar ice surrounding waters investigations (Table 5.1, Westerlund and Öhman, 1991; Sedwick et al., 2000, Grotti et al. 2001, Sanudo et al., 2002) and would support the role of the ice cover in fuelling Fe to the water column.

Chapters 3 and 4 give information on the overall TDFe ranges in pack ice: 2.3 - 97.8 nM TDFe. The reported concentrations are in accordance with the first sea ice values measured by Löscher et al. (range 10.8 - 99.3 nM TDFe, 1997) and de Jong et al. (one bottom sea ice sample = 95 nM TDFe, 1999) (Table 5.1). Iron profiles in bulk ice are globally C-shaped, with the highest Fe levels encountered in the lower most section of the ice cover, just at the ice-water interface (see bottom ice Fe values in Table 5.1). Bulk sea ice indeed appears to be the medium with the highest Fe contents, followed respectively by the brine, snow and underlying seawater media. Brine (6.0 - 34.3 nM TDFe) and snow (1.8 - 23.7 nM TDFe) from our two pack ice studies do exhibit Fe contents consistent with the previously published data listed in Table 5.1.

5.1.2.2. DFe/TFe partitioning in the western Weddell pack ice

According to the DFe/TFe results from collected western Weddell pack ice, DFe fraction would be enhanced in the brine system (60 ± 16%, n=14, 1σ) as compared to the other collected media. This is meant to be a consequence of salts rejection together with dissolved Fe into the liquid phase of the brine pockets when sea ice forms, while particulate Fe would remain attached to the walls of the brine system and thus would not be recovered upon "sack hole" brine sampling. For seawater sampled at the ice-water interface, 1 m and 30

m deep, the DFe would represent on average 41 ± 16% (n=12, 1σ) of the total Fe content. The averaged DFe/TFe in the ice cores is 20 ± 11% DFe/TFe (n=25, 1σ); this means most of the Fe entrapped in bulk sea ice would be associated with the particulate matter. Only two PFe values in snow are reported for the western Weddell pack ice study, with DFe/TFe ratio being at 5% and 24%. Complementary snow filters analysis will bring further information to address the many questions related to DFe/TFe partitioning in the sea ice environment.

5.1.3. Spatial and temporal studies: what controls Fe distribution in sea ice primarily?

Most of the ship-based expeditions rely on a few hours stays per visited stations (e.g. our East Antarctic cruise) and barely allow the long-term study of a given Fe pool. An alternative for this is long-term observation of pack ice from a drifting ice station (e.g. our western Weddell campaign) which enables the temporal study of Fe distribution together with the thermodynamic and biological features.

5.1.3.1. Spatial variability

The overall ranges reported along our two Antarctic pack ice studies are fairly similar. The spatio- temporal East Antarctic study showed TDFe and DFe levels ranging from 3.3 to 65.8 nM TDFe and 2.6 to 20.5 nM DFe for ice cores 0.3 to 0.8 m thickness. On the opposite side of the Antarctic continent, Fe levels in the western Weddell drifting ice station ranged from 2.3 to 97.8 nM TDFe and 0.7 to 36.8 nM DFe for sea ice 0.9 m thick.

Table 5.2. Overview of the estimated averaged bulk ice concentrations (in nM) of total-dissolvable Fe (TDFe) and dissolved Fe (DFe) in pack ice from the East Antarctic sector (stations IV to IX) and the western Weddell ice drifting study (stations 29.11.04 to 30.12.04). The seasonal regime of the sampled ice is indicated in brackets

ice station	Date	lat, long	TDFe (nM)	DFe (nM)
IV (winter)	01th Oct	64°3 S, 117°4 E	48.9	18.3
XIII (winter)	07th Oct	64°4 S, 116°3 E	40.7	11.4
VII (transition)	09th Oct	64°3 S, 116°4 E	17.7	13.1
XII (transition)	11th Oct	64°2 S, 115°1 E	9.5	9.3
V (spring)	14th Oct	63°5 S, 114°2 E	13.5	5.6
IX (spring)	20th Oct	65°1 S, 109°3 E	24.0	6.7
29.11.04 (spring)	29th Nov	68°0 S, 54°5 W	51.2	14.8
04.12.04 (spring)	04th Dec	68°1 S, 55°0 W	25.5	14.5
09.12.04 (summer)	09th Dec	68°0 S, 55°1 W	10.8	4.8
14.12.04 (summer)	14th Dec	67°3 S, 55°2 W	9.3	2.8
19.12.04 (summer)	19th Dec	67°4 S, 55°1 W	7.7	2.2
25.12.04 (summer)	25th Dec	67°4 S, 55°3 W	6.1	1.3
30.12.04 (summer)	30th Dec	67°3 S, 55°2 W	8.3	2.0

Table 5.2 gives an overview of TDFe mean averaged bulk ice concentrations estimated for both pack ice studies. The ranges are roughly equivalent for both expeditions: 9.5 - 48.9 nM TDFe and 5.6 - 18.3 nM DFe in the East Antarctic sector and 6.1 - 51.2 nM TDFe and 1.3 - 14.8 nM DFe in the Weddell pack ice. Based on the two data sets collected, large-scale spatial distribution does not globally seem to affect much the Fe ranges encountered in the visited Antarctic pack ice floes. Iron distribution can probably vary as much at scales less than one meter than it can at scales of several thousands of kilometres.

5.1.3.2. Temporal variability

Chapter 3 both displays a spatial study where cores were collected on different ice floes in the East Antarctic sector together with temporal approach of the ice cover with regards to Fe distribution in late winter-early spring (i.e. 1st to 20th October 2003). Based on the ice permeability and texture, seasonal regimes were characterized for each visited station and compared with each others when possible (i.e. when similar genetic ice types were observed). Winter, transition and spring type regimes were displayed, the coldest station being the station IV. This winter station IV was thus considered as representative of the initial pool of Fe in the ice cover. Even if the visited ice floes were distanced from each others by sometimes more than 200 km, a clear decrease in Fe levels between the cold winter and warm spring type stations was observed (see bulk levels in Table 5.2, or chapter 3 for a detailed understanding).

The western Weddell ice drifting station enabled the long-term study of one single area (20x20m surface) for assessing Fe biogeochemical behaviour as a function of time. While starting the 29th of November, the ice core collection was more than 1 month delayed as compared to the East Antarctic cruise. The late spring-early summer regime was further supported by the high permeability of the ice cover; the 1st sampled station exhibited sea ice temperature already above -5°C throughout the whole ice depth. Iron drawdown in the visited ice sheet was observed as a function of time (Table 5.2 and Chapter 4) with a very efficient loss of Fe at the two first stations because of the brine drainage and convection processes.

The initial stocks of Fe were similar for both studies (i.e. 48.9 nM TDFe at station IV and 51.2 nM TDFe at station 29.11.04, Table 5.2). One should bear in mind that the sampling site from the Weddell pack ice time series was in a spring regime when arriving on site. The

melting of the ice cover was already initiated on the 1st day of sampling as evidenced by the ice temperature being >-5°C and brine volume fraction >5%. Weddell pack ice Fe winter stock was therefore presumably even higher initially than the estimated East Antarctic Fe winter stock. This comparison only stands because the ice cover from the Weddell time series and the winter station (station IV) collected in the East Antarctic pack ice are both first-year pack ice. As the summer progresses, our time series investigation shows that Fe contents in the ice cover can decrease drastically within a few days. In the light of chapters 3 and 4, Fe distribution in the sea ice ecosystem is highly controlled by the ongoing thermodynamic and biological features, which both depend on the temporal evolution of the ice cover.

5.1.4. Limiting factors for sea ice algae in the Southern Ocean

Within the ice habitat, algal growth can be limited by different parameters such as irradiance, high salinity and low temperature (Eicken, 1992; Palmisano and Garrison, 1993; Kirst and Wiencke, 1995), size of the brine channels, grazers (e.g. Garrison and Buck, 1991; Krembs et al., 2001; Schnack-Schiel et al., 1998; 2001) and deficiency in macro- and micro-nutrients such as Fe. Surface and near-surface assemblages may have optimal irradiance and Fe levels for growth, but are often restricted by nutrients supply. Micro-organisms residing in the internal layers of the ice cover are exposed to steep gradients in salinities and temperatures that can severely constrain their growth (e.g. salinity up to 100 and ice temperature down to -10°C in our East Antarctic study). When enough light is available, most of sea ice algae are living in the bottom of the ice sheet where temperature and salinity conditions are more stable and favourable for growth over spring and summer time (Arrigo, 2003). Iron winter pool does not seem to be limiting but the steep gradients in temperatures and salinity conditions together with low irradiance may constrain algal biomass within the sea ice habitats over winter time.

In the light of the chapter 3, Fe levels do not seem to yield limiting concentrations for sea ice algae over winter-early spring season. The late spring-early summer time series study revealed subnanomolar DFe levels in some part of the bulk ice as the season evolves, but DFe brine contents remained high and presumably sufficient to sustain biological uptake. Macro-nutrients were nevertheless severely exhausted in much of the ice a few days after the arrival on site and would have presumably been the first limiting factor for algal growth within the sea ice matrix. For the algal communities living at the snow-ice interface, infiltration and/or flooding events into the snow pack can provide sporadic resupply of nutrients from seawater

which could induce important algal development (e.g. Arrigo et al, 1995; Thomas et al., 1998; top section the 9th Dec in this study). Bottom ice phytoplankton communities usually manage to stand high crops while presumably feeding on the macro-nutrients from the underlying seawater and Fe supplied from the ice medium. Finally, bottom ice communities constitute major feeding ground for a wide variety of organisms, including krill, in autumn, winter and early spring when the phytoplankton biomass in the water column is scarce. Grazing pressure may thus co-limit primary production within the ice (Schnack-Schiel, 2003).

5.1.5. Sources and pathways for Fe accumulation in pack ice

5.1.5.1. Iron and ice texture: an indicator for Fe accumulation pathway

Ice texture provides information on the ice growth history, and may help in deciphering Fe sources and pathways in the ice column. Apart from enhanced values in the top and lower most sections,no clear overall relationship was observed between ice texture and Fe content within our cores.

Snow ice is of granular type and originates from seawater infiltration into the snow pack. Iron in snow ice thus could both originate from eolian deposition (i.e. snow events) on the top of the ice sheet. The increased Fe values encountered in the top most sections may be induced by physical sequestration of planktonic organisms along the course of frazil ice formation. Within the few days of its formation, frazil ice would accumulate micro-organisms which adhere to the ice crystals rising in the water column and thus become trapped onto/in between ice crystals when the frazil ice coagulates (Garrison et al., 1983; 1989; Horner et al., 1992; Gleitz et al., 1998; Arrigo, 2003). Alternatively, the filtering and trapping of micro-organisms suspended in the water column can be induced by the pumping effect of the Langmuir circulation or by wave field pumping (Garrison et al., 1990; Weissenberger and Grossmann, 1998; Brierley and Thomas, 2002). These 3 mechanisms would presumably enable the physical enrichment of particulate or colloidal Fe within the pack ice, together with planktonic organisms and derived detritus organic matter (Schoemann et al., 2006; in prep). Finally, the high PFe levels observed at the ice-water interface in both pack ice studies could be associated with gravity driven export of Fe from the ice matrix towards the ice water-interface and/or freshly formed algae. Phytoplankton cells use the ice as a living

platform, the latter being the optimal spot where algae can feed on macro-nutrients from the water column and Fe supplied from the ice column.

5.1.5.2. Sources of Fe to Antarctic pack ice

The possible Fe sources to Antarctic surface waters are presumably similar as the ones leading to Fe segregation in the pack ice. The Fe fluxes required to accumulate over 9 months about 16.5 nM DFe (i.e. averaged initial DFe bulk ice concentration based on our initial stocks from the 2 investigated areas) in a 1 m thick ice sheet would be estimated at 0.06 $\mu mol/m^2/d$ DFe.

Based on the calculated Fe fluxes to the whole Southern Ocean surface waters (Table 3.4), the added aerosol (J_{atm}) and extraterrestrial (J_{space}) DFe fluxes would equate 0.0016 $\mu mol/m^2/d$ DFe. Upwelling ($J_{upwelling}$) and vertical diffusion (J_{diapyc}) would respectively yield 0.13 $\mu mol/m^2/d$ and 0.009 $\mu mol/m^2/d$ DFe. When considering a pack ice forming at 200 km from the coast with near-shore waters averaging at 4.0 nM DFe (estimated from 0.4-4.1 nM DFe at Terra Nova Bay from Grotti et al., 2005 and 4.7-7.4 nM DFe in the Gerlache Strait after Martin et al., 1990), the continental shelf lateral advection (J_{advec}) to the pack ice would be 0.00002 $\mu mol/m^2/d$ DFe and can thus be deemed insignificant. Atmospheric inputs would indeed remain low as compared to upward Fe inputs. Upwelling of Fe rich deep waters would be the main supplier of Fe to the Antarctic surface waters. When integrating atmospheric dust and extraterrestrial deposition, vertical diffusion, upwelling and lateral advection from the continent, the total DFe flux to the ocean surface would be 0.13 $\mu mol/m^2/d$ DFe. This flux would be sufficient in supplying the 0.06 $\mu mol/m^2/d$ required to incorporate 16.5 nM DFe in a 1 m thick pack ice over 9 months.

5.1.5.3. Geographic location of the ice pack

It is worth noting that these Fe fluxes are calculated when considering the whole surface waters of the Southern Ocean. Concerning the current study, we do not know precisely where the pack ice formed over fall/winter time and how these Fe fluxes affected locally the Fe levels at one visited site. Because vertical supply from below could represent up to 90% of the total DFe fluxes to the upper ocean, stability and depth of the water column may play a crucial role in the estimation of Fe fluxes towards the pack ice and therefore could control Fe bulk ice levels. However the very few Fe ranges measured at widespread sites around the Antarctic continent (list in Table 5.1) were in agreement with each others, and may hint that the large-scale Fe distribution in pack ice may perhaps not be as heterogeneous

as one would intuitively think. (Land-)fast ice has not been approached in this study but one can presume that land-attached sea ice might be significantly influenced by lateral advection from the continent. Conversely, fast ice may be less efficient as compared to pack ice in scavenging Fe-organic matter upon sea ice formation because of the stable quiescent characteristic of coastal waters.

5.1.6. Is pack ice a significant source of Fe to Fe-depleted Antarctic surface waters?

5.1.6.1. Iron flux from melting pack ice

Based on an averaged estimated bulk level of 16.5 nM DFe and considering a melting period of 30 days for an ice floe 1 m thick, the estimated DFe flux from decaying sea ice to the Antarctic surface waters would be $J_{melting}$ = 0.55 µmol/m^2/d DFe (Fig. 5.1). During this short-time melting period, this flux would be major as compared to the other conceivable fluxes estimated in section 5.1.3.2 here above. Melting pack ice would actually represent ¾ of the total estimated DFe input upon this 1 month of sea ice decay (i.e. $J_{melting}+J_{atm}+J_{space}+J_{advec}+J_{diapyc}+J_{upwelling}$=0.68 µmol/m^2/d DFe).

One should bear in mind that pack ice does not fuel Fe to the upper ocean all year round but exclusively during the short-time period of melting, whereas the other sources are able to supply Fe along the 4 seasons. Over fall and winter, strong winds blowing and digging the mixed layer may actually favour upwards fluxes of Fe-rich deep waters and atmospheric deposition of Fe dusts to the upper ocean/pack ice. Ultimately, one can consider the resident pack ice as a storage reservoir which would scavenge over fall/winter time the Fe supplied from upwelling, vertical diffusion and in a lesser extent atmospheric deposition and continental shelf advection. This Fe accumulated and stored in pack ice over 9 months becomes a pool of potentially bio-available Fe for Fe-depleted Antarctic surface waters when spring arrives, and would possibly induce and explain the observed algal blooms occurring in the marginal ice zone.

5.1.6.2. What would this flux represent as a source of Fe when spring arrives?

When spring arrives, the introduction of low salinity melted sea ice at the ocean surface is likely to both stabilize and seed the upper water column with Fe and sea ice algae. The 16.5 nM DFe in a 1 m thick pack ice would give rise to an increase of 0.33 nM DFe over a 50 m deep mixed layer upon sea ice decay. When considering the averaged DFe/TFe fraction is 20% in Antartcic pack ice, the input of total Fe to the upper ocean could be up to

1.65 nM. These values would constitute a considerable input compared to other conceivable Fe sources as supported by sea ice based and ice-edge algal blooms.

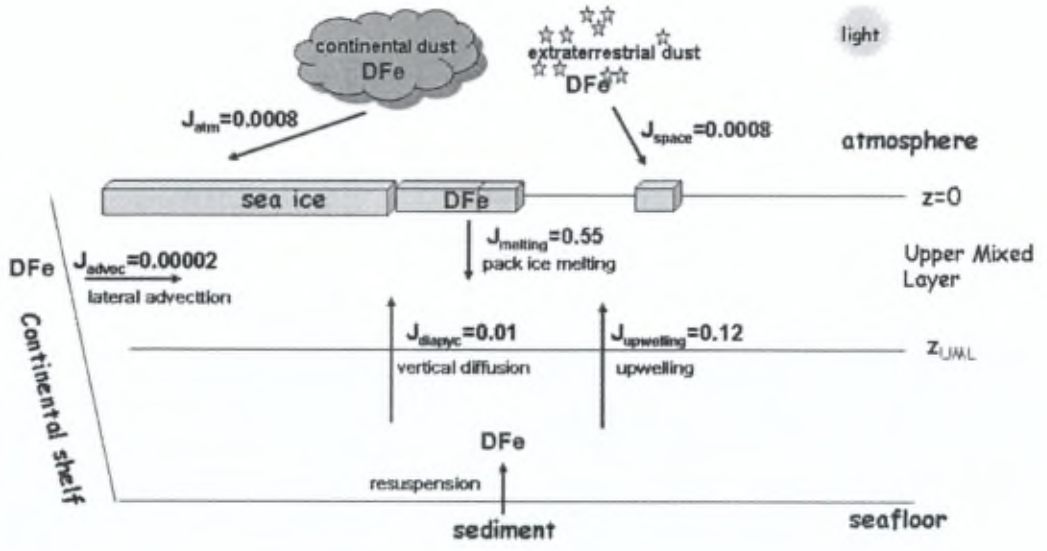

Figure 5.1. Summary of the estimated averaged dissolved Fe fluxes (in µmol/m^2/d) to the Antarctic surface waters upon 1 month sea ice decay.

5.2. Conclusion and perspectives

We developed a sensitive and reliable method to measure Fe concentrations in the sea ice environment. We demonstrated the ability of this method to deal with high gradients of salinity and Fe concentrations. Accuracy and reproducibility were satisfactory. Our methodology has been successfully applied to Antarctic sea ice samples and Fe data were consistent with previously reported values.

The East Antarctic and Weddell pack ice investigated in the present study revealed high Fe contents in sea ice as compared to under-ice seawater. A major part of the Fe sequestred in the ice matrix would be associated to particles. Both thermodynamic and

biological processes are likely key factors controlling the Fe distribution in sea ice, as spring progresses and the ice warms.

When integrating the estimated atmospheric dust and extraterrestrial deposition, vertical diffusion, upwelling and lateral advection, the total DFe flux to the Southern Ocean surface waters would yield 0.13 $\mu mol/m^2/d$ DFe, of which upwelling of Fe-rich deep waters would represent 90% o the total DFe flux. This calculated estimation based on data from the literature, would be sufficient to accumulate the DFe levels reported in the present study. Finally, using data from both investigated areas the Fe calculated fluxes from melting sea ice would represent an important source of Fe when spring arrives, compared to other conceivable sources and could therefore induce algal blooms in the marginal ice zone.

Future spatial (small-scale and large-scale collection around Antarctica) and temporal (seasonal or even full year cycle) field data collection will bring complementary insights on Fe biogeochemistry and speciation in the sea ice environment. This will help evaluating the Fe bio-availability in the sea ice habitat for sea ice based and pelagic algal growth. Laboratory experiments simulating ice growth may would also provide further mechanistic insights for the enrichment processes of Fe in the sea ice structure.

References

Allison, I. (1997) Physical processes determining the Antarctic sea ice environment. Australian Journal of Physics, 50 (4): 759-771.

Anderson, M.A. and Morel, F.M. (1982) The influence of aqueous iron chemistry on the uptake of iron by the coastal diatom Thalassiosira weissflogii. Limnology and Oceanography 27, 789–813.

Arrigo, K.R., Dieckmann, G.S., Gosselin, M., Robinson, D.H., Fritsen, C.H. and Sullivan, C.W. (1995) High resolution study of the platelet ice ecosystem in McMurdo Sound, Antarctica: biomass, nutrient, and production profiles within dense microalgal bloom. Marine Ecology Progress Series 127, 255-268..Arrigo, K.R., Worthen, D.L., Dixon, P. and Lizotte, M.P. (1998a) Primary productivity of near surface communities within Antarctic pack ice. Antarctic Research Series 73, 23-43.

Arrigo, K.R., Worthen, D., Schnell, A. and Lizotte, M.P. (1998b) Primary production in Southern Ocean waters. Journal of Geophysical Research, 103(C8): 15587-15600.

Arrigo, K.R., Weiss, A.M. and Smith, W.O.Jr (1998c) Physical forcing of phytoplankton dynamics in the southwestern Ross Sea. Journal of Geophysical Research, 103(C1): 1007-1021.

Arrigo, K.R. (2003) Primary production in sea ice. The importance of sea ice: an overview. In: Thomas, D.N., Dieckmann, G.S., (Eds.), Sea Ice - An introduction to its physics, chemistry, biology and geology. Oxford: Blackwell Science, pp. 143-183.

Arrigo, K.R. and Thomas, D.N. (2004) Large scale importance of sea ice biology in the Southern Ocean. Antarctic Science, 16 (4), 471-486.

Baker, A.R., Jickells, T.D., Witt, M. and Linge, K.L. (2006) Trends in the solubility of iron, aluminium, manganese and phosphorus in aerosol collected over the Atlantic Ocean. Marine Chemistry, 98 (1): 43-58.

Barbeau, K., Rue, E.L., Bruland, K.W. and Butler, A. (2001) Photochemical cycling of iron in the surface ocean mediated by microbial iron(III)-binding ligands. Nature 413, 409-413.

Blain, S., Tréguer, P., Belviso, S., Bucciarelli, E., Denis, M., Desabre, S., Fiala, M., Martin-Jézéquel, V., Le Fèvre, J. and Mayzaud, P. (2001) A biogeochemical study of the island mass effect in the context of the iron hypothesis: Kerguelen Islands, Southern Ocean. Deep Sea Research, 48(1): 163-187.

Bopp, L., Monfray, P., Aumont, O., Dufresne, J.L., Le Treut, H., Madec, G., Terray, L. and Orr, J.C. (2001) Potential impact of climate change on marine export production. Global Biogeochemical Cycles, 15(1): 81-99.

Bowie, A.R., Achterberg, E.P., Mantoura, R.F.C. and Worsfold, P.J. (1998) Determination of sub-nanomolar levels of iron in seawater using flow injection with chemiluminescence detection. Analytica Chimica Acta 361, 189-200.

Bowie, A.R., Maldonado, M.T., Frew, R.D., Croot, P.L., Achterberg, E.P., Mantoura, R.F.C., Worsfold, P.J., Law, C.S. and Boyd, P.W. (2001) The fate of added iron during a mesoscale fertilisation experiment in the Southern Ocean. Deep-Sea Research Part II, 48: 2703-2743.

Bowie, A.R., Achterberg, E.P., Blain, S., Boye, M., Croot, P.L., Laan, P., Sarthou, G., de Baar, H.J.W. and Worsfold, P.J. (2003) Shipboard analytical intercomparison of dissolved iron in surface waters along a north-south transect of the Atlantic Ocean. Marine Chemistry 84, 19-34.

Bowie, A.R., Sedwick, P.N. and Worsfold, P.J. (2004) Analytical intercomparison between flow injection-chemiluminescence and flow injection-spectrophotometry for the determination of picomolar concentrations of iron in seawater. Limnology and Oceanography: Methods 2, 42-54.

Bowie, A.R., Achterberg, E.P.; Croot, P.L., de Baar, H.J.W., Laan, P., Moffett, J.W., Ussher, S., and Worsfold, P.J. (2006) A community-wide intercomparison exercise for the determination of dissolved iron in seawater. Marine Chemistry 98, 81-99

Bowman, J.P., McCammon, S.A., Brown, M.V., Nichols, D.S. and McMeekin, T.A. (1997) Diversity and association of psychrophilic bacteria in Antarctic sea ice, Applied and Environmental Microbiology, 63 (8), 3068-3078.

Boyd, P.W., Watson, A.J., Law, C.S., Abraham, E.R., Trull, T., Murdoch, R., Bakker, D.C.E., Bowie, A.R., Buesseler, K.O., Chang, H., Charette, M., Croot, P., Downing, K., Frew, R., Gall, M., Hadfield, M., Hall, J., Harvey, M., Jameson, G., LaRoche, J., Liddicoat, M., Pickmere, S., Pridmore, R., Rintoul, S., Safi, K., Sutton, P., Strzepek, R., Tanneberger, K., Turner, S., Waite, A. and Zeldis, J. (2000). A mesoscale phytoplankton bloom in the polar Southern Ocean stimulated by iron fertilization. Nature, 407: 695-702.

Boyd, P.W., Law, C.S., Wong, C.S., Nojiri, Y., Tsuda, A., Levasseur, M., Takeda, S., Rivkin, R., Harrison, P.J., Strzepek, R., Gower, J., McKay, R.M., Abraham, E., Arychuk, M., Barwell-Clarke, J., Crawford, W., Crawford, D., Hale, M., Harada, K., Johnson, K., Kiyosawa, H., Kudo, I., Marchetti, A., Miller, W., Needoba, J., Nishioka, J., Ogawa, H., Page, J., Robert, M., Saito, H., Sastri, A., Sherry, N., Soutar, T., Sutherland, N., Taira, Y., Whitney, F., Wong, S.K.E. and Yoshimura, T. (2004) The decline and fate of an iron induced subarctic phytoplankton bloom. Nature 428, 549-553.

Boyd, P.W., Law, C.S., Hutchins, D.A., Abraham, E.R., Croot, P.L., Ellwood, M., Frew, R.D., Hadfield, M., Hall, J., Handy, S., Hare, C., Higgins, J., Hill, P., Hunter, K.A., LeBlanc, K., Maldonado, M.T., McKay, R.M., Mioni, C., Oliver, M., Pickmere, S., Pinkerton, M., Safi, K., Sander, S., Sanudo-Wilhelmy, S.A., Smith, M., Strzepek, R., Tovar-Sanchez, A. and Wilhelm, S.W. (2005) FeCycle: Attempting an iron biogeochemical budget from a mesoscale SF6 tracer experiment in unperturbed low

iron waters. Global Biogeochemical Cycle, 19, GB4S20, doi:10.1029/2005GB002494.

Boye, M., van den Berg, C.M.G., de Jong, J.T.M., Leach, H., Croot, P.L. and de Baar, H.J.W. (2001) Organic complexation of iron in the Southern Ocean. Deep Sea Research Part I 48, 1477-1497.

Boyle, E.A., Handy, B. and van Geen, A. (1987) Cobalt determination in natural waters using cation-exchange liquid chromatography with luminol chemiluminescence detection, Analytical Chemistry, 59:1499-1503

Brierley, A.S. and Thomas, D.N. (2002) Ecology of Southern Ocean pack ice, Advances in Marine Biology, 43, 171-278.

Broecker, W.S. and Peng, T.-H. (1991) Interhemispheric transport of carbon dioxide by ocean circulation, Nature, 356, 587-589.

Bruland, K.W. and Rue, E.L. (2001) Analytical methods for the determination of concentrations and speciation of iron. In: Turner, D.R., Hunter, K.H., (Eds.), The Biogeochemistry of Iron in Seawater, IUPAC Series on Analytical and Physical Chemistry of Environmental Systems. Volume 7, pp. 255-289.

Bucciarelli, E., Blain, S. and Tréguer, P. (2001) Iron and manganese in the wake of the Kerguelen Islands (Southern Ocean). Marine Chemistry 73, 21-36.

Buesseler, K.O., Andrews, J.E., Pike, S.M. and Charette, M.A. (2004) The effects of iron fertilization on carbon sequestration in the Southern Ocean. Science, 304(5669): 414-417.

Buffle, J. (1988) Complexation reactions in aquatic systems. An analytical approach. Ellis Horwood.

Buma, A.G.J., deBaar, H.J.W., Nolting, R.F. and Van Bennekom, A.J. (1991) Metal enrichment experiments in the Weddell-Scotias Seas:effect of iron and manganese on various plankton communities. Limnology and Oceanography, 36: 1865-1878.

Chen, M., Dei, R.C.H., Wang, W.-X. and Guo, L. (2003) Marine diatom uptake of iron bound with natural colloids of different origins. Marine Chemistry 81, 177-189.

Chereskin, B.M. and Castelfranco, P.A. (1982) Effects of iron and oxygen on chlorophyll biosynthesis. 2. Observations on the biosynthetic-pathway in isolated etiochloroplasts. Plant Physiology 69, 112-116.

Coale, K.H., Johnson, K.S., Chavez, F.P., Buesseler, K.O., Barber, R.T., Brzezinski, M.A., Cochlan, W.P., Millero, F.J., Falkowski, P.G., Bauer, J.E., Wanninkhof, R.H., Kudela, R.M., Altabet, M.A., Hales, B.E., Takahashi, T., Landry, M.R., Bidigare, R.R., Wang, X., Chase, Z., Strutton, P.G., Friederich, G.E., Gorbunov, M.Y., Lance, V.P., Hilting, A.K., Hiscock, M.R., Demarest, M., Hiscock, W.T., Sullivan, K.F., Tanner, S.J., Gordon, M.R., Hunter, C.N., Elrod, V.A., Fitzwater, S.E. Jones, J.L., Tozzi, S., Koblizek, M., Roberts, A.E., Herndon, J., Brewster, J., Ladizinsky, N., Smith, G., Cooper, D., Timothy, D., Brown, S.L., Selph, K.E., Sheridan, C.C.,

Twining, B.S., Johnson, Z.I. (2004) Southern Ocean iron enrichment experiment: carbon cycling in high- and low-Si waters. Science, 304: 408-414.

Croot, P.L. and Laan, P. (2002) Continuous shipboard determination of Fe (II) in polar waters using flow injection analysis with chemiluminescence detection. Analytica Chimica Acta, 466, 261-273.

Croot, P.L., Andersson, K., Öztürtk, M. and Turner, D.R. (2004) The distribution and speciation of iron along 64°E in the Southern Ocean. Deep-Sea Research, 51: 2857-2879.

Cullen, J.J. (1991) Hypothesis to explain high-nutrient conditions in the open sea. Limnology and Oceanography, 36(8): 1578-1599.

de Baar, H.J.W., Buma, A.G.J., Nolting,R.F., Cadée, G.C., Jacques, G. and Tréguer, P. (1990) On iron limitation of the Southern Ocean: experimental observations in the Weddell and Scotia Seas. Marine Ecology Progress Series, 65: 105-122.

de Baar, H.J.W. (1994) Von Liebig's Law of the minimum and plankton ecology (1899-1991). Progress in Oceanography, 33, 347-386.

de Baar, H.J.W., de Jong, J.T.M., Bakker, D.C.E., Löscher, B.M., Veth, C., Bathmann, U. and Smetacek, V. (1995) Importance of iron for plankton blooms and carbon dioxide drawdown in the Southern Ocean. Nature, 373: 412- 415.

de Baar, H.J.W., van Leeuwe M. A., Scharek, R., Goeyens, L., Bakker, K.M.J. and Fritsche, P. (1997). Nutrient anomalies in Fragilariopsis kerguelensis blooms, iron deficiency and the nitrate/phosphate ratio (A.C. Redfield) of the Antarctic Ocean. Deep-Sea Research II, 44(1-2): 229-260.

de Baar, H.J.W., de Jong, J.T.M., Nolting, R.F., Timmermans, K.R., van Leeuwe, M.A., Bathmann, U., van der Loeff, M.R. and Sildam, J. (1999) Low dissolved Fe and the absence of diatom blooms in remote Pacific waters of the Southern Ocean. Marine Chemistry 66, 1-34.

de Baar, H.J.W., P.M. Boyd (2000) The role of iron in plankton ecology and Carbon Dioxide transfer of the global Oceans. Chapter 4 in: Hanson, R.B., Ducklow, H.W. and Field, J.G. (Eds.), The Dynamic Ocean Carbon Cycle: A Midterm Synthesis of the Joint Global Ocean Flux Study, , International Geosphere Biosphere Programme Book Series, Vol. 5, Cambridge University Press, (ISBN 0 521 65603 6), 61-140.

de Baar, H.J.W. and de Jong, J.T.M., (2001) Distribution, sources and sinks of iron in seawater. In: Turner, D.R., Hunter, K.H., (Eds.), The Biogeochemistry of Iron in Seawater, IUPAC Series on Analytical and Physical Chemistry of Environmental Systems. Volume 7, pp. 123-253.

de Baar, H.J.W., Boyd,P.W., Coale, K.H., Landry, M.R., Tsuda, A.,, Assmy, P., Bakker, D.C.E., Bozec, Y., Barber, R.T., Brzezinski, M.A., Buesseler, K.O., Boye, M., Croot, P.L., Gervais, F., Gorbunov, M.Y., Harrison, P.J., Hiscock, W.T., Laan, P., Lancelot, C., Levasseur, M., Marchetti, A., Millero, F.J., Nishioka, J., , Nojiri, Y., van Oijen,T.,

Riebesell, U., Rijkenberg, M.J.A., Saito, H., and Takeda, S., Timmermans, K.R., Veldhuis, M.J.W., (2005) Synthesis of Iron Fertilization Experiments: from the Iron Age in the Age of Enlightenment. Journal of Geophysical Research, 110, C09S16, doi: 10.1029/2004JC002601.

de Jong J.T.M., den Das, J., Bathmann, U., Stoll, M.H.C., Kattner, G., Nolting, R.F. and de Baar, H.J.W., (1998). Dissolved iron at subnanomolar levels in the Southern Ocean as determined by ship-board analysis. Analytica Chimica Acta, 377: 113-124.

de Jong, J.T.M., Croot, P.L. and de Baar, H.J.W., (1999). Distribution of iron in the surface and deep waters of the Southern Ocean along 20°E (abstract). EOS, Trans. Amer. Geophys. Union, 80 (49), 161.

de Jong, J.T.M., Boyé, M., Schoemann, V.F., Nolting, R.F. and de Baar, J.W. (2000) Shipboard techniques based on flow injection analysis for measuring dissolved Fe, Mn and Al in seawater. Journal of Environmental Monitoring 2, 496-502.

Dieckmann, G.S., Hellmer, H.H., (2003). The importance of sea ice: an overview, In Thomas D.N., Dieckmann G.S. (editors), Sea ice: an introduction to its physics, chemistry, biology and geology, Blackwell publishing, Blackwell Science Ltd, 1-21.

Duce, R.A. and Tindale, N.W., (1991) Atmospheric transport of iron and its deposition in the ocean. Limnology and Oceanography, 36: 1715-1726.

Dugdale, R.C., Wilkerson, F.P. and Minas, H.J. (1995) The role of a silicate pump in driving new production. Deep-Sea Research I, 42 (5): 697-719.

Edwards, R., Sedwick, P.N., Morgan, V., Boutron, C.F. and Hong, S., (1998) Iron in ice cores from Law Dome, East Antarctica: implications for past deposition of aerosol iron. Annals of Glaciology, 27: 365-370.

Edwards, P.R., (1999) Iron in modern and ancient east Antarctic snow: implications for phytoplankton production in the Southern Ocean., University of Tasmania.

Edwards, R. and Sedwick, P.N., (2001). Iron in East Antarctic snow: Implications for atmospheric iron deposition and algal production in Antarctic waters. Geophysical Research Letters, 28 (20): 3907-3910.

Eicken, H., Lange, M. A. and Dieckmann, G. S., (1991b) Spatial variability of sea ice properties in the northwestern Weddell Sea. Journal of Geophysical Research, 96 (C6): 10603-10615.

Eicken, H., (1992) Salinity profiles of Antarctic sea ice: field data and model results. Journal of Geophysical Research, 97 (C10): 15545-15557.

Eicken, H., (1998) Factors determining microstructures, salinity and stable-isotope composition of Antarctic sea ice: Deriving modes and rates of ice growth in the Weddell Sea. In: Jeffries, M.O. (Ed.), Antarctic Sea Ice: Physical Processes, Interactions and Variability. AGU, Washington, D.C. Antarctica Research Series 74, pp. 89-122.

Eicken, H., (2003) From the microscopic, to the macroscopic, to the regional scale: growth, microstructure, and properties of sea ice. In: Thomas, D.N., Dieckmann, G.S., (Eds.), Sea Ice - An introduction to its physics, chemistry, biology and geology. Oxford: Blackwell Science, pp. 22-83.

Erickson D.J., Walton, J.J., Ghan, S.J., Penner, J.E. (1991) Atm. Environ., 25A, 2513.

Erickson, I.D.J., Hernandez, J.L., Ginoux, P., Gregg, W.W., MC Clain, C. and Christian J. (2003) Atmospheric iron delivery and surface ocean biological activity in the Southern Ocean and Patagonian regions. Geophysical Research Letters, 30: 1-4.

Falkowski, P., Scholes, R.J., Boyle, E., Canadell, J., Canfield, D., Elser, J., Gruber, N., Hibbard, K., Högberg, P., Linder, S., Mackenzie, F. T., Moore III, B., Pedersen, T., Rosenthal, Y., Seitzinger, S., Smetacek, V., Steffen, W., (2000) The global carbon cycle: a test of our knowledge of earth as a system. Science, 290: 291-296.

Falkowski, P.G., Barber, R.T., Smetacek, V., (1998) Biogeochemical controls and feedbacks on ocean primary production. Science, 281: 200-206.

Fichefet, T., Tartinville, B. and Goosse, H. (2003) Antarctic sea ice variability during 1958–1999: A simulation with a global ice-ocean model, Journal of Geophysical Research, 108(C3): 3102.

Gao, Y., Fan, S-M, Sarmiento, J., (2003) Aeolian iron input to the ocean through precipitation scavenging: a modeling perspective and its implication for natural iron fertilization in the ocean. Journal of Geophysical Research, 108(D7): 4221, doi:10.1029/2002JD002420.

Gao, Y., Kaufman, Y.J., Tanre, D., Kolber, D. and Falkowski, P.G., (2001) Seasonal distributions of aeolian iron fluxes to the global ocean. Geophysical Research Letters, 28: 29-32.

Garrison, D.L., Ackley, S.F. and Buck, K.R. (1983) A physical mechanism for establishing algal populations in frazil ice. Nature, 306: 363-365.

Garrison, D.L., Close, A.R. and Reimnitz, E., (1989) Algae concentrated by frazil ice: evidence from laboratory experiments and field measurement. Antarctic Science, 1 (4): 313-316.

Garrison, D.L. and Buck, K.R. (1991). Surface-layer sea ice assemblages in Antarctic pack ice during the austral spring: environmental conditions, primary production and community structure. Marine Ecology Progress Series 75, 161-172.

Garrison, D.L. and Close, A.R. (1993). Winter ecology of the sea ice biota in Weddell Sea pack ice. Marine Ecology Progress Series 96, 17-31.

Geider, R.J., la Roche, J., Greene, R.M. and Olaizola, M., (1993) Response of the photosynthetic apparatus of Phaeodactylum tricornutum (Bacillariophyceae) to nitrate, phosphate, or iron starvation. J. Phycol., 29(6): 755-766.

Gervais, F., Riebesell, U., Gorbunov, M.Y., (2002) Changes in the size-fractionated primary

productivity and chlorophyll a in response to iron fertilization in the southern Polar Frontal Zone. Limnology and Oceanography, 47: 1324-1335.

Gill, A.E. (1973) Circulation and bottom water production in the Weddell Sea. Deep-Sea Research, 20, 111-240.

Ginoux, P., Chin, M., Tegen, I., Prospero, J.M, Holben, B., Dubovik, O. and Lin, S.-J. (2001) Sources and distributions of dust aerosols simulated with the GOCART model, Journal of Geophysical Research, 106(D17): 20,255-20,274,.

Gledhill, M., and van den Berg, C.M.G. (1994) Determination of complexation of iron (III) with natural organic complexing ligands in seawater using cathodic stripping voltametry. Marine Chemistry, 47, 41-54.

Gledhill, M., van den Berg, C.M.G., Nolting, R.F. and Timmermans, K.R. (1998) Variability in the speciation of iron in the northern North Sea. Marine Chemistry 59, 283-300.

Gleitz, M., Bartsch, A., Dieckmann, G.S. and Eicken, H. (1998) Composition and succession of sea ice diatom assemblages in the eastern and southern Weddell Sea, Antarctica. Antarctic Research series 73, 107-120.

Gloersen, P., Campbell, W.J., Cavalieri, D.J., Comiso, J.C., Parkinson, C.L. and Zwally, H.J. (1992) Arctic and Antarctic sea ice, 1978-1987: Satellite passive microwave observations and analysis. NASA, Washington, D.C., 290pp.

Golden, K.M., Ackley, S.F. and Lytle, V.I., (1998) The percolation phase transition in sea ice. Science, 282: 2238-2241.

Goldman, J.C. and Dennett, M.R. (1985) Susceptibility of some marine phytoplankton species to cell breakage during filtration and post-filtration rinsing. J. Exp. Mar. Biol. Ecol. 86:47.

Gonye, E.R. and Carpenter, E.J. (1974) Production of iron-binding compounds by marine micro-organisms, Limnology and Oceanography, 19, 840-841.

Goosse, H. and Fichefet, T. (1999) Importance of ice-ocean interactions for the global ocean circulation: a model study. Journal of Geophysical Research, 104: 23337–23355.

Goosse, H and Renssen, H. (2001) A Two-phase response of the Southern Ocean to an increase in greenhouse gas concentrations. Geophysical Research Letters vol. 28, N° 18, 3469-3472.

Gow, A.J., Ackley, S.F., Govoni J.W. and Weeks, W.F., (1998) Physical and structural properties of land-fastice in Mc Murdo Sound, Antarctica. In: Jeffries, M.O. (Ed.), Antarctic Sea Ice: Physical Processes, Interactions and Variability. AGU, Washington, D.C. Antarctic Research Series 74, pp. 355-374.

Gran, H.H. (1931) On the conditions for the production of plankton in the Sea. Rapport Procès Verbal de la Réunion du Conseil International pour l'Exploration de la Mer, 75: 37-46.

Greene, R.M., Geider, R.J., Falkowski, P.G. (1991) Effect of iron limitation on

photosynthesis in a marine diatom. Limnology and Oceanography, 36(8): 1772-1782.

Grotti, M., Soggia, F., Ianni, C. and Frache, R. (2005) Trace metals distributions in coastal sea ice of Terra Nova Bay, Ross Sea, Antarctica. Antarctic Science, 17 (2): 289-300.

Haas, C., Thomas, D.N. and Bareiss, J. (2001) Surface properties and processes of perennial Antarctic sea ice in summer, Journal of Glaciology, 47 (159), 613-625.

Hart, T.J., (1934) On the phytoplankton of the Southwest Atlantic and the Bellingshausen Sea, 1929-1931. Discovery Rep, 8: 1-268.

Hill, J. M. (1973) The preparation of 8-hydroxyquinoline substituted silica gel for the chelation chromatography of some trace metals. Journal of Chromatography 76, 455-458.

Hoffmann, L., Peeken, I., Assmy, P., Veldhuis, M.J.W. and Lochte, K. (2005) Response of pico-, nano-, and microphytoplankton during the Southern Ocean iron fertilization experiment EIFEX, paper presented at the Summer Meeting, Am. Soc. of Limnology and Oceanography, Santiago de Compostela, Spain, 24 june.

Hoppema, M., de Baar, H.J.W., Fahrbach, E., Hellmer, H.H. and Klein, B. (2003) Substantial advective iron loss diminishes phytoplankton production in the Antarctic Zone. Global Biogeochemical Cycle, 17(1): 1025.

Horner, R.A. (1985a). History of ice algal investigations. In: Horner, R.A. (Ed.) Sea Ice Biota. Boca Raton, CRC Press, pp. 1-19.

Hudson, R.J. and Morel, F.M.M. (1990) Iron transport in marine phytoplankton: kinetics of cellular and medium coordination reactions. Limnology and Oceanography 34, 1113-1120.

Hutchins D.A., Witter, A. E., Butler, A. and Luther III, G.W. (1999) Competition among marine phytoplankton for different chelated iron species. Nature 400: 858–861.

Hutchins, D.A. and Rueter, J.G. (1991). Siderophore production and nitrogen fixation are mutually exclusive strategies in Anabaena 7120. Limnology and Oceanography, 36, 1-12.

IPCC, 2001: Climate Change 2001: The Scientific Basis. Contribution of Working Group I to the Third Assessment Report of the Intergovernmental Panel on Climate Change. [J.T. Houghton et al. (eds.)]. Cambridge University Press, Cambridge, 881 pp.

Jeffries, M.O., Weeks, W.F., Shaw, R. and Morris, K. (1993) Structural characteristics of congelation and platelet ice and their role in the development of Antarctic land-fast sea ice. Journal of Glaciology, 39 (132), 223-238

Jickells, T.D., An, Z.S., Anderson, K.K., Baker, A.R., Bergametti, G., Brooks, N., Cao, J.J., Boyd, P.W., Duce, R.A., Hunter, K.A., Kawahata, H., Kubilay, N., La Roche, J., Liss, P.S., Mahowald, N., Prospero, J.M., Ridgwell, A.J., Tegen, I. and Torres., R. (2005) Global iron connections between desert dust, ocean biogeochemistry and climate. Science, 308: 67-71.

Johnson, K.S. (2001). Iron supply and demand to the upper ocean: Is extraterrestrial dust a significant source of bioavailable iron? Global Biogeochemical Cycle, 15 (1): 61-63.

Johnson, K.S., Chavez, F.P. and Frederich G.E. (1999) Continental-shelf sediment as a primary source of iron for coastal phytoplankton. Nature, 398: 697-700.

Jones, G.J., Palenik, B.P. and Morel, F.M.M. (1987) Trace metal reduction by phytoplankton: The role of plasmalemma redox enzymes. Journal of Phycology, 23, 237-244.

Kirst, G.O. and Wiencke, C. (1995) Ecophysiology of polar algae. Journal of Phycology 31:181–99

King, D.W., Lounsbury, H.A. and Millero, F.J. (1995) Rates and mechanism of Fe(II) oxidation at nanomolar total iron concentrations. Environmental Science and Technology 29 (3) 818-824.

Kivi, K. and Kuosa, H. (1994) Late winter microbial communities in the western Weddell Sea (Antarctica). Polar Biology 14: 389-399.

Krembs, C., Mock, T. and Gradinger, R. (2001a) A mesocosm study of physical-biological interactions in artificial sea ice: effects of brine channel surface evolution and brine movement on algal biomass. Polar Biology, 24: 356-364.

Krembs, C., Tuschling, K. and Juterzenka, K.V. (2001b) The topography of the ice-water interface - its influence on the colonization of sea ice by algae, Polar Biology, 25 (2), 106-117.

Lancelot, C., Veth, C. and Mathot, S. (1991) Modelling ice-edge phytoplankton bloom in the Scotia-Weddell Sea sector of the Southern Ocean during spring 1988. Journal of Marine Systems, 2: 333-346.

Lancelot, C., Billen, G., Veth, C., Mathot, S. and Becquevort, S. (1991) Modelling carbon cycling through phytoplankton and microbes in the Scotia-Weddell Sea area during sea ice retreat. Marine Chemistry, 35: 305-324.

Lancelot, C., Mathot, S., Veth, C. and deBaar, H.J.W. (1993) Factors controlling phytoplankton ice-edge blooms in the marginal ice-zone of the north western Weddell Sea during sea ice retreat 1988: field observations and mathematical modelling. Polar Biology, 13: 337-387.

Landing, W.M., Haraldsson, C. and Paxeus, N. (1986) Vinyl polymer agglomerate based transition metal cation chelating ion-exchange resin containing the 8-hydroxyquinoline functional group. Analytical Chemistry 58, 3031-3035.

Lange, M.A., Ackley, S.F., Wadhams, P., Dieckmann, G.S. and Eicken, H. (1989) Development of sea ice in the Weddell Sea, Annals of Glaciology, 12, 92-96.

Lange, M.A. and Eicken, H. (1991) Textural characteristics of sea ice and the major mechanisms of ice growth in the Weddell Sea, Annals of Glaciology, 15, 210-215.

Langway, C.C. (1958) Ice fabrics and the universal stage. USA Cold Regions Research and Engineering Laboratory, CRREL Technical Report, 62.

Lannuzel, D., de Jong, J.T.M., Schoemann, V., Trevena, A., Tison, J.-L. and Chou, L. (2006a). Development of a sampling and flow injection analysis technique for iron determination in the sea ice environment. Analytica Chimica Acta, 556 (2): 476-483.

Lannuzel, D., Schoemann, V., de Jong, J.T.M., Tison, J.-L. and Chou, L. (2006b). Distribution and biogeochemical behaviour of iron in the East Antarctic sea ice. Marine Chemistry, in Press.

Law, C.S., Abraham, E.R., Watson, A.J. and Liddicoat, M.I. (2003) Vertical eddy diffusion and nutrient supply to the surface mixed layer of the Antarctic Circumpolar Current. Journal of Geophysical Research, 108 (C8): 3272.

Levitus, S., Burgett, R. and Boyer,T.P. (1994) World Ocean Atlas, vol. 4, Temperature. Natl. Ocean and Atmos. Admin., Washington, D. C., pp. 117p.

Longhurst, A., Sathyendranath, S., Platt, T. and Caverhill, C. (1995) An estimate of global primary production in the ocean from satellite radiometer data. J. Plankton Res., 17 (6): 1245-1271.

Löscher, B.M., de Baar, H.J.W., de Jong, J.T.M., Veth, C. and Dehairs, F. (1997) The distribution of Fe in the Antartic Circumpolar Current. Deep-Sea Research Part II, 44: 143-187.

Mahowald, N.M. and Luo, C. (2003) A less dusty future? Geophysical Research Letters, 30 (17), 1903.

Maldonado, M.T. and Price, N.M. (1999) Utilization of iron bound to strong organic ligands by plankton communities in the subarctic Pacific Ocean. Deep Sea Research Part II: Topical Studies in Oceanography, 46(11-12): 2447-2473.

Maranger, R, Bird, D.F. and Price, N.M. (1998) Iron acquisition by photosynthetic marine phytoplankton from ingested bacteria. Nature 396: 248-251.

Maranger, R. and Pullin, M.J. (2003) Elemental complexation by dissolved organic matter in lakes: Implications for Fe speciation and the bioavailability of Fe and P. In Aquatic Ecosystems: Interactivity of Dissolved Organic Matter, Findlay, S. and Sinsabaugh, R., eds., Academic Press.

Marsland, S.J., Bindoff, N.L., Williams, G.D. and Budd, W.F. (2004) Modeling water mass formation in the Mertz Glacier Polynia and Adélie Depression, East Antarctica. Journal of Geophysical Research, 109, C11003.

Martin, J.H. and Fitzwater, S.E. (1988) Iron deficiency limits phytoplankton growth in the north-east Pacific subarctic. Nature, 331: 341-343.

Martin, J.H. (1990a) Glacial-interglacial CO2 change: the iron hypothesis. Paleoceanography, 5: 1-13.

Martin, J.H., Fitzwater, S.E. and Gordon, R.M. (1990b) Iron deficiency limits phytoplankton growth in Antarctic waters, Global Biogeochemical Cycles, 4(1), 5-12, 10.

Maykut, G.A. (1985) The ice environment. In: Horner, R.A. (Ed.) Sea Ice Biota. Boca Raton, CRC Press, pp21-82.

Measures, C.I., Yuan, J. and Resing J.A. (1995) Determination of iron in seawater by flow injection analysis using in-line preconcentration and spectrophotometric detection. Marine Chemistry 50, 3-12.

Millero, F.J. and Sotolongo, S. (1989) The oxidation of Fe(II) with H_2O_2 in seawater. Geochimica Cosmochimica Acta, 53(8): 1867-1873.

Millero, F.J., Yao, W. and Aicher, J.A. (1995) The speciation of Fe(II) and Fe (III) in natural waters. Marine Chemistry 50, 21–39.

Mills, M.M., Ridame, C., Davey, M., La Roche, J. and Geider, R. J.(2004) Iron and phosphorus co-limit nitrogen fixation in the eastern tropical North Atlantic, Nature, 429, 292–294.

Mitchell, G.B., Brody, E.A., Holm-Hansen, O., McClain, C. and Bishop, J. (1991) Light limitation of phytoplankton biomass and macronutrient utilization in the Southern Ocean. Limnology and Oceanography, 36(8): 1662-1677.

Moore, J.K. and Abbot, M.R. (2000) Phytoplankton chlorophyll distributions and primary production in the Southern Ocean. Journal of Geophysical Research, vol 105, C12, 28709-28722.

Moore, J.K. and M.R. Abbott (2002) Surface chlorophyll concentrations in relation to the Antarctic Polar Front: seasonal and spatial patterns from satellite observations. Journal of Marine Systems 37: 69- 86.

Nakawo, M. and Sinha, N.K. (1981) Growth rate and salinity profile of first-year sea ice in the Arctic. Journal of Glaciology, 27 (96): 315-330.

Nelson, D.M. and Smith, W.O. Jr (1991) Sverdrup revisited: Critical depths, maximum chlorophyll levels, and the control of Southern Ocean productivity by the irradiance-mixing regime. Limnology and Oceanography, 36(8): 1650-1661.

Nodwell, L.M. and Price, N.M., (2001) Direct use of inorganic colloidal iron by marine mixotrophic phytoplankton. Limnology and Oceanography 46(4), 765-777.

Nolting, R.F., de Baar, H.J.W., van Bennekom, A.J. and Masson, A. (1991)Cadmium, copper and iron the Scotia Sea, Weddell Sea and Weddell/Scotia Confluence (Antarctica). Marine Chemistry, 35, 219-243.

Obata, H., Karatani, H. and Nakayama, E. (1993) Automated determination of iron in seawater by chelating resin concentration and chemiluminescence detection. Analytical Chemistry 65, 1524-1528.

O'Sullivan, D.W., Hanson Jr,. A.K. and Kester, D.R. (1995) Stopped flow luminol chemiluminescence determination of Fe(II) and reducible Fe in seawater at subnanomolar levels. Marine Chemistry 49, 65-77.

Palmisano, A.C. and Garrison, D.L. (1993) Micro-organisms in Antarctic sea ice. In:

Friedman, E.I. (Ed.) Antarctic Microbiology. Wiley-Liss, New York, pp. 167-218.

Penrose, J.D., Conde, M. and Pauly, T.J. (1994) Acoustic detection of ice crystals in Antarctic waters. Journal of Geophysical Research 99, 12573-12580.

Petit, J.R., Jouzel, J., Raynaud, D., Barkov, N.I., Barnola, J.M., Basile, I., Bender, M., Chappellaz, J., Davis, M., Delaygue, G., Delmotte, M., Kotlyakov, V.M., Legrand, M., Lipenkov, V.Y., Lorius, C., Pepin, L., Ritz, C., Saltzman, E. and Stievenard, M. (1999) Climate and atmospheric history of the past 420,000 years from the Vostok ice core, Antarctica. Nature, 399: 429-436.

Powell, R.T., King, D.W. and Landing, W.M. (1995) Iron distributions in surface waters of the south Atlantic. Marine Chemistry 50, 13-20.

Powell, R.T. and Wilson-Finelli, A. (2003) Photochemical degradation of organic iron complexing ligands in seawater. Aquatic Science 65, 367-374.

Reimnitz, E., Kempema, E.W., Wefer, W.S., Clayton, J.R. and Payne, J.R. (1990) Suspended-matter scavenging by rising frazil ice. In: Ackley, S.F., Weeks, W.F. (Eds.), Sea ice properties and processes: Proceedings of the Sea ice symposium. CRREL Monograph 90-1. Cold Region Research and Engineering Laboratory, Hanover, pp. 97-100.

Rintoul, S.R., Hughes, C.W. and Olbers, D. (2001) The Antarctic Circumpolar Current System. In: Siedler, G., Church, J. & Gould, J. (Eds.) Ocean Circulation & Climate. Blackwell, 271-302.

Rose, A.L. and Waite, T.D. (2001) Chemiluminescence of luminol in the presence of iron(II) and oxygen: oxidation mechanism and implications for its analytical use. Analytical Chemistry, 73:5909-5920.

Sakshaug, E., Slagstad, D. and Holm-Hansen, O. (1991) Factors controlling the development of phytoplankton blooms in the Antarctic Ocean - a mathematical model. Marine Chemistry, 35: 259-271.

Sanudo-Wilhelmy, S.A., Olsen, K.A., Scelfo, J.M.; Foster, T.D. and Flegal, A.R. (2002) Trace metal distributions off the Antarctic Peninsula in the Weddell Sea. Marine Chemistry, 77: 157-170.

Sarmiento, J.L., Hughes, T.M.C., Stouffer, R.J. and Manabe, S. (1998) Simulated response of the ocean carbon cycling to anthropogenic carbon warming. Nature 393, 245.

Sarthou, G. (1996). Géochimie du fer dans les eaux de surface océaniques en rapport avec la production primaire. Etude de deux environnements contrastés : l'Océan Austral et la Mer Méditerranée. Thèse de doctorat, Université de Toulouse III.

Schoemann, V., de Baar, H.J.W., de Jong, J.T.M. and Lancelot C. (1998) Effects of phytoplankton blooms on the cycling of manganese and iron in coastal waters. Limnology and Oceanography 43(7): 1427-1441.

Schoemann, V., Lannuzel, D., Becquevort, S., Tison, J.-L., Trevena, A., de Jong, J.T.M., Delille, B., Sauvée, M.-L., Lancelot, C. and Chou, L. (2005) The role of microbiological processes in the cycling of Fe in Antarctic sea ice during spring. Gordon Research Conference on Polar Marine Science, Ventura, USA, March 13-18, 2005.

Schoemann, V., Lannuzel, D., Becquevort, S., Tison, J.-L., Trevena, A., de Jong, J.T.M., Delille, B., Sauvée, M.-L., Lancelot, C. and Chou, L. (2006) Impact of microbiological processes in the cycling of Fe in Antarctic sea ice. AGU/TOS/ASLO meeting, Honolulu, Hawaii, USA, February 20-24, 2006.

Schnack-Schiel, S.B., Thomas, D.N., Haas, C., Mizdalski, E. and Dahms, H.-U. (1998) Copepods in Antarctic sea ice. Antarctic Research Series 73, 173-182.

Schnack-Schiel, S.B. (2003) The macrobiology of sea ice a Ice - An introduction to its physics, chemistry, biology and geology. Oxford: Blackwell Science, pp. 211-239.

Sedwick, P.N. and DiTullio, G.R. (1997) Regulation of algal blooms in Antarctic shelf waters by the release of iron from melting sea ice. Geophysical Research Letters, 24(20): 2515-2518.

Sedwick, P.N., DiTullio, G.R. and Mackey, D.J. (2000) Iron and manganese in the Ross Sea, Antarctica: seasonal iron limitation in Antarctic shelf waters. Journal of Geophysical Research, 105: 11321-11336.

Sedwick, P.N., Harris, P.T., Robertson, L.G., McMurtry, G.M., Cremer, M.D. and Robinson, P. (2001) Holocene sediment records from the continental shelf of Mac. Robertson Land, East Antarctica, Paleoceanography, 16(2), 212-225.

Siegenthaler, U. and Sarmiento, J.L. (1993) Atmospheric carbon dioxide and the ocean. Nature, 365: 119-125.

Sigman, D.M. and Boyle, E.A. (2000) Glacial/interglacial variations in atmposheric carbon dioxide. Nature, 407, 859-869.

Smetacek, V. (2001) EisenEx, International team conducts iron experiment in the Southern Ocean. US JGOFS News 11:11–4.

Smetacek, V., Assmy, P. and Henjes, J. (2004) The role of grazing in structuring Southern Ocean pelagic ecosystems and biogeochemical cycles. Antarctic Science, 14(4): 541-558.

Smith, W.O.Jr. and Nelson, D.M. (1985) Phytoplankton bloom produced by a receding ice edge in the Ross Sea: Spatial coherence with the density field. Science, 227: 163-166.

Sorria-Dengg, S. and Horstmann, U. (1995) Ferrioxamines B and E as iron sources for the marine diatom Phaeodactylum Tricornutum. Marine Ecology Progress Series, 127, 269-277.

Speer, K.G., Rintoul, S.R. and Sloyan, B.M. (2000) The diabatic Deacon cell. Journal of Physical Oceanography 30, 3212-3222.

Sullivan, C.W., Arrigo, K.R., McClain, C.R., Comiso, J.C. and Firestone, J. (1993) Distributions of phytoplankton blooms in the Southern Ocean. Science, 262, 1832–1837.

Sunda, W.G. and Huntsman, S.A. (1995) Iron uptake and growth limitation in oceanic and coastal phytoplankton. Marine Chemistry, 50: 189-206.

Sunda, W.G. and Huntsman, S.A. (1997) Interrelated influence of iron, light and cell size on marine phytoplankton growth. Nature, 390: 389-392.

Sunda, W.G. (2001) Bioavailability and bioaccumulation of iron in the sea. In: Turner, D.R., Hunter, K.H., (Eds.) The Biogeochemistry of Iron in Seawater, IUPAC Series on Analytical and Physical Chemistry of Environmental Systems. Volume 7, pp. 41-84.

Stocker, T.F. and Schmittner, A. (1997) Influence of CO2 emission rates on the stability of the thermohaline circulation. Nature, 388: 862-865.

Tegen, I., Werner, M. Harrison, S.P., Kohfeld, K.E. (2004) Geophysical Research Letters 31, L05105.

Thomas, D.N., Lara, R., Hass, C., Schnack-Schiel, S.B., Nötig, E.-M., Dieckmann, G.S., Kattner, G. and Mizdalski, E. (1998) Biological soup within decaying summer sea ice in the Amundsen Sea, Antarctica. Antarctic Research Series 73, 161-171.

Thomas, D.N. (2003) Iron limitation in the Southern Ocean. Science, 302: 565.

Timmermans, K.R., Stolte, W. and de Baar, H.J.W. (1994) Iron-mediated effects on nitrate reductase in marine phytoplankton. Marine Biology 121: 389 - 396.

Trenberth, K.E., Large, W.G. and Olson, J.G. (1990) The mean annual cycle in global ocean wind stress. Journal of Physical Oceanography, 20, 1742-1760.

Trick, C.G., Andersen, R.J., Price, N.M., Gillam, A. and Harrison, P.J. (1983) Examination of hydroxamate-siderophore production by neritic euryotic phytoplankton. Marine Biology, 75, 9-17.

Trull, T., Rintoul, S.R., Hadfield, M. and Abraham, E.R. (2001) Circulation and seasonal evolution of polar waters south of Australia: implications for iron fertilization of the Southern Ocean. Deep-Sea Research II, 48, 2439-2466.

Van Leeuwe, M.A. (1997) Iron and light interactions with phytoplankton growth in the Southern Ocean. PhD thesis, NIOZ, pp. 189.

Voelker, B.M. and Sedlak, D.L. (1995) Iron reduction by photoproduced superoxide in seawater. Marine Chemistry 50: 93–102.

Watson, A.J. and Orr, J.C. (2003) Carbon dioxide fluxes in the global ocean. In: Fasham, M.J.R. (Ed.), Ocean biogeochemistry: The role of the ocean carbon cycle in global change. Springer-Verlag, Berlin.

Watson, A.J. (2001) Iron limitation in the Oceans. In: Turner, D.R., Hunter, K.H., (Eds.), the biogeochemistry of iron in seawater, IUPAC Series on Analytical and Physical Chemistry of Environmental Systems. Volume 7, pp. 9-39.

Wedepohl, K.H. (1995) The composition of the continental crust. Geochimica Cosmochimica Acta, 59: 1217-1232.

Weeks, D.A. and Bruland, K.W. (2002) An improved flow injection analysis method for the determination of iron in seawater. Analytica Chimica Acta, 453: 21-32

Weeks, W.F. and Ackley, S.F. (1982) The growth, structure, and properties of sea ice.

Weeks, W.F. and Ackley, S.F. (1986) The growth, structure and properties of sea ice. In: Untersteiner, N. (Ed.), The Geophysics of sea ice. NATO ASI series, pp. 9-164.

Weissenberger, J. and Grossmann, S. (1998) Experimental formation of sea ice: importance of water circulation and wave action for incorporation of phytoplankton and bacteria. Polar Biology, 20: 178-188.

Wells, M.L., Price, N.M. and Bruland, KW. (1995). Iron chemistry in seawater and its relationship to phytoplankton: a workshop report. Marine Chemistry, 48, 157-182.

Westerlund, S. and Öhman, P. (1991) Iron in the water column of the Weddell Sea. Marine Chemistry, 35: 199-217.

Worby, A.P., Massom, R.A., Allison, I., Lytle, V.I. and Heil, P. (1998) East Antarctic sea ice: a review of its structure, properties and drift, In Jeffries M.O. (editor), Antarctic sea ice: physical processes, interactions and variability, Antarctic Research Series, vol. 74, American Geophysical Union, 41-67.

Wu, J., Boyle, E., Sunda, W. and Wen, L.-S. (2001) Soluble and colloidal iron in the oligotrophic North Atlantic and North Pacific. Science 293, 847-849.

Yentsch, C.S. and Menzel, D.W. (1963) A method for the determination of phytoplankton chlorophyll and phaeophytine by fluorescence, Deep-Sea Research, 10: 221-231.

APPENDICES

Available online at www.sciencedirect.com
SCIENCE DIRECT
Analytica Chimica Acta 556 (2006) 476–483
ANALYTICA CHIMICA ACTA
www.elsevier.com/locate/aca

Development of a sampling and flow injection analysis technique for iron determination in the sea ice environment

Delphine Lannuzel[a,*], Jeroen de Jong[a], Véronique Schoemann[b], Anne Trevena[c,1], Jean-Louis Tison[c], Lei Chou[a]

[a] *Laboratoire d'Océanographie Chimique et Géochimie des Eaux, Université Libre de Bruxelles, Campus de la Plaine CP208, Bd. du Triomphe, B-1050 Bruxelles, Belgium*
[b] *Ecologie des Systèmes Aquatiques, Université Libre de Bruxelles, Campus de la Plaine CP221, Bd. du Triomphe, B-1050 Bruxelles, Belgium*
[c] *Unité de Glaciologie, Université Libre de Bruxelles CP 160/03, 50 Av. F. D. Roosevelt, B-1050 Bruxelles, Belgium*

Received 1 June 2005; received in revised form 19 September 2005; accepted 26 September 2005
Available online 27 October 2005

Abstract

A trace metal clean method for sampling and analysis of iron is set up and applied to sea ice and its associated snow, brine, and underlying seawater sampled during the Antarctic expedition "ARISE in the East" (Antarctic Remote Ice Sensing Experiment, AA03-V1, September–October 2003, 64–65°S/112–119°E, RV *Aurora Australis*). For clean sampling, a non-contaminating electropolished stainless steel ice corer is designed in conjunction with a polyethylene lathe equipped with Ti chisels to remove possibly contaminated outer layers of ice cores. A portable peristaltic pump with clean tubing is used on the ice to sample the underlying seawater (interface ice–water = 0, 1 and 30 m) and sea ice brine from access holes. Considering the extreme range of salinities (1–100) and Fe concentrations (0.1–100 nM) previously observed in similar environments, it is of paramount importance to set up a simple and sensitive Fe analyser adapted to such gradients. We use a flow injection analysis (FIA) technique and successfully demonstrate its capability to measure Fe concentrations directly in the sample without an on-line preconcentration/matrix separation step. We test the sensitivity, accuracy, precision and long-term stability of the analytical procedure. Also we explore and remediate interferences from a suite of other trace elements, such as Ni, Cd, Cr, Mn, Cu, Zn and Co. Analysis of reference materials NASS-5 and CASS-3 gives a good agreement with the certified values. Repeated measurements over a period of 5 months of an "in-house" Antarctic seawater standard yields a concentration of 1.02 ± 0.07 nM ($n = 17$, 1σ). The detection limit (3σ of the blank) is on average 0.12 nM. We report here results of the Fe distribution in sea ice that are in good agreement with previously published data. To our knowledge, this work provides the first complete profiles of total dissolvable and dissolved Fe in sea ice.

Keywords: Iron; FIA; Sea ice; Direct measurement; Chemiluminescence

1. Introduction

As a potentially limiting micro-nutrient for algal growth in the oceans, iron (Fe) is strongly involved in marine biogeochemical cycling [1,2]. Sea ice is of importance to global climate as it covers large areas of the polar oceans and this coverage shows strong seasonal changes [3,4]. Present at the interface between atmosphere and ocean, sea ice may play an important role in the ocean–atmosphere exchange of carbon (CO_2), sulphur (DMS) and Fe. The scarcity of reliable Fe data in sea ice [5,6] mainly results from the analytical challenges encountered in this extreme environment, which makes the biogeochemical cycle of iron in sea ice virtually unknown as to date.

Recent advances in shipboard flow injection techniques for the measurement of iron in seawater have greatly facilitated the collection of reliable data [7,8]. Not only can data now be collected in near real-time mode, but also contamination problems can be quickly identified during sampling campaigns. Most of these methods use luminol chemiluminescence for detection [9–13], though some rely on spectrophotometric detection [14–16]. Another characteristic of the Fe-FIA methods used today, is that they nearly all apply on-line preconcentra-

* Corresponding author. Tel.: +32 2 650 52 78.
E-mail address: dlannuze@ulb.ac.be (D. Lannuzel).
[1] Present address: Department of Environment North West Region, P.O. Box 836, Karratha, WA 6714, Australia.

0003-2670/$ – see front matter © 2005 Elsevier B.V. All rights reserved.
doi:10.1016/j.aca.2005.09.059

tion/matrix separation using resins of 8-hydroxyquinoline (8-HQ) immobilized on a carrier of PVC based polymer [17] or alkoxyglass [13]. Exceptions are the stopped-flow method by O'Sullivan et al. that measures total dissolved Fe directly in the sample, and those FIA applications for analysing reduced Fe(II) directly in ambient seawater in which it is required to measure the sample immediately in order not to loose any Fe(II) by rapid re-oxidation [18,19].

The use of a column packed with 8-HQ resin aims at reaching low detection limits by on-line preconcentration followed by elution in a small volume of dilute acid. It also rejects sea-salts due to its high affinity for transition metals and low affinity for the major ions. Major ions would not only interfere with iron–luminol chemiluminescence, but would also clog the detector flow cell due to precipitation at the optimal high pH of the luminol reaction. The preconcentration technique requires tedious resin synthesis schemes, as well as column set up that can be problematic. Not every attempt to synthesize 8-HQ resin is successful and every new batch of the resin product needs careful characterization of its chromatographic properties and blank levels before it can be brought into use. Various factors control potential occurrence of backpressure problems, which may lead to limited flow-through and even severe leaking problems. They are the type of carrier resin (porosity, particle size), the length and diameter of the column, the connectors, the Teflon or polypropylene frits or nylon net to hold the resin in the column, and the flow speed. Another complication associated with 8-HQ resins is that their yields may be influenced by competition between natural organic ligands and the 8-HQ, leading to underestimations of the concentration. This is especially crucial when standard additions are performed on one seawater sample only and all the others are related to this calibration. When not using a preconcentration step, dissolved organic matter can also interfere by absorbing the luminescent signal, competing for radical intermediates or complexing Fe(II) [12]. In any case, these matrix interferences can be cancelled out by applying standard addition calibration to every sample.

Luminol (3-aminophtalhydrazide) is well known to produce strong chemiluminescence with Fe or cobalt and, to a lesser extent, with other transition metals. FIA methods for Fe are based on the Fe-mediated chemiluminescent reaction between luminol and O_2 or H_2O_2. During the oxidation of luminol, blue light is emitted and detected by a photon counter. The peak area or peak height of the signal is proportional to the amount of dissolved Fe present in the analyte. The use of O_2 or H_2O_2 depends on whether Fe(II) or Fe(III) is the Fe species of interest [13,20]. The advantage of the Fe(II) driven chemiluminescence is that the reaction is instantaneous and can take place inside the detector flow cell so that analysis time can be kept short. Peak shapes are sharp and sensitivity is generally high, so that preconcentration volumes and times can be minimized. In the case of Fe(III) driven chemiluminescence, the Fe sample is delayed in a long reaction loop while being mixed with luminol, reaction buffer and H_2O_2 before being introduced in the detector flow cell. This leads to a longer analysis time, smearing of the signal due to wall friction in the flow circuit and lower sensitivity. The latter requires higher preconcentration factors hence higher sample volume. The Fe(II) based methods involve a lengthy reduction step, with for instance sodium sulphite to convert thermodynamically favoured Fe(III) into Fe(II), while the Fe(III) method can measure samples without this preliminary step. All FIA methods for total dissolved Fe measurement require that filtered samples are acidified at least 24 h before analysis to solubilize the iron, while unfiltered seawater samples for total dissolvable Fe should be kept for several weeks to months at low pH in order to release as much as possible the leachable particulate Fe species.

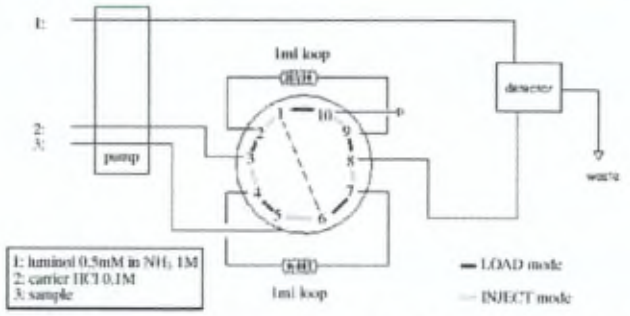

Fig. 1. Schematic diagram of FeLume. Pump runs at 8 rpm (1: 3.9 ml/min; 2: 2.0 ml/min; 3: 2.0 ml/min).

In this paper, we report a new FIA application, which can measure total dissolvable (unfiltered) and total dissolved Fe (0.2 μm filtered) directly in the sample at subnanomolar levels in natural waters with a wide range of salinities, without a preconcentration step. This application takes advantage of the high sensitivity of Fe(II) driven chemiluminescence, whilst eluding the aforementioned problems associated with the use of 8-HQ resins.

2. Experimental

2.1. Instrumental

Our FIA instrument (Fig. 1) is an automated continuous flow system (FeLume, Waterville Analytical, USA) that detects chemiluminescence from the reaction of luminol and dissolved Fe(II) by directly injecting a natural water sample from a 1 ml sample loop into the detector flow cell. Sample preparation is adapted from Bowie et al. and O'Sullivan et al. To ensure that all the Fe is under the Fe(II) form, the reductant sodium sulphite (Na_2SO_3) in dilute ammonium acetate (NH_4Ac) is added to the acidified sample and allowed to react for 24 h before analysis [12]. A Valco 10-port selection valve (VICI, Switzerland, not shown in Fig. 1) switches between the samples to be analysed. A Valco 10-port injection valve with two 1 ml sample loops switches between load and inject mode. While one loop is being loaded with a sample (240 s), the sample already in the other loop is being injected (240 s) with a 0.1 M HCl carrier into the detector where it mixes with a 0.5 mM luminol–1 M NH_3 ammonia buffer at an optimal reaction pH 10.1. The detector consists of a 0.3 cm^3 Plexiglas spiral flow cell facing the photon counter (Hamamatsu HC-135). Pump tubing (Tygon), polypropylene reagents straws (Bran and Luebbe) and 1/8 in. and 1/16 in. ID teflon FEP tubing (Cole-Parmer) are used to transport reagents

and sample to the detector via an 8-channel peristaltic pump (Minipuls 3, Gilson) at a rate of 8 rpm. The flow rates (Fig. 1) were optimised to minimize backpressure and to obtain a narrow peak.

Each sample is measured by the method of standard additions (sample plus increasing additions of fresh Fe(II) to three aliquots of the same sample). Each sample solution is measured in triplicate using peak area integrations. One analytical run takes 45 min and requires about 60 ml sample volume.

2.2. Cleaning procedures

All plasticware (LDPE, HDPE, FEP, PFA) used for trace metal work was cleaned as follows: first soaking in a detergent bath (RBS 5%, v/v) for 24 h, followed by rinsing 3× with deionized water and then 3× with ultra high purity water (UHP) (18.2 MΩ Millipore milli-Q system) before being filled with 6 M HCl (Merck, reagent grade) for 1 week. In a trace metal clean room, items were then rinsed 5× with UHP water and dried inside a class-100 laminar flow hood. Bottles and containers acid-cleaned were sealed in triple plastic bags until use.

Polycarbonate filters (0.2 μm porosity, 47 mm diameter, Nuclepore) were treated in 1 M HCl ultrapure (Ultrex, J.T. Baker) for 1 week before being gently rinsed 5× and stored in UHP before use. Pipette tips were manipulated inside a class-100 laminar flow hood and rinsed 5× with 6 M HCl (J.T. Baker) and 5× with UHP before use.

Large polyethylene plastic bags (Vink) dedicated to sea ice core storage were acid-cleaned in 1 M HCl for 1 week and then rinsed 5× with UHP water, before being sealed in three zip-lock bags.

LDPE bottles for Fe measurement by standard additions (three additions per sample) were rinsed 5× with UHP water between uses, filled with 6 M HCl overnight and rinsed again 5× with UHP water.

Between runs, FIA lines were filled with UHP water to avoid memory effects or adsorption of the last sample analysed on the walls of the Teflon tubing. The lines are also rinsed with 1 M HCl and UHP water at the beginning and at the end of each analytical session.

2.3. Reagents

2.3.1. Acids

Samples are acidified to pH 1.8 with 14 M HNO_3 (J.T. Baker, Ultrex, 100 μl per 100 ml sample). A 0.1 M HCl carrier and 0.2 M HCl for Fe(II) working solutions are prepared by dilutions of 30% HCl (Merck, suprapure) in 1 l UHP water. One molar HCl cleaning acid is prepared by diluting 32% HCl (Merck, reagent grade) in UHP water.

2.3.2. Fe(II) standards

Fe(II) stock solution (4 mM) is prepared by dissolution in 0.2 M HCl of 784.28 mg $FeSO_4{\cdot}2H_2O$ in a 500 ml PE volumetric flask. This solution can be stored for 1 month. Two Fe(II) working solutions (40 μM and 400 nM) are prepared daily by serial dilutions of the stock solution in 0.2 M HCl.

2.3.3. Luminol/ammonia buffer 1 M NH_3

One molar NH_3 is prepared by dilution of 73 ml of 25% NH_3 (Merck, reagent grade) in 1 l UHP water. Luminol stock solution (10 mM) is prepared by the dissolution of 250 mg K_2CO_3 (Merck, suprapure) and 177 mg luminol (3-aminophtalhydrazide, Fluka) in 100 ml 1 M NH_3, followed by ultrasonication for 30 min [9]. Luminol working solution (0.5 mM) is prepared at least 24 h in advance to ensure a stable pH by diluting 25 ml of luminol stock solution in 500 ml 1 M NH_3. The luminol powder is used as received and solutions are not further purified.

2.3.4. Ammonium acetate buffer 2 M NH_4Ac

Two molar NH_4Ac buffer is prepared by adding 23.5 ml of 25% NH_3 (Merck, reagent grade) to 11.5 ml of 96% HAc (Merck, reagent grade) and made up to 100 ml with UHP water. The pH is then adjusted to 6.5 by dropwise addition of either NH_3 or HAc. Finally, the buffer is purified by pumping the solution at a rate of 1 ml min^{-1} through two sequential columns packed with Silicagel based 8-HQ resin. 0.1 M NH_4Ac buffer is prepared by diluting 20 times a 2 M NH_4Ac buffer in UHP water.

2.3.5. Reducing agent

Reducing agent is prepared daily by adding 108 mg Na_2SO_3 (Fluka) in 20 ml of 0.1 M NH_4Ac buffer. Complete dissolution is achieved by a 10 min ultrasonicating step. The reducing agent solution is then cleaned by pumping through two sequential Si-8HQ columns prior to its addition to the sample. Seventy-five microliter of reducing agent solution is added per 30 ml sample at pH 1.8 and allowed to react for 24 h. The final reducing agent concentration in the sample is 100 μM [12].

2.3.6. Si-8HQ resin column set up

Si-8HQ resin used to purify the reagents (see above) was made following the procedure of Hill [21]. Columns were constructed from 5 cm Tygon tube (3.17 mm i.d.) and filled with Si-8HQ resin by pipetting. Columns were closed at both ends with nylon nets (63 μm) tightly folded to keep the resin in the tube. Polycarbonate connectors (Cole-Parmer) were used and attached to the Tygon tubing with some cyclohexanone glue (Technilab). Columns were cleaned by passing 1 M HCl and UHP water prior and after use.

2.3.7. Metals solutions

For interference testing, metal solutions were prepared by serial dilutions in 0.2 M HCl of 1000 ppm standards (Merck, CertiPUR) of $Co(NO_3)_2$, $Ni(NO_3)_2$, $Mn(NO_3)_2$, $Cu(NO_3)_2$, $Cd(NO_3)_2$, $Cr(NO_3)_3$ and $Zn(NO_3)_2$. The reducing agent and 2 nM freshly prepared Fe(II) were first added to the unfiltered seawater matrix before spiking with other metals.

2.4. Field sampling

Samples were collected and processed under trace metal clean conditions during the Antarctic expedition "ARISE in the East" (AA03-V1, September–October 2003, 64–65°S/

112–119°E, RV *Aurora Australis*). Samples of snow, brine (collected at 2 depths), seawater (0, 1 and 30 m deep) and sea ice (four sections chosen depending on the ice texture and visual observation of ice algae) were collected upwind from the ship under trace metal clean conditions. Great attention was paid to prevent contamination: the sampling site was off-limits to unauthorized personnel, analysts were wearing clean room garments (Tyvek overall, overshoes and polyethylene gloves) over their warm clothes, and items dedicated to sample collection and storage were acid-cleaned and sealed in plastic bags. First, snow was collected with polyethylene shovels, upon which the ice–water interface was accessed using electropolished stainless steel ice corer and seawater was pumped up with a portable peristaltic pump (Cole-Parmer, Masterflex E/P) and trace metal clean tubing. Access holes ("sack holes") were drilled into the sea ice cover at various depths to allow gravity-driven brine collection and sampling with the latter device. Finally, a set of sea ice cores was collected using the same non-contaminating ice corer.

For the ice corer different materials were considered in order to comply with the following characteristics: (1) trace metal cleanliness, (2) mechanical strength and (3) resistance to below 0 °C temperatures. Teflon, the material of choice for trace metal clean sampling, is unsuitable for sea ice coring because of its high plasticity. Teflon coated PVC and acrylate were also deemed unfit because these materials become brittle at low temperatures. Teflon coated stainless steel would be a good choice if the Teflon would not erode away during use. Titanium is a good option but its high cost makes it less attractive, although it could still be a useful alternative for smaller ice cutting accessories. The material finally chosen was electropolished stainless steel (Lichtert Industry, Belgium).

Cores retrieved for Fe study were kept in acid-cleaned plastic bags and stored frozen at −28 °C in the dark until further processing. Inside a shipboard clean laboratory under a class-100 laminar flow hood, sea ice was cut in slices of 6–10 cm thick using a titanium coated stainless steel saw (Lichtert Industry, Belgium). Ice core slices were melted in PE containers and the meltwater was subsequently filtered using a Sartorius polycarbonate filtration device with Teflon O-rings. A gentle pressure of not more than 0.3 atm was maintained with a hand pump to avoid the rupture of phytoplankton cells [22,23]. Brine, snow and seawater were filtered on board as well. Membrane filtration (0.2 μm) operationally separates "dissolved" Fe species from suspended particulate matter. The filtrate (containing dissolved Fe, DFe hereafter) is acidified to pH 1.8 (14 M HNO_3, J.T. Baker, Ultrex) at least 24 h before being analysed. Total dissolvable Fe (TDFe, unfiltered) is acidified and stored at pH 1.8 at least 6 months before measurement by FIA [7] to release all but the most refractory Fe species into the dissolved form.

3. Results and discussion

3.1. Metal ions interferences

Experiments to examine metal ion interferences were conducted with unfiltered Antarctic seawater from 30 m depth to which 2 nM fresh Fe(II) was added. Individual metal ions (Co(II), Mn(II), Cu(II), Zn(II), Cr(III), Cd(II) and Ni(II)) were then spiked to study possible changes in the Fe(II) signal as a function of the type and amount of metal added. Independent tests were performed on samples at pH 1.8 and 5.3. The pH of the sample was brought from 1.8 to 5.3 by adding purified 2 M NH_4Ac buffer to the sample (1 ml buffer pH 6.5 per 30 ml sample at pH 1.8) 4 h prior to analysis by FIA. The 4 h delay allows the sodium sulphite in the sample to reduce any Fe(III), which could have formed as a result of the increase of pH [12]. An overview of the spike experiment with added concentrations of each metal is given in Table 1.

The addition of 20 nM Zn, Cd, Cr or Ni seems to result in an increased chemiluminescent Fe(II) signal at a sample pH 1.8 whereas no perturbation was encountered at a sample pH 5.3 (Table 1). No Mn interferences were observed at both pH 1.8 and 5.3. Co(II) did not interfere at sample pH 1.8 and 5.3 when added at similar or lower concentrations as Fe(II). At higher Co(II) concentrations there is an Fe overestimation (e.g. 146 ± 10% when 3.4 nM added). However, Co(II) is unlikely to interfere since it would be present at picomolar levels in most natural samples [1,24,25].

In the case of Cu, an underestimation of Fe was observed with only 67% (±5%) of the signal recovered at pH 1.8 with an 8 nM Cu addition to 2 nM Fe, whereas at pH 5.3 the yield is 91% (±13%) of the signal (Table 1). This result was confirmed with CASS-3 seawater, measured at both pH (1.8 and 5.3). This certified reference seawater contains 8.5 nM Cu and 22.56 nM Fe. At sample pH 1.8, the instrument measured 59% (±3.5%, $n = 5$) of the true value, whereas the results were satisfactory at pH 5.3 (Table 2). The reduced Fe signal can be explained by the fact that at pH 1.8, Cu is in its free ionic form and oxidizes Fe(II) present in the sample, which results in a suppression of

Table 1
Response at pH 1.8 and 5.3 of interfering metals in 30 m Antarctic seawater with 2 nM Fe(II) added, normalised to the response of 2 nM Fe(II) in 30 m Antarctic seawater

	Metal added						
	1.7 nM Co	17 nM Mn	8 nM Cu	20 nM Zn	20 nM Cr	20 nM Cd	20 nM Ni
% (signal metal added)/(signal Fe) pH 1.8	108 ± 2	103 ± 6	67 ± 5	113 ± 12	122 ± 4	140 ± 5	121 ± 8
% (signal metal added)/(signal Fe) pH 5.3	102 ± 2	96 ± 10	91 ± 13	98 ± 5	99 ± 5	102 ± 4	103 ± 8

Uncertainties represent the standard deviation for $n = 3$ independent analysis.

Table 2
Results for dissolved Fe(II + III) in certified seawater solutions

	NASS-5	CASS-3
Certified value (nM Fe)	3.70 ± 0.63	22.56 ± 3.04
FIA value (nM Fe) pH 5.3	3.95 ± 0.61 (n = 4, 2σ)	21.99 ± 4.61 (n = 5, 2σ), 19.6 (n = 1)[a]
FIA value (nM Fe) pH 1.8	3.81 (n = 1)	13.22 ± 1.08 (n = 5, 2σ)

[a] 3× diluted CASS-3 in MQ (salinity 11.3 after dilution).

the signal:

$$Cu(II) + Fe(II) = Fe(III) + Cu(I)$$

The Cu(I) formed is oxidized by O_2 at the reaction pH causing a catalytic oxidation of Fe(II) without involving luminol [12]. Tests were conducted by adding Cu(II) at different timing prior to and during analyses, however, observations were the same independently of the timing of the Cu addition, meaning the reaction is probably instantaneous.

An explanation for the absence of positive or negative interference at pH 5.3, could be that the interfering metal ions recombine with the natural organic ligands present in the sample, which impedes their reaction with Fe(II) or with luminol. The metals we tested for interference are predominantly complexed by organic ligands in natural waters. Another explanation could be that these metals no longer contribute (or at least much less) to luminol chemiluminescence as a result of the pH shift to somewhat higher values inside the flow cell. This would lead to a stronger formation of $Mg(OH)_2$ precipitates, effectively masking these metals (see Section 3.2).

3.2. Sensitivity

The sensitivity of a method can be deduced from the slope of the linear regression line from the calibration curve. Rose and Waite [19] used a model to study the chemiluminescence of luminol in the presence of Fe(II) and O_2: they obtained a non-linear response, which has been observed by Croot and Laan [18] as well. In our case, the calibrations show a slight upward curvature which can be fitted with a second order polynomial of the form $y = ax^2 + bx + c$. The first derivative of the latter equation, when x approaches x_0, gives the slope of the tangent at the point of abscissa x_0 on the curve. We chose a concentration of x_0 at halfway the standard addition range (e.g. $x_0 = 2$ when range is 0–4 nM Fe added) where we compared sensitivities.

As can be seen in Table 3, one of the consequences of measuring the in-house standard at pH 5.3 is a lower sensitivity by nearly a factor 3. At reaction pH > 10, Mg^{2+} precipitates as $Mg(OH)_2$. At sample pH 1.8 and reaction pH 10.1 there is only a weak formation of precipitates in the flow cell, but at sample pH 5.3 this happens more intensely because the pH shift upon mixing of sample and luminol/buffer is smaller. These magnesium hydroxides can interfere by either scavenging Fe(II) and/or scattering the luminescent emission, which results in decreasing the signal intensity [12]. However, the accuracy of the method is not affected (see in-house value Table 3).

Table 3
Fe values and sensitivities (slope of the tangent at x_0 = 2nM) for n independent calibrations of the in-house standard at pH 1.8 and 5.3

	In-house value (nM Fe)	Sensitivity (counts/nM Fe)
pH 1.8 (n = 13, 1σ)	1.02 ± 0.09	8661 ± 4227
pH 5.3 (n = 4, 1σ)	1.03 ± 0.05	3405 ± 1607

Table 4
Fe values and sensitivities (slope of the tangent at x_0 = 4 nM) for a brine sample salinity 80.1 (TDFe = 36.7 nM) diluted 2.5×, 5× and 10× in UHP water

Salinity	32.0	16.0	8.0
TDFe value (nM) pH 5.3	34.1	35.1	34.7
Sensitivity (counts/nM Fe)	22020	17050	11395

Salinity in samples from the sea ice environment may range from 0 up to 100. Experiments conducted at different salinities exhibited higher sensitivity at higher salinity (Table 4). This may be due to an enhancing effect of chloride ions on the chemiluminescence reaction [9].

The age of luminol and carrier solutions seems to affect the sensitivity of the instrument also. Practically, the sensitivity was improved when using luminol working solution prepared at least 24 h before analysis.

3.3. Blanks and detection limit

The reagent blank of the FeLume results from the addition to a sample of the following chemicals: (1) HNO_3 (J.T. Baker, Ultrex) used to acidify the samples, (2) sodium sulphite reducing agent in dilute NH_4Ac buffer and (3) 2 M NH_4Ac buffer to change the pH of the sample from 1.8 to 5.3 in order to minimize possible metal interferences. These three reagents were all added in single and double volumes to assess their possible contamination. The Fe content of the added reagents was not detectable. The detection limit was estimated by repeated analysis of UHP water and calculated as 3σ of the UHP concentration. This was done at sample pH 1.8 and 5.3. At pH 1.8 the DL is 0.12 ± 0.07 nM (n = 12) and at pH 5.3 DL is 0.20 ± 0.08 nM (n = 8).

3.4. Accuracy and reproducibility

Certified reference materials CASS-3 (coastal seawater) and NASS-5 (open ocean) available from the National Research Council of Canada, were both measured and results were in good agreement with certified values (Table 2). For quality control purpose (monitoring long-term stability and accuracy of the FeLume) a low Fe in-house standard that was cross-calibrated with above reference materials, was measured together with the samples. Our "in-house" standard is a batch of filtered under-ice seawater from 30 m depth acidified to pH 1.8 with 14 M HNO_3 (J.T. Baker, Ultrex). The long-term stability over a period of 5 months was excellent and averaged 1.02 ± 0.07 nM, n = 17, 1σ.

3.5. Test of possible contamination from the ice corer

A leaching experiment was conducted on a piece of electropolished stainless steel, which was soaked in UHP water

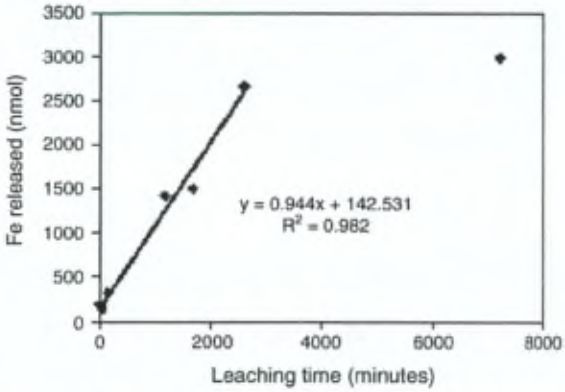

Fig. 2. Fe released (nmol) as a function of time during a leaching experiment on an electropolished stainless steel testing piece in 100 ml of MQ.

for several days. Subsamples taken at regular intervals from the leaching experiment were analysed by ICP-MS and the results indicated low Fe diffusion fluxes from the ice corer (Fig. 2 and Table 5). During the time between drilling an ice core and transferring it from the corer into its protective plastic bags the contamination by the corer is thus negligible.

3.6. Sea ice re-sampling procedure

To assess possible contamination during sampling, processing and/or storage, a duplicate sea ice core was decontaminated at the Glaciology Unit of the University of Brussels (AA03-V1 station XIII/ULB) and compared with the non-decontaminated core processed on board (AA03-V1 station XIII/Field). The decontamination procedure took place at −27 °C, in a class-100 laminar flow bench. The core was mounted in a polyethylene lathe and the 5 mm outer layer was removed mechanically using Ti chisels (Fig. 3). The chisels are made of a glass/Epoxy handle with a Ti blade, which is the only part that comes into contact with the ice core. The inner core and ice chips falling off during the cleaning procedure were collected in clean polyethylene containers and melted, acidified to pH 1.8 and analysed by FIA. On the treated section, outer layer and inner core TDFe values (24.3 ± 1.9 and 23.3 ± 2.7 nM, respectively) suggest that there is no significant difference for the station XIII/Field core at approximately the same depth (22.6 ± 3.5 nM TDFe).

Table 5
Fe leaching electropolished metal object[a]

Slope (nmol min^{-1})	0.943
R	0.991
Dissolution flux (fmol cm^{-2} min^{-1})	12.6
Typical sea ice Fe concentration (nmol l^{-1})	20
Total Fe amount core (nmol)	308
Fe added after 10 min exposure (nmol)	0.6
Contamination (%)	0.2

[a] Testing object surface area = 75.2 cm^2, inner surface ice corer = 4396 cm^2, volume ice corer = 15.4 dm^3.

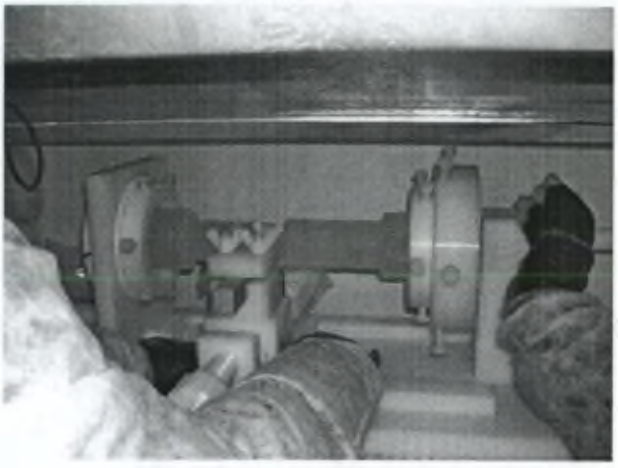

Fig. 3. Sea ice re-sampling procedure (see Section 3.6).

3.7. Fe results in Antarctic sea ice

Vertical profiles of the TDFe and DFe concentrations in a first-year sea ice core at AA03-V1 station XIII (65°15′S, 109°27′E; 20th October 2003), including surface snow, is shown in Figs. 4 and 5. "Sack hole" brine concentrations are indicated by dotted lines. Fig. 6 plots seawater concentrations in the upper 30 m (0, 1 and 30 m) of the under-ice water column at the same station.

Our TDFe and DFe results are in the same range as those reported in previous studies (Table 6) and tend to show relatively high Fe contents in sea ice compared to under-ice seawater. Some TDFe snow concentration levels from previous data sets show that it could potentially contribute to the high observed sea ice values. However, the snow layer at our location was limited to a fine veneer, a few centimetres thick. High snow salinity at this station (20.1) suggests infiltration by low Fe seawater

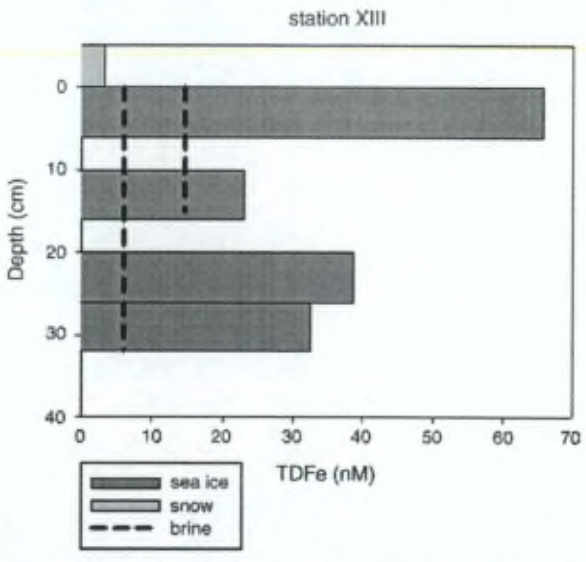

Fig. 4. TDFe (nM) profile in four sections of 32 cm sea ice core, snow and brine at 15 and 30 cm deep at station XIII (20th October, 2003) sampled during the ARISE in the East Antarctic cruise.

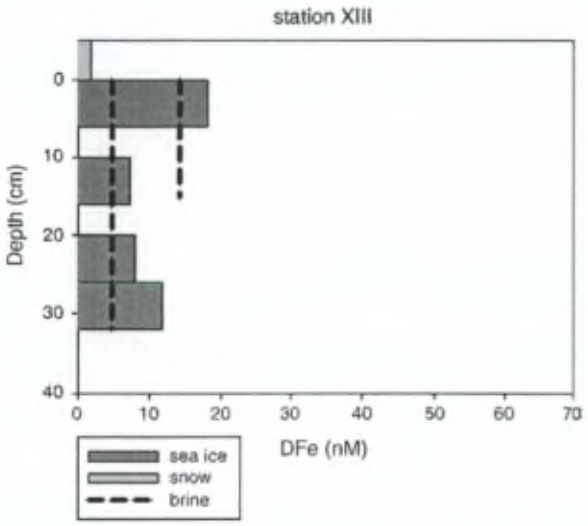

Fig. 5. DFe (nM) profile in four sections of 32 cm sea ice core, snow and brine at 15 and 30 cm deep at station XIII (20th October, 2003) sampled during the ARISE in the East Antarctic cruise.

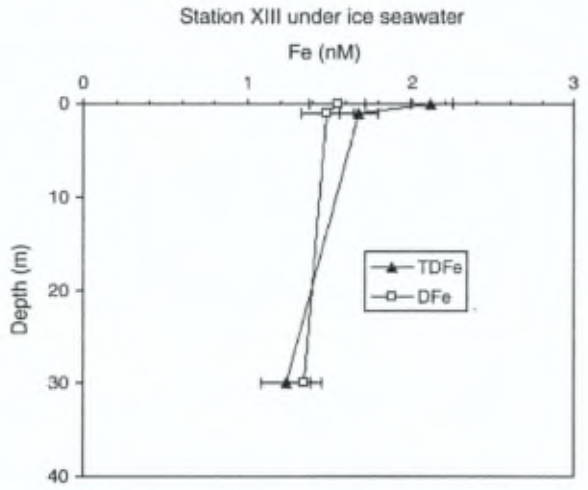

Fig. 6. Under ice seawater profile (0, 1 and 30 m deep) at station XIII.

(Table 6). Long-term dry deposition of Fe-rich aerosols at the sea ice surface could be responsible for the high TDFe values in the sea ice topmost layer at station XIII, but the low ice temperature in the upper half of the sea ice cover (Fig. 7) prevents transfer

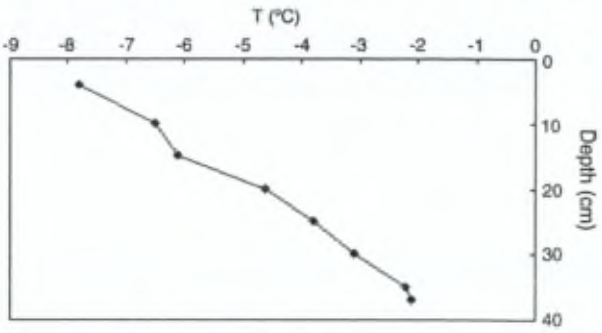

Fig. 7. Temperature profile in sea ice at station XIII.

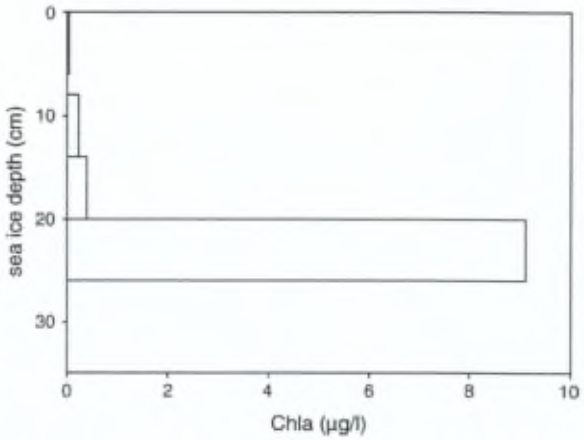

Fig. 8. Chlorophyll *a* (µg/l) profile in sea ice at station XIII.

of this surface signal to the intermediate levels via the brine system [26]. Enhanced Fe values in the warmer bottom ice may be associated with the presence of ice algae as evidenced by high Chlorophyll *a* concentrations (Fig. 8).

As can be seen from the temperature profile in Fig. 7 in the sea ice, the upper layer is colder than the bottom layer because of the relatively low air temperature compared with underlying seawater. At temperatures of −5 °C and higher, the hyper-saline brine channels and brine pockets in the sea ice, formed by the rejection of sea salt during ice formation, start to melt and become interconnected [26]. We observed Fe concentrations that were higher in shallow brine (15 cm depth, <−5 °C) than in deep brine (30 cm depth, >−5 °C). This is likely to result from dilution of

Table 6
Overview of reported data of total dissolvable and dissolved Fe in Antarctic

	This work (nM)		(a) (nM)		(b) (nM)		(c) (nM)		(d) (nM)		(e) (nM)		(f) (nM)	
	TDFe	DFe	TDFe	DFe	TDFe	DFe	TDFe	DFe	TDFe	DFe	TDFe	DFe	TDFe	DFe
Snow	3.1	1.7	1.2–31.7	–	–	–	31.3–52.6	–	–	–	–	–	5.7–16.0	–
Brine	6.0–14.6	4.7–14.1		–	–	–	19.8–64.6	–	–	–	–	–	–	–
Sea ice	23.9–65.8	7.2–18.2		–	–	–	10.8–99.3	–	–	–	–	–	–	–
Under ice seawater	1.2–2.1	1.3–1.5	–	–	–	0.4–4.1	–	–	0.27–9.17	0.09–3.8	–	0.5–31	0.4–12.9	0.2–8.62

Note: (a) Edwards (2000), snow sampled at sea ice surface Prydz Bay (64–66°S, 75–76°E), September 1994 [27]; (b) Grotti et al. (2001), Terra Nova Bay, Western Ross Sea (74°S, 164°E), November 1997–February 1998 [28]; (c) Löscher et al. (1997), Polarstern Cruise ANTX/6 (58–60°S, 7–9°W), September–November 1992; (d) Sedwick et al. (2000), Ross Sea (66–77°S, 164–179°E), November–December 1994 and December 1995–January 1996; (e) Sanudo et al. (2002), Weddell Sea (63–65°S, 41–56°W), February–March 1991; (f) Westerlund and Öhman (1991), Surface seawater Weddell Sea 50 m, December 1988–January 1989.

the initially rejected Fe present in cold brine through progressive melting of fresh water ice from the brine channel walls as the ice temperature increases. Further support for this comes from the salinity values, which are 93.7 in cold shallow brine and 88.0 in warm deep brine. It is also worth comparing TDFe and DFe concentrations in sea ice and in brine at station XIII. Figs. 4 and 5 show that the TDFe and DFe are nearly identical in the brine whilst the TDFe is considerably higher than the DFe in the ice. This suggests that particulate iron might not be easily drained into the brine sack hole and is somehow retained in the ice medium.

Finally, density difference between brine and underlying seawater will initiate brine convection as rising temperatures in the bottom ice re-establish connection between brine in the lower half of the sea ice cover and seawater below. This process is likely to favour transfer of particulate Fe from brine to the underlying seawater, as suggested in the graphs of the Fig. 6.

Further insights into the controlling factors for Fe incorporation and pathways in the sea ice system will be discussed elsewhere in more detail in the light of complementary physical and biogeochemical data sets.

4. Conclusions

We developed a sensitive and reliable method to measure Fe concentrations in the sea ice environment. We demonstrated the ability of this method to deal with high gradients of salinity and Fe concentrations. Accuracy and reproducibility were satisfactory. Our methodology has been successfully applied to Antarctic sea ice samples and Fe data were consistent with previously reported values. Results from the first data set reveal the potential of such measurements in shedding more light on biogeochemical cycles interacting in sea ice polar regions.

Acknowledgements

We would like to thank the Australian Antarctic Division, especially Ian Allison (Expedition Leader) and Rob Massom (Chief Scientist), for inviting us on the "ARISE in the East" endeavor. Captain, officers and crew of the RV *Aurora Australis* are thanked for all their efforts to help making our work a success. We are also grateful to the Australian Antarctic Division for arranging the loan of a clean laboratory container. The logistic support in the laboratory provided by Nathalie Roevros is greatly appreciated. The authors would like to thank the two anonymous referees and the editor for their helpful comments on the manuscript. This work was funded by the Belgian French Community (ARC contract 2/07-287) and by the Belgian Federal Science Policy Office (contract EV/12/7E).

References

[1] J.H. Martin, R.M. Gordon, S.E. Fitzwater, Nature 345 (1990) 156.
[2] J.H. Martin, S.E. Fitzwater, Nature 331 (1988) 341.
[3] G.S. Dieckmann, H.H. Hellmer, in: D.N. Thomas, G.S. Dieckmann (Eds.), Sea Ice. An Introduction to its Physics, Chemistry, Biology and Geology, Blackwell, Oxford, 2003, p. 1.
[4] D.J. Erickson, J.J. Walton, S.J. Ghan, J.E. Penner, Atm. Environ. 25A (1991) 2513.
[5] B.M. Löscher, J.T.M. de Jong, H.J.W. de Baar, C. Veth, F. Dehairs, Deep-Sea Res. II 44 (1997) 143.
[6] S. Westerlund, P. Öhman, Mar. Chem. 35 (1991) 199.
[7] A.R. Bowie, P.N. Sedwick, P.J. Worsfold, Limnol. Oceanogr.: Methods 2 (2004) 42.
[8] A.R. Bowie, E.P. Achterberg, S. Blain, M. Boye, P.L. Croot, H.J.W. de Baar, P. Laan, G. Sarthou, P.J. Worsfold, Mar. Chem. 84 (2003) 19.
[9] A.R. Bowie, E.P. Achterberg, R.F.C. Mantoura, P.J. Worsfold, Anal. Chim. Acta 361 (1998) 189.
[10] J.T.M. de Jong, J. den Das, U. Bathmann, M.H.C. Stoll, G. Kattner, R.F. Nolting, H.J.W. de Baar, Anal. Chim. Acta 377 (1998) 113.
[11] R.T. Powell, D.W. King, W.M. Landing, Mar. Chem. 50 (1995) 13.
[12] D.W. O'Sullivan, A.K. Hanson Jr., D.R. Kester, Mar. Chem. 49 (1995) 65.
[13] H. Obata, H. Karatani, E. Nakayama, Anal. Chem. 65 (1993) 1524.
[14] D.A. Weeks, K.W. Bruland, Anal. Chim. Acta 453 (2002) 21.
[15] P.N. Sedwick, G.R. DiTullio, D.J. Mackey, Geophys. Res. 105 (2000) 11321.
[16] C.I. Measures, J. Yuan, J.A. Resing, Mar. Chem. 50 (1995) 3.
[17] W.M. Landing, C. Haraldsson, N. Paxeus, Anal. Chem. 58 (1986) 3031.
[18] P.L. Croot, P. Laan, Anal. Chim. Acta 466 (2002) 261.
[19] A.L. Rose, T.D. Waite, Anal. Chem. 73 (2001) 5909.
[20] D.W. King, H.A. Lounsbury, F.J. Millero, Environ. Sci. Tech. 29 (1995) 818.
[21] J.M. Hill, J. Chromatogr. 76 (1973) 455.
[22] V. Schoemann, H.J.W. de Baar, J.T.M. de Jong, C. Lancelot, Limnol. Oceanogr. 43 (7) (1998) 1427.
[23] J.C. Goldman, M.R. Dennett, J. Exp. Mar. Ecol. 86 (1985) 47.
[24] S.A. Sanudo-Wilhelmy, K.A. Olsen, J.M. Scelfo, T.D. Foster, A.R. Flegal, Mar. Chem. 77 (2002) 157.
[25] E.A. Boyle, B. Handy, A. van Green, Anal. Chem. 59 (1987) 1499.
[26] K.M. Golden, S.F. Ackley, V.I. Lytle, Science 282 (1) (1998) 2238.
[27] P.R. Edwards, Ph.D. Thesis, 2000, 177pp.
[28] M. Grotti, F. Soggia, M.L. Abelmoschi, P. Rivaro, E. Magi, R. Frache, Mar. Chem. 76 (2001) 189.

Available online at www.sciencedirect.com

ScienceDirect

ELSEVIER

Marine Chemistry xx (2006) xxx – xxx

MARINE CHEMISTRY

www.elsevier.com/locate/marchem

Distribution and biogeochemical behaviour of iron in the East Antarctic sea ice

Delphine Lannuzel [a,*], Véronique Schoemann [b], Jeroen de Jong [a,1], Jean-Louis Tison [c], Lei Chou [a]

[a] *Laboratoire d'Océanographie Chimique et Géochimie des Eaux, Université Libre de Bruxelles, Campus de la Plaine CP 208, Bd. du Triomphe, B-1050 Bruxelles, Belgium*

[b] *Ecologie des Systèmes Aquatiques, Université Libre de Bruxelles, Campus de la Plaine CP 221, Bd. du Triomphe, B-1050 Bruxelles, Belgium*

[c] *Unité de Glaciologie, Université Libre de Bruxelles CP 160/03, 50 Av. F. D. Roosevelt, B-1050 Bruxelles, Belgium*

Received 30 January 2006; received in revised form 16 June 2006; accepted 19 June 2006

Abstract

We have attempted to evaluate the relative importance, compared to other possible sources, of sea ice in supplying Fe to East Antarctic surface ocean waters. Samples of snow, brine, seawater and sea ice were collected and processed for Fe analysis during the "ARISE in the East" Antarctic cruise during September–October 2003 (64°–65°S/112°–119°E, *RV Aurora Australis*). Total-dissolvable and dissolved Fe concentrations were measured together with relevant physical, chemical and biological parameters. The most striking feature we observed is that total-dissolvable Fe concentrations in sea ice were up to an order of magnitude higher than those measured in the underlying seawater. Moreover, total-dissolvable Fe in sea ice is more concentrated at cold "winter" type stations than at the warm "spring" ones. This probably results from the enhanced ice permeability as spring arrives, which allows brine drainage within the ice cover and renders exchanges with the water column possible. During the melting period, iron inputs to surface waters from sea ice may represent as much as 70% of the estimated daily total flux into surface seawater when taking into account available data on dust deposition, extraterrestrial iron, vertical diffusion and upwelling. Our results highlight the potentially important contribution of pack ice to the Fe biogeochemical cycle in the East Antarctic oceanic Ecosystem.

Keywords: Iron biogeochemistry; Fe inputs; Sea ice; East Antarctica

1. Introduction

As an essential nutrient for phytoplankton growth, and hence involved in marine primary productivity and carbon export, iron (Fe) is a key element in the study of ocean–atmosphere biogeochemical interactions. This micro-nutrient has been shown to limit algal growth in "High-Nutrient, Low-Chlorophyll" (HNLC) areas such as the Southern Ocean, where external Fe inputs are low. Potential Fe sources for Antarctic surface waters are: (1) continental and extraterrestrial dust via atmospheric deposition, (2) upwelling and turbulent diffusion, (3) sediment resuspension and lateral advection, and (4) melting sea ice and icebergs (Löscher et al., 1997; Sedwick and DiTullio, 1997; Johnson et al., 1999; Johnson, 2001; Sedwick et al., 2001; Grotti et al., 2005).

* Corresponding author. Tel.: +32 2 650 5278; fax: +32 2 650 5228.
E-mail address: dlannuze@ulb.ac.be (D. Lannuzel).
[1] Current address: Unité de Glaciologie, Université Libre de Bruxelles CP 160/03, 50 Av. F. D. Roosevelt, B-1050 Bruxelles, Belgium.

0304-4203/$ - see front matter © 2006 Elsevier B.V. All rights reserved.
doi:10.1016/j.marchem.2006.06.010

Sea ice covers seasonally large areas of the Southern Ocean and could constitute a significant pool of bioavailable Fe, which in turn could support algal blooms when this ice melts (Sedwick et al., 2000).

The Southern Ocean covers 30% of the global ocean and plays an important role in regulating the Earth's climate as seasonal sea ice formation around Antarctica provide a major drive to the global thermohaline overturning circulation through intermediate and bottom water formation (Sarmiento et al., 1998). Also, low temperatures and strong wind mixing facilitate physical removal of carbon dioxide to the deep sea (Watson and Orr, 2003). In recent years, Fe has been recognized as a key element in ocean biogeochemistry. Martin and Fitzwater (1988) highlighted the role of Fe as a limiting nutrient for phytoplankton growth in HNLC regions of the oceans. Since solubility of Fe in oxygenated seawater is low, and dissolved Fe can be strongly scavenged from the water column due to biological uptake and/or to rapid precipitation and sedimentation of iron oxyhydroxides, dissolved Fe is present in very low concentrations in open ocean surface waters (de Baar and de Jong, 2001). The eolian pathway of Fe may constitute an additional source, but it is typically small in remote ocean regions (Gao et al., 2001; Jickells et al., 2005). Martin (1990) speculated that enhanced dust transport to the Southern Ocean during glacial periods might have fertilized the region, enhancing the "biological carbon pump" and drawing down atmospheric CO_2. Today, atmospheric Fe inputs from the deserts of South Africa, South America, Australia and the Transantarctic Mountains may provide the main inputs of eolian Fe to Antarctic waters. Because of its assumed role as a "dust collector" while covering a large part of the Southern Ocean, sea ice might be a significant pool of bioavailable Fe in Antarctic surface waters, compared to other possible Fe sources.

Sea ice forms as the seawater temperature drops below −1.86 °C, producing frazil ice under agitated conditions or a uniform thin sheet called nilas when the ocean is calm. Congelation or columnar ice may then grow downward by freezing of the water, forming more uniformly oriented crystals (e.g. Weeks and Ackley, 1986; Gow et al., 1998). Snowfalls are frequent in the Southern Ocean, so that a snow layer generally accumulates on top of young sea ice within a few days. Under heavy snow pack, seawater may infiltrate and form the so-called "snow ice". Sea ice textures are important for reconstructing the ice history and for evaluating the conditions under which sea ice was formed. Temporally and spatially, sea ice is a highly heterogeneous medium, with regard to physical, chemical and biological features. Thermodynamics and physical forcing both control ice texture and thickness, thus influencing temperature, salinity, porosity, nutrient content, light penetration and biological activity. These parameters are closely linked, and their relations are highly complex. Thermodynamically, East Antarctic sea ice can grow only to a thickness of 0.5–1 m. However, rafting and ridge building can considerably increase thickness to several meters (e.g. Allison, 1997).

Away from the coast, Antarctic sea ice consists mostly of first-year ice, because most of sea ice melts during the first summer after its formation. The differences in sea ice area in the Southern Ocean between maximum extent in September and minimum extent in February is about 15×10^6 km^2 (Allison, 1997). This vast area provides a habitat for marine organisms, which develop within and beneath the ice column. Although frozen coastal waters (land-fast ice) appear to be a favourable zone for primary production due to land vicinity, open ocean pack ice can sustain high algal biomass as well. Chlorophyll *a* (Chl *a*) levels up to 6 mg/l in land-fast ice (Mc Murdo) and 0.2 mg/l in pack ice (Weddell Sea) have been reported (Arrigo, 2003). Algal communities are observed at different levels within sea ice (e.g. Horner, 1985a). Bottom assemblages are the most common. They grow often under low light conditions and consume major nutrients from the underlying seawater. Internal communities live in brine channels, where salinities and temperatures can be extreme as compared to bottom ice. Surface assemblages are thought to originate from seawater infiltration into the snow pack. Theoretically, sea ice should contain little Fe since it is formed from Fe-deficient waters (Thomas, 2003). But this extreme environment obviously can meet chemical and physical conditions favourable to algal growth. In other words, Fe concentrations must be high enough to sustain biological activity in much of the sea ice.

Sea ice may be a substrate not only for algal production within the ice column itself (surface, internal and bottom assemblages), but also for pelagic phytoplankton communities growing beneath or adjacent to the ice floe. Once the ice starts to melt, Fe may be released and eventually become available for the pelagic algal communities. These phenomena are difficult to quantify, since sea ice Fe data are scarce (Löscher et al., 1997; Grotti et al., 2005; Lannuzel et al., 2006) due in large part to the challenges encountered in this extreme environment with regard to sampling and analysis.

The present study focuses on the biogeochemistry of Fe in Antarctic pack ice in order to assess Fe pools, sources and pathways. The objectives were to characterize the Fe distribution in sea ice, and its associated snow, brine and underlying seawater at 6 stations sampled in the East Antarctic sector of the Southern Ocean during early

austral spring 2003. Iron speciation was determined by measuring the total-dissolvable Fe (TDFe) and dissolved Fe (DFe) pools, and calculating the particulate-dissolvable Fe (PDFe). Based on these data and their possible correlations to sea ice physical properties (ice texture, salinity, temperature), chemistry and biology, we have attempted to assess the possible Fe inputs and pathways, and the importance of sea ice as an Fe source to Southern Ocean surface waters in the seasonal sea ice zone.

2. Material and methods

2.1. Sea ice environment and sample collection

Samples of sea ice and associated snow, brine and underlying seawater were collected during the "ARISE in the East" Antarctic expedition (Antarctic Remote Ice Sensing Experiment, voyage AA03-01, September–October 2003, 64°–65°S/112°–119°E, *RV Aurora Australis*). The 6 stations sampled were located in the seasonal sea ice zone in the deep ocean (Fig. 1A,B).

A full description of the sample collection technique for Fe measurement in sea ice is detailed by Lannuzel et al. (2006). Briefly, snow was first collected in Polyethylene (PE) containers using polypropylene (PP) shovels. A set of closely spaced ice cores (10–20 cm apart from each other) was then sampled on a uniform, levelled sea ice cover, using an electropolished stainless-steel corer previously tested for trace-metal clean conditions in order to assess relevant physical, chemical and biological parameters (temperature, salinity, nutrients and Chl *a*). Cores were stored in a plastic bag (acid-cleaned for the cores dedicated to Fe study) at −28 °C in the dark until further processing. Access holes ("sack holes") were drilled into the sea ice cover at one or two different depths to allow gravity-driven brine collection (ice levels above or below −5 °C threshold when applicable as described by Golden et al., 1998; see Section 3.2). Brines and under ice seawater (0 m, 1 m and 30 m deep) were then pumped up using a portable peristaltic pump (Cole-Parmer, Masterflex E/P) and plastic tubing (sampling system adapted from de Jong et al., 1998). Snow and ice sections of 5–10 cm thickness were melted in trace-metal clean containers in the dark at shipboard ambient temperature.

2.2. Physical and biological parameters

In situ ice temperatures were measured on site using a calibrated probe (TESTO 720) inserted every 5 or 10 cm along the freshly sampled core. Bulk salinity was determined from conductivity using a WP-84-TPS meter. Vertical ice thin-section photographs taken under polarized light (Langway, 1958) indicated ice crystalline shapes and were used as an indicator for ice texture (e.g. columnar vs. granular).

Sea ice sections for Chl *a* determination were melted in seawater filtered through 0.2 μm filters (1:4 volume ratio) to avoid cell lysis by osmotic shock. Chl *a* was quantified fluorimetrically following Yentsch and Menzel (1963) after 90% v:v acetone extraction of the particulate material retained on glass-fibre filters (Whatman GF/F) for 12 h at 4 °C in the dark.

2.3. Iron

Seawater, brine, and melted snow and sea ice samples dedicated for Fe analysis were processed onboard ship. All labware was acid-cleaned according to the procedure described in Lannuzel et al. (2006). Total-dissolvable Fe (TDFe, unfiltered) was stored at pH 1.8 (addition of 100 μl 14 M HNO_3, J.T. Baker, Ultrex for 100 ml of sample) for a period of at least 6 months before Fe measurement by flow injection analysis (FIA), which should dissolve all but the most refractory Fe species. The dissolved Fe fraction (DFe) was collected after filtration through 0.2 μm pore nuclepore polycarbonate (PC) membrane filters, mounted on Sartorius PC filtration devices equipped with Teflon O-rings. The filtrate was acidified to pH 1.8 with 14 M HNO_3 (J.T. Baker, Ultrex) at least 24 h prior to analysis. We adapted a FIA technique (FeLume, Waterville Analytical) to measure TDFe and DFe concentrations in our samples without a pre-concentration step. Analysis of reference material NASS-5 and CASS-3 gives a good agreement with the certified values and detection limit (3σ of the blank) is on average 0.12 nM (Lannuzel et al., 2006). Particulate-dissolvable Fe (PDFe) refers to the difference in concentration between TDFe and DFe.

3. Results

3.1. Ice texture

Sea ice thickness at our selected sampling sites ranged from 0.3 m (station XIII) to 0.8 m (station V) thickness. Thin section observations reveal a typical pack ice structure, with snow ice and/or frazil ice, underlain by congelation ice (Fig. 2). Station IV apparently underwent a similar genesis as station IX, with about 15 cm of frazil ice growing then into columnar ice (~30 cm). Both stations V and VII show a thick snow ice layer (~20 cm deep) with contrasted snow metamorphism, then a frazil ice layer followed by a columnar structure. Stations XII and XIII display a somewhat more complex sequence of

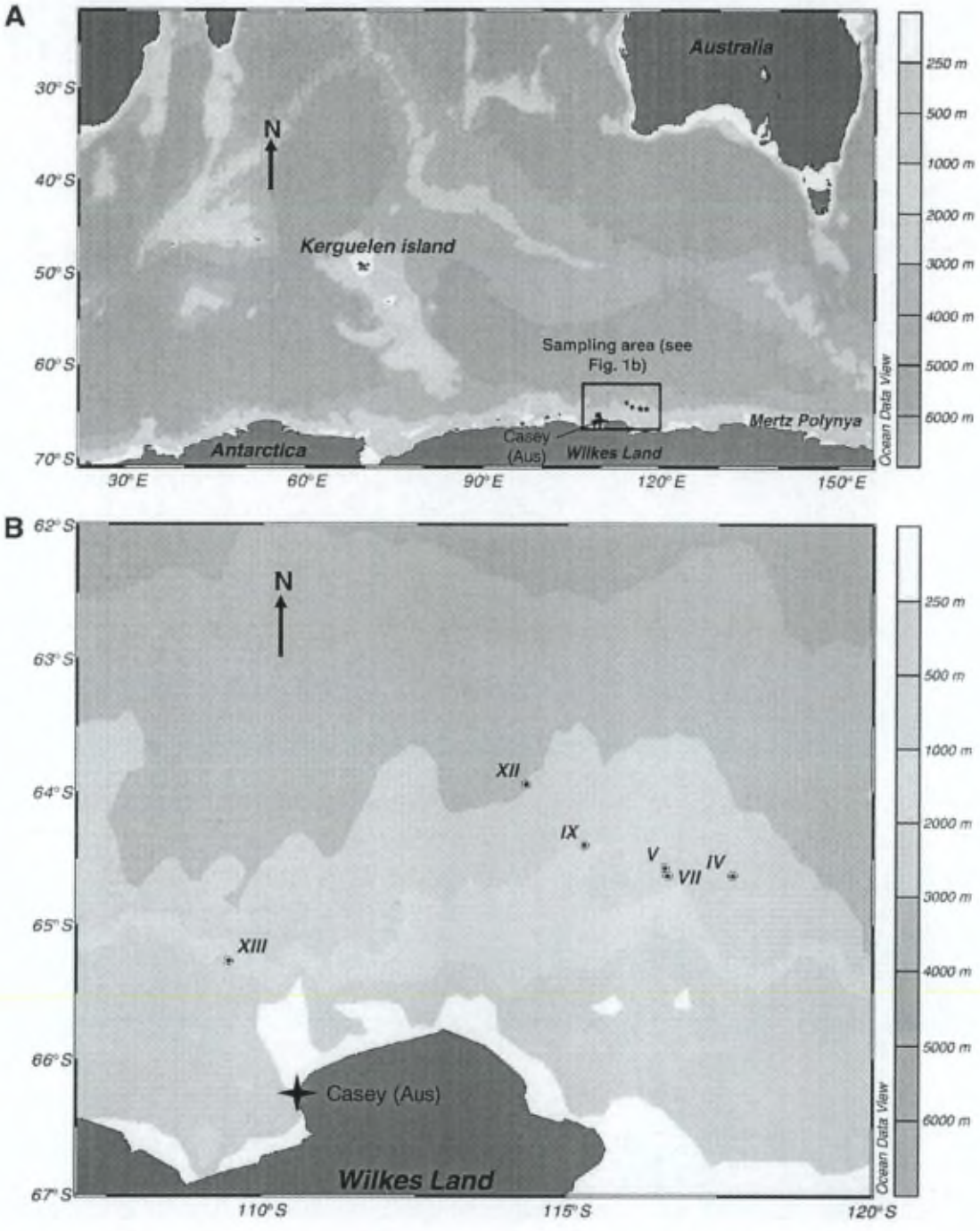

Fig. 1. (A and B) Location of the sampling area (Schlitzer, R., Ocean Data View, http://www.awi-bremerhaven.de/GEO/ODV, 2005).

genetic processes, probably involving rafting. This is suggested by the repeated occurrence of bent columnar crystals at station XII and the "flattened" frazil ice crystals in the lower part of the core XIII (Fig. 2). Stations IV, V, VII and IX are located at the same latitude (64.3°S), whereas stations XII and XIII are located at 63.6°S and 65.2°S, respectively.

3.2. Temperature, bulk ice salinity, brine volume and Chl a profiles

In sea ice, the upper layer is colder than the bottom layer because of the relatively low air temperature compared to underlying seawater. Sea ice indeed exhibits a marked transition in its fluid transport

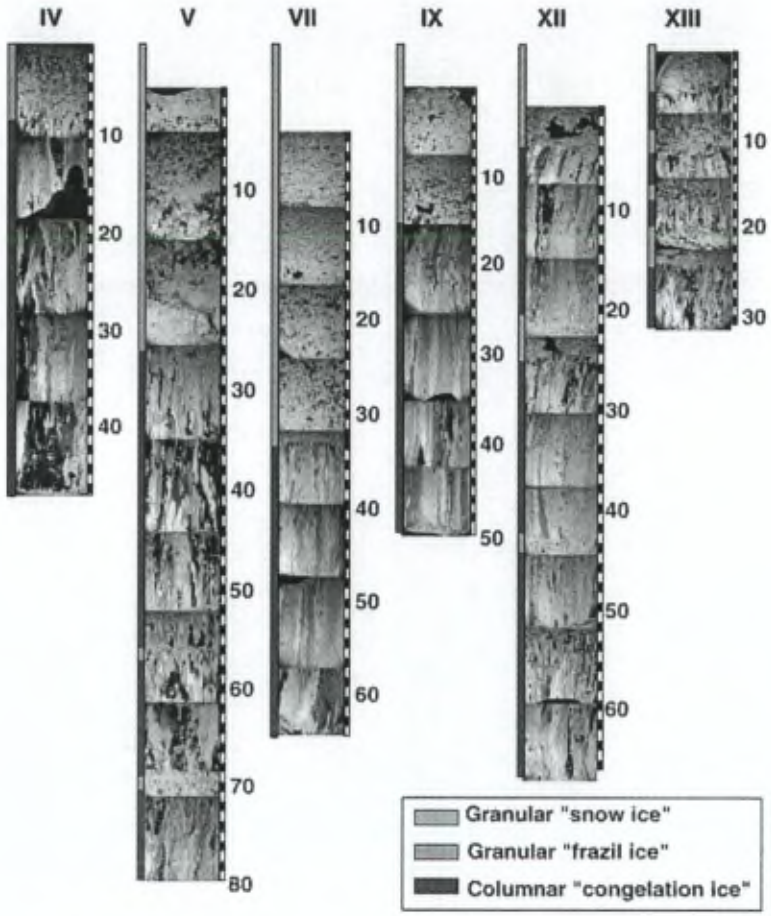

Fig. 2. Ice textures from vertical thin sections, viewed under crossed polarizers of ice cores for each stations. Depths have been adjusted so that snow thickness is taken into account.

properties at a brine volume fraction of about 5%, which roughly corresponds to a −5 °C ice temperature at a bulk ice salinity of 5 (Golden et al., 1998). For brine volume fractions higher than 5%, brine inclusions become interconnected and can carry heat and nutrients through the ice, whereas for lower porosities the ice is impermeable. Golden et al. (1998) referred this threshold behaviour as the "law of fives".

Temperature profiles allow a possible classification in terms of the thermal stages at our stations (Fig. 3). Station IV had the coldest ice, with its upper half exhibiting the lowest ice temperatures. Then ice at

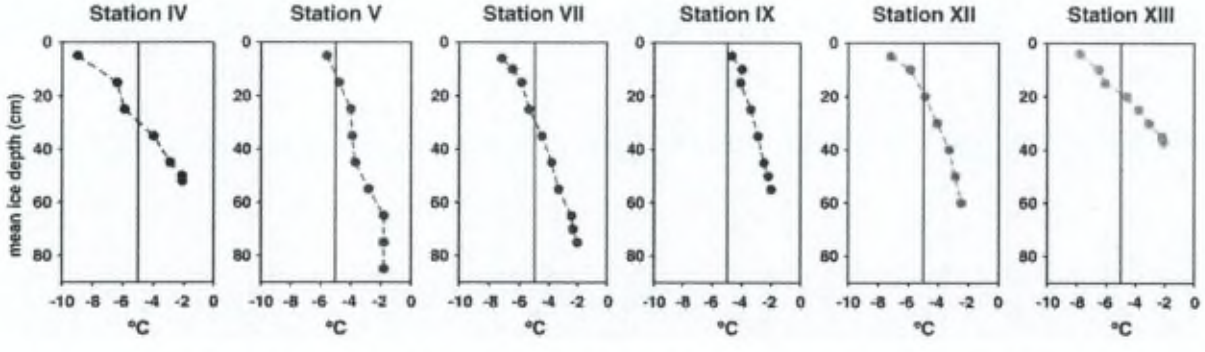

Fig. 3. Temperature (°C) profiles in sea ice. The −5 °C critical temperature is indicated by the vertical line.

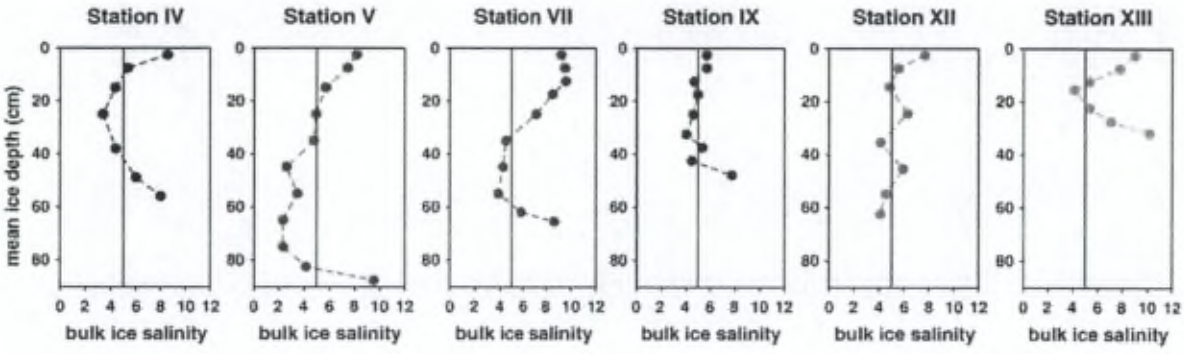

Fig. 4. Bulk salinity profiles in sea ice. The critical salinity 5 is indicated by the vertical line.

stations VII, XII and XIII appeared to be in a later seasonal stage compared to station IV, as ice temperatures were slightly higher in the upper half of the ice cover. Finally, both stations V and IX showed a warmer regime as most of the ice cover was above −5 °C.

Most stations showed the typical C-shaped bulk salinity profile described in many other field studies of sea ice (e.g. Nakawo and Sinha, 1981; Weeks and Ackley, 1986; Eicken, 1992, 1998) (Fig. 4). Higher salinities at the top result from enhanced initial entrapment under faster growth rates, brine expulsion upwards on cooling, and eventually seawater infiltration in snow ice, later in the season. Lower salinities in the middle levels reflect enhanced salt rejection after initial entrapment under slower growth rates and brine drainage, whilst higher salinities in the warmer bottom layers result from higher porosities and lack of brine drainage in the fragile skeletal layer. Sea salts tend to be more easily trapped in surface frazil ice because of its rapid formation (a few hours to a few days, depending on air temperature), whereas congelation ice forms slowly (weeks to months) and expels salts more efficiently. This contrast supports the previous assumption of ice rafting at station XII, which shows the repetition of such a sequence with depth.

The evolutionary stages described from the various temperatures profiles are also shown in the calculated brine volume fraction (V_b/V=brine volume/bulk ice volume; Eicken, 2003) profiles (Fig. 5). This variable is of critical importance since brine drainage within the ice towards the underlying water can be regarded as a key physical process for Fe transfer. Station IV clearly shows $V_b/V<5\%$ in the upper ice column because cold ice temperature favours smaller brine volumes and higher brine salinity. On the contrary, the lower section of this core indicates increased porosity and permeability (V_b/V being $>5\%$), and possible exchanges with underlying seawater. In contrast, ice porosity at stations V, VII and IX was considerably higher, with brine volumes typically being $\geq 5\%$ along all cores. Stations XII and XIII displayed a somewhat intermediate profile in the upper half of the ice cover. One should bear in mind that air temperature, ice thickness and texture, snow cover and solar irradiance all contribute to the control of ice temperature, salinity and permeability. Within a few hours, meteorological conditions may act together and affect the brine volumes at different locations along the core. It is thus not surprising that the complex links between different physical properties render a clear seasonal characterization for all stations difficult, especially in the spring.

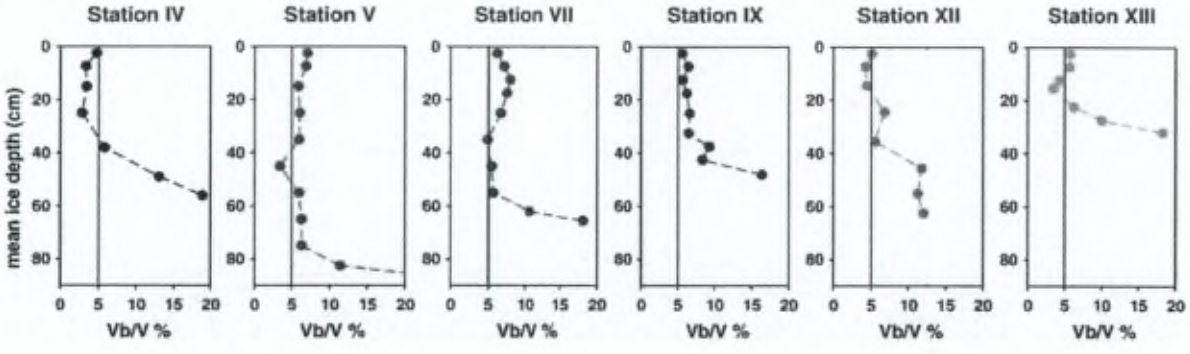

Fig. 5. Brine volume fraction V_b/V (%) profiles in sea ice. The 5% critical brine volume is indicated by the vertical line.

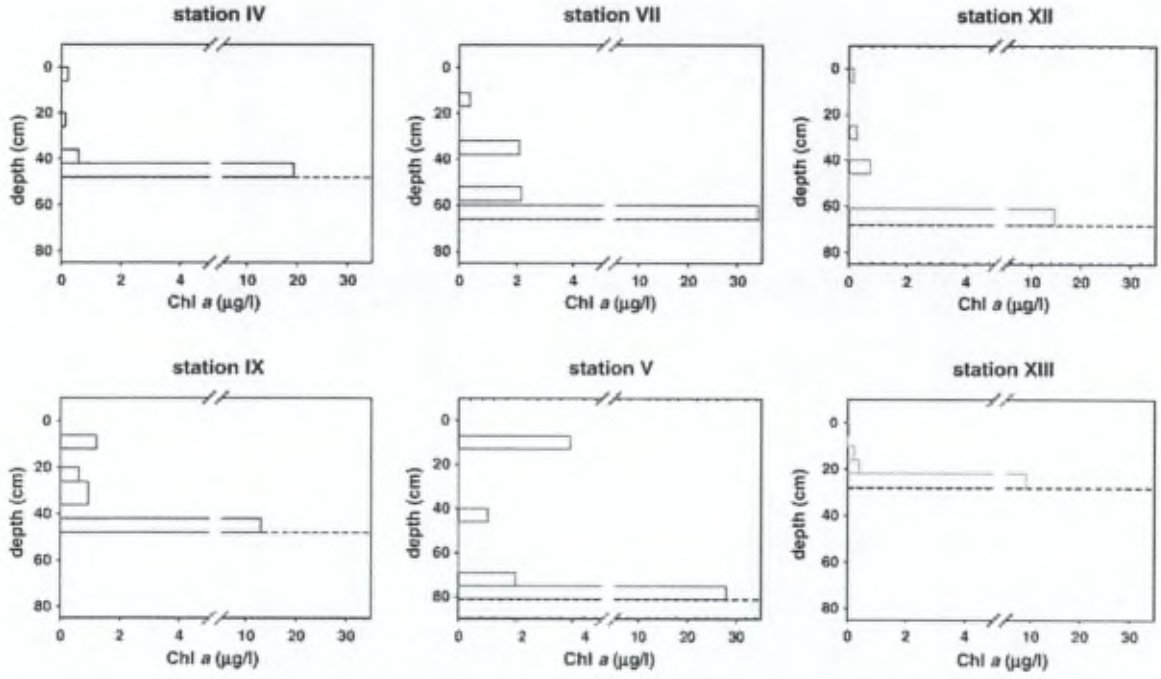

Fig. 6. Chlorophyll *a* (µg/l) profiles in four sea ice sections. The dashed horizontal black line represents the ice–water interface.

Chl *a* profiles indicate maximum values (i.e. from 9.1 to 34.2 µg/l) were systematically located in the lower portions of the ice at all stations (Fig. 6). Algal biomass was however also observed at other levels in the cores of stations V, VII and IX. This probably reflects increased ice permeability at these stations, supplying major

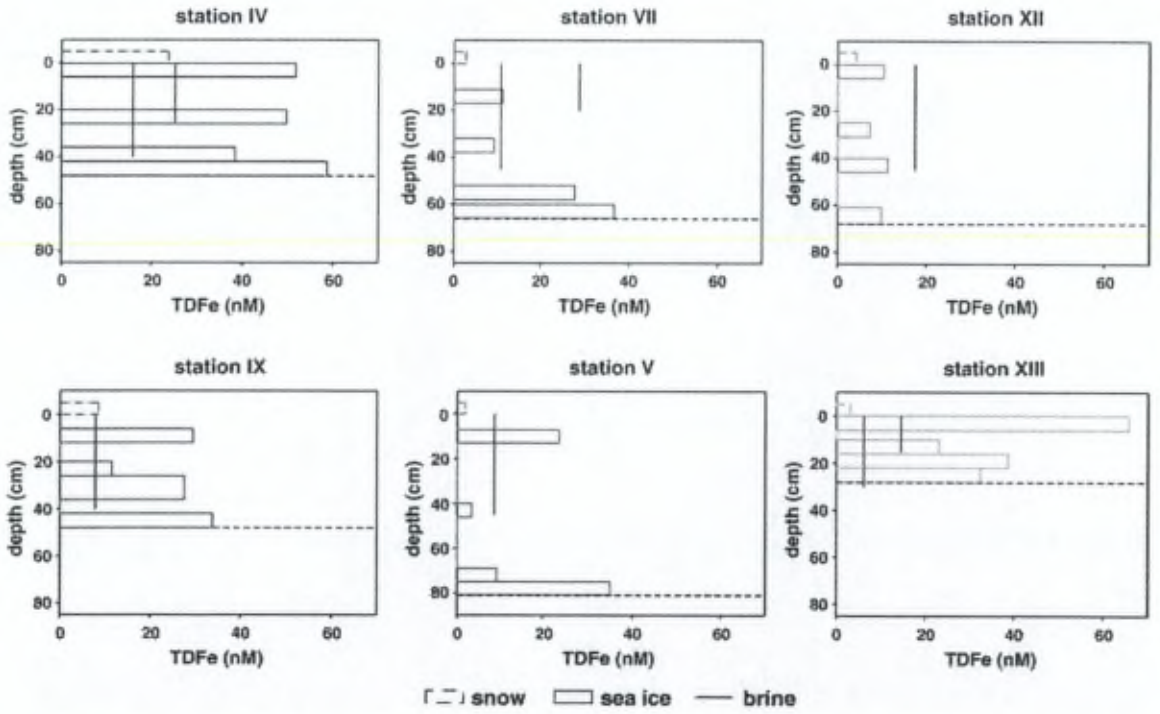

Fig. 7. TDFe (nM) profiles in four sea ice sections (solid bars), snow (dotted bars) and brines (vertical lines for cold<−5 °C shallow brine and warm>−5 °C deep brine).

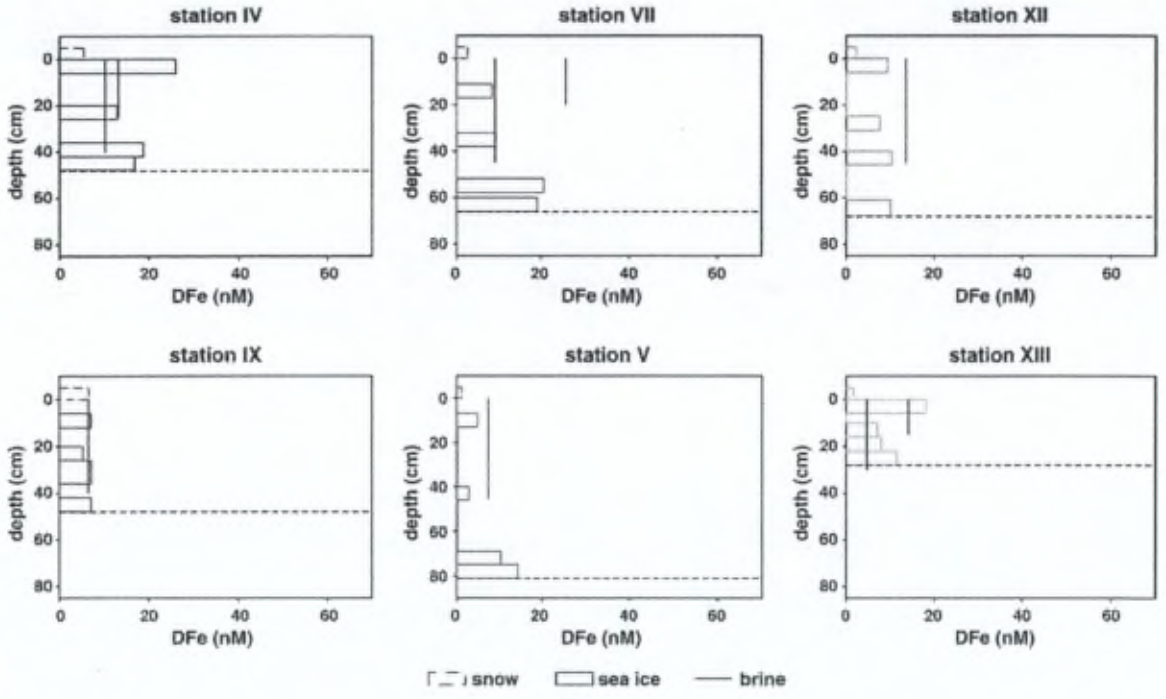

Fig. 8. DFe (nM) profiles in four sea ice sections (solid bars), snow (dotted bars) and brines (vertical lines for cold<−5 °C shallow brine and warm>−5 °C deep brine).

nutrients from seawater and possibly Fe from the sea ice, in addition to improved light conditions.

In light of the physical parameters and Chl *a* profiles, stations V and IX can be regarded as typical "spring" stations as revealed by ice temperatures>−5 °C and brine volume fractions >5% throughout the ice cover. The latter physical characteristic allows vertical ice–water exchanges, thus algal development along the whole core (Fig. 6). Note that in the case of station V, one cannot preclude snow ice formation (i.e. seawater infiltration into the snow pack) as an efficient process for initial algal "seeding" and major nutrients enrichment of the top ice layer. In contrast, station IV is more likely a "winter" type station: Figs. 3 and 5 demonstrate that the ice is impermeable to brine exchange in the upper part of the ice cover, therefore preventing algal development in the upper ice (Fig. 6). Stations VII, XII and XIII exhibit a transitional regime, with the upper 30 cm of stations XII and XIII still reflecting low permeability.

3.3. Spatial and temporal distribution of Fe

Figs. 7–9 show the profiles of TDFe, DFe and PDFe in our East Antarctic pack ice cores (bars), including surface snow (dashed bars). "Sack hole" brine (>−5 °C and <−5 °C when present) concentrations are indicated by solid vertical lines.

Our results tend to show relatively high Fe contents in the sea ice compared to under-ice seawater (Table 1). Generally, sea ice and brines exhibit the highest Fe levels, followed by snow. These three media are more concentrated in Fe than the underlying seawater. The ranges are: 3.3–65.8 nM TDFe and 2.6–26.0 nM DFe in sea ice, 6.0–28.9 nM TDFe and 4.7–25.5 nM DFe in brines, 1.8–23.7 nM TDFe and 1.0–6.5 nM DFe in snow, and 1.2–3.8 nM TDFe and 1.1–4.5 nM DFe in under-ice seawater. Seawater shows a major DFe fraction compared to the sea ice as reflected by DFe percentages of 78±23% (1σ, n=15) in seawater and 60±32% (1σ, n=24) in sea ice.

On the whole, station IV exhibits higher levels of TDFe, DFe and PDFe in sea ice, brines and snow compared to other sampled stations (Figs. 7–9). Based on the data collected at 4 levels along the core, we vertically integrated the concentrations of TDFe, DFe and PDFe per core at each station. This provides an estimate of a mean bulk concentration of Fe in ice at each station (Table 2). The mean TDFe bulk concentration estimated for station IV is the highest at 48.9 nM, followed by stations XIII and IX, where average integrated TDFe concentrations are 40.7 and 24.0 nM, respectively. The averaged integrated bulk concentrations of Fe (1σ standard deviation) estimated in sea ice for all stations investigated are respectively 25.7±15.8 nM TDFe, 10.7±4.6 nM DFe and 15.0±12.8 nM PDFe.

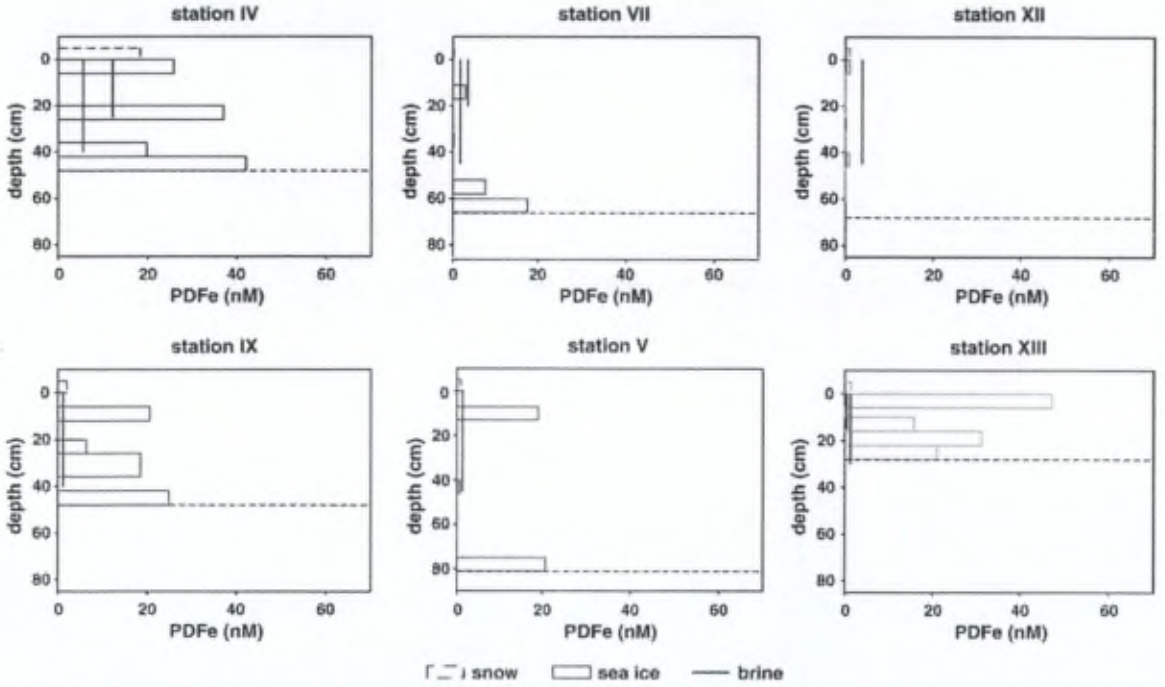

Fig. 9. PDFe (nM) profiles in four sea ice sections (solid bars), snow (dotted bars) and brines (vertical lines for cold<−5 °C shallow brine and warm>−5 °C deep brine).

In the same ice core, the Fe concentration measured in cold shallow brine is typically higher than in warm deep brine; for example, TDFe at station VII is 28.9 nM at 20 cm and 10.4 nM at 45 cm sampled depths (Table 1). Another notable feature is that most of the Fe of the brines is in the dissolved phase, as can be observed at station XIII, where DFe and TDFe are 14.1 nM and 14.6 nM at 15 cm depth. As a result, DFe represents on average 78±14% (1σ, n=9) of TDFe in brines. Both brines and seawater therefore exhibit a high DFe percentage of TDFe, as compared to sea ice.

Finally, Fe levels in snow are relatively low, with a somewhat higher value at "winter" station IV (Table 1); concentrations of TDFe range from 1.8 nM (station XIII) to 23.7 nM (station IV). Dissolved Fe is on the average 56±26% (1σ, n=6) of TDFe in the snow.

4. Discussion

4.1. Distribution and biogeochemical behaviour of Fe

4.1.1. Sea ice, seawater and snow

Patchiness can be a recurrent factor within the same ice floe (Eicken et al., 1991). Sea ice is indeed a highly dynamic and heterogeneous medium in terms of thickness, texture, nutrients distribution, gas content, light penetration, biological activity and probably Fe distribution. As we present here a spatial study of cores collected on different ice floes, it is important to compare stations exhibiting similar ice structure. Hypothetically, stations IV, V, VII and IX, which are located at the same latitude and similar water depth, should have received similar Fe inputs from atmospheric deposition and advection from the continent shelf. Ice at station XII (farther from the coast) and station XIII (closer to the coast) probably reflect rafting processes; it is therefore difficult to assess whether stations XII and XIII received the same external Fe inputs as stations IV, V, VII and IX. Based on similarities in ice textures, we thus compare here below station IV to station IX, station V to station VII, and finally stations XII to XIII.

Station IV clearly shows high DFe and TDFe contents in the sea ice compared to station IX. This is probably due to the difference in the stage of seasonal ice evolution. Station IV can be associated with "winter" type ice in terms of ice temperature, brine volume and Chl *a* profiles (Figs. 3, 5, and 6). In contrast, station IX ice demonstrates "spring" type features, which could favour brine drainage and Fe transfer from the ice pack to the water column below. Besides thermodynamic controls, biological activity is likely to have a strong impact on Fe distribution in the sea ice environment. In nutrient-replete Antarctic waters, light conditions are improving in spring and Fe may become available from the sea ice as it starts to

Table 1
TDFe (nM), DFe (nM), PDFe (nM), temperature (°C) and salinity at the visited stations

		Depth	Ice texture	T (°C)	Salinity	TDFe	DFe	PDFe
Station IV	Snow					23.7	5.4	18.3
01-oct-03	Sea ice	0–6 cm	Frazil	−8.9	8.6	51.8	26.0	25.8
64°37.7′S		20–26 cm	Columnar	−5.9	3.6	49.8	12.9	37.0
117°44.5′E		36–42 cm	Columnar	−3.7	4.4	38.5	18.8	19.7
		42–48 cm	Bottom	−3.0	6.0	58.8	16.7	42.1
	Brine	0–25 cm		−8.2	103.5	25.2	13.1	12.1
		0–40 cm		−6.0	89.9	15.8	10.1	5.6
	Seawater	0 m			34.3	3.0	2.4	0.5
		1 m			34.3	2.7	2.4	0.3
		30 m			34.3	1.4	1.1	0.2
Station V	Snow					1.8	1.0	0.9
07-oct-03	Sea ice	7–13 cm	Snow ice	−5.2	6.6	23.7	4.5	19.2
64°34.0′S		40–46 cm	Columnar	−3.5	3.1	3.3	2.6	0.6
116°37.8′E		69–75 cm	Columnar	−1.9	2.3	8.9	9.8	[a]
		75–81 cm	Bottom	−1.8	3.3	34.9	14.1	20.8
	Brine	0–45 cm			78.6	8.2	6.9	1.3
	Seawater	0 m			34.3	3.0	1.3	1.7
		1 m			34.2	2.3	1.3	1.0
Station VII	Snow					2.7	2.6	0.1
09-oct-03	Sea ice	11–17 cm	Snow ice	−6.2	9.1	10.9	8.0	2.9
64°38.0′S		32–38 cm	Columnar	−4.7	4.5	8.9	8.8	0.1
116°40.7′E		52–58 cm	Columnar	−3.2	3.8	27.9	20.5	7.4
		60–66 cm	Bottom	−2.7	7.3	36.6	19.0	17.6
	Brine	0–20 cm			89.1	28.9	25.5	3.4
		0–45 cm		−6.7	80.1	10.4	8.7	1.7
	Seawater	0 m			34.2	2.0	1.1	0.9
		1 m			34.2	2.9	1.9	1.0
Station IX	Snow					8.4	6.5	1.9
11-oct-03	Sea ice	6–12 cm	Frazil	−4.3	5.2	29.5	8.0	21.5
64°24.1′S		20–26 cm	Columnar	−3.6	4.7	11.5	4.8	6.7
115°17.5′E		36–42 cm	Columnar	−2.8	4.9	27.6	7.1	20.5
		42–48 cm	Bottom	−2.4	6.1	33.8	7.0	26.8
	Brine	0–40 cm		−2.8	61.5	7.6	6.4	1.1
	Seawater	0 m			34.3	1.9	1.7	0.2
		1 m			34.3	3.3	1.9	1.4
		30 m				2.1	1.7	0.4
Station XII	Snow					4.1	2.3	1.8
14-oct-03	Sea ice	0–6 cm	Snow ice	−6.7	7.7	10.3	9.3	1.0
63°56.2′S		25–31 cm	Columnar	−4.7	5.2	7.2	7.6	[a]
114°19.4′E		40–46 cm	Frazil/columnar	−3.4	5.9	11.3	10.4	0.9
		61–68 cm	Bottom	−1.9	4.1	9.8	10.0	[a]
	Brine	0–40 cm		−3.8	63.0	17.4	13.5	3.9
	Seawater	0 m			34.2	2.2	2.1	0.1
		1 m			34.2	3.8	4.5	[a]
Station XIII	Snow					3.1	1.7	1.4
20-oct-03	Sea ice	0–6 cm	Frazil/columnar	−7.9	9.0	65.8	18.1	47.6
65°16.1′S		10–16 cm	Frazil/columnar	−6.1	5.3	23.1	7.2	15.9
109°27.8′E		16–22 cm	Frazil/columnar	−5.1	4.7	38.8	8.0	30.8
		22–28 cm	Bottom	−4.0	6.2	32.5	11.5	21.0
	Brine	0–15 cm		−6.0	93.7	14.6	14.1	0.5
		0–25 cm		−4.2	88.0	6.0	4.7	1.4
	Seawater	0 m			34.3	2.1	1.5	0.6
		1 m			34.3	1.7	1.4	0.3
		30 m			34.3	1.2	1.3	[a]

The sampling date and location are indicated for each site, in addition to media, sampling depths and sea ice textures.
[a] Not detectable within measurement error.

Table 2
Estimated averaged bulk concentrations (nM) of total-dissolvable Fe (TDFe), dissolved Fe (DFe) and particulate-dissolvable Fe (PDFe)

Stations	TDFe (nM)	DFe (nM)	PDFe (nM)
Station IV	48.9	18.3	30.6
Station V	13.5	5.6	7.9
Station VII	17.7	13.1	4.6
Station IX	24.0	6.7	17.3
Station XII	9.5	9.3	0.3
Station XIII	40.7	11.4	29.2

melt. All environmental conditions are then met to favour an algal bloom. Although internal melting has probably occurred, lower DFe and relatively high PDFe concentrations in sea ice at station IX together with increases in Chl *a* levels suggest biological Fe uptake within the ice (see Table 1 and Fig. 7). Decreases in major nutrients concentrations throughout the ice core between the winter and spring type stations are also observed (ranges for station IV and IX are respectively: 0.4–14.4 μM and 0.4–5.65 μM NO_3, 1.3–12.8 and 2.2–10.2 μM $Si(OH)_4$, and 0.04–10.4 and 0.03–4.0 μM PO_4; data not shown). This comparison is only valid if the two stations had similar initial inventory; a situation that is likely since similar ice structures suggest similar sea ice history, and thus similar Fe accumulation processes.

In the same way, station VII can be regarded as a colder station with regard to station V (see temperature profile in Fig. 3). Chl *a* profiles (Fig. 6) and apparent DFe "drawdown" (Table 2) support the idea that station V is in a later stage of the seasonal ice evolution compared to station VII.

Stations XII and XIII both underwent a perturbed genesis as revealed by the succession of frazil and congelation ice sections which lead to strong differences in thickness and probably age. Comparisons of Fe distributions between these two stations are therefore difficult, as we cannot assume that initial Fe stocks were similar. Note, however, that station XII shows a larger proportion of ice with increased permeability, suggesting that it is in a later seasonal stage as compared to station XIII.

To summarize, comparisons of station IV with station IX, station VII with station V, and station XIII with station XII suggest that, as the spring progresses, both ice melting and biological activity are important processes in controlling the distribution and speciation of Fe in the sea ice.

The inferred release of Fe from the ice pack as spring progresses is not obvious from the seawater Fe profiles. This may reflect rapid scavenging, vertical mixing and/or diffusion below the ice, both leading to Fe removal from the upper water column and transfer to deeper water. Seawater Fe concentrations are nevertheless relatively high compared to levels usually encountered in ice-free surface waters (e.g. 0.05–0.3 nM DFe, de Jong et al., 1998; 0.1 nM DFe, Bowie et al., 2001).

Reported Fe concentration levels in snow from previous studies suggest that this medium could potentially contribute to the high Fe values observed in sea ice and underlying seawater (Westerlund and Öhman, 1991; Löscher et al., 1997; Edwards et al., 1998). However, the snow sampled at our locations did not, in general, exhibit Fe concentrations as high as those we observed in sea ice, possibly reflecting the remoteness of our study area with respect to dust sources, compared to other investigated sites. Our snow TDFe values are consistent with other published data for the East Antarctic sector, ranging from 1.2 to 31.7 nM (Edwards and Sedwick, 2001). Long-term deposition of aerosol Fe could be responsible for the high Fe values in the sea ice topmost layers, with the low ice temperature in the upper half of the sea ice cover preventing transfer of this surface enrichment to the lower levels via the brine system (e.g. station IV).

Table 3
Upper ocean iron input estimates during sea ice melting

		Remarks
Sea ice formation Fe uptake		
Winter TDFe (nM)	49	Station IV
Winter DFe (nM)	18	Station IV
Thickness (m)	0.5	Station IV
Residence time of sea ice (9 months) in days	274	
Required TDFe flux to sea ice (μmol/m²/day)	0.09	External supply 0.13, Table 4
Required DFe flux to sea ice (μmol/m²/day)	0.03	External supply 0.28, Table 4
Sea ice melting Fe release		
TDFe inventory (μmol/m²)	24.5	0.49 nM TDFe addition to upper 50 m if melted at once
DFe inventory (μmol/m²)	9	
Melting time (day)	30	
Release TDFe (μmol/m²/day)	0.82	
Release DFe (μmol/m²/day)	0.30	
DFe total flux to the upper ocean during sea ice melting	μmol/m²/day	
Atmospheric/ extraterrestrial	0.0016	
Vertical diffusion	0.01	
Upwelling	0.12	
Sea ice melting	0.30	
Total	0.43	

Table 4
Estimates of iron input to the upper Antarctic Ocean

$J_{diff} = Kz \times d[DFe]/dz$
$J_{upwelling} = v_{upwelling} \times [DFe]_{deep}$
$J_{tot} = J_{atm} + J_{space} + J_{diff} + J_{upwelling}$

		Remarks	References
Aerosol flux J_{atm}			
Dust input (mg/m^2/year)	5	Range 1–10	Duce and Tindale, 1991
TDFe flux (μmol/m^2/day)	0.011	Assuming 4.3% Fe content	Wedepohl, 1995
DFe flux (μmol/m^2/day)	0.0005	Solubility mineral dust 5%	Baker et al., 2006
TDFe flux (μmol/m^2/day)	0.003	SSIZ, 32% mean solubility	Edwards and Sedwick, 2001
DFe flux (μmol/m^2/day)	0.0010		Edwards and Sedwick, 2001
Average DFe flux (μmol/m^2/day)	0.0008		
Extraterrestrial flux J_{space}			
DFe (μmol/m^2/day)	0.0008	Assumed 100% soluble	Johnson, 2001
Vertical diffusion J_{diff}			
K_z (m^2/s)	3.0e−05	ACC (56°S, 15°W)	de Baar et al., 1995
d[DFe]/dz (μmol/m^4)	0.006		
DFe flux (μmol/m^2/day)	0.016		
TDFe flux (μmol/m^2/day)	0.031[a,b]		
K_z (m^2/s)	2.4e−05	SOIREE (61°S, 140°E)	Law et al., 2003
d[DFe]/dz (μmol/m^4)	0.003		Bowie et al., 2001
DFe flux (μmol/m^2/day)	0.006		
TDFe flux (μmol/m^2/day)	0.012[a,b]		
K_z (m^2/s)	6.6e−05	FeCycle (46°S, 179°E)	Boyd et al., 2005
d[DFe]/dz (μmol/m^4)	0.00066		
DFe flux (μmol/m^2/day)	0.004		
TDFe flux (μmol/m^2/day)	0.008[a,b]		
Average DFe flux (μmol/m^2/day)	0.009		
Average TDFe flux (μmol/m^2/day)	0.017		
Upwelling $J_{upwelling}$			
Upwelling velocity (m/s)	1.5e−06	ACC (56°S, 15°W)	de Baar et al., 1995
Deep water concentration (nM)	1		
DFe flux (μmol/m^2/day)	0.13		
TDFe flux (μmol/m^2/day)	0.26[a]		
Surface (m^2)	1.08e+13[c]		Watson, 2001
Upwelling flux (Sv)	25		
Deep water concentration (nM)	0.6		
DFe flux (μmol/m^2/day)	0.12		
TDFe flux (μmol/m^2/day)	0.24[a]		
Average DFe flux(μmol/m^2/day)	0.12		
Average TDFe flux (μmol/m^2/day)	0.25		
Total flux J_{tot}			
Average DFe flux (μmol/m^2/day)	0.13		
Average TDFe flux (μmol/m^2/day)	0.28		

[a] Assuming TDFe = 2 × DFe.
[b] Assuming the same vertical diffusivity for TDFe and DFe.
[c] Surface based on biogeochemical provinces from Longhurst et al. (1995).

4.1.2. Brines

Concentrations of TDFe and DFe in sea ice were up to two orders of magnitude higher than in typical Antarctic seawater. When seawater freezes, sea-salts are expelled together with other impurities (e.g. gases, particles) into the brine system and the water below (Eicken, 1998). In this context, and given the mean calculated brine volumes at our stations (V_b/V=3–27%, Fig. 5) the TDFe and DFe concentrations should be about 4 to 33 times higher in brine than in bulk sea ice. However, we observed similar levels in both media. A potential explanation for this apparent discrepancy is that the brine collection technique ("sack-hole") might lead to an underestimation of the particulate Fe content in brines. Due to its high particle affinity, the Fe associated with micro-organisms and derived organic matter could remain attached to the walls of the brine channels during sample collection, thus not be recovered (Krembs et al., 2001). For the same reason, it might well be that Fe does not behave in the same way as other nutrients during sea ice formation. Iron would not be expelled into the liquid brine, but could use the solid phase, such as wall channels, pure ice crystals or even particulate matter (organic or inorganic), as sorptive surfaces. Comparing TDFe and DFe concentrations in sea ice and brine at station XIII provides evidence to support this hypothesis. Indeed, TDFe and DFe concentrations are nearly identical in the brine, while TDFe is considerably higher than DFe in the ice. This suggests that particulate Fe might not be easily drained into the brine sack hole, and is perhaps retained in the ice medium.

The difference in Fe content between shallow (<−5 °C) and deep (>−5 °C) brines could be a consequence of brine exchanges between the bottom ice cover and the surface seawater. Density difference between brine and underlying seawater can initiate brine convection, as rising temperatures in the bottom ice re-establish connection between brine in the lower sea ice and the seawater below. Comparison of winter and spring brine profiles also tends to show a decline in salinity and Fe, as spring progresses. This can be explained by both brine dilution by freshwater from melting pure ice and/or dilution by seawater due to brine convection.

4.2. Fe and ice texture relationships

Ice texture provides information on the ice growth history, and may help in deciphering Fe sources and pathways in the ice column. Iron accumulates within pack ice at concentrations clearly exceeding that of the underlying seawater. In the case of planktonic organisms, enrichment has been attributed to physical concentration mechanisms, via scavenging by frazil ice crystals rising through the water column (Garrison et al., 1983, 1989; Reimnitz et al., 1990). In this process, suspended organisms are thought to adhere to individual ice crystals (frazil ice) that develop and rise in the surface waters. Alternatively, micro-organism particulates may be concentrated by wave fields pumping water through the freshly formed frazil ice layer, causing particles to become attached to, or trapped between, the ice crystals (Weissenberger and Grossmann, 1998). Thus, sea ice genesis could eventually lead to physical enrichment of particulate or colloidal Fe within the pack ice, together with planktonic organisms. However, such enrichment would mainly be confined to frazil ice layers as it is probably the case for stations IV and XIII.

Within our cores, however, no clear overall relationship was observed between ice texture and Fe content (Table 1). For example at station IV, TDFe is 51.8 nM in frazil ice, 49.8 nM and 38.5 nM in columnar sections, and 58.8 nM in bottom ice (also of columnar nature). Bottom ice TDFe enrichment could be caused by phytoplankton DFe uptake in the bottom ice assemblages. On one hand, we might expect higher Fe levels in snow ice, because of accumulation of atmospheric deposition, and in frazil ice via planktonic enrichment. But on the other hand, columnar ice should more efficiently expel sea salts and particles during formation, especially at depth, and therefore might not accumulate Fe. Our observations support neither scenario, and point toward the need for further research on the processes of Fe enrichment and transfer in sea ice.

4.3. Requirements and potential sources for Fe inputs to the sea ice cover

In our investigation, station IV can be regarded as a "winter" type station and its iron content might thus be taken as representative of the initial Fe distribution before significant melting (Table 2). Considering a 9-month residence time of 0.5 m thick ice, the required Fe flux into sea ice in order to accumulate 49 nM TDFe and 18 nM DFe would be 0.09 μmol TDFe/m^2/day and 0.03 μmol DFe/m^2/day (Table 3).

Based on data from the literature, we attempted to estimate Fe inputs to the Southern Ocean surface waters from various possible sources including atmospheric dust deposition (J_{atm}), extraterrestrial input (J_{space}), vertical diffusion (J_{diff}) and upwelling ($J_{upwelling}$). The calculations suggest a possible total flux of 0.28 μmol TDFe/m^2/day and 0.13 μmol DFe/m^2/day to the surface Antarctic waters (Table 4). Amongst the considered sources, upwelling should dominate the Fe inputs, accounting for about 90% of the total. This means that potential sources

of Fe to the upper waters of the Southern Ocean are sufficient to account for the total DFe and TDFe trapped in pack ice based on our data (Table 4).

4.4. Importance of sea ice as a source of Fe to Antarctic surface waters

Table 3 shows estimated TDFe and DFe fluxes from melting East Antarctic pack ice to the upper water column. For an ice floe of 0.5 m thickness containing an average of 49 nM TDFe and 18 nM DFe (station IV), and assuming a melting period of 1 month, the estimated releases to the upper ocean would be 0.82 μmol TDFe/m^2/day and 0.30 μmol DFe/m^2/day – this equates to a 0.49 nM TDFe addition over a 50 m mixed layer. During spring melting, compared to other sources, sea ice could thus represent a significant Fe source to the Antarctic surface waters (Table 4). When integrating atmospheric dust and extra-terrestrial deposition (0.0016 μmol DFe/m^2/day), vertical diffusion (0.01 μmol DFe/m^2/day), upwelling (0.12 μmol DFe/m^2/day) and sea ice melting (0.30 μmol DFe/m^2/day), the total DFe flux to the ocean surface would be 0.43 μmol DFe/m^2/day (Table 3), of which sea ice could represent 70% of the total input. Hence, sea ice melting during austral spring may be important, as a source of Fe, in favouring ice edge spring blooms.

5. Conclusions

The East Antarctic pack ice investigated in the present study reveals high Fe contents in sea ice as compared to under-ice seawater. Both thermodynamic and biological processes are likely key factors controlling the Fe distribution, as spring progresses and the ice warms. Comparison of Fe content and ice texture sheds some light on possible Fe pathways to pack ice. Complementary field data and laboratory experiments simulating ice growth could provide further mechanistic insights into the enrichment processes for Fe in the sea ice environment. Melting sea ice may provide a significant input of Fe to Antarctic surface waters during spring, in comparison to other sources, and may thus play an important role in fuelling algal blooms in the seasonal ice zone.

Acknowledgments

The authors would like to thank the Australian Antarctic Division, especially Ian Allison (Expedition Leader) and Rob Massom (Chief Scientist), for inviting us on the "ARISE in the East" endeavour. We are also grateful to the captain and crew of the *RV Aurora Australis* for their logistic assistance throughout the duration of the cruise. The support from Bruno Delille for field assistance, Anne Trevena for ice core sub-sampling and salinity measurements and Marie-Line Sauvée for processing samples for nutrient analysis is greatly acknowledged. The two anonymous reviewers are greatly acknowledged for their valuable comments, which improved the clarity of our paper. This work was funded by the Belgian French Community (ARC contract no. 2/07-287) and by the Belgian Federal Science Policy Office (contracts EV/12/7E and SD/CA/03A). This is also a contribution to the SOLAS international research initiative, the European Network of Excellence EUR-OCEANS (contract no. 511106-2) and to the European Integrated Project CarboOcean (contract no. 511176-2).

References

Arrigo, K.R., 2003. Primary production in sea ice. The importance of sea ice: an overview. In: Thomas, D.N., Dieckmann, G.S. (Eds.), Sea Ice – An Introduction to its Physics, Chemistry, Biology and Geology. Blackwell Science, Oxford, pp. 143–183.

Allison, I., 1997. Physical processes determining the Antarctic sea ice environment. Aust. J. Phys. 50 (4), 759–771.

Baker, A.R., Jickells, T.D., Witt, M., Linge, K.L., 2006. Trends in the solubility of iron, aluminium, manganese and phosphorus in aerosol collected over the Atlantic Ocean. Mar. Chem. 98 (1), 43–58.

Bowie, A.R., Maldonado, M.T., Frew, R.D., Croot, P.L., Achterberg, E.P., Mantoura, R.F.C., Worsfold, P.J., Law, C.S., Boyd, P.W., 2001. The fate of added iron during a mesoscale fertilisation experiment in the Southern Ocean. Deep-Sea Res., Part 2, Top. Stud. Oceanogr. 48, 2703–2743.

Boyd, P.W., Law, C.S., Hutchins, C.S., Abraham, D.A., Croot, E.R., Ellwood, P.L., Frew, M., Hadfield, R.D., Hall, M., Handy, J., Hare, S., Higgins, C., Hill, J., Hunter, P., LeBlanc, K.A., Maldonado, K., McKay, M.T., Mioni, R.M., Oliver, C., Pickmere, M., Pinkerton, S., Safi, M., Sander, K., Sanudo-Wilhelmy, S., Smith, S.A., Strzepek, M., Tovar-Sanchez, R., Wilhelm, S.W., 2005. FeCycle: Attempting an iron biogeochemical budget from a mesoscale SF_6 tracer experiment in unperturbed low iron waters. Glob. Biogeochem. Cycles 19, GB4S20, doi:10.1029/2005GB002494.

de Baar, H.J.W., de Jong, J.T.M., 2001. Distribution, sources and sinks of iron in seawater. In: Turner, D.R., Hunter, K.H. (Eds.), The Biogeochemistry of Iron in Seawater, IUPAC Series on Analytical and Physical Chemistry of Environmental Systems, vol. 7, pp. 123–253.

de Baar, H.J.W., de Jong, J.T.M., Bakker, D.C.E., Loscher, B.M., Veth, C., Bathmann, U., Smetacek, V., 1995. Importance of iron for phytoplankton spring blooms and CO_2 drawdown in the Southern Ocean. Nature 373, 412–415.

de Jong, J.T.M., den Das, J., Bathmann, U., Stoll, M.H.C., Kattner, G., Nolting, R.F., de Baar, H.J.W., 1998. Dissolved iron at subnanomolar levels in the Southern Ocean as determined by ship-board analysis. Anal. Chim. Acta 377, 113–124.

Duce, R.A., Tindale, N.W., 1991. Atmospheric transport of iron and its deposition in the ocean. Limnol. Oceanogr. 36, 1715–1726.

Edwards, R., Sedwick, P.N., 2001. Iron in East Antarctic snow: implications for atmospheric iron deposition and algal production in Antarctic waters. Geophys. Res. Lett. 28 (20), 3907–3910.

Edwards, R., Sedwick, P.N., Morgan, V., Boutron, C.F., Hong, S., 1998. Iron in ice cores from Law Dome, East Antarctica: implications for past deposition of aerosol iron. Ann. Glaciol. 27, 365–370.

Eicken, H., 1992. Salinity profiles of Antarctic sea ice: field data and model results. J. Geophys. Res. 97 (C10), 15545–15557.

Eicken, H., 1998. Factors determining microstructures, salinity and stable-isotope composition of Antarctic sea ice: deriving modes and rates of ice growth in the Weddell Sea. In: Jeffries, M.O. (Ed.), Antarctic Sea Ice: Physical Processes, Interactions and Variability. Antarct. Res. Ser., vol. 74. AGU, Washington, D.C., pp. 89–122.

Eicken, H., 2003. From the microscopic, to the macroscopic, to the regional scale: growth, microstructure, and properties of sea ice. In: Thomas, D.N., Dieckmann, G.S. (Eds.), Sea Ice – An introduction to its physics, chemistry, biology and geology. Blackwell Science, Oxford, pp. 22–83.

Eicken, H., Lange, M.A., Dieckmann, G.S., 1991. Spatial variability of sea ice properties in the northwestern Weddell Sea. J. Geophys. Res. 96 (C6), 10603–10615.

Gao, Y., Kaufman, Y.J., Tanre, D., Kolber, D., Falkowski, P.G., 2001. Seasonal distributions of aeolian iron fluxes to the global ocean. Geophys. Res. Lett. 28, 29–32.

Garrison, D.L., Ackley, S.F., Buck, K.R., 1983. A physical mechanism for establishing algal populations in frazil ice. Nature 306, 363–365.

Garrison, D.L., Close, A.R., Reimnitz, E., 1989. Algae concentrated by frazil ice: evidence from laboratory experiments and field measurement. Antarct. Sci. 1 (4), 313–316.

Golden, K.M., Ackley, S.F., Lytle, V.I., 1998. The percolation phase transition in sea ice. Science 282, 2238–2241.

Gow, A.J., Ackley, S.F., Govoni, J.W., Weeks, W.F., 1998. Physical and structural properties of land-fastice in Mc Murdo Sound, Antarctica. In: Jeffries, M.O. (Ed.), Antarctic Sea Ice: Physical Processes, Interactions and Variability. Antarct. Res. Ser., vol. 74. AGU, Washington, D.C., pp. 355–374.

Grotti, M., Soggia, F., Ianni, C., Frache, R., 2005. Trace metals distributions in coastal sea ice of Terra Nova Bay, Ross Sea, Antarctica. Antarct. Sci. 17 (2), 289–300.

Horner, R.A., 1985a. History of ice algal investigations. In: Horner, R.A. (Ed.), Sea Ice Biota. CRC Press, Boca Raton, pp. 1–19.

Jickells, T.D., An, Z.S., Anderson, K.K., Baker, A.R., Bergametti, G., Brooks, N., Cao, J.J., Boyd, P.W., Duce, R.A., Hunter, K.A., Kawahata, H., Kubilay, N., La Roche, J., Liss, P.S., Mahowald, N., Prospero, J.M., Ridgwell, A.J., Tegen, I., Torres, R., 2005. Global iron connections between desert dust, ocean biogeochemistry and climate. Science 308, 67–71.

Krembs, C., Mock, T., Gradinger, R., 2001. A mesocosm study of physical–biological interactions in artificial sea ice: effects of brine channel surface evolution and brine movement on algal biomass. Polar Biol. 24, 356–364.

Johnson, K.S., 2001. Iron supply and demand to the upper ocean: is extraterrestrial dust a significant source of bioavailable iron? Glob. Biogeochem. Cycles 15 (1), 61–63.

Johnson, K.S., Chavez, F.P., Frederich, G.E., 1999. Continental-shelf sediment as a primary source of iron for coastal phytoplankton. Nature 398, 697–700.

Langway, C.C., 1958. Ice fabrics and the universal stage. CRREL Technical, vol. 62. USA Cold Regions Research and Engineering Laboratory.

Lannuzel, D., de Jong, J.T.M., Schoemann, V., Trevena, A., Tison, J.-L., Chou, L., 2006. Development of a sampling and flow injection analysis technique for iron determination in the sea ice environment. Anal. Chim. Acta 556 (2), 476–483.

Law, C.S., Abraham, E.R., Watson, A.J., Liddicoat, M.I., 2003. Vertical eddy diffusion and nutrient supply to the surface mixed layer of the Antarctic Circumpolar Current. J. Geophys. Res. 108 (C8), 3272.

Longhurst, A., Sathyendranath, S., Platt, T., Caverhill, C., 1995. An estimate of global primary production in the ocean from satellite radiometer data. J. Plankton Res. 17 (6), 1245–1271.

Löscher, B.M., de Baar, H.J.W., de Jong, J.T.M., Veth, C., Dehairs, F., 1997. The distribution of Fe in the Antarctic Circumpolar Current. Deep-Sea Res., Part 2, Top. Stud. Oceanogr. 44, 143–187.

Martin, J.H., Fitzwater, S.E., 1988. Iron deficiency limits phytoplankton growth in the north-east Pacific subarctic. Nature 331, 341–343.

Martin, J.H., 1990. Glacial–interglacial CO_2 change: the iron hypothesis. Paleoceanography 5, 1–13.

Nakawo, M., Sinha, N.K., 1981. Growth rate and salinity profile of first-year sea ice in the Arctic. J. Glaciol. 27 (96), 315–330.

Reimnitz, E., Kempema, E.W., Wefer, W.S., Clayton, J.R., Payne, J.R., 1990. Suspended-matter scavenging by rising frazil ice. In: Ackley, S.F., Weeks, W.F. (Eds.), Sea Ice Properties and Processes: Proceedings of the Sea Ice Symposium. CRREL Monograph, vol. 90-1. Cold Region Research and Engineering Laboratory, Hanover, pp. 97–100.

Sarmiento, J.L., Hughes, T.M.C., Stouffer, R.J., Manabe, S., 1998. Simulated response of the ocean carbon cycling to anthropogenic carbon warming. Nature 393, 245.

Sedwick, P.N., DiTullio, G.R., 1997. Regulation of algal blooms in Antarctic shelf waters by the release of iron from melting sea ice. Geophys. Res. Lett. 24 (20), 2515–2518.

Sedwick, P.N., DiTullio, G.R., Mackey, D.J., 2000. Iron and manganese in the Ross Sea, Antarctica: seasonal iron limitation in Antarctic shelf waters. J. Geophys. Res. 105, 11321–11336.

Sedwick, P.N., Harris, P.T., Robertson, L.G., McMurtry, G.M., Cremer, M.D., Robinson, P., 2001. Holocene sediment records from the continental shelf of Mac, Robertson Land, East Antarctica. Paleoceanography 16 (2), 212–225.

Thomas, D., 2003. Iron limitation in the Southern Ocean. Science 302, 565.

Watson, A.J., 2001. Iron limitation in the oceans. In: Turner, D.R., Hunter, K.H. (Eds.), The Biogeochemistry of Iron in Seawater. IUPAC Series on Analytical and Physical Chemistry of Environmental Systems, vol. 7, pp. 9–39.

Watson, A.J., Orr, J.C., 2003. Carbon dioxide fluxes in the global ocean. In: Fasham, M.J.R. (Ed.), Ocean Biogeochemistry: The Role of the Ocean Carbon Cycle in Global Change. Springer-Verlag, Berlin.

Wedepohl, K.H., 1995. The composition of the continental crust. Geochim. Cosmochim. Acta 59, 1217–1232.

Weeks, W.F., Ackley, S.F., 1986. The growth, structure and properties of sea ice. In: Untersteiner, N. (Ed.), The Geophysics of Sea Ice. NATO ASI Series, pp. 9–164.

Weissenberger, J., Grossmann, S., 1998. Experimental formation of sea ice: importance of water circulation and wave action for incorporation of phytoplankton and bacteria. Polar Biol. 20, 178–188.

Westerlund, S., Öhman, P., 1991. Iron in the water column of the Weddell Sea. Mar. Chem. 35, 199–217.

Yentsch, C.S., Menzel, D.W., 1963. A method for the determination of phytoplankton chlorophyll and phaeophytine by fluorescence. Deep-Sea Res. 10, 221–231.